

Manipulation of Ring Strain and Antiaromaticity in the Design and Synthesis of Unique Optoelectronic Materials

by

Rebecca R. Parkhurst

B. A. *summa cum laude* Chemistry, French
Hamilton College, 2007

Submitted to the Department of Chemistry
In Partial Fulfillment of the Requirements for the Degree of

DOCTOR OF PHILOSOPHY IN CHEMISTRY

at the

MASSACHUSETTS INSTITUTE OF TECHNOLOGY

June 2012

© Massachusetts Institute of Technology. All Rights Reserved.

Signature of Author: _____
Department of Chemistry
May 16, 2012

Certified by: _____
Timothy M. Swager
Thesis Supervisor

Accepted by: _____
Robert W. Field
Chairman, Departmental Committee on Graduate Students

This doctoral thesis has been examined by a Committee at the Department of Chemistry as follows:

Professor Rick L. Danheiser: _____
Chairman

Professor Timothy M. Swager: _____
Thesis Supervisor

Professor Timothy F. Jamison: _____
Department of Chemistry

Dedicated to Barbara Hildreth Parkhurst (1920-2011)

Manipulation of Ring Strain and Antiaromaticity in the Design and Synthesis of Unique Optoelectronic Materials

by

Rebecca R. Parkhurst

Submitted to the Department of Chemistry on May 16, 2012
In Partial Fulfillment of the Requirements for the Degree of
Doctor of Philosophy in Chemistry

ABSTRACT

Polycyclic aromatic hydrocarbons (PAHs) and fully-conjugated ladder polymers are leading candidates for organics electronics, as their inherent conformational rigidity encourages electron delocalization. Many of these systems consist of fused benzenoid or heterocyclic aromatic rings. Less frequently, however, PAHs are reported with character that alternates between the aromaticity of benzene fragments and the antiaromaticity of a nonbenzenoid moiety. Due to its high degree of unsaturation and ring strain, 3,4-bis(methylene)cyclobutene presents an intriguing building block for a variety of polycyclic macromolecules.

The syntheses of several derivatives of 3,4-bis(benzylidene)cyclobutene are reported. Previously unknown 1,2-dibromo-3,4-bis(benzylidene)cyclobutene was obtained through *in situ* generation of 1,6-diphenyl-3,4-dibromo-1,2,4,5-tetraene followed by electrocyclic ring closure. Ensuing reduction and metal-catalyzed cross-coupling provided additional derivatives. The effects of ring strain on the geometry and electronics of these derivatives were examined.

The synthesis of new class of fully unsaturated ladder structures, phenylene-containing oligoacenes (POAs), using 3,4-bis(methylene)cyclobutene as a building block for sequential Diels-Alder reactions is described. The electronic effects of strain and the energetic cost of antiaromaticity can be observed *via* the optical and electrochemical properties of the reported compounds. The resulting shape-persistent ladder structures contain neighboring chromophores that are partially electronically isolated from one other while still undergoing a reduction in the band gap of the material.

Singlet fission, a phenomenon in which two triplet excitons are generated from a single photon of light, has the potential to improve the efficiency of organic solar cells by increasing the theoretical quantum efficiency. Singlet fission is observed for the first time in dithienyl-substituted pentacene and tetracene. Dissociation of the triplets at the donor-acceptor interface in a solar cell constructed with 6,13-di(thien-2-yl)pentacene is demonstrated. The synthesis of a POA containing pentacene is also investigated.

The chain-growth mechanism of polymerization allows for greater control of molecular weight and polydispersity than does the step-growth mechanism, however is currently limited to only a few reactions. Due to its unique Diels-Alder reactivity, 3,4-bis(methylene)cyclobutene and related structures are investigated as monomers for chain-growth Diels-Alder polymerization.

Thesis Supervisor: Timothy M. Swager
Title: John D. MacArthur Professor of Chemistry

Table of Contents

Abstract	4
Table of Contents	5
List of Figures	7
List of Schemes	11
List of Tables	14
Chapter 1: Introduction: Antiaromaticity in Nonbenzenoid Oligoarenes and Ladder Polymers	16
1.1 Introduction	17
1.2 [N]Phenylenes and Related Materials	17
1.3 Recent Synthetic Developments in [N]Phenylenes	21
1.4 Photophysical Properties of [N]Phenylenes	27
1.5 Reactivity of [N]Phenylenes and Related Materials	30
1.6 Applications of Phenylene-Containing Materials	34
1.7 Polymeric and Graphitic [N]Phenylenes	43
1.8 Conclusions and Outlook	47
1.9 References	48
Chapter 2: Synthesis of 3,4-Bis(benzylidene)cyclobutenes	52
2.1 Introduction	53
2.2 Synthesis of 1,2-Dibromo-3,4-bis(benzylidene)cyclobutene	54
2.3 Characterization of 1,2-Dibromo-3,4-bis(benzylidene)cyclobutene	56
2.4 Synthesis of Additional Derivatives of 3,4-Bis(benzylidene)cyclobutenes	61
2.5 Conclusions	64
2.6 Experimental Section	64
2.7 References	72
Appendix	74
Chapter 3: Synthesis and Optoelectronic Properties of Phenylene-Containing Oligoarenes (POAs)	86
3.1 Introduction	87
3.2 Diels-Alder Reactivity of 3,4-Bis(methylene)cyclobutene	90
3.3 Synthesis of [2-3]Phenylene-Containing Oligoarene	92
3.4 Synthesis of [2-3-2] and [3-3-3]Phenylene-Containing Oligoarene	94
3.5 Optical and Electrochemical Properties of POAs	95
3.6 X-Ray crystallography of POAs	99
3.7 Conclusions	99
3.8 Experimental Section	100
3.9 References	111
Appendix	114

Chapter 4: Acenoid Candidates for Singlet Fission in Organic Solar Cells	137
4.1 Introduction	138
4.2 Singlet Fission in Dithienyl-Acenes	141
4.3 Towards POAs for Singlet Fission	146
4.4 Conclusions	149
4.5 Experimental Section	150
4.6 References	155
Appendix	157
Chapter 5: Towards Chain-Growth Diels-Alder Polymerization	161
5.1 Introduction	162
5.2 Initial Polymerization Studies	164
5.3 Improved Monomer Design	166
5.4 Towards a Monomer for Chain-Growth Diels-Alder Polymerization	169
5.5 Conclusions	172
5.6 Experimental Section	173
5.7 References	178
Appendix	180
Curriculum Vitae	184
Acknowledgements	186

List of Figures

Chapter 1.

Figure 1.1	Structures of (a) cyclobutadiene, (b) linear and (c) angular [N]phenylenes.	18
Figure 1.2	(a) Kekulé structures of biphenylene and (b) theoretical π -bond orders based on the above structures.	20
Figure 1.3	X-Ray crystal structures: (a) Front and (d) side views of 12 , (b) front and (e) side views of 13 , and (c) front and (f) side views of 14 .	26
Figure 1.4	Structure of [N]phenylenes 20-25 .	28
Figure 1.5	Structures of [N]Phenylenes 26 and 27 .	29
Figure 1.6	Structures of <i>anti</i> -[2.2]-(1,4)-biphenylenophane 38 and [2.2]paracyclophane 39 .	37
Figure 1.7	Triangular [4]phenylene dyad 44 .	39
Figure 1.8	Thioether-substituted fluorenes 48 and 49 .	40
Figure 1.9	Structure of 52 : (a) X-ray crystal structure of major contributor (methyl groups and H atoms omitted for clarity) (b) Calculated geometry (c) Disorder in the crystal (d) Crystal packing.	43
Figure 1.10	Convergent bond lengths in extended [N]phenylenes.	44
Figure 1.11	Archimedene 53 .	45
Figure 1.12	Insertion of 2-carbon fragment into C ₆₀ .	46
Figure 1.13	Structures of phenylene-containing graphitic materials: (a) biphenylene sheet, (b) biphenylene nanoribbons with armchair and zigzag edge morphology, (c) biphenylene nanotubes, and (d) biphenylene dimer.	47

Chapter 2.

Figure 2.1	Space-filling (a–c) and front/side ellipsoid views (d–f) of X-ray crystal structures of isomers of 7 (a, d) (<i>in,out</i>) (b, e) (<i>in,in</i>) (c, f) (<i>out,out</i>). Aromatic hydrogens omitted for clarity.	56
Figure 2.2	Photolysis of (a) 7 (<i>in,out</i>) after (b) 1.5h (c) 17h. Photolysis of (d) 7 (<i>in,in</i>) after (e) 1.5h (f) 17h. Photolysis of (g) 7 (<i>out,out</i>) after (h)1.5h (i)17h.	58
Figure 2.3	Comparison of ¹ H NMR spectra of compounds 7 and 8 . Deshielding of H ^b is evident.	62
Figure 2.4	Absorption and emission curves of 10 (<i>out,out</i>) in CHCl ₃ .	64
Figure A2.1	Crystal packing in the X-ray crystal structure of 7 (<i>in,out</i>).	75
Figure A2.2	Crystal packing in the X-ray crystal structure of 7 (<i>in,in</i>).	76
Figure A2.3	Crystal packing in the X-ray crystal structure of 7 (<i>out,out</i>).	76

Chapter 3.

Figure 3.1	Rapidly decreasing band gap (E_g , estimated from lowest energy λ_{max}) versus number of fused aromatic rings (nFAR) of the trialkylsilylethynyl-substituted acenes.	88
Figure 3.2	(a) Brick-like crystal packing of TIPS-Pentacene. (b) Front and (c) side views of herringbone crystal packing of pentacene. Crystal structure data gathered from the Cambridge Structural Database (CSD).	89
Figure 3.3	General structures of (a) acenes, (b) [N]phenylenes, and (c) phenylene-containing oligoacenes (POAs).	90
Figure 3.4	Determination of the stereochemistry of 2a . (a) HSQC-NMR, (b) HMBC-NMR, (c) <i>exo</i> -product, and (d) <i>endo</i> -product.	91
Figure 3.5	(a) X-Ray crystal structure of 3 . (b) LUMO of 1 (B3LYP/6-31g**) (c) <i>Endo</i> and (d) <i>exo</i> approaches of 1 to a furan diene.	92
Figure 3.6	(a) DSC of POA 6 recrystallized from EtOAc to give kinetic polymorph A, which reorganizes to thermodynamic polymorph B after heating. (b) PXRD of POA 6 taken at various points during the DSC heating/cooling cycle.	94
Figure 3.7	Absorbance overlay of TIPS-Anth , compound 5 , and compound 6 in CHCl ₃ .	96

Figure 3.8	(a) Overlay of the absorbance curves of TIPS-Anth , 6 , and 9a/b . Absorbance and Emission of (b) TIPS-Anth , (c) 6 , (d) 9a , and (e) 9b .	96
Figure 3.9	Cyclic Voltammetry of (a) TIPS-Anth , (b) 6 , (c) 9a , and (d) 9b .	98
Figure 3.10	Crystal structures of (a) 6 and (b) 9a . Localization of π -bonds in (c) 6 and (d) 9a .	99
Figure A3.1	X-ray crystal structure of 3 .	115
Figure A3.2	X-ray crystal structure of 4 .	116
Figure A3.3	Two views of the crystal packing of 4 .	116
Figure A3.4	X-ray structure of 6 .	117
Figure A3.5	Two views (rotated about the y-axis) of crystal packing of 6 .	117
Figure A3.6	X-ray structure of 9a .	118
Figure A3.7	Two views (rotated about the x-axis) of crystal packing of 9a .	118
 Chapter 4.		
Figure 4.1	Singlet Fission to produce two triplet excitons.	138
Figure 4.2	Schematic representation of the theoretical efficiency as a function of the S_0 - T_1 energy difference (ΔE) of a standard organic photovoltaic cell (OPV, blue) and a singlet fission OPV (red).	139
Figure 4.3	Two views of the crystal packing of 1 . Crystal structure data gathered from the American Chemical Society.	141
Figure 4.4	(a) Absorbance and emission of 2 , (b) Absorbance of 2 in solution state and thin film.	143
Figure 4.5	Percent change in instant fluorescence of 1 with increasing magnetic field.	144
Figure 4.6	(a) Device architecture, (b) J - V curve, $V_{OC} = 0.33$ V, (b) plot of external quantum efficiency (EQE), and (d) plot of magnetic field dependence of photocurrent.	145
Figure 4.7	Chemical structure of PDI-2CN .	145
Figure 4.8	Absorbance spectrum of compound 5 .	147

Figure 4.9 (a) ^1H NMR spectrum of compound **5** in CDCl_3 , and (b) ^1H NMR spectrum of the short-lived presumed monodehydration product. 149

Chapter 5.

Figure 5.1 (a) Schematic representation, and (b) plot of molecular weight versus monomer conversion of step-growth polymerization. (c) Schematic representation, and (d) plot of molecular weight versus monomer conversion of chain-growth polymerization. 163

Figure 5.2 Two classical examples of Diels-Alder polymerization: (a) A_2/B_2 polymerization (b) AB polymerization. (c) Proposed chain-growth Diels-Alder polymerization of 3,4-bis(methylene)cyclobutene. 164

Figure 5.3 Infrared spectrum of **P1**. 165

Figure 5.4 IR spectra of insoluble solids resulting from heating of **1** in the presence of (a) 5%, (b) 50 %, and (c) 0% of initiator **2**. 166

Figure 5.5 (a) Diels-Alder reactivity of *s-cis* dienes dependent on internuclear distance “*r*.” For the specific *k* values plotted, the dienophile is TCNE. Calculated geometries of (a) **1** and (b) **3** (Spartan, B3LYP/6-31g**). 167

Figure 5.6 Proposed chain-growth Diels-Alder polymerization of isobenzofuran[*b*]cyclobutadiene monomer. 169

List of Schemes

Chapter 1.

Scheme 1.1	Catalytic cycle in the metal-catalyzed [2 + 2 + 2] cycloaddition of aryl alkynes to yield [N]phenylenes.	19
Scheme 1.2	Synthesis of (a) bent [4]Phenylene (2a) and (b) 2b . Synthesis of (c) <i>anti</i> (5) and (d) <i>syn</i> double bent [5]phenylene (6).	22
Scheme 1.3	Synthesis of singly bent [5]phenylene 10 .	23
Scheme 1.4	Hexahydrogenation of ring C of 2b .	24
Scheme 1.5	Pd-catalyzed cyclization of 2,3-dehydrobiphenylene derivatives.	27
Scheme 1.6	Proposed mechanism of two-photon photoreactivity of 20 .	31
Scheme 1.7	Mechanism of phenyl group migration in FVP of phenylene-containing PAHs.	31
Scheme 1.8	FVP of 28 , 21 , and 29 .	32
Scheme 1.9	Reactivity of 22 .	34
Scheme 1.10	Synthesis of unsymmetric, substituted η^6 -Cr(CO) ₃ -complexes of biphenylene.	35
Scheme 1.11	Photo-thermal IRHR of η^4 -CpCo-complexed linear [N]phenylenes.	36
Scheme 1.12	Synthesis of benzo[3]phenylene-C ₆₀ dyad 43 .	38
Scheme 1.13	Synthesis of thioether-substituted biphenylene 47 .	40
Scheme 1.14	Synthesis of quadrannulene 52 .	42
Scheme 1.15	Three-fold cyclotrimerization to give archimedene fragment 54 .	45
Scheme 1.16	One-pot synthesis of C ₆₂ analogue 55 .	46

Chapter 2.

Scheme 2.1	Rearrangement of 1,5-hexadiyne to 1 .	53
Scheme 2.2	Synthesis of 2 and 3 reported by Toda <i>et al.</i>	54
Scheme 2.3	Synthesis of intermediates 4 and 5 .	55
Scheme 2.4	Rearrangement and irreversible cyclization to form 7 .	55
Scheme 2.5	Stereochemistry of the rearrangement and ring closure of 6 to 7 .	57
Scheme 2.6	Proposed mechanisms of Cu(I)-catalyzed 4π -electrocyclic ring closure; (a) ring closure <i>via</i> radical anion intermediate, (b) ring closure <i>via</i> cupracyclopentane.	59
Scheme 2.7	Reduction of a single isomer 7 to a single isomer of 8 with retention of <i>E/Z</i> configuration.	62
Scheme 2.8	Examples of metal-catalyzed cross-coupling of 7 .	63

Chapter 3.

Scheme 3.1	Proposed pathways of photo-oxidation of pentacene; (a) [4 + 2] cycloaddition with singlet oxygen, or (b) charge transfer to oxygen followed by recombination.	89
Scheme 3.2	Sequential Diels-Alder reactions to yield 3 .	90
Scheme 3.3	Synthesis of POA 6 from compound 3 .	93
Scheme 3.4	Bisaryne Diels-Alder reaction and aromatization to yield POAs 9a/b .	95

Chapter 4.

Scheme 4.1	Simplified mechanism of singlet fission (forward direction) and triplet-triplet annihilation (reverse direction).	140
-------------------	---	-----

Scheme 4.2	Synthesis of dithienyl-substituted acenes 1 and 2 .	142
Scheme 4.3	Synthesis of pentacene-containing 5 .	147
Scheme 4.4	Attempted dehydration of 5 to [2-5-2]POA.	148
 Chapter 5.		
Scheme 5.1	Attempted polymerization of 1 to polymer P1 .	165
Scheme 5.2	(a) Retrosynthetic analysis of Ph ₂ - 3 to 4 . (b) Attempted Paal-Knorr furan synthesis resulting in rearrangement of 4 to unsymmetrical furan 5 .	168
Scheme 5.3	(a) Generic example of [2 + 2] ring closure of <i>o</i> -substituted phenyl bisallenes to naphthocyclobutenes. (b) Reported synthesis of 1,3-diphenylisobenzofuran-containing 6 .	170
Scheme 5.4	Retrosynthetic analysis of monomer 7 .	170
Scheme 5.5	New synthetic route to 1,2-dibromonaphtho[<i>b</i>]cyclobutadiene 9 as a model system, and Diels-Alder trapping of naphtho[<i>b</i>]cyclobutadiene to give 10 .	171
Scheme 5.6	Attempted synthesis of monomer precursor 13 , resulting instead in diketone 14 .	172

List of Tables

Chapter 1.

Table 1.1	Synthesis of [N]heliphenes (N = 6-9).	25
Table 1.2	Photophysical properties of [N]phenylenes in THF.	28
Table 1.3	Lowest energy λ_{\max} for some [4]- and [5]phenylenes.	30
Table 1.4	Photostationary state of IRHR of [N]phenylenes 35-37 .	36
Table 1.5	Photophysical and electrochemical properties of 38, 39 , and 20 .	38
Table 1.6	Conductance and first oxidation potential of PAHs 47-49 .	41

Chapter 2.

Table 2.1	Thermal distribution of isomers of 7 .	57
Table 2.2	Structural information of 1 (B3LYP/6-31G**) and crystal structures of 7 . Redundant bond and torsion angles for symmetrical compounds have been omitted.	60
Table A2.1	X-ray crystallographic data.	75

Chapter 3.

Table 3.1	Electrochemical Data for POAs.	97
Table A3.1	X-ray crystallographic data.	115

Chapter 4.

Table 4.1 Literature values for E(S₁) and 2E(T₁) for acenes n = 3-5. 140

Table 4.2 Dehydrations conditions screened for compound **5**. 148

Chapter 1

Introduction: Antiaromaticity in Nonbenzenoid Oligoarenes and Ladder Polymers

Adapted from: Parkhurst, R. R.; Swager, T. M. "Antiaromaticity in Nonbenzenoid Oligoarenes and Ladder Polymers," *Topics in Current Chemistry*, **2012**, *in press*.

1.1 Introduction

The concepts of aromaticity and antiaromaticity have long been employed to explain certain chemical phenomena, however there is still much to be explored regarding the effect of these simultaneously opposing and intertwined theories on the properties of materials. Aromatic molecules are generally characterized by several properties including unexpectedly high thermal stability, nonalternant bond lengths, and diamagnetic anisotropy.¹ Since it was first proposed by Hückel in the 1930s, it has held that these properties belong to cyclic arrays containing $4n + 2 \pi$ -electrons.² On the other hand, those species containing $4n \pi$ -electrons later came to be classified as antiaromatic, and alternatively can be high energy and difficult to isolate.³

Organic molecules consisting of multiple fused aromatic rings are commonly known as polycyclic aromatic hydrocarbons (PAHs). Due to the extended conjugation and ring current inherent in these materials, they make a class of important candidates for use in organic electronics.⁴ Antiaromatic compounds, on the other hand, are also appealing candidates for optoelectronic applications due to small HOMO-LUMO gaps relative to analogous aromatic systems, and theoretically high polarizability, which could improve intermolecular interactions. Although attempts have been made to computationally predict the structure and solid-state properties of polycyclic antiaromatic hydrocarbons (PAAHs), there is still much that is not well understood.⁵ In this regard, one area of interest is to study the interplay of these two concepts in polycyclic systems consisting of alternating aromatic and antiaromatic character.⁶

1.2 [N]Phenylenes and Related Materials

The most basic example of antiaromaticity is found in the 4π -electron system of cyclobutadiene (Figure 1.1a).⁷ There has been a great deal of theoretical interest in the

antiaromaticity of cyclobutadiene, however experimental analysis has been difficult as a result of the very high reactivity of the parent hydrocarbon.

The [N]phenylenes are a family of PAHs in which benzene rings are fused together by cyclobutadiene rings, resulting in a ladder structure with alternating aromatic and antiaromatic character (Figure 1.1b,c).⁸ The simplest member of this family, biphenylene (N = 2), was first synthesized in 1941 from 2,2'-dibromobiphenyl after a fairly long history of eluding synthetic chemists.⁹ Other classic methods to access this scaffold include the dimerization of arynes or contraction of bridged biaryls through extrusion of a small molecule such as N₂, CO₂, or CO.¹⁰ Over the last several decades the synthesis has been dominated by the metal-catalyzed [2 + 2 + 2] cycloaddition methodology (Scheme 1.1), developed primarily by Vollhardt and coworkers.⁸ This approach has improved the synthesis of biphenylene as well as provided access to longer derivatives. It has been demonstrated both experimentally and theoretically that the π -bonds in these systems tend to localize within the six-membered rings thereby minimizing the 4π antiaromatic character of the cyclobutadiene linkage.¹¹

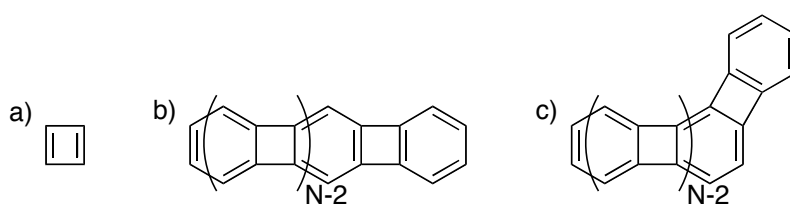
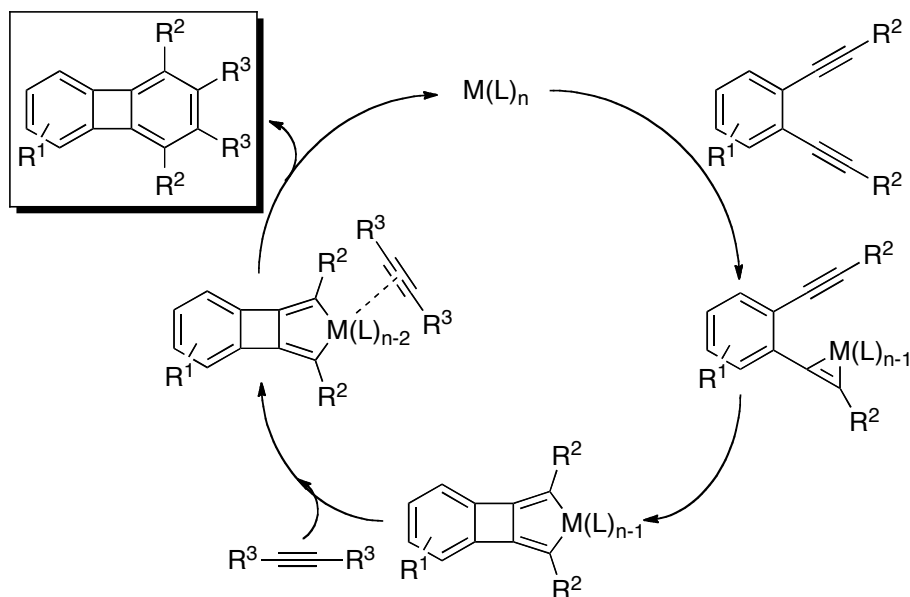


Figure 1.1. Structures of (a) cyclobutadiene, (b) linear and (c) angular [N]phenylenes.



Scheme 1.1. Catalytic cycle in the metal-catalyzed [2 + 2 + 2] cycloaddition of aryl alkynes to yield [N]phenylenes.

In the past, the model of conjugated circuits, traditionally employed to determine the resonance energy of PAHs, has failed to explain some of the properties observed in [N]phenylenes.¹² Most significantly, the model does not account for the increased stability of angular [N]phenylenes (Figure 1.1c) over linear [N]phenylenes (Figure 1.1b).^{8,13} Recently, Randić and coworkers have sought to develop a revised theory to determine the aromaticity of [N]phenylenes that can compensate for this discrepancy.¹²

The five possible Kekulé resonance structures of biphenylene are shown in Figure 1.2a. According to these structures, the C—C bond connecting the two benzenoid rings should have a bond order of $1\frac{1}{5}$. In reality, this bond has been shown to have even less double bond character than this value suggests. The authors propose excluding the fifth and final structure that does not contain any Clar sextets¹⁴ as a contributor to the resonance hybrid. This leads to $1\frac{1}{2}$ bond order for all π bonds except for the connecting C—C bond with a bond order of 1. This solution

appears to improve the theory for one aspect of the observed bond lengths in biphenylene, however it does not yet account for the decreased bond alternation within the benzenoid rings.

The authors also considered the effect of the proposed reduced set of Kekulé structures on the ring currents of biphenylene, following a structural approach in which aromaticity is a combination of the local ring current of each conjugated circuit in the resonance structures. This model leads to a reduction in the diamagnetic current of benzenoid rings to $\frac{1}{2}$ that of benzene, and a paramagnetic current of $\frac{1}{3}$ the magnitude of the same reference in the four-membered rings. Therefore, although fusion of the aromatic and antiaromatic systems results in a reduced contribution by both, the aromatic character of these PAHs is still stronger.

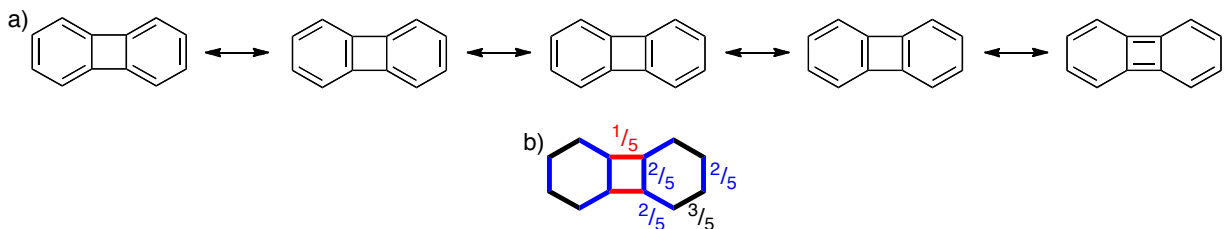


Figure 1.2. (a) Kekulé structures of biphenylene and (b) theoretical π -bond orders based on the above structures.

The revised model also provides promising results when applied to longer [N]phenylenes. In the case of linear (Figure 1.1b, $N = 3$) and angular [3]phenylene (Figure 1.1c, $N = 3$), each have 12 and 13 respective Kekulé structures. Elimination of those that do not contain at least 3 Clar sextets leaves only 8 possible structures for each. The resonance energy determined from these revised structures (by summing the positive contribution of $4n + 2$ π -electrons and the negative contribution of $4n$ π -electrons) is indeed higher for angular [3]phenylene, consistent with previous experimental and theoretical findings.

1.3 Recent Synthetic Developments in [N]Phenylenes

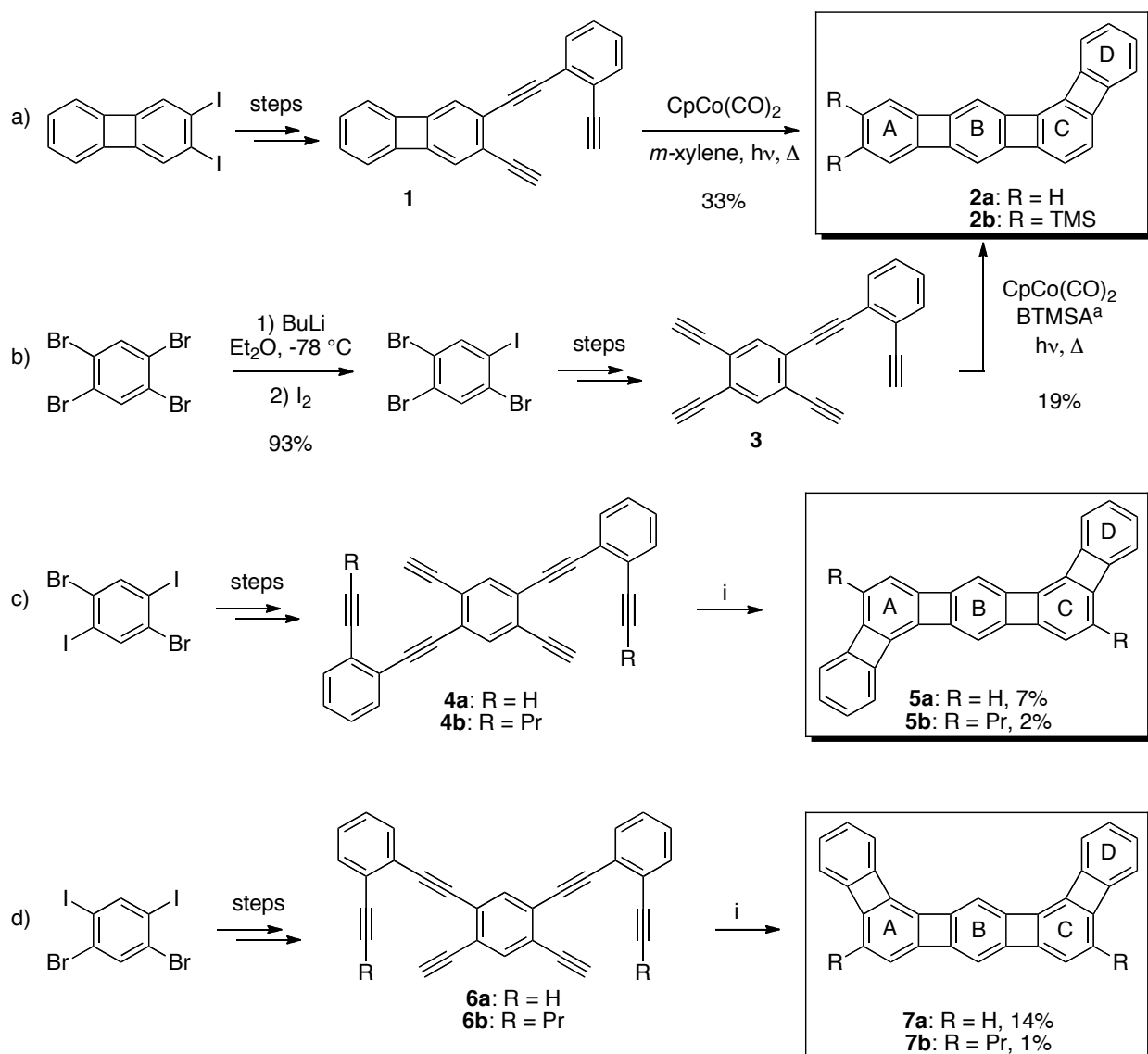
As mentioned previously, the most general route to accessing a wide variety of linear, angular, zigzag, and branched [N]phenylenes is *via* the appropriate phenylethynyl precursor and subsequent [2 + 2 + 2] cycloaddition. This chemistry is relatively well-established through work by Vollhardt and coworkers and has been reviewed previously,⁸ therefore this discussion will focus on developments made in the last ten years.

Several derivatives of bent [N]phenylenes have been reported by Vollhardt and coworkers since 2002. Bent [4]phenylene (**2**), the final isomer of the [4]phenylene family, was synthesized in 2002 (Scheme 1.2a).¹⁵ Starting from 2,3-diiodobiphenylene, non-selective Pd-catalyzed Sonogashira coupling with mono-silated *o*-diethynyl benzene, followed by a second Sonogashira coupling with trimethylsilylacetylene and subsequent deprotection provided the desired triyne precursor **1**. Cobalt-catalyzed [2 + 2 + 2] cyclization of **1** yielded the air-sensitive compound **2a** in 1.7% overall yield over 8 steps.

An alternative synthesis, resulting in the relatively more stable bis(trimethylsilyl)-**2** (**2b**) and involving double [2 + 2 + 2] cycloaddition, was also reported (Scheme 1.2b). In this case, 5-iodo-1,2,4-tribromobenzene was generated in high yields by regioselective lithiation of 1,2,4,5-tetrabromobenzene followed by quenching with iodine. Consecutive Sonogashira coupling reactions yielded compound **3**. This pentayne underwent a two-fold intra- and intermolecular [2 + 2 + 2] cyclization to yield **2b** in an improved 7% yield over 5 steps. However, attempts to perform the protodesilylation of **2b** to parent hydrocarbon **2a** resulted in decomposition.

In a fashion similar to that discussed above, Vollhardt and coworkers were also able to access *anti* (**5**) and *syn* (**7**) doublebent [5]phenylenes by first constructing the appropriate hexayne precursor (Scheme 1.2c,d).¹⁶ Both isomers are accessible through successive

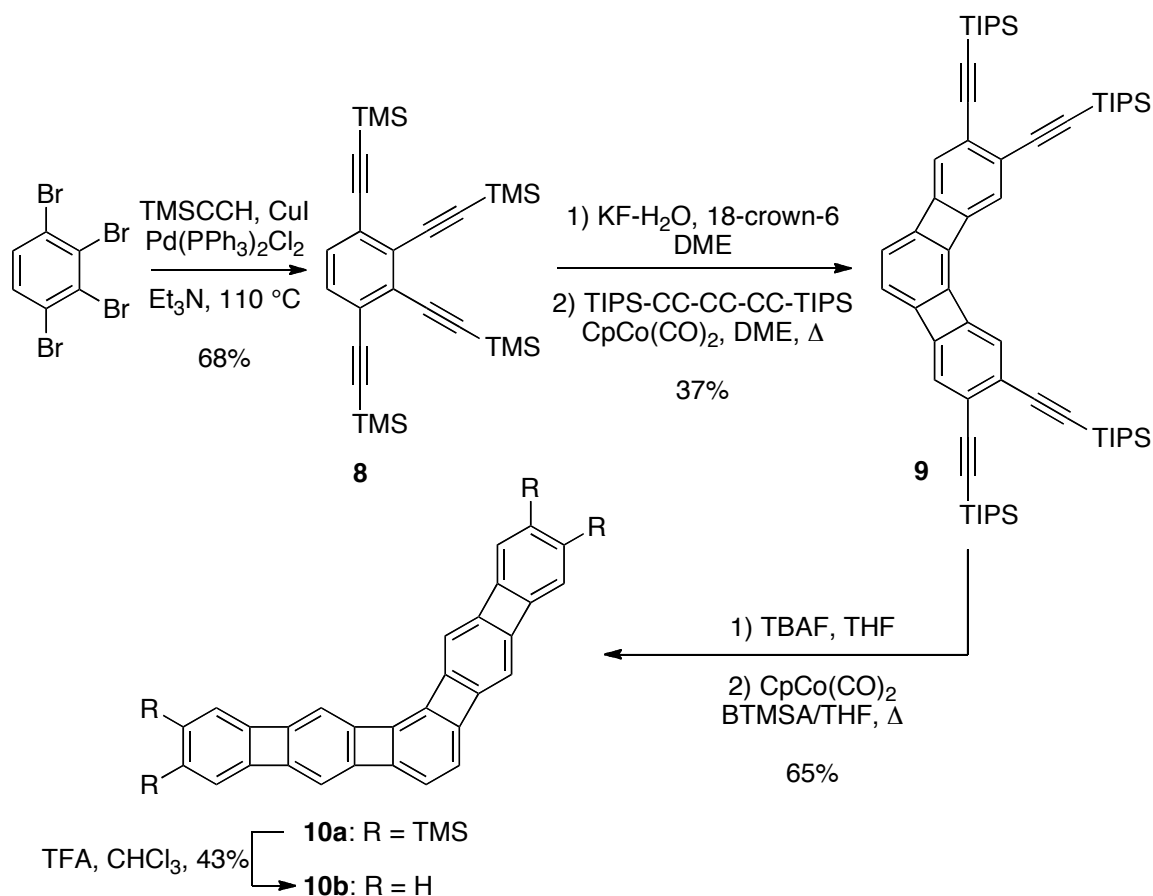
Sonogashira couplings of the appropriately substituted 1,2,4,5-tetrahalobenzene, followed by intramolecular [2 + 2 + 2] cyclization.



Scheme 1.2. Synthesis of (a) bent [4]Phenylene (**2a**) and (b) **2b**. Synthesis of (c) *anti* (**5**) and (d) *syn* double bent [5]phenylene (**6**). For **5a** and **7a**: (i) (1) $\text{CpCo(C}_2\text{H}_4)_2$, THF, $-25\text{ } ^\circ\text{C}$ (2) 1,3-cyclohexadiene, THF, $110\text{ } ^\circ\text{C}$. For **5b** and **7b**: (i) CpCo(CO)_2 , *m*-xylene, hv, Δ . ^aBTMSA = bis-(trimethylsilyl)acetylene.

The simpler singly bent [5]phenylene **10** is also available through a somewhat different route (Scheme 1.3).¹⁷ In this case, tetrayne **8** was synthesized *via* a four-fold Sonogashira coupling of 1,2,3,4-tetrabromobenzene with trimethylsilylacetylene. Compound **8** was then

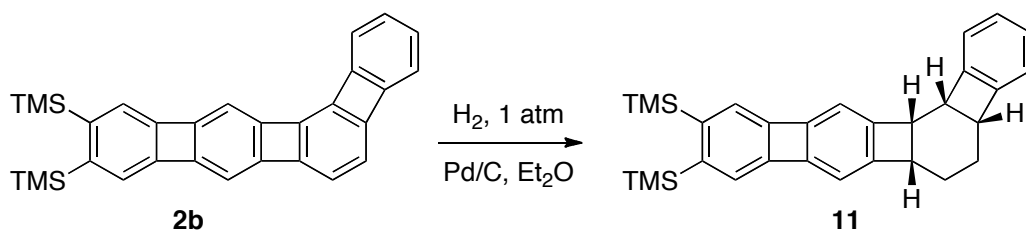
deprotected *in situ* followed by a twofold [2 + 2 + 2] cyclization with bis(triisopropylsilyl)-protected 1,3,5-hexatriyne to give angular [3]phenylene-containing tetrayne **9**. A second twofold [2 + 2 + 2] with bis(trimethylsilyl)acetylene (BTMSA) and deprotection yielded **10b**. All the bent [5]phenylenes were air-sensitive, and the parent hydrocarbons (**5a**, **7a**, and **10a**) were relatively insoluble.



Scheme 1.3. Synthesis of singly bent [5]phenylene **10**.

The aromaticity of the reported [4]- and [5]phenylenes was examined using a number of criteria. For **2**, shielding of the protons bound to ring C relative to those on ring B confirm the increased cyclohexatrienic character of the former and benzenoid character of the latter.¹⁵ As shown in Scheme 1.4, ring C of compound **2b** can be all *cis*-hexahydrogenated, proving it to be

the most activated. This is comparable to the reactivity of the central ring in angular [3]phenylene.⁸ In the case of **7a**, deshielding of ring B protons is even more pronounced than in **2a** especially in the bay region, however chemical shifts of the ring C protons are comparable.¹⁶ The same pattern is seen in comparing the calculated NICS (Nucleus Independent Chemical Shifts) values from **2a** and **7a**: the diatropicity of ring B increases from NICS = -6.4 to NICS = -7.5, whereas for ring C NICS = -2.9 in each case. In **10b**, there is even greater shielding of ring C protons, which is again consistent with decreasing diatropicity of NICS = -2.5 for that ring.¹⁷



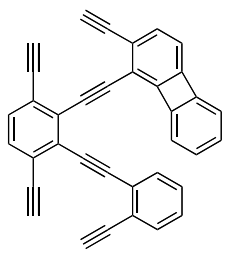
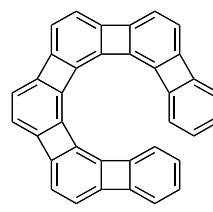
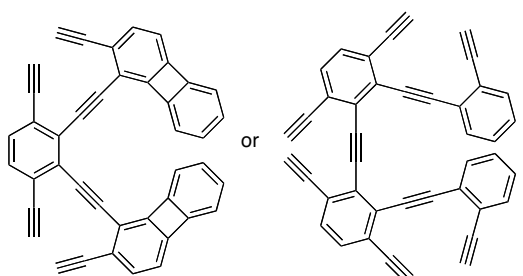
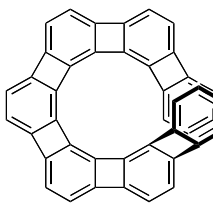
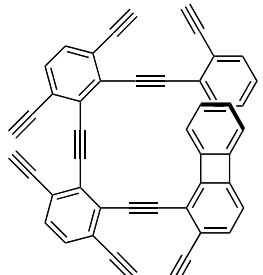
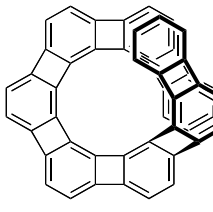
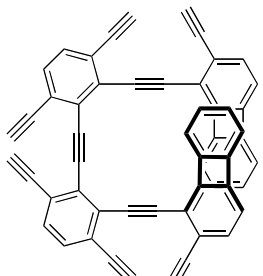
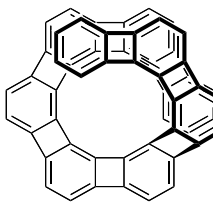
Scheme 1.4. Hexahydrogenation of ring C of **2b**.

The longer angular [N]phenylenes are of both experimental and theoretical interest, becoming helical with $N > 5$ and referred to as [N]heliphenes.¹⁸ Syntheses of angular [6]-[9]phenylenes were reported in 2002.¹⁹ In each case the [N]heliphene was accessed by a two- or threefold [2 + 2 + 2] cycloaddition of the appropriate ethynyl precursor as outlined in the Table 1.1. Heliphenes **12** and **13** are stable in the solid state while **14** and **15** are only moderately so.

The ¹H NMR spectra of these compounds are consistent with the pattern seen in lower angular phenylenes.^{13b,20} The terminal benzenoid rings are the most aromatic, having the most deshielded protons, whereas the penultimate ring has the most shielded protons and therefore the most cyclohexatrienic character.¹⁹ In the case of heliphenes **13-15** where the termini begin to overlap only those protons lying over the terminal (aromatic) ring are shielded. The protons that

reside over the penultimate ring are actually slightly deshielded. Crystal structures demonstrating the helical turn and overlapping termini of heliphenes **12** through **14** are shown in Figure 1.3

Table 1.1. Synthesis of [N]heliphenes (N = 6-9). Conditions: CpCo(CO)₂, *m*-xylene, hv, Δ.

Precursor	[N]Heliphene	Name and Yield
		[6]Heliphene (12), 12%
		[7]Heliphene (13), 8% or 2%
		[8]Heliphene (14), 2%
		[9]Heliphene (15), 2%

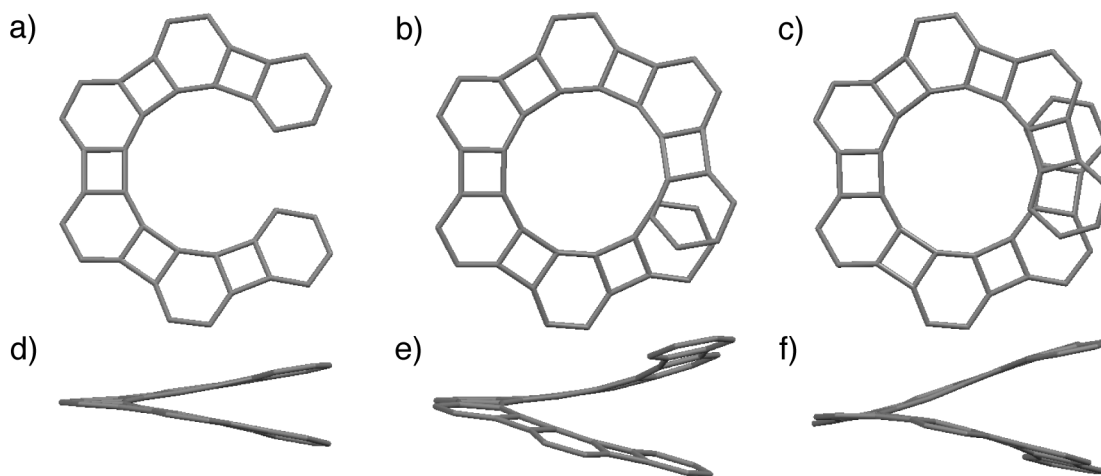
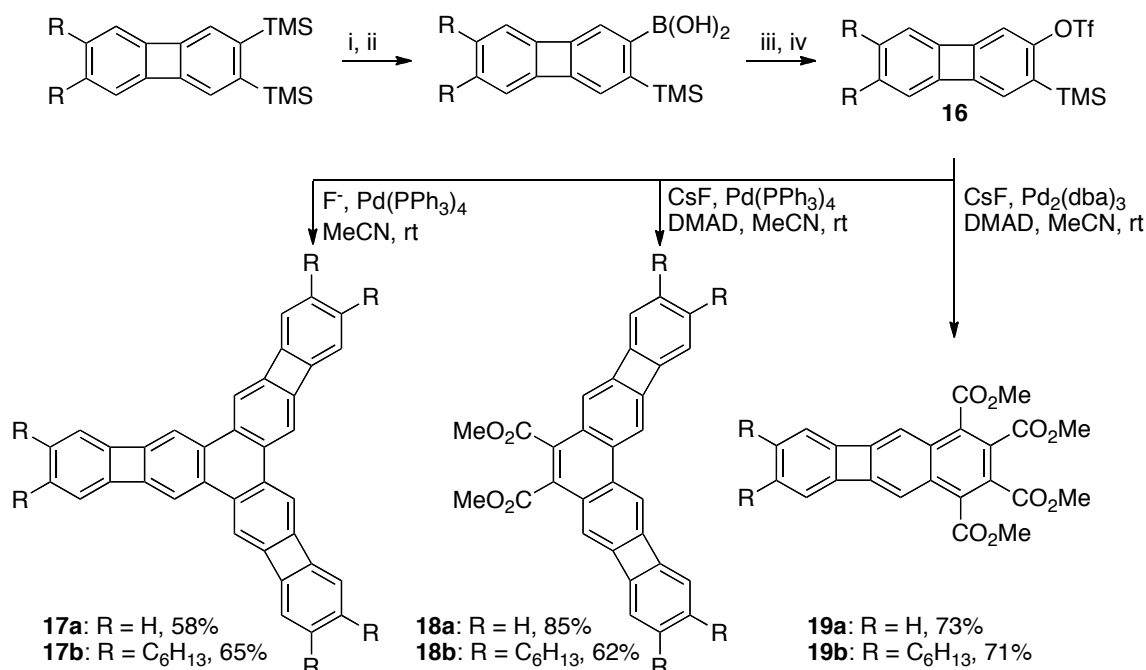


Figure 1.3. X-Ray crystal structures: (a) Front and (d) side views of **12**, (b) front and (e) side views of **13**, and (c) front and (f) side views of **14**. Crystal structure data from ref. 19a and ref. 19b was gathered from the Cambridge Structural Database (CSD).

Fewer reports have focused on the development of synthetic methods to access materials containing aromatic segments larger than one benzene ring. Taking advantage of the ability of palladium to catalyze the [2 + 2 + 2] cycloaddition of aryne, the synthesis of tris(benzocyclobutadieno)triphenylene **17** and related phenylene-containing PAHs, **18-19**, was reported.²¹ Key to this strategy was the synthesis of a 2,3-dehydrobiphenylene precursor **16** from 2,3-bis(trimethylsilyl)biphenylene as demonstrated in Scheme 1.5. The aryne was then generated by addition of the fluoride ion and followed by either trimerization to give **17** or cyclization with dimethylacetylene dicarboxylate (DMAD) and the appropriate Pd(0) source to give **18** or **19**.



Scheme 1.5. Pd-catalyzed cyclization of 2,3-dehydrobiphenylene derivatives. Conditions: (i) NBS, AgNO₃, acetone, rt, (ii) (1) BuLi, THF, -78 °C, (2) B(OMe)₃, -78 °C, (3) HCl (1 M), (iii) oxone, NaHCO₃(aq), acetone-H₂O, 0 °C, (iv) DIPEA, TF₂O, CH₂Cl₂, -78 °C. The source of F⁻ is TBAF for **17a** and CsF for **17b**.

1.4 Photophysical Properties of [N]Phenylenes

Examination of photophysical properties of [N]phenylenes of a variety of topologies can also be useful in probing relative levels of conjugation within each chromophore. Consistent with the earlier discussion of relative resonance energies, calculations predict larger HOMO-LUMO gaps for zigzag [N]phenylenes than for the linear isomer due to increased bond alternation.²²

The photophysical behavior of biphenylene (**20**) and both the linear (**21**) and angular (**22**) isomers of [3]phenylene were well-studied prior to the scope of this review, however this foundation is important for understanding properties observed in longer isomers. Biphenylene is only weakly fluorescent ($\phi_F = 2 \times 10^{-4}$),²³ and only low levels of triplet state population are observed upon direction excitation ($\phi_{ISC} < 10^{-2}$).²⁴

The values corresponding to the energy of S_1 - S_0 transition in compounds **20-22** as well as zigzag [4]- (**23**) and [5]phenylene (**24**), and triangular [4]phenylene (**25**, Figure 1.4) are summarized in Table 1.2.²² The bathochromic shift in energy going from **20** to linear **21** is much larger (0.87 eV) than that from **20** to angular **22** (0.13 eV). The rapidly decreasing band gap with linear annulation is consistent with the prediction that linear [N]phenylenes of infinite length could serve as conductive organic wires.^{13c} Interestingly, angular [3]phenylene is emissive while linear [3]phenylene is not. The band gap decreases with angular extension of the [N]phenylene going from **22-24** but at a much slower rate.

The larger [N]phenylenes **23-25** have very small Stokes shifts (65-150 cm^{-1}) as compared to both **22** (750 cm^{-1}) and **20** (4750 cm^{-1}) indicating a more rigid structure in which the geometry does not change much in going from S_0 to S_1 .²² This data together with increased fluorescence quantum yields indicate slower rates of internal conversion for these species. As indicated in Table 1.2, the zigzag [N]phenylenes, **22-24** undergo intersystem crossing (ISC) fairly efficiently with ISC quantum yields ranging from 25-45%. Therefore this process is a likely contributor to the deactivation of the S_1 state. However, this is not the case for **20** and **21** for which energy is presumably lost *via* fast internal conversion.

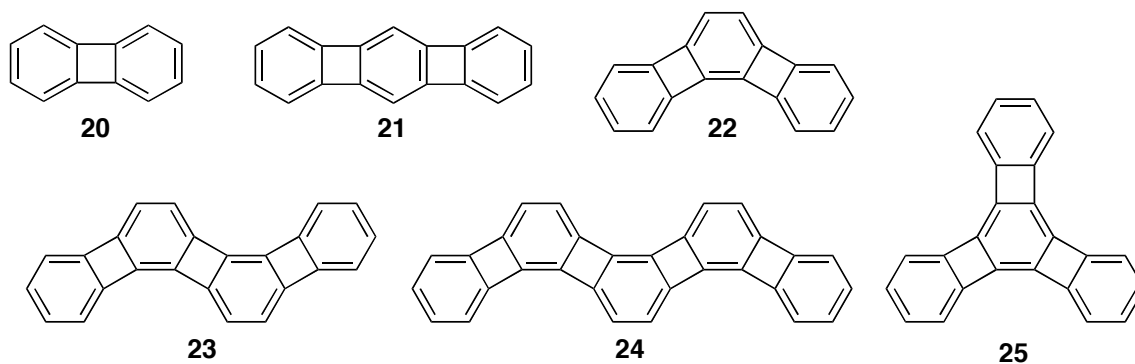


Figure 1.4. Structure of [N]phenylenes **20-25**.

Table 1.2. Photophysical properties of [N]phenylenes in THF.

Compound	E(S ₁) (eV)	Stokes shift (cm ⁻¹)	φ _F	φ _{ISC}
20	2.98	4750	2.6 × 10 ⁻⁴	< 0.01
21	2.11	–	< 10 ⁻⁴	< 0.01
22	2.85	750	0.07	0.30
23	2.66	70	0.12	0.25
24	2.57	65	0.21	0.45
25	2.81	150	0.15	0.03

An interesting pattern also emerges in examination of the band gap (estimated from the lowest energy absorption) of the bent [N]phenylene derivatives discussed in the previous section (Table 1.3). The lowest energy absorptions of linear 2,3-bis(trimethylsilyl)-[4]phenylene²⁵ (**26**) and 2,3,9,10-tetrakis(trimethylsilyl)-[5]phenylene²⁶ (**27**, Figure 1.5) are also included in Table 1.3 for comparison. Bent [4]phenylene **2a**, has almost the same lowest energy λ_{max} as its linear counterpart,¹⁵ as does singly bent [5]phenylene **10b**.¹⁷ The λ_{max} of doublebent [5]phenylene **5a**, on the other hand, lies in between that of the linear **27** and the higher energy absorption of other known isomers including zigzag (see above).¹⁶ From examination of this data, it appears that the first angular ring annelation has a stronger effect on the band gap than does a second.

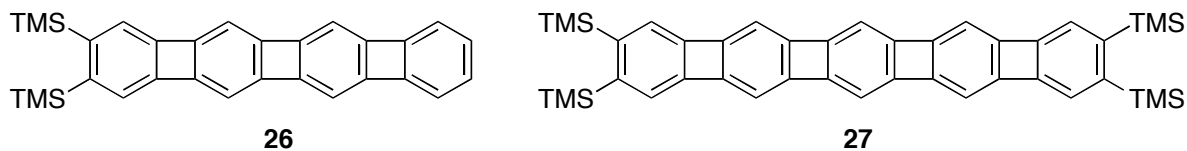
**Figure 1.5.** Structures of [N]Phenylenes **26** and **27**.

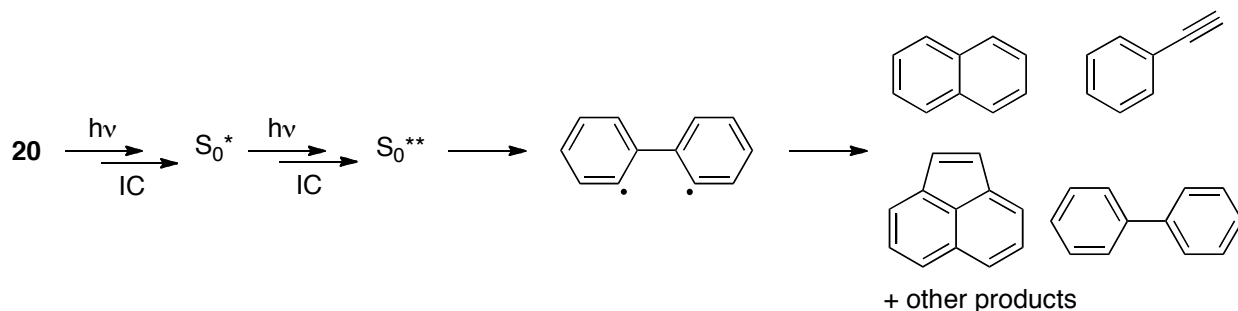
Table 1.3. Lowest energy λ_{\max} for selected [4]- and [5]phenylenes.

Compound	Lowest E λ_{\max} (nm)	E_g (eV)
2a	486	2.55
26	488	2.54
5a	505	2.46
10b	523	2.37
27	530	2.34

The lowest energy λ_{\max} of the heliophenes also increases with length as expected.¹⁹ The bathochromic shift decreases in going from **12** to **13** (12 nm), **13** to **14** (10 nm) **14** to **15** (9 nm). A plot of λ_{\max} versus $1/(N+0.5)$ provides a straight line that can be extrapolated to 578 nm, possibly indicating the theoretical band gap of polyheliophene.

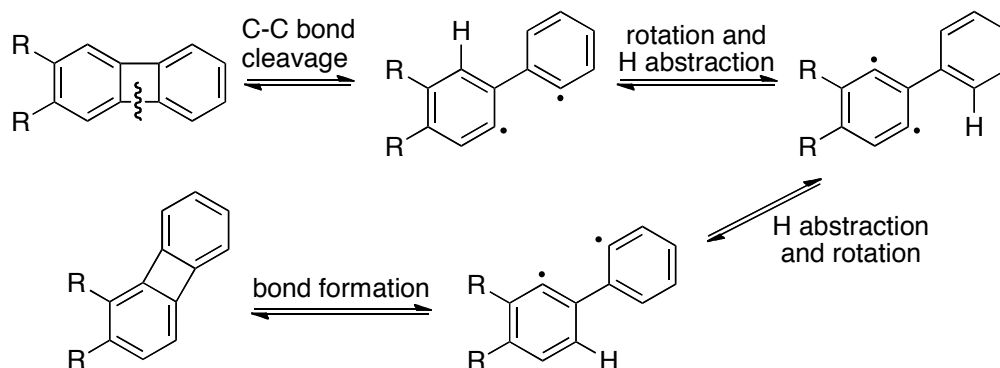
1.5 Reactivity of [N]Phenylenes and Related Materials

Biphenylene (**20**) was long believed to be photoinert, however evidence of high internal conversion rates indicated that the picture is more complex.²⁷ Transient absorption measurements of **20** indicate the formation of an initial, vibrationally hot ground state S_0^* formed by internal conversion, followed by chemical reaction to form stable products. Correlation between the transient absorbance and laser influence data suggest that hot biphenylene must absorb a second photon to become chemically reactive, further raising its internal energy to compete with collisional deactivation. Several photo-products were identified including phenylacetylene, biphenyl, naphthalene, and acenaphthylene as well as three unknown. The authors suggest a mechanism involving initial C—C bond cleavage to form the 2,2-biphenyl biradical (Scheme 1.6).



Scheme 1.6. Proposed mechanism of two-photon photoreactivity of **20**.

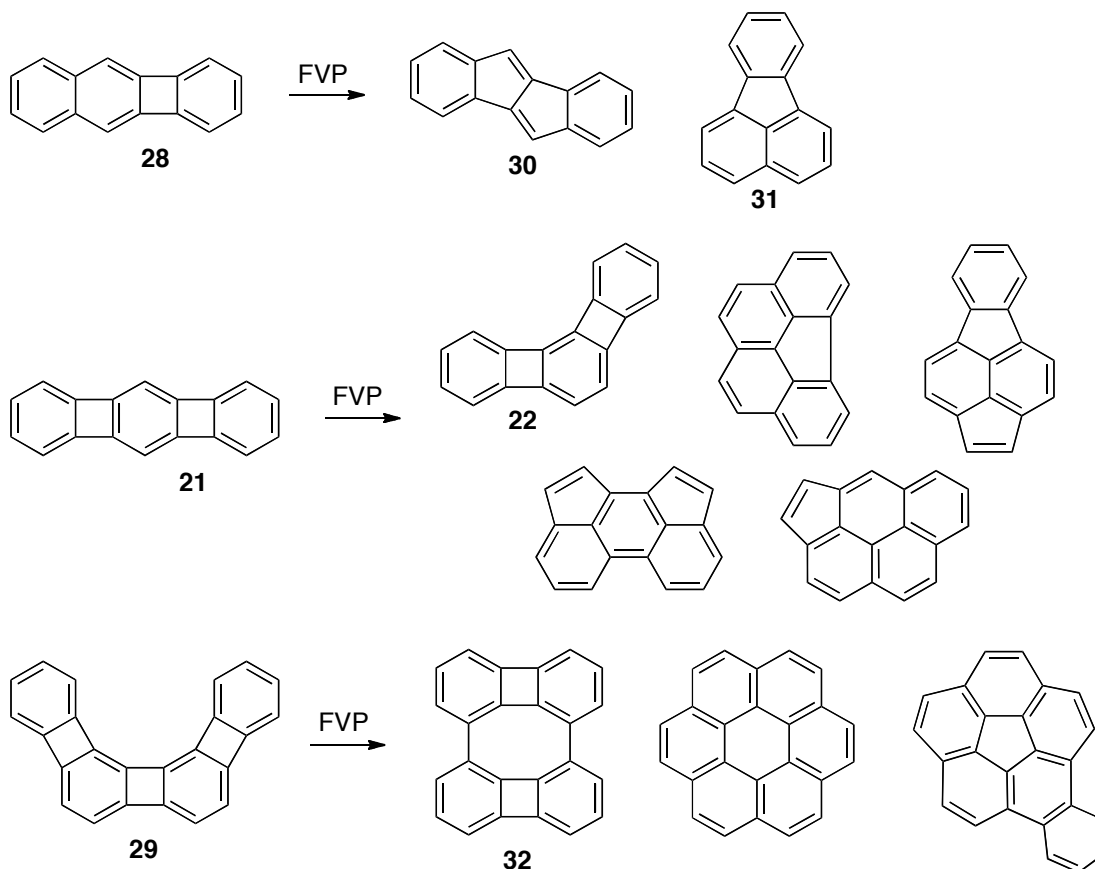
Work reported in the early 1990's showed that benzo[*a*]pentalene is produced as an intermediate in the Flash Vacuum Pyrolysis (FVP) of biphenylene, further rearrangement leading to acenaphthylene as the major product.²⁸ The driving force of this skeletal rearrangement is believed to be the relief of strain in the four-membered ring. More recently, however, several groups have revealed another mechanistic pathway involved in rearrangements of larger PAHs containing the phenylene-linkage.²⁹ Phenyl groups are able to migrate by a process in which C—C bond cleavage occurs as described above, followed by several 1,5- or 1,6-hydrogen transfers, and ring closure at a new position and so on (Scheme 1.7).



Scheme 1.7. Mechanism of phenyl group migration in FVP of phenylene-containing PAHs.

Together, the above mechanism and ring contraction/expansion to relieve strain can be used to explain most of the products obtained from FVP of phenylene-containing materials. The

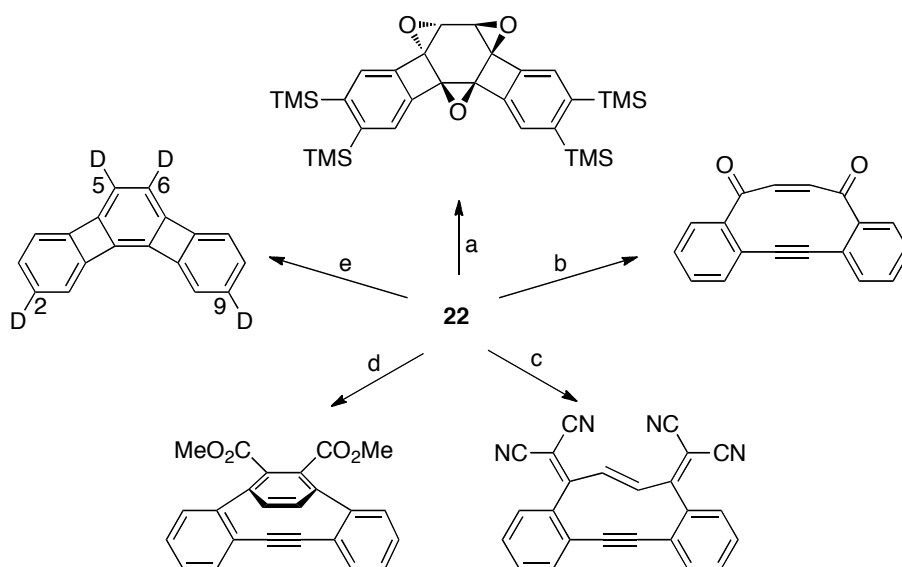
major products obtained from FVP of benzo[*b*]biphenylene (**28**), linear [3]phenylene (**21**) and angular [4]phenylene (**29**) are summarized in Scheme 1.8. Scott and coworkers investigated the FVP of **28** which resulted in two major products: dibenzo[*a,e*]pentalene (**30**) from benzene ring contraction, and fluoranthene (**31**) from phenyl migration.^{29a} Vollhardt and coworkers showed that FVP of **21** resulted in four major PAH products (the same four products as FVP of angular [3]phenylene **22**)³⁰ as well as 1% of **22**.^{29b} The conversion of **21** to **22** clearly occurs through the phenyl migration mechanism, whereas the other PAH products appear to result from various benzene ring contraction rearrangements of **22** once it has formed. Finally, **29** is converted to the major product biphenylene dimer **32**, by a mechanism similar to phenyl migration, as well as two additional PAHs.^{29c}



Scheme 1.8. FVP of **28**, **21**, and **29**.

As mentioned previously, it has been shown that angular annulation causes greater bond alternation and decreased diatropicity in the benzene ring at the bend (ring C, Schemes 1.2 and 1.3), increasing the reactivity of those double bonds. In addition to hydrogenation as shown in Scheme 1.4, it has been demonstrated that the central benzene ring in angular [3]phenylene (**22**) is susceptible to a number of reactions (Scheme 1.9).³¹ All three double bonds in the central ring of 2,3,8,9-tetrakis(trimethylsilyl)-substituted **22** underwent epoxidation (Scheme 1.9a) analogously to the reactivity of triangular [4]phenylene (**25**).³² Epoxidation of the unsubstituted **22**, however only proceeded twice leaving the bay region double bond unreacted.³¹ The diene composed of the more reactive double bonds underwent [4 + 2] cycloadditions with singlet oxygen (¹O₂), tetracyanoethylene (TCNE), and DMAD, followed by a second electrocyclic reaction to give the product shown (Scheme 1.9b-d).

Lastly, the deuteration of **22** was attempted in order to examine more generally its reactivity towards electrophiles. Biphenylene^{10a} and **25**³³ both undergo deuteration exclusively at the β position (C2/9). However, for **22** deuteration occurs preferentially at the α position (C5/6) and then secondarily at the β position under harsher conditions (Scheme 1.9e).³¹ Calculations (HF/6-31G*) of the protonated intermediates indicated that attack at C5/6 results in the fewest resonance forms with cyclobutadienoid character. Additionally, this reactivity trend corresponds to the relative size of the HOMO coefficients (HF/STO-3G) at those positions.



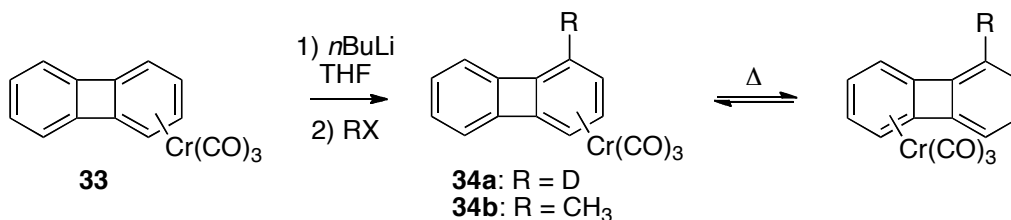
Scheme 1.9. Reactivity of **22**. Conditions: (a) using 2,3,8,9-tetrakis(trimethylsilyl)-**22** as the starting material, dimethyldioxirane (DMDO), acetone, 26% (b) methylene blue (0.9 eq), O₂, CH₂Cl₂, hv, 70% (c) TCNE (1 eq), CH₃CN, Δ, 78% (d) DMAD (1.6 eq), AlCl₃ (0.1 eq), PhCH₃, 74% (e) (1) CF₃CO₂D, CDCl₃, 60 °C, 80% (2) CF₃CO₂D, CDCl₃, 100 °C, 82%.

1.6 Applications of Phenylene-Containing Materials

There is a fair amount of interest in the effect of incorporating antiaromatic moieties into systems that normally rely on aromatics to perform a function. In these cases, biphenylene is often turned to as a stable substitute for cyclobutadiene. Previous work has clearly demonstrated that this scaffold is not purely antiaromatic, however the model systems have had some informative results.

In several cases, π -complexes of [N]phenylenes have been shown to undergo intramolecular inter-ring haptotropic rearrangements (IRHR). Depending on the metal and ligand, the metal atom migrates between either benzene (η^6 - η^6)³⁴ or cyclobutadiene (η^4 - η^4)³⁵ ligands. In both the η^6 - η^6 and η^4 - η^4 cases of IRHR in [N]phenylenes, DFT calculations show that the migration occurs through a mechanism in which the metal atom “walks” the periphery of the PAH.

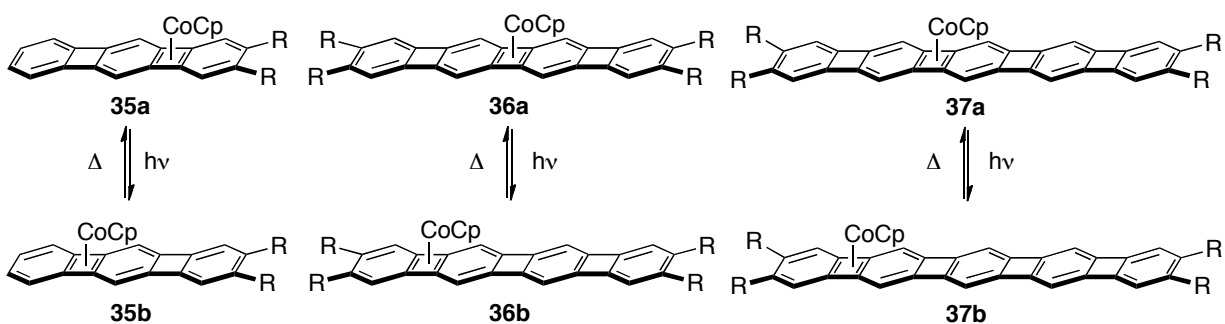
In the case of the former, the mono-chromium tricarbonyl $[\text{Cr}(\text{CO})_3]$ complex of biphenylene **33** can be selectively lithiated on the complexed benzene ring and subsequently substituted with an electrophile to give two non-degenerate ligand sites on biphenylenes **34a/b** (Scheme 1.10).³⁴ The equilibria of IRHR of these species were studied by NMR at 130 °C. Whereas **34a** equilibrated to a ratio of 1:1 of the two ligand sites after about 20 hours, decomposition of the complex competed with IRHR in **34b** and after 56 hours equilibrium had still not been reached. The activation for IRHR in **34a** was determined to be 32.2 kcal mol⁻¹, which expectedly lies between the analogous values in naphthalene (28.5 kcal mol⁻¹) and biphenyl (35.1 kcal mol⁻¹).



Scheme 1.10. Synthesis of unsymmetric, substituted η^6 -Cr(CO)₃-complexes of biphenylene.

More recently it has been shown that cyclobutadiene-metal complexes of the longer linear [N]phenylenes can undergo photo-thermal reversible IRHR.³⁵ Systems such as these have potential for a variety of applications including solar energy storage and switches. The cyclopentadienyl-cobalt {CpCo} complexes of substituted linear [3]-, [4]-, and [5]phenylenes can be isolated directly from the [2 + 2 + 2] cycloaddition of the appropriate precursor with BTMSA, under modified conditions employing stoichiometric [CpCo(CO)₂] and THF as a co-solvent. As indicated by deshielding in the NMR and calculated NICS values, complexation of {CpCo} has an aromatizing effect on the entire PAH, however most strongly on the metal-bound cyclobutadiene ring.

When irradiated with light, [N]phenylene complexes **35-37a** under go IRHR to give the higher energy haptomer **35-37b** (Scheme 1.11) reaching a photostationary state as indicated in Table 1.4. The calculated heat of activations for the thermal reversal of the unsubstituted [N]phenylenes are all very close in value, around 27 kcal mol⁻¹. However, the exothermicity increases going down the series from [3]-[5]phenylene. This trend can be attributed to the decreasing HOMO-LUMO gap and increasing antiaromaticity along the series, which result in stronger {CpCo} bonds.



Scheme 1.11. Photo-thermal IRHR of η^4 -CpCo-complexed linear [N]phenylenes, for **35** and **36** R = TMS, for **37** R = H or TMS.

Table 1.4. Photostationary state of IRHR of [N]phenylenes **35-37**. Irradiated with ^a350 nm lamp, ^b310 + 365 nm lamp. ^cCalculated values for R = H in kcal mol⁻¹.

[N]phenylene-CpCo	Haptomer a	Haptomer b	$\Delta H^{\neq(c)}$	ΔH^c
35^a	1	1	26.9	0
36^a	1	2	27.1	-7.6
37^b	7	3	27.3	-9.7

The π -stacking interaction of aromatic materials in the solid state is a key variable to consider in achieving high charge mobilities for electronic applications. The [2.2]paracyclophane motif, with an inter-ring distance shorter than the 3.4 Å necessary for effective π -stacking, has

been a useful tool for investigating the effects of stacking on the optoelectronic properties.³⁶ In 2005 Leung and coworkers synthesized *anti*-[2.2]-(1,4)-biphenylenophane (**38**), employing the biphenylene framework to investigate the phane properties of antiaromatics (Figure 1.6). An X-ray crystal structure of **38** confirmed the *anti* relationship of the biphenylene rings. The inter-ring distance of 3.09 Å is identical to that of the parent [2.2]paracyclophane (**39**), however the ethano C—C bridge in **38** is significantly shorter likely due to the increased flexibility of biphenylene.³⁷ Additional thermal stability is imparted to **38** by a decrease in the strain of this bond.

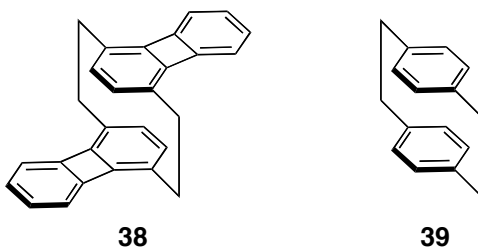


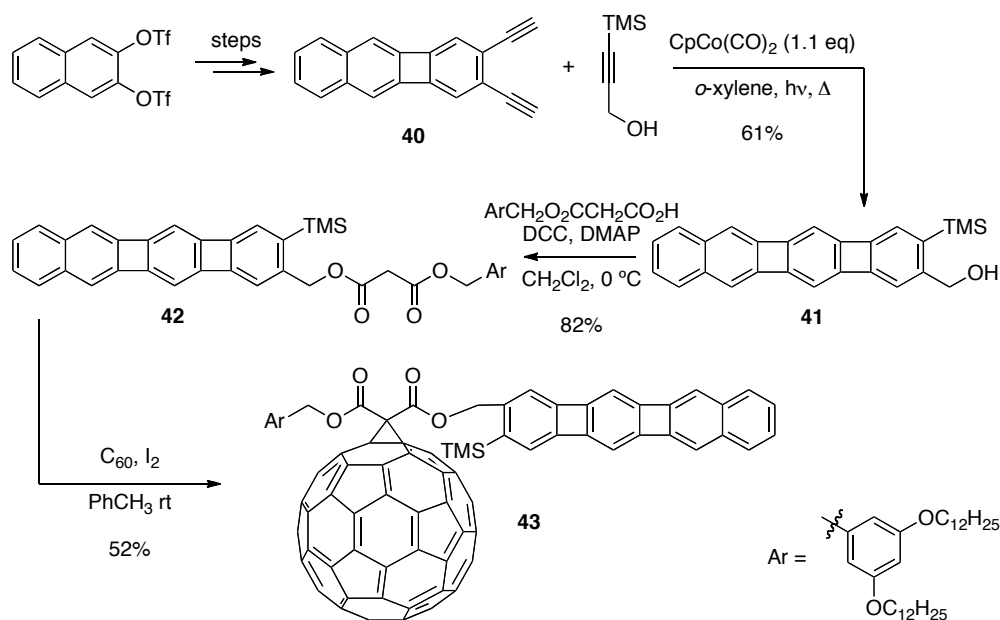
Figure 1.6. Structures of *anti*-[2.2]-(1,4)-biphenylenophane **38** and [2.2]paracyclophane **39**.

The photophysical properties of **38** as compared to those of biphenylene **20** and the electrochemical properties of **38** as compared to **20** and **39** are summarized in Table 1.5.³⁶ A bathochromic shift and spectral broadening in going from **20** to **38** is consistent with ground-state interactions between the biphenylene units in the cyclophane. Since the Stokes shifts in **38** and **20** are similar, it is difficult to determine whether or not emission in **38** is the result of an excimer-like phane-state. However, the authors suggest that the longer lifetime of **38** implies participation of the phane state. Cyclophane **38** is more easily oxidized than both **39** and **20**.

Table 1.5. Photophysical and electrochemical properties of **38**, **39**, and **20**.

Compound	Lowest E λ_{\max} (nm)	λ_{em} (nm)	τ (ps)	E _{ox} (V vs. Ag/Ag ⁺)
38	378	537	229	1.37, 1.55
39	-	-	-	1.59
20	359	518	194	1.72

To investigate the use of [N]phenylenes for photovoltaic applications, the synthesis of linear benzo[3]phenylene-C₆₀ dyad **43** was reported in 2005.³⁸ The synthesis employed iterative Co-catalyzed [2 + 2 + 2] cyclizations, using 3-trimethylsilylpropargyl alcohol to install a tether in the final cyclization to yield **41** (Scheme 1.12). Lastly, diester **42** was reacted with C₆₀ using the Bingel conditions³⁹ to give the desired dyad. The absorbance spectrum of dyad **43** closely resembles the sum of its constituents, signifying that there are not significant ground state interactions between the [N]phenylene and fullerene which could otherwise inhibit charge separation.

**Scheme 1.12.** Synthesis of benzo[3]phenylene-C₆₀ dyad **43**.

As with other linear [3]phenylenes, **41** and **42** are reportedly not fluorescent. This is likely due to high rates of internal conversion, which would indicate that this particular dyad is not a good candidate for photovoltaic applications.⁴⁰ This led researchers to investigate the photoinduced electron transfer of angular phenylenes, with much slower rates of internal conversion, in dyads. The fluorescence and quantum yield of triangular [4]phenylene dyad **44** (Figure 1.7) displays a solvent polarity dependence characteristic of intramolecular charge transfer, however levels of the charge-transfer complex are low at equilibrium.

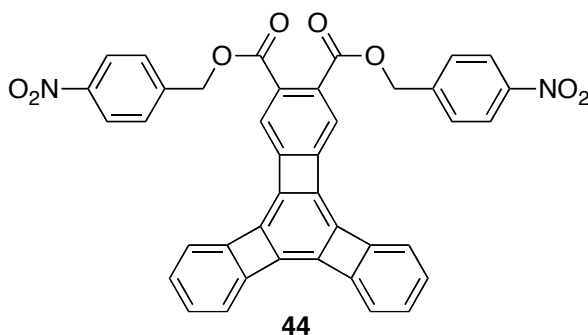
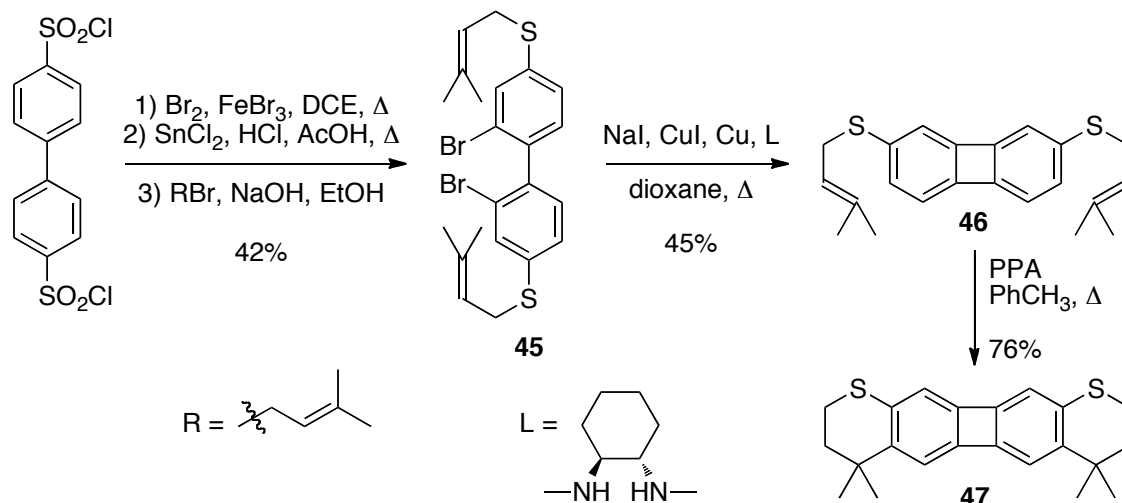


Figure 1.7. Triangular [4]phenylene dyad **44**.

The small HOMO-LUMO gap of antiaromatics led researchers to investigate the use of biphenylene as a molecular wire in a single molecule device.⁴¹ Research on single molecule devices made from acenes has shown that increasing conductivity can be correlated to decreasing HOMO-LUMO gap and increasing quinoidal stability.⁴² Thioether-substituted biphenylene **47** was synthesized according to the procedure outline in Scheme 1.13 and its conductance compared with that of fluorenes **48** and **49** (Figure 1.8).⁴¹ The essential biphenylene-forming reaction was achieved by Ullman coupling of the 2,2-dibromobiaryl **45**. Acidic cyclization of **46** is completely regioselective at the β position to give **47**, as cyclization at the α position would involve a carbocation cation intermediate with greater cyclobutadiene character.



Scheme 1.13. Synthesis of thioether-substituted biphenylene **47**.

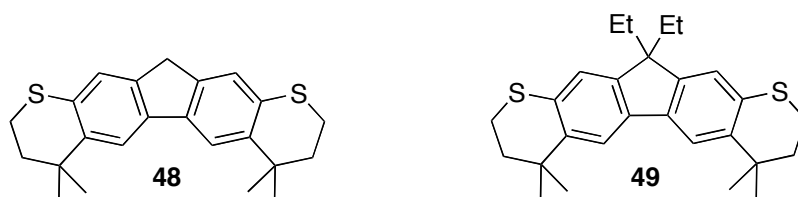


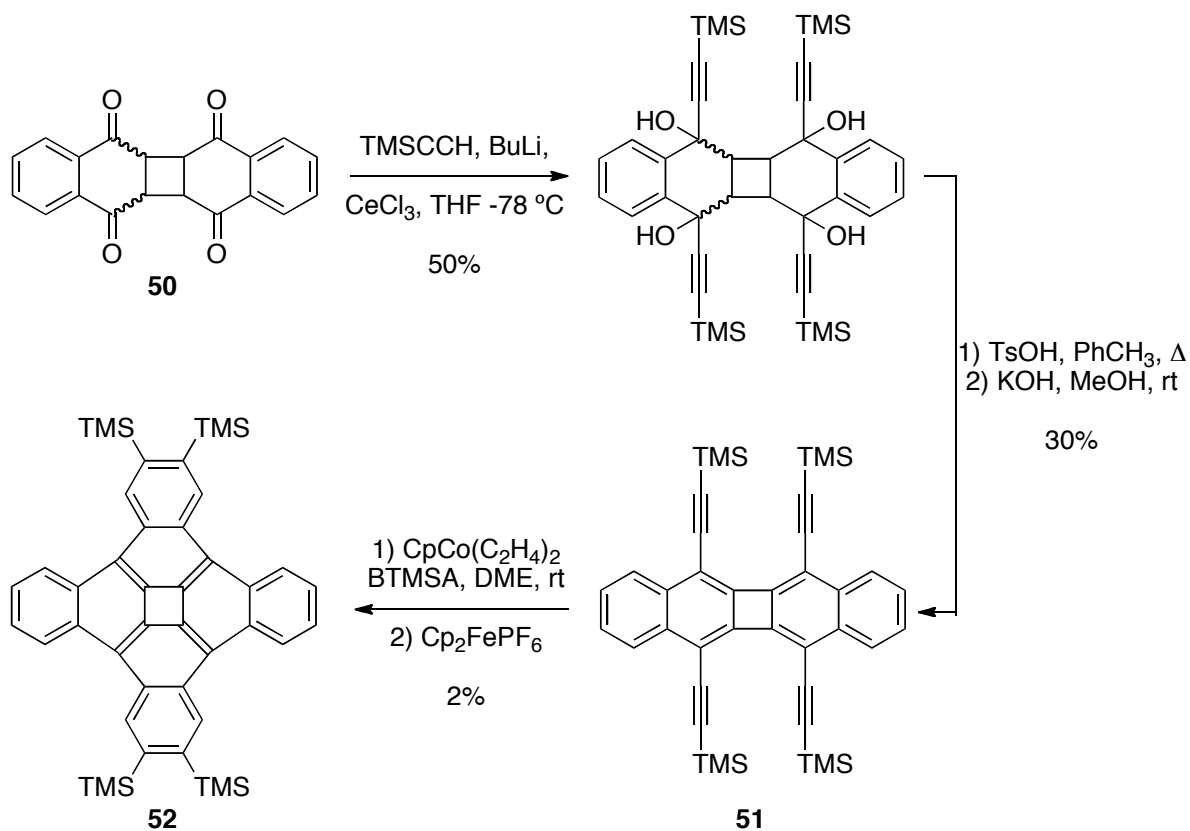
Figure 1.8. Thioether-substituted fluorenes **48** and **49**.

The conductances of compounds **47-49** were measured using a scanning tunnel microscope (STM) based break-junction technique. Results from the conductance and first oxidation potentials are summarized in Table 1.6. Surprisingly, although biphenylene **47** is more easily oxidized than the fluorene analogues, decreasing oxidation potential did not seem to correlate with increasing conductivity. These results reflect the complexities of materials designs and difficulties in translating molecular properties to solid-state and device properties.

Table 1.6. Conductance and first oxidation potential of PAHs **47-49**.

Compound	Conductance ($G_0 \times 10^3$)	$E_{1/2}$ (V vs Ag/Ag ⁺)
47	3.6 ± 0.2	0.509
48	3.5 ± 0.3	0.633
48	4.4 ± 0.3	0.627

Nonbenzenoid rings in graphitic structures induce curvature, the most classic example being the twelve five-membered rings that allow the spherical shape of C₆₀. The [n]circulenes are a class of PAHs derived from the fusion of benzenoid rings to the corresponding [n]radialene frame.⁴³ The curvature and bowl-to-bowl inversion barrier of these materials is expected to increase with decreasing size of the central ring. The first synthesis of benzannulated [4]circulene, quadrannulene (**52**) was reported by King and coworkers in 2010.⁴⁴ The four-membered ring is derived from the photodimer of naphthoquinone (**50**, Scheme 1.14). The authors take advantage of the Co-catalyzed cyclotrimerization's well-established ability to form highly-strained rings to form the bridges in going from tetrayne **51** to **52**.



Scheme 1.14. Synthesis of quadrannulene **52**.

The X-ray crystal structure and calculated geometry (B3LYP/6-311G**) of **52** are shown in Figure 1.9. Calculated bond lengths and NICS value support the radialene-structure as depicted in Scheme 1.14, with ring A having a NICS value of 4.5 ppm. The bowl depth, the distance between the plane containing ring A and the plane formed by the eight atoms that fuse rings B and C, is 1.36 Å, significantly deeper than a depth of 0.87 Å for [5]circulene.

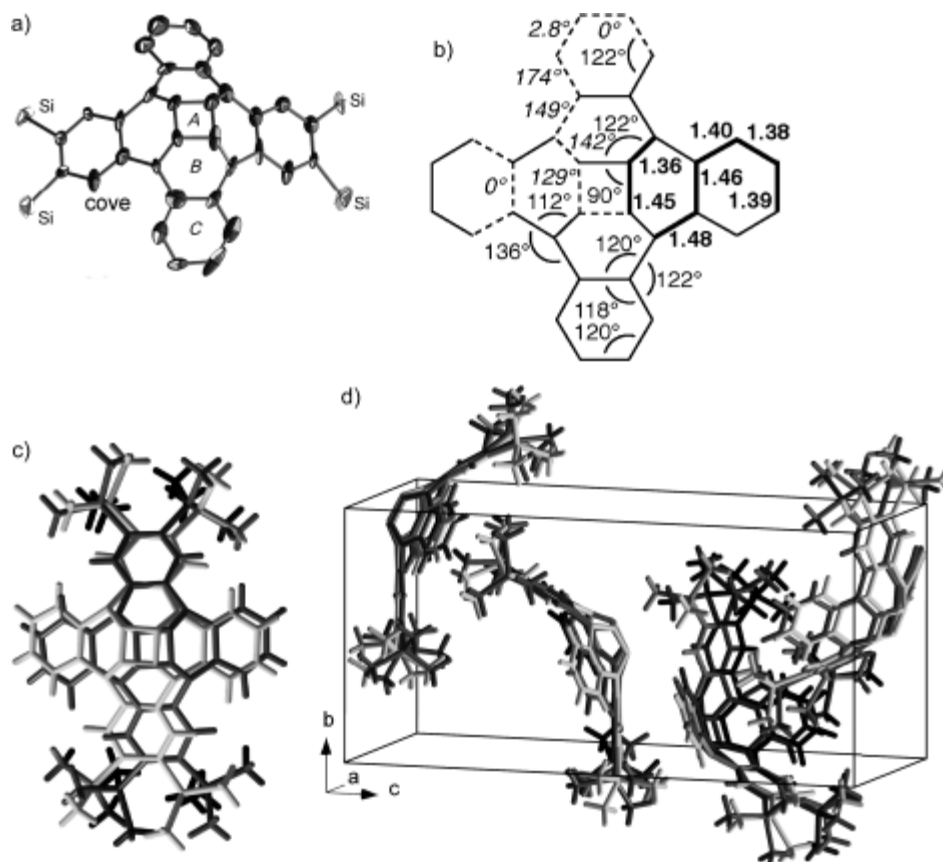


Figure 1.9. Structure of **52**: (a) X-ray crystal structure of major contributor (methyl groups and H atoms omitted for clarity) (b) Calculated geometry (c) Disorder in the crystal (d) Crystal packing. Reprinted with permission from ref. 44. Copyright 2009 John Wiley and Sons.

1.7 Polymeric and Graphitic [N]Phenylenes

Currently, ladder polymers and 2 or 3D graphitic materials containing phenylenes have mostly been an area of theoretical interest due to synthetic challenges. Inspired by the successful synthesis of the [N]heliphenes up to $N = 9$,¹⁹ calculations on the properties of even longer linear, angular, and helical phenylenes, of $N=14$, 19 and 24, were reported in 2003.⁴⁵ Notably, in each case the authors found that bond lengths and NICS value converge on the center most rings (Figure 1.10); the zigzag and helical topologies taking on increased bond alternation, while all bonds of the six-membered rings are nearly equal in the linear topology.

Despite the increase in bond alternation, isotropic magnetic susceptibility calculations indicate that the zigzag topology is the most aromatic followed closely by the helical analogue. For zigzag and helical topologies the terminal benzenoid ring is the most aromatic while the penultimate is the least, whereas for the linear case aromaticity decreases from the terminus towards the center. The four-membered rings in the linear topology are more antiaromatic than their zigzag and helical counterparts.

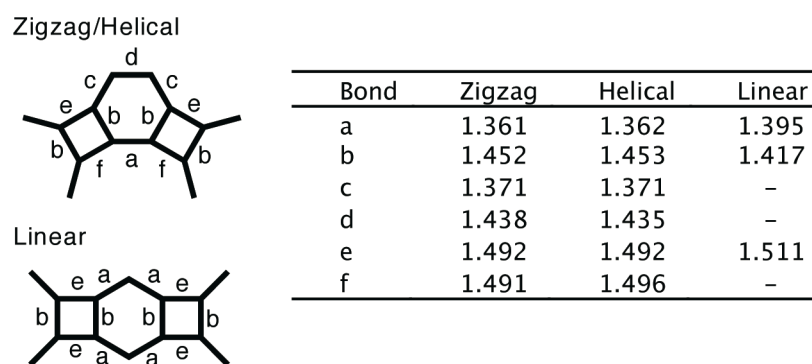


Figure 1.10. Convergent bond lengths in extended [N]phenylenes.

The polyhedral carbon allotrope containing phenylene units and a molecular formula of C_{120} is known as archimedene **53** (Figure 1.11).⁴⁶ *Ab initio* calculations were performed on **53** as well as eight related bowl-shaped hydrocarbons in 2005 by Schulman And Disch.⁴⁷ The resulting geometries are very consistent with what has been shown experimentally for angular and branched [N]phenylenes: the six-membered rings have significant bond alternation, 1.479 Å and 1.364 Å, and the four-membered rings are nearly square. NICS values for the six- and ten-membered rings are slightly negative, NICS = -1.9 and -0.2 respectively, while those of the four-membered ring are slightly positive, NICS = 3.2, indicating that the system is neither strongly aromatic nor antiaromatic.

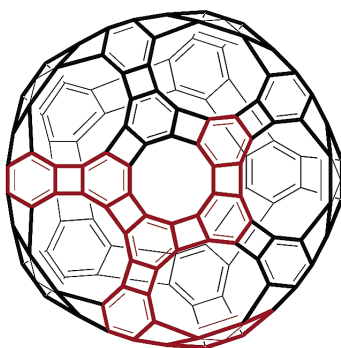
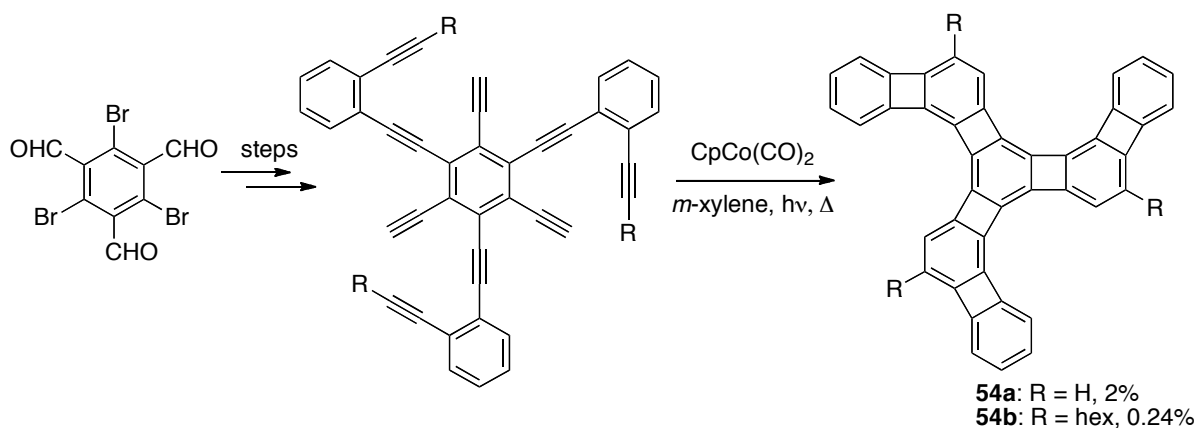


Figure 1.11. Archimedene **53**. Reprinted with permission from ref. 48. Copyright 2003 American Chemical Society.

Synthetic attempts towards **53** have so far focused on assembling smaller fragments. In 2003, Vollhardt and coworkers reported the synthesis of the C_{3h} -symmetric fragment [7]phenylene **54** (highlighted in red in Figure 1.11), by a threefold cyclotrimerization of the appropriate nonayne precursor (Scheme 1.15).⁴⁸ Unfortunately, insolubility prevented some NMR studies and X-ray analysis. However, DFT and NICS calculations of **54a** indicated that the central ring has greater diatropic character than the triangular [7]phenylene with linear arms.



Scheme 1.15. Threefold cyclotrimerization to give archimedene fragment **54**.

There is also interest in incorporating rings of different sizes into the standard C_{60} skeleton, in the hopes of creating new functional materials. Rubin and coworkers proposed a

conceptual approach for inserting a two-carbon fragment into fullerene to generate C_{62} in 2000 (Figure 1.12).^{49a} Attempts to isolate the parent hydrocarbon C_{62} were not successful, likely due to its predicted high reactivity. Therefore the authors turned to a related system that allowed them to access diaryl- C_{62} **55**.^{49b} The one-pot reaction commencing with the Diels-Alder reaction of diaryltetrazine and C_{60} , involves a sequence of electrocyclic reactions and the eventual extrusion of two equivalents of nitrogen gas (Scheme 1.16).

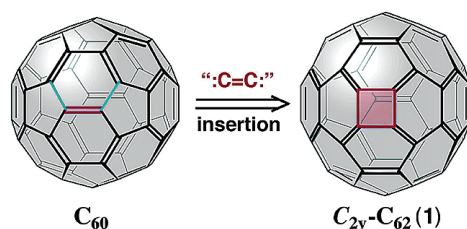
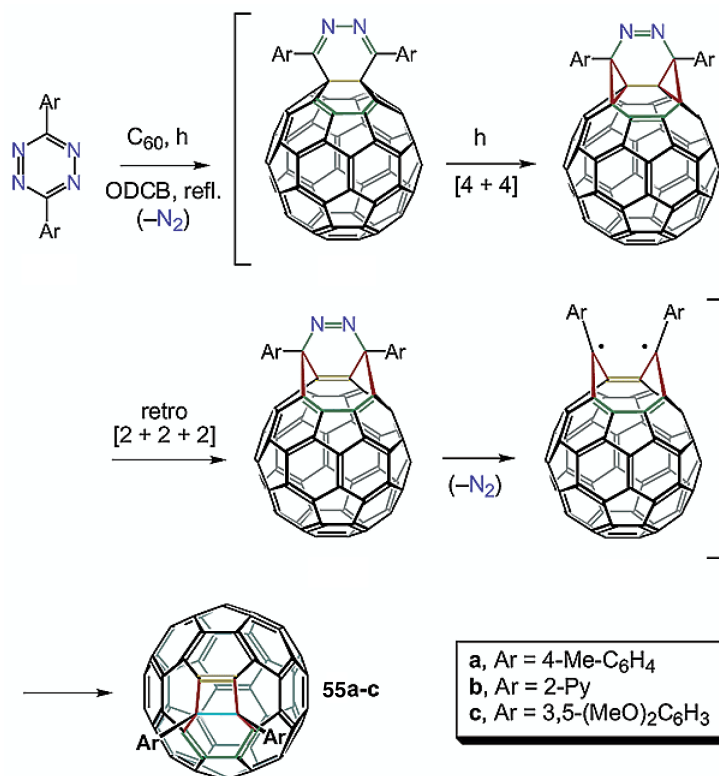


Figure 1.12. Insertion of 2-carbon fragment into C_{60} . Reprinted with permission from ref. 49b. Copyright 2003 American Chemical Society.



Scheme 1.16. One-pot synthesis of C_{62} analogue **55**. Adapted with permission from ref. 49b. Copyright 2003 American Chemical Society

Other graphitic materials containing phenylenes, such as nanoribbons, sheets, and nanotubes, can also be imagined and have been a subject of theoretical interest (Figure 1.13).⁵⁰ The biphenylene nanoribbons (BNR, Figure 1.13b) were dubbed either armchair or zigzag depending on the edge morphology, analogously to graphene nanoribbons (GNR). For the armchair BNR, calculations predict the bandgap will decrease monotonically with the width of the ribbon, whereas zigzag BNR are predicted to have metallic character for all but the narrowest ribbon. Spin-polarized calculations predict both edge configurations to be diamagnetic, unlike GNR for which the zigzag morphology is predicted to have interesting magnetic properties.⁵¹ Both armchair and zigzag tubes are predicted to possess metallic character.

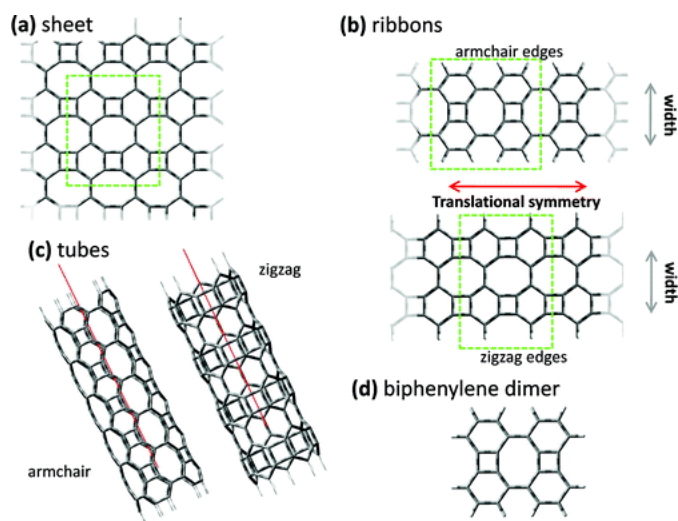


Figure 1.13. Structures of phenylene-containing graphitic materials: (a) biphenylene sheet, (b) biphenylene nanoribbons with armchair and zigzag edge morphology, (c) biphenylene nanotubes, and (d) biphenylene dimer. Reproduced with permission from ref. 50. Copyright 2010 American Chemical Society.

1.8 Conclusions and Outlook

Much can be learned by studying the interplay of aromaticity and antiaromaticity, and how these dueling theories affect synthetic access to and properties of organic materials. Fully-

conjugated ladder structures, both small molecules and polymers, are interesting candidates for optoelectronic applications in that they provide conformationally-rigid systems that promote electron delocalization. The chemistry and properties surrounding the [N]phenylenes are quite well-established, however the synthesis of polymeric and graphitic materials that reflect those properties still remains a challenge. Continued development of synthetic methodology will allow researchers to experimentally confirm some of the theoretical predictions, and to expand our understanding of the effects of electron delocalization in ladder systems.

1.9 References

-
- (1) (a) Minkin, V. I. Glukhovtsev, M. N.; Simkin, B. Y. *Aromaticity and Antiaromaticity. Electronic and Structural Aspects*, J. Wiley & Sons: New York, **1994**. (b) Garratt, P. J. *Aromaticity*, Wiley: New York, **1986**.
- (2) Hückel, E. *Z. Phys.* **1931**, *70*, 204.
- (3) (a) Dewar, M. J. S. *Adv. Chem. Phys.* **1965**, *8*, 65. (b) Breslow, R. *Acc. Chem. Res.* **1973**, *6*, 393. (c) Maier, G. *Angew. Chem. Int. Ed.* **1988**, *27*, 309. (d) Wilber, K. B. *Chem. Rev.* **2001**, *101*, 1317.
- (4) Randić, M. *Chem. Rev.* **2003**, *103*, 3449.
- (5) Jusélius, J.; Sundholm, D. *Phys. Chem. Chem. Phys.* **2001**, *3*, 2433.
- (6) Jusélius, J.; Sundholm, D. *Phys. Chem. Chem. Phys.* **2008**, *10*, 6630
- (7) Deniz A. A.; Peters, K. S.; Snyder, G. J. *Science*, **1999**, *286*, 1119, and references within.
- (8) For a review on [N]Phenylenes see: Miljanić, O. Š.; Vollhardt, K. P. C. in *Carbon-Rich Compounds: From Molecules to Materials*, Haley, M. M.; Tykwinski, R. R., Eds. Wiley-VCH: Weinheim, **2006**, pp 140-197.
- (9) Lothrop, W. C. *J. Am. Chem. Soc.* **1941**, *63*, 1187.
- (10) (a) Shepherd, M. L. *Cyclobutarenes: The Chemistry of Benzocyclobutene, Biphenylene, and Related Compounds*, Elseiver: New York, **1991**. (b) Toda, F.; Garratt, P. J. *Chem. Rev.* **1992**, *92*, 1685.

-
- (11) Schleifenbam, A.; Feeder, N.; Vollhardt, K. P. C. *Tetrahedron Lett.* **2001**, *42*, 7329.
- (12) Randić, M.; Balaban, A. T.; Plavšić, D. *Phys. Chem. Chem. Phys.* **2011**, *13*, 20644.
- (13) (a) Vollhardt, K. P. C. *Pure Appl. Chem.* **1993**, *65*, 153. (b) Vollhardt, K. P. C.; Mohler, D. I. in *Advances in Strain in Organic Chemistry*, Halton, B., Ed. JAI Press: London, **1996**, *5*, pp 121–160. (c) Trinajstić, N.; Schmalz, T. G.; Nikolić, S.; Hite, G. E.; Klein, D. J.; Seitz, W. A. *New J. Chem.* **1991**, *15*, 27. (d) Gutman, I.; Tomović, Ž. *Monatsh. Chem.*, **2001**, *132*, 1032. (e) Schulman, J. M.; Disch, P. L. *J. Am. Chem. Soc.*, **1996**, *118*, 8470. (f) Schulman, J. M.; Disch, P. L. *J. Phys. Chem. A*, **1997**, *101*, 5596.
- (14) (a) Clar, E. *Polycyclic Hydrocarbons*; Academic Press: London, 1964. (b) Clar, E. *The Aromatic Sextet*; Wiley: London, 1972. (c) Havenith, R. W. A.; van Lenthe, J. H.; Dijkstra, F.; Jenneskens, L. W. *J. Phys. Chem. A* **2001**, *105*, 3838.
- (15) Bong, D. T.-Y.; Gentric, L.; Holmes, D.; Matzger, A. J.; Scherhag, F.; Vollhardt, K. P. C. *Chem. Commun.* **2002**, *3*, 278.
- (16) Bong, D. T.-Y.; Chan, E. W. L.; Diercks, R.; Dosa, P. I.; Haley, M. M.; Matzger, A. J.; Miljanić, O. Š.; Vollhardt, K. P. C. *Org. Lett.* **2004**, *6*, 2249.
- (17) Mohler, D. L.; Kumaraswamy, S.; Stanger, A.; Vollhardt, K. P. C. *Synlett*, **2006**, 2981.
- (18) Schulman, J. M.; Disch, R. L. *J. Phys. Chem. A*, **1997**, *101*, 5596.
- (19) (a) Han, S.; Bond, A. D.; Disch, R. L.; Holmes, D.; Schulman, J. M.; Teat, S. J.; Vollhardt, K. P. C.; Whitener, G. D. *Angew. Chem. Int. Ed.* **2002**, *41*, 3223. (b) Han, S.; Anderson, D. R.; Bond, A. D.; Chu, H. V.; Disch, R. L.; Holmes, D.; Schulman, J. M.; Teat, S. J.; Vollhardt, K. P. C.; Whitener, G. D. *Angew. Chem. Int. Ed.* **2002**, *41*, 3227.
- (20) Schmidte-Radde, R. H.; Vollhardt, K. P. C. *J. Am. Chem. Soc.* **1992**, *114*, 9713.
- (21) Iglesias, B.; Cobas, A.; Pérez, D.; Guitián, E.; Vollhardt, K. P. C. *Org. Lett.* **2004**, *6*, 3557.
- (22) Dosche, C.; Löhmansröben, H.-G.; Bieser, A.; Dosa, P. I.; Han, S.; Iwamoto, M.; Schleifenbaum, A.; Vollhardt, K. P. C. *Phys. Chem. Chem. Phys.* **2002**, *4*, 2156, and references within.
- (23) (a) Shizuka, H.; Ogiwara, T.; Cho, S.; Morita, T. *Chem. Phys. Lett.* **1976**, *42*, 311. (b) Otha, N.; Fujita, M.; Baba, H.; Shizuka, H. *Chem. Phys.* **1980**, *47*, 389. (c) Elsaesser, T.; Lärmer, F.; Kaiser, W.; Dick, B.; Niemeyer, M.; Lüttke, W. *Chem. Phys.* **1988**, *126*, 405.
- (24) (a) Tetrau, C.; Lavalette, D.; Land, E. J.; Peradejordi, F. *Chem. Phys. Lett.* **1972**, *17*, 245. (b) Hertzberg, J.; Nickel, B. *Chem. Phys.* **1988**, *132*, 235. (c) Swiderek, P.; Michaud, M.;

Hohlneicher, G.; Sanche, L. *Chem. Phys. Lett.* **1991**, *178*, 289. (d) Suarez, M.; Devadoss, C.; Schuster, G. B. *J. Phys. Chem.* **1993**, *97*, 9299.

(25) Hirthammer, M.; Vollhardt, K. P. C. *J. Am. Chem. Soc.* **1986**, *108*, 2481.

(26) Blanco, L.; Helson, H. E.; Hirthammer, M.; Mestdagh, H.; Spyroudis, S.; Vollhardt, K. P. C. *Angew. Chem. Int. Ed.* **1987**, *26*, 1246.

(27) Yatsushashi, T.; Akiho, T.; Nakashima, N. *J. Am. Chem. Soc.* **2001**, *123*, 10137.

(28) (a) Wiersum, U. E.; Jenneskens, L. W. *Tetrahedron Lett.* **1993**, *34*, 6615. (b) Brown, R. F. C.; Choi, N.; Coulson, K. J. Eastwood, F. W. Wiersum, U. E.; Jenneskens, L. W. *Tetrahedron Lett.* **1994**, *35*, 4405.

(29) (a) Preda, D. V.; Scott, L. T. *Org. Lett.* **2000**, *2*, 1489. (b) Dosa, P. I.; Schleifenbaum, A.; Vollhardt, K. P. C. *Org. Lett.* **2001**, *3*, 1017. (c) Dosa, P. I.; Gu, Z.; Hager, D.; Karney, W. L.; Vollhardt, K. P. C. *Chem. Commun.* **2009**, 1967.

(30) Matzger, A. J.; Vollhardt, K. P. C.; *Chem. Commun.* **1997**, 1415.

(31) Kumaraswamy, S.; Jalisatgi, S. S.; Matzger, A. J.; Miljanić, O. Š.; Vollhardt, K. P. C. *Angew. Chem. Int. Ed.* **2004**, *43*, 3711.

(32) Mohler, D. L.; Vollhardt, K. P. C.; Wolff, S. *Angew. Chem. Int. Ed.* **1995**, *34*, 563.

(33) Berris, B. C.; Hovakeemian, B. G. H.; Lai, Y.-H.; Mestdagh, H. Vollhardt, K. P. C.; *J. Am. Chem. Soc.* **1985**, *107*, 5670.

(34) Oprunenko, Y.; Gloriov, I.; Lyssenko, K.; Malyugina, S.; Mityuk, D.; Mstislavsky, V.; Günther, H.; von Firks, G.; Ebener, M. *J. Organomet. Chem.* **2002**, *656*, 27.

(35) (a) Albright, T. A.; Dosa, P. I.; Grosmann, T. N.; Khrustalev, V. N.; Oloba, O. A.; Padilla, R.; Paubelle, R.; Stanger, A.; Timofeeva, T. V.; Vollhardt, K. P. C. *Angew. Chem. Int. Ed.* **2009**, *48*, 9853. (b) Albright, T. A.; Oldenhof, S.; Oloba, O. A.; Padilla, R.; Vollhardt, K. P. C. *Chem. Commun.* **2011**, *47*, 9039.

(36) Leung, M.-k.; Viswanath, M. B.; Chou, P.-T.; Pu, S.-C.; Lin, H.-C. Jin, B.-Y. *J. Org. Chem.* **2005**, *70*, 3560.

(37) Holmes, D.; Kumaraswamy, S.; Matzger, A. J.; Vollhardt, K. P. C. *Chem. Eur. J.* **1999**, *5*, 3399.

(38) Taillemite, S.; Aubert, C.; Fichou, D.; Malacria, M. *Tetrahedron Lett.* **2005**, *46*, 8325.

-
- (39) (a) Bingel, C. *Chem. Ber.* **1993**, *126*, 1957. (b) Nierengarten, J.-F.; Gramlich, V.; Cardullo, F.; Diederich, F. *Angew. Chem. Int. Ed.* **1996**, *35*, 2101.
- (40) Dosche, C.; Mickler, W.; Lohmannsroben, H.-G.; Agenet, N.; Vollhardt, K. P. C. *J. Photochem. Photobiol. A: Chem.* **2007**, *188*, 371.
- (41) Schneebeli, S.; Kamenetska, M.; Foss, F.; Vazquez, H.; Skouta, R.; Hybertsen, M.; Venkataraman, L.; Breslow, R. *Org. Lett.* **2010**, *12*, 4114.
- (42) Quinn, J. R.; Foss, F. W. Venkataraman, L.; Breslow, R. *J. Am. Chem. Soc.* **2007**, *129*, 12376.
- (43) Christoph, H.; Grunenberg, J.; Hopf, H.; Dix, I.; Jones, P. G.; Scholtissek, M.; Maier, G. *Chem. Eur. J.* **2008**, *14*, 5604.
- (44) Bharat, Bhola, R.; Bally, T.; Valente, A.; Cyranski, M. K.; Dobrzycki, L.; Spain, S. M.; Rempala, P.; Chin, M. R.; King, B. T. *Angew. Chem. Int. Ed.* **2010**, *49*, 399.
- (45) Schulman, J. M.; Disch, R. L. *J. Phys. Chem. A* **2003**, *107*, 5223.
- (46) (a) Haymet, A. D. J. *J. Chem. Phys. Lett.* **1985**, *122*, 421. (b) Fowler, P. W.; Woolrich, J. *Chem. Phys. Lett.* **1986**, *127*, 78. (c) Kovačević, K.; Graovac, A. *Int. J. Quantum Chem. Quantum Chem Symp.* **1987**, *21*, 589. (d) Coulombeau, C.; Rassat, A. *J. Chem. Phys.* **1987**, *84*, 875. (e) Kurita, N.; Kobayashi, K.; Kumahora, H.; Tago, K. Ozawa, K. *Chem Phys. Lett.* **1992**, *188*, 181. (f) Schulman, J. M.; Disch, R. L. *Chem. Phys. Lett.* **1996**, *262*, 813. (g) De La Vaissière, B.; Fowler, P. W.; Deza, M. *J. Chem. Inf. Comput. Sci.* **2001**, *41*, 376.
- (47) Schulman, J. M. Disch, R. L. *J. Phys. Chem. A*, **2005**, *109*, 6947.
- (48) Bruns, D.; Miura, H.; Vollhardt, K. P. C. *Org. Lett.* **2003**, *5*, 549.
- (49) (a) Qian, W.; Bartberger, M. D.; Pastor, S. J.; Houk, K. N.; Wilkins, C. L.; Rubin, Y. *J. Am. Chem. Soc.* **2000**, *122*, 8333. (b) Qian, W.; Chuang, S.-C.; Amador, R. B.; Jarrosson, T.; Sander, M.; Pieniazek, S.; Khan, S. I.; Rubin, Y. *J. Am. Chem. Soc.* **2003**, *125*, 2066.
- (50) Hudspeth, M. A.; Whitman, B. W.; Barone, V.; Peralta, J. E. *ACS Nano*, **2010**, *4*, 4565.
- (51) Son, Y.-W.; Cohen, M. L.; Louie, S. G. *Nature*, **2006**, *444*, 347.

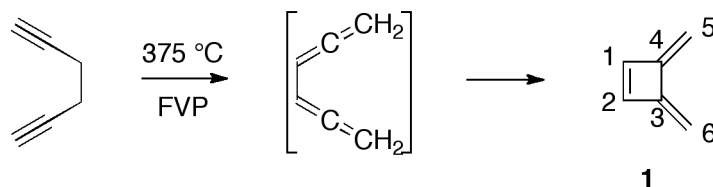
Chapter 2

Synthesis of 3,4-Bis(benzylidene)cyclobutenes

Adapted from: Parkhurst, R. R.; Swager, T. M. "Synthesis of 3,4-Bis(benzylidene)cyclobutenes," *Synlett*, **2011**, 1519.

2.1 Introduction

3,4-Bis(methylene)cyclobutene (**1**) is a highly strained and air-sensitive isomer of benzene that was first detected in 1961 from the Hofmann elimination of 3,4-bis[(trimethylammonio)methyl]cyclobutene dihydroxide.¹ The relative thermal stability of derivatives of **1** initially came as a surprise due to the significant ring strain. As a result, there has been much fascination with the synthesis and reactivity of compounds bearing this core structure. Unsubstituted **1** can be generated quantitatively through the thermal rearrangement of 1,5-hexadiyne: an initial [3,3]-sigmatropic rearrangement affords hexa-1,2,4,5-tetraene, which undergoes conrotatory 4π -electrocyclic ring closure to yield **1** (Scheme 2.1).²

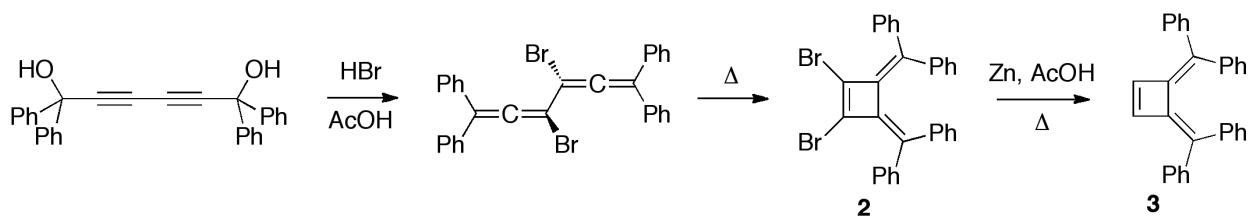


Scheme 2.1. Rearrangement of 1,5-hexadiyne to **1**.

Compound **1** has a significant dipole ($\mu = 0.616 \pm 0.002$ D) for a simple hydrocarbon, as increased electron density at C5 and C6 reduces the antiaromatic character of the ring.^{2c} Theoretical and experimental studies have shown that **1** is more similar to a cross-conjugated diene than to a triene. Additionally, the *exo*-methylene groups in **1** do not react as a Diels–Alder diene, as the resulting product would contain antiaromatic cyclobutadiene. The primary factor influencing the unique structure and reactivity of **1** is the energetic cost of antiaromaticity.³

The highly strained and unsaturated nature of **1** makes it an intriguing building block for the synthesis of unique polycyclic macromolecules, however the methodology for accessing substituted derivatives of **1** must first be expanded. Although **1** is highly air-sensitive, it is

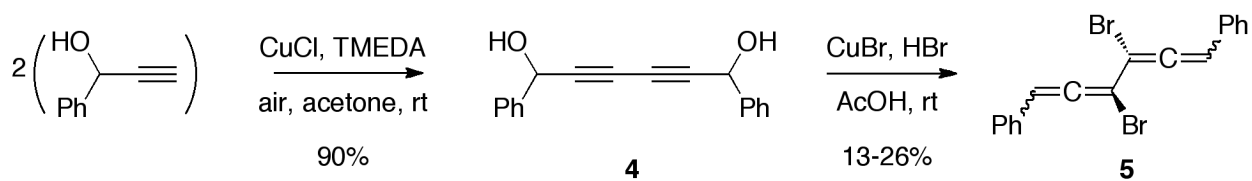
possible to synthesize air-stable analogs by installing electron-withdrawing groups, thereby reducing antiaromatic character.⁴ The most prominent example of this is 1,2-dibromo-3,4-bis(diphenyl-methylene)cyclobutene (**2**),⁵ originally synthesized by Toda *et al.*⁶ The debrominated derivative **3** is readily available via reduction with zinc metal in acetic acid and is moderately air-stable as compared to **1** (Scheme 2.2).⁷ This synthetic scheme is limited in scope and functional-group tolerance, due to its dependence on the use of tertiary propargyl alcohols and harsh, acidic conditions. A new scheme is required to access less substituted derivatives and a wider range of functional groups.



Scheme 2.2. Synthesis of **2** and **3** reported by Toda *et al.*

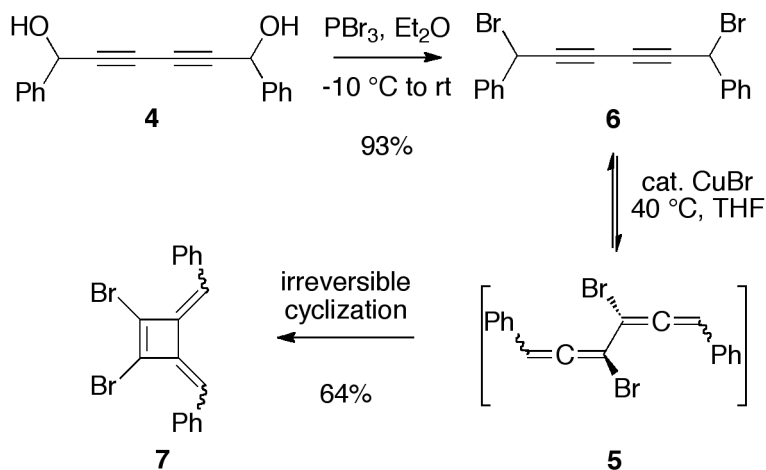
2.2 Synthesis of 1,2-Dibromo-3,4-bis(benzylidene)cyclobutene

The rearrangement of propargyl alcohols to allenyl halides is a well-studied transformation.⁸ Glaser coupling of the corresponding terminal alkyne produces 1,6-diphenyl-2,4-diyne-1,6-diol (**4**) on a large scale in good yield (100 g, 90%).⁹ Treatment of **4** with substoichiometric amounts of copper(I) bromide (CuBr) and concentrated hydrobromic acid (HBr) in acetic acid provides the desired 1,6-diphenyl-3,4-dibromo-1,2,4,5-tetraene (**5**, Scheme 2.3).¹⁰ Unfortunately, isolation of **5** is difficult, leading to decomposition and low yields (13–26%). Therefore, a synthesis that circumvents the direct isolation of **5** was pursued.



Scheme 2.3. Synthesis of intermediates **4** and **5**.

Copper(I) salts catalyze the reversible rearrangement of propargyl halides to allenyl halides.¹¹ Jacobs *et al.* reported a maximum conversion of alkyne to allene of 65% in the case of 3-bromopropyne. Interestingly, copper(I) salts have also been shown to catalyze the electrocyclic ring closure of diallenes to 3,4-bis(methylene)cyclobutenes.¹² The present system exploits the dual ability of copper(I) salts to achieve tandem rearrangement and irreversible electrocyclic ring closure (Scheme 2.4). Upon treatment with phosphorus tribromide (PBr_3), diol **4** is converted in high yield to dibromide **6**. Compound **6** was found to rearrange to **5** (ca. 50%) and hydrolyze to **4** (ca. 50%) upon chromatography on silica gel and decomposed partially during recrystallization attempts, therefore it was used without further purification. As expected, upon heating to 40 °C in THF in the presence of 5 mol% copper(I) bromide (CuBr), the crude product **6** was converted to a mixture of three isomers of 1,2-dibromo-3,4-bis(benzylidene)cyclobutene (**7**).



Scheme 2.4. Rearrangement and irreversible cyclization to form **7**.

2.3 Characterization of 1,2-Dibromo-3,4-bis(benzylidene)cyclobutene

The three isomers arise from the *E/Z* stereochemistry about the exocyclic double bonds and have been labeled as **7**(*in,out*), (*in,in*), and (*out,out*) referring to the position of the phenyl groups using nomenclature analogous to that used by Toda *et al.*¹³ The isomers of **7** are separable by column chromatography, and the structure of each has been confirmed by X-ray crystallography (Figure 2.1).

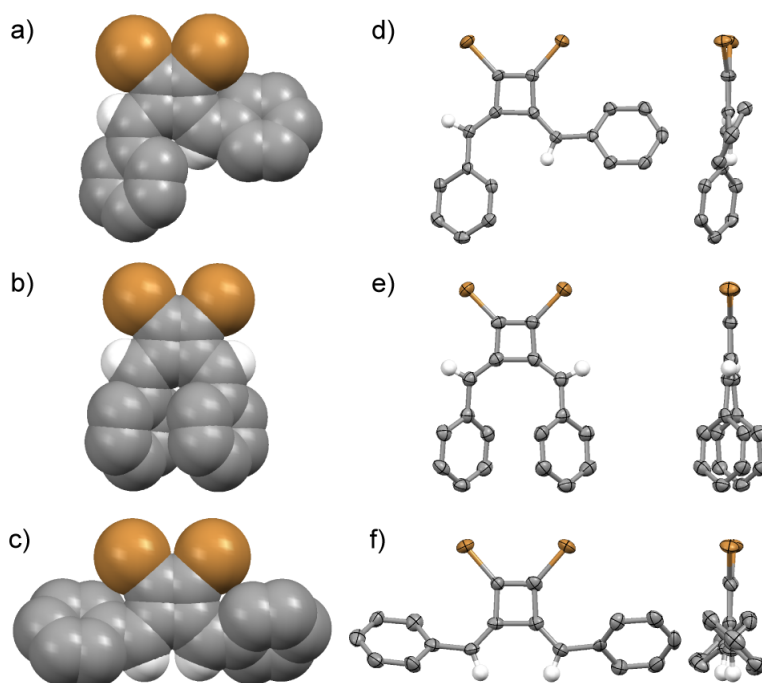
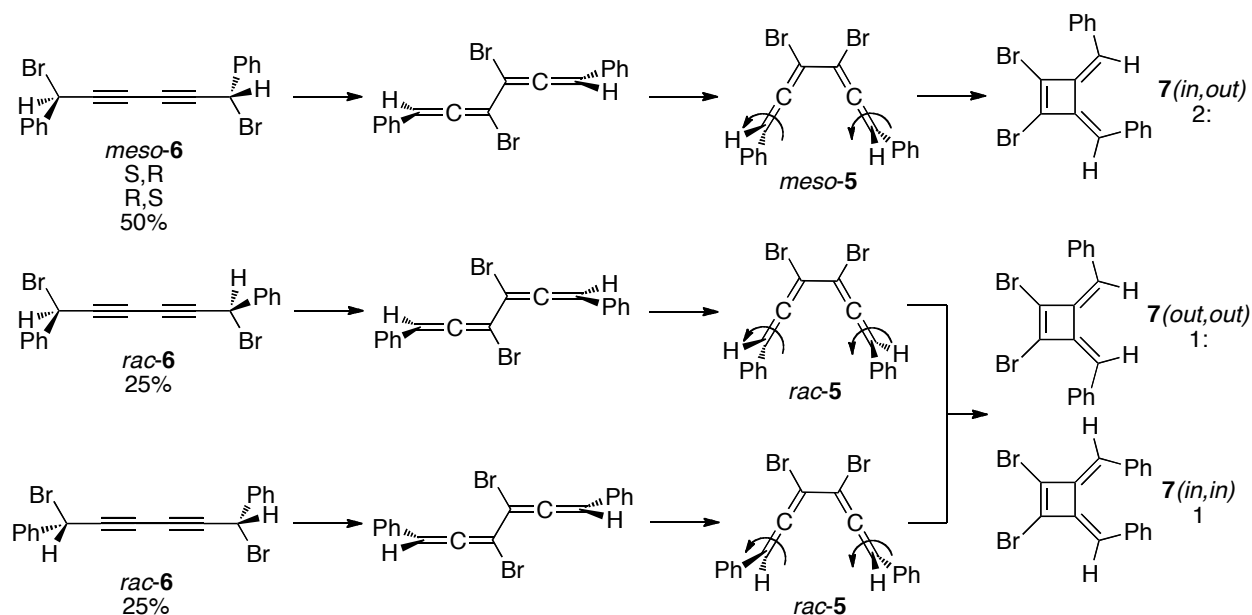


Figure 2.1. Space-filling (a–c) and front/side ellipsoid views (d–f) of X-ray crystal structures of isomers of **7** (a, d) (*in,out*) (b, e) (*in,in*) (c, f) (*out,out*). Aromatic hydrogens omitted for clarity. Anisotropic thermal ellipsoids set at 50% probability.

The formation of three isomers is consistent with the mechanism of the overall transformation (Scheme 2.5). Starting from racemic 1-phenyl-2-propyn-1-ol, compounds **4** and **6** are a 1:1 mixture of the *rac* and *meso* stereoisomers, which rearrange to the corresponding isomers of **5**. The *meso* isomer then undergoes conrotatory cyclization to form exclusively **7** (*in,out*) while the *rac* isomers cyclize to either **7**(*in,in*) or **7**(*out,out*). Therefore, a 2:1:1 ratio of

(*in,out*)/(*in,in*)/(*out,out*) isomers is expected. The distribution of products at different loadings of CuBr as determined by ^1H NMR is listed in Table 2.1. The (*in,out*) isomer consistently accounts for approximately 50% of the product. When a pure sample of a single isomer in hexane was irradiated with UV light (Hg pen-lamp), each isomerized to a mixture of approximately 67% (*in,out*), 23% (*in,in*), and 10% (*out,out*) isomers (Figure 2.2). This observation is consistent with calculations (B3LYP/6-31+g*) that predict the (*out,out*) isomer to be the highest in energy, with relative E (kcal mol $^{-1}$) of $7(\textit{in,out}) = -0.4487$, $7(\textit{in,in}) = 0$, $7(\textit{out,out}) = 0.0056$.



Scheme 2.5. Stereochemistry of the rearrangement and ring closure of **6** to **7**.

Table 2.1. Distribution of isomers of **7** from Cu(I)-catalyzed ring closure.

CuBr (%)	Ratio of (<i>in,out</i>) : (<i>in,in</i>) : (<i>out,out</i>)
5	4.9 : 3.1 : 2.0
50	4.6 : 2.5 : 2.9
100	4.8 : 2.1 : 3.1
250	5.0 : 1.9 : 3.1

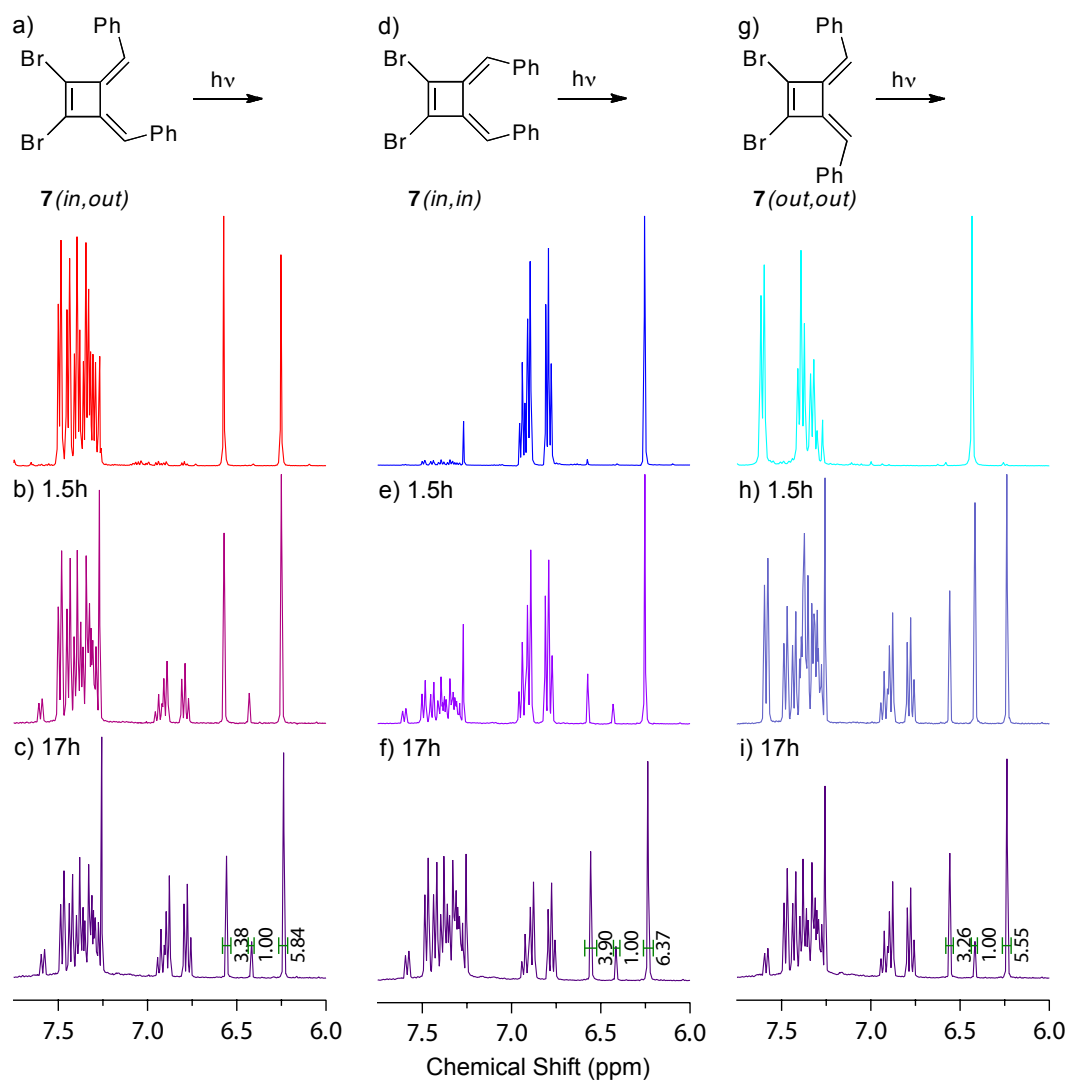
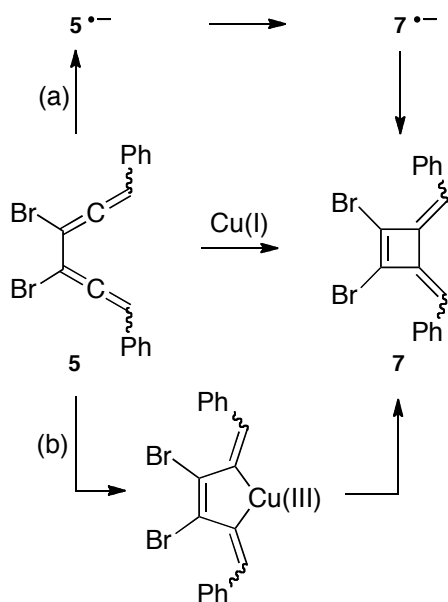


Figure 2.2. Photolysis of (a) **7**(*in,out*) after (b) 1.5h (c) 17h to yield 66% (*in,out*), 24% (*in,in*), and 10% (*out,out*). Photolysis of (d) **7**(*in,in*) after (e) 1.5h (f) 17h to yield 69% (*in,out*), 22% (*in,in*), and 9% (*out,out*). Photolysis of (g) **7**(*out,out*) after (h)1.5h (i)17h to yield 67% (*in,out*), 23% (*in,in*), and 10% (*out,out*).

The increased energy of **7**(*out,out*) indicates the energetic cost of the phenyl groups twisting out of plane to reduce steric repulsion with the bromine atoms. The ability of the phenyl groups to π -stack is able to somewhat counterbalance the effect of steric repulsion and twisting in **7**(*in,in*). As shown in Table 2.1, the ratio of **7**(*out,out*) to **7**(*in,in*) increases with increased levels of the copper(I) source. Similarly, Pasto *et al.* found greater yields of sterically congested

products with copper(I)-catalyzed ring closure of diallenes to 3,4-bisalkylidenecyclobutenes as compared to the strictly thermal process.^{12c,14} They proposed that the copper(I)-catalyzed cyclization occurs through a radical-anion process (Scheme 2.6a). Theoretical investigation of the transformation of 1,2,4,5-hexatriene to **1** performed by Pasto *et al.* indicates that ring closure of the radical anion is more exothermic than that of the neutral compound, creating an earlier transition state in which steric congestion [in the case of **7**(*out,out*)] or π -stacking [as in **7**(*in,in*)] in the product are less important. An alternative mechanism involves the formation of a metallocycle intermediate (Scheme 2.6b). This pathway has been proposed for the metal-catalyzed intramolecular [2 + 2] ring closure in a variety of allene-containing compounds.¹⁵

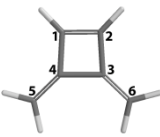
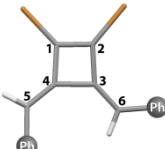
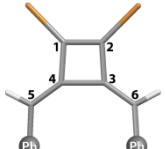
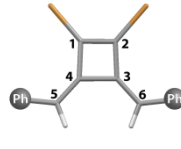


Scheme 2.6. Proposed mechanisms of Cu(I)-catalyzed [2+2] ring closure; (a) ring closure *via* radical anion intermediate, (b) ring closure *via* cupracyclopentane.

The structural differences between the isomers of **7** and the calculated structure of parent compound **1** (B3LYP/6-31G**) are summarized in Table 2.2. There is a notable deviation in internuclear distance between C5 and C6. This value is related to the bonding angle of C2–C3–

C6 (and C1–C4–C5) and is determined by the steric interaction between either a phenyl ring and a bromine atom or between two phenyl rings. In the case of compound **1**, which lacks this steric interaction, the C5–C6 distance is 3.409 Å with a corresponding angle of 137°. The corresponding values of compound **7**(*out,out*) deviate the least from those of **1**, 0.069 Å and 2°, respectively. Compound **7**(*in,in*), where the phenyl rings must twist in order to stack face-to-face and reduce steric repulsion, deviates the most from **1** with an increase in C5–C6 distance of 0.270 Å and a 7° decrease in the C2–C3–C6 angle.

Table 2.2. Structural information of **1** (B3LYP/6-31G**) and crystal structures of **7**. Redundant bond and torsion angles for symmetrical compounds have been omitted.

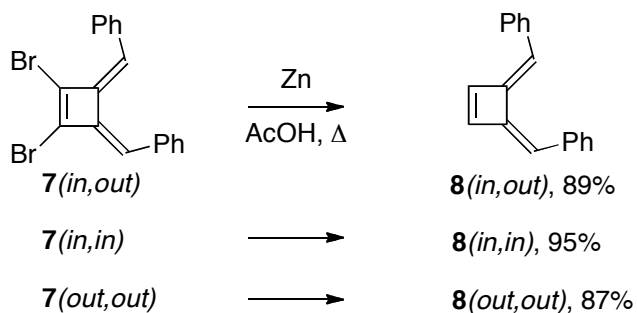
					
		1	7 (<i>in,out</i>)	7 (<i>in,in</i>)	7 (<i>out,out</i>)
Bond Length (Å)	C1–C2	1.336	1.357	1.345	1.375
	C1–C4	1.484	1.472	1.479	1.494
	C2–C3	1.484	1.495	1.482	1.477
	C3–C4	1.509	1.522	1.531	1.507
Distance (Å)	C5–C6	3.409	3.508	3.679	3.340
Angle (°)	C1–C2–H(Br)	134	130	134	131
	C2–C1–H(Br)	-	133	-	-
	C2–C3–C6	137	131	130	139
	C1–C4–C5	-	140	-	-
Torsion (°)	C2–C3–C6–Ph	0	29	43	42
	C1–C4–C5–Ph	-	30	-	-

The effects of steric bulk are also evident in variations of the angle defined by C1–C2–H(Br) [or C2–C1–H(Br)]. In this regard, **7**(*in,in*) is the most similar to **1**. The angle is decreased by 3° in **7**(*out,out*) as the bromine atoms are forced closer together to accommodate the outward-pointing phenyl rings and minimize their twisting. As expected unsymmetrical **7**(*in,out*) exhibits both types of bond angles dependent on the position of the phenyl group.

Finally, and perhaps most significantly, is the difference in torsion angle caused by the twisting of the phenyl groups. In **7**(*in,out*) the phenyl groups only twist 29° and 30° out of plane whereas in **7**(*in,in*) and **7**(*out,out*) the corresponding values are 43° and 42°, respectively. Increased planarity (and therefore conjugation) of the benzylidene group in **7**(*in,out*) is a likely explanation for its favored formation in the photochemical isomerization.

2.4 Synthesis of Additional Derivatives of 3,4-Bis(benzylidene)cyclobutenes

Single isomers of **7** can be reduced to 3,4-bis(benzylidene)cyclobutene (**8**) with retention of the *E/Z* configuration by heating with zinc powder in acetic acid (Scheme 2.7). Compound **8** is moderately stable, but decomposes slowly under air. Attempts to purify compound **8** *via* column chromatography or recrystallization were unsuccessful due to its limited stability. The ¹H NMR spectra of **7** and crude **8** are compared in Figure 2.3. In each case, growth of the new H^b peak is evident. As expected from the dipole moment and antiaromatic character of parent compound **1**, the vinyl peaks for H^b are significantly deshielded and positioned downfield of the aromatic region. Previously, the synthesis of a single symmetrical isomer of **7** from the iron tricarbonyl complex of substituted cyclobutadiene was reported.¹⁶ Based on our findings, however, it seems likely the authors had actually generated a mixture of symmetrical isomers [**8**(*in,in*) and **8**(*out,out*)].



Scheme 2.7. Reduction of a single isomer **7** to a single isomer of **8** with retention of *E/Z* configuration.

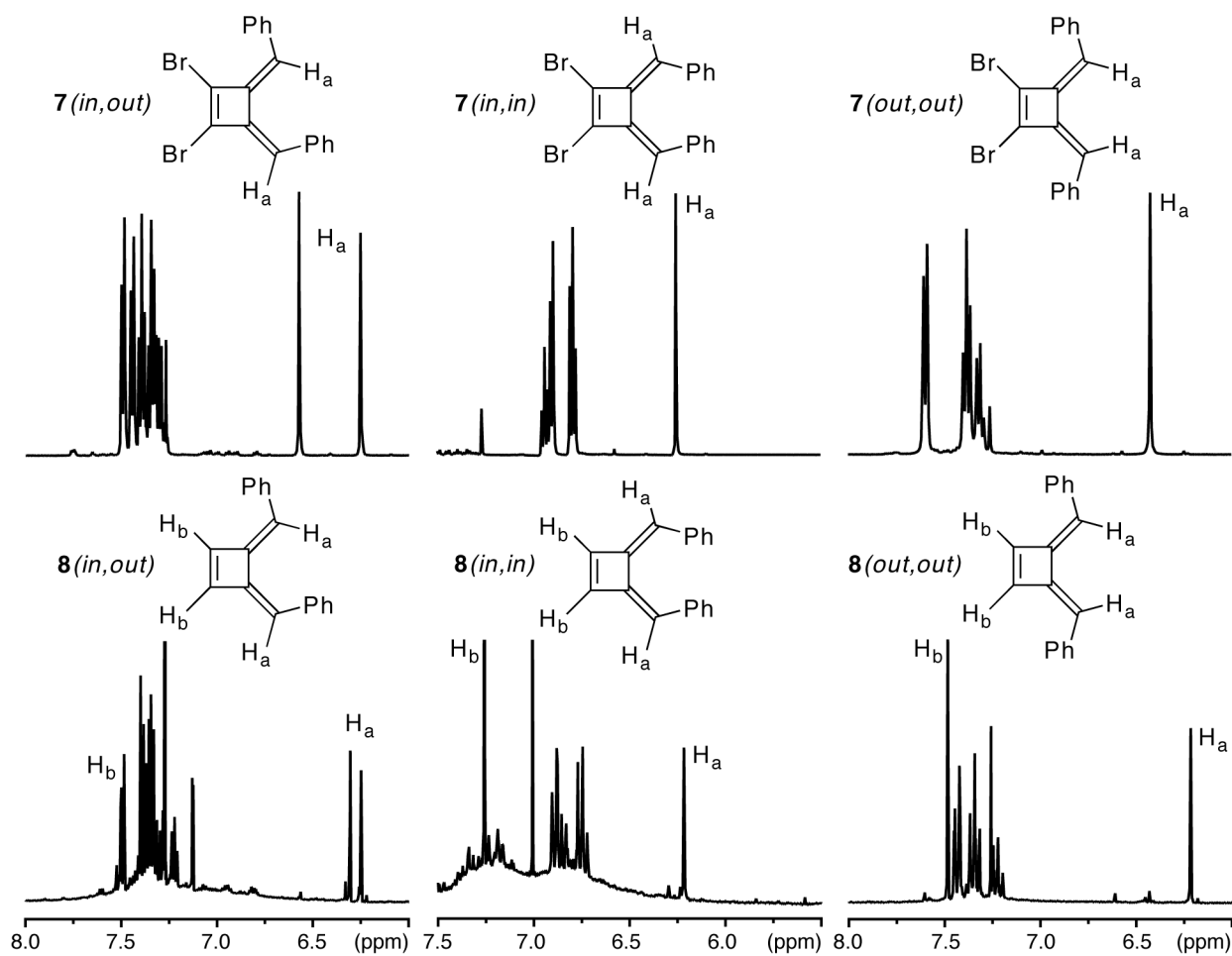
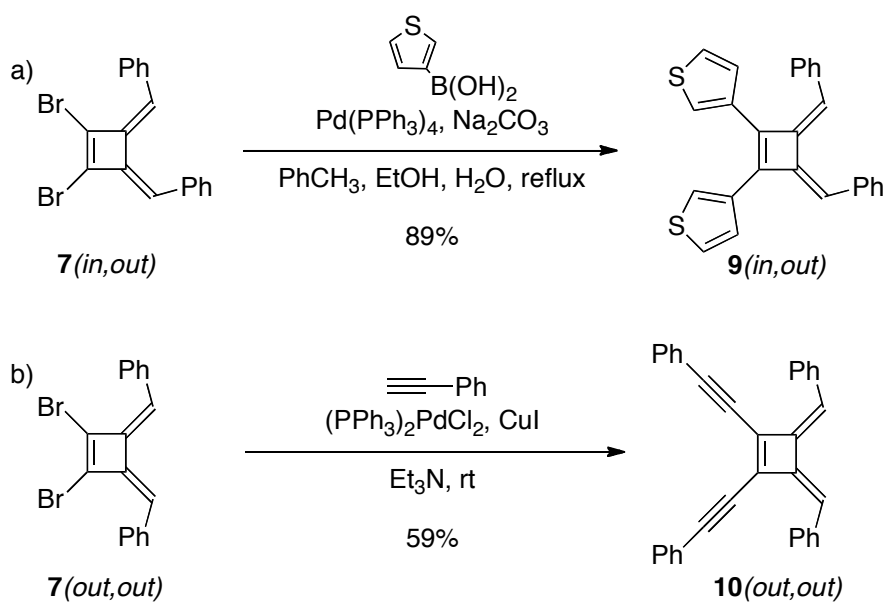


Figure 2.3. Comparison of ^1H NMR spectra of compounds **7** and **8**. Deshielding of H^b is evident.
^aImpurities are believed to be primarily high molecular weight decomposition products.

Compound **7** can also be used as a coupling partner for metal-catalyzed cross-coupling reactions (Scheme 2.8). Coupling reactions were generally carried out using a single isomer of **7**,

however, no difference in efficiency of the reaction between isomers was observed. Twofold Suzuki cross-coupling reaction between 3-thiophene boronic acid and **7** gave compound **9** in 89% yield. Attempts at oxidative cyclization between the thiophene rings of **9** to form benzodithiophene¹⁷ were unsuccessful due to the increased bond angles around the four-membered ring. Compound **7** also successfully participated in twofold Sonogashira cross-coupling with phenylacetylene to produce **10** in 59% yield. The absorption and emission spectra of **10**(*out,out*) are shown in Figure 2.4; a difference in the optical characteristics between different isomers of **10** was not observed.



Scheme 2.8. Examples of metal-catalyzed cross-coupling of **7**.

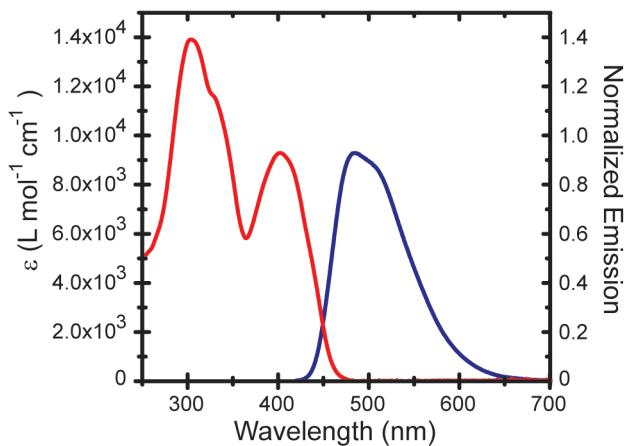


Figure 2.4. Absorption and emission curves of **10**(*out,out*) in CHCl_3 ($\phi_{\text{em}} = 0.63$, $t = 5.77$ ns).

2.5 Conclusions

In conclusion, we have developed a method for the synthesis of previously unknown 1,2-dibromo-3,4-bis(benzylidene)cyclobutene (**7**). Each of the three possible isomers of **7** were isolated and characterized by X-ray crystallography. The utility of **7** as a starting material in the synthesis of additional highly strained molecules *via* reduction and metal-catalyzed cross coupling has also been demonstrated.

2.6 Experimental

Materials: All reactions were carried out under argon using standard Schlenk techniques unless otherwise noted. All solvents were of ACS reagent grade or better unless otherwise noted. Anhydrous tetrahydrofuran (THF) and diethyl ether (Et_2O) were obtained from J. T. Baker and dried on a solvent column purification system. Silica gel (40 μm) was purchased from SiliCycle Inc. $\text{Pd}(\text{PPh}_3)_4$ and $(\text{PPh}_3)_2\text{PdCl}_2$ were purchased from Strem Chemicals. All other reagent grade materials were purchased from Alfa Aesar or Sigma-Aldrich and used without further

purification. Compound **2** was prepared by a Glaser coupling (copper(I) chloride, N,N,N',N'-tetramethylethylenediamine, air, in acetone) as described by Adlington *et al.*^{9b} The ¹H NMR data was consistent with that reported in the literature.^{9a}

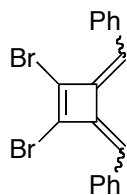
NMR Spectroscopy: ¹H and ¹³C NMR spectra for all compounds were acquired in CDCl₃ on a Bruker Avance Spectrometer operating at (400 MHz and 100 MHz, respectively), or on a Varian Inova Spectrometer (500 MHz or 125 MHz, respectively). Chemical shifts (δ) are reported in parts per million (ppm) and referenced with residual CHCl₃ (7.27 ppm).

Mass Spectrometry: High-resolution mass spectra (HRMS) were obtained at the MIT Department of Chemistry Instrumentation Facility employing either electron impact (EI), electrospray (ESI), or Direct Analysis in Real Time (DART) as the ionization technique.

Infrared (IR) spectroscopy: IR spectra were recorded on a Perkin-Elmer Model 2000 FT-IR spectrophotometer at the MIT Department of Chemistry Instrumentation Facility. Peaks are reported as strong (s), medium (m) or weak (w).

Absorption and Emission Spectroscopy: Ultraviolet-visible absorption spectra were measured with an Agilent 8453 diode array spectrophotometer and corrected for background signal with a solvent-filled cuvette. Fluorescence spectra were measured on a SPEX Fluorolog-τ 3 fluorimeter (model FL- 321, 450 W Xenon lamp) using right-angle detection. Fluorescence quantum yields in Chloroform (CHCl₃) were determined relative to perylene in ethanol (EtOH) and are corrected for solvent refractive index and absorption differences at the excitation wavelength. Fluorescence lifetimes were measured *via* frequency modulation using a Horiba-Jobin-Yvon MF2 lifetime

spectrometer equipped with a 365 nm laser diode and using the modulation of POPOP (1,4-bis(5-phenyloxazol-2-yl)benzene) as a calibration reference.

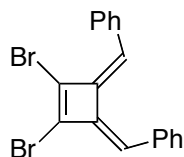


Compound 7, step 1: A solution of 1,6-diphenylhexa-2,4-diyne-1,6-diol (10.000g, 38.1 mmol) in anhydrous Et₂O (200 mL) was cooled to -10 °C in a brine/ice bath and flushed with argon for 10 minutes. Phosphorus tribromide (PBr₃, 2.36 mL, 25.2 mmol) was added to the solution dropwise and the reaction mixture was allowed to warm to room temperature over 2 hours. The reaction mixture was poured over ice and neutralized with a saturated solution of sodium bicarbonate (NaHCO_{3(aq)}). The two layers were separated, then the aqueous phase was extracted with Et₂O (2 × 100 mL). The combined organics were washed with brine (100 mL), and dried over anhydrous magnesium sulfate (MgSO₄). The solvent was removed under reduce pressure to give 13.715g of **6** (93% crude yield) as a mixture of stereoisomers which was used in the next step without further purification.

¹H NMR (400 MHz, CDCl₃): 7.57 (dd, *J*=8.0 Hz, 1.4 Hz, 2H), 7.38 (m, 3H), 5.78 (s, 1H)

Step 2: To a solution of **6** (5.743g, 14.8 mmols) in anhydrous THF (100 mL) was added catalytic copper(I) bromide (CuBr) (106 mg, 0.7 mmols). The reaction mixture was flushed with Argon for 10 minutes then heated to 40 °C for 4 hours. After cooling to room temperature, the reaction mixture was diluted with dichloromethane (CH₂Cl₂, 200 mL) and washed with saturated aqueous ammonium chloride (NH₄Cl_(aq), 100 mL). The layers were separated and the organic layer was

dried over anhydrous sodium sulfate (Na_2SO_4) and concentrated under reduced pressure. Flash column chromatography of the residue (SiO_2 , hexanes) yielded 3.707 g of an isomeric mixture of **7** (64% yield). Analytically pure samples of each isomer were obtained by flash column chromatography (SiO_2 , hexanes) followed by recrystallization from hot methanol (MeOH).



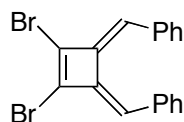
7(*in,out*):

$^1\text{H NMR}$ (500 MHz, CDCl_3): 7.49 (d, $J=7.6$ Hz, 2H), 7.44 (d, $J=7.4$ Hz, 2H), 7.40 (app t, $J=7.4$ Hz, 2H), 7.34 (ψt, $J=6.0$ Hz, 2H), 7.32-7.27 (m, 2H), 6.57 (s, 1H), 6.23 (s, 1H)

$^{13}\text{C NMR}$ (125 MHz, CDCl_3): 141.0, 138.7, 134.9, 134.6, 134.1, 129.9, 129.5, 128.6, 128.3, 128.2, 127.80, 127.78, 116.1, 113.6

HRMS (EI): calc for $\text{C}_{18}\text{H}_{12}\text{Br}_2$ $[\text{M}]^+$ 385.9300, found 385.9288

Melting point (MeOH): 84-88 °C



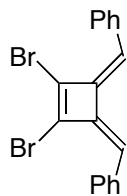
7(*in,in*):

$^1\text{H NMR}$ (500 MHz, CDCl_3): 6.94 (app t, $J=7.4$ Hz, 1H), 6.90 (d, $J=7.0$ Hz, 2H), 6.79 (app t, $J=7.7$ Hz, 2H), 6.26 (s, 1H)

$^{13}\text{C NMR}$ (125 MHz CDCl_3): 139.6, 134.9, 130.7, 129.5, 127.4, 127.3, 114.5

HRMS (DART): calc for $\text{C}_{18}\text{H}_{12}\text{Br}_2$ $[\text{M}+\text{H}]^+$ 388.9366, found 388.9380

Melting point (MeOH): 74-77 °C



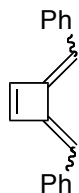
7(out,out):

¹H NMR (400 MHz, CDCl₃): 7.61 (d, *J*=7.4 Hz, 2H), 7.39 (app t, *J*=7.7 Hz, 2H), 7.32 (app t, *J*=7.3 Hz, 1H), 6.43 (s, 1H)

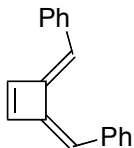
¹³C NMR (100 MHz, CDCl₃): 139.6, 134.2, 132.0, 129.8, 128.5, 127.9, 110.6

HRMS (DART): calc for C₁₈H₁₂Br₂ [M+H]⁺ 388.9366, found 388.9380.

Melting point (MeOH): 138-140 °C



Compound 8, representative procedure: A reaction tube was charged with **7(in,in)** (100 mg, 0.26 mmols), zinc dust (35 mg, 0.54 mmols), and acetic acid (AcOH, 1.3 mL). The suspension was flushed with argon for 10 minutes than heated to 120 °C for 30 minutes. After cooling to room temperature, the reaction mixture was diluted with H₂O (5 mL). The precipitate was collected by filtration and washed with methanol to give 57 mg (95%) of **8(in,in)**.

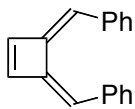


7(*in,out*) → **8**(*in,out*), 89%:

¹H NMR (400 MHz, CDCl₃): 7.49 (d, *J*=7.4 Hz, 2H), 7.40-7.28 (m, 8h), 7.22 (app t, *J*=7.1 Hz, 1H), 7.12 (d, *J*=2.6 Hz, 1H), 6.30 (s, 1H), 6.24 (s, 1H)

¹³C NMR (100 MHz, CDCl₃): 147.9, 144.6, 144.1, 142.7, 137.5, 136.6, 129.4, 128.7, 128.4, 128.0, 127.04, 127.01, 115.2, 115.1

IR (ν_{\max} , cm⁻¹, KBr): 517 (m), 694 (s), 748 (s), 913 (s), 1028 (m), 1077 (m), 1179 (w), 1448 (m), 1493 (m), 1598 (m), 1685 (w), 2926 (w), 3024 (m), 3058 (w)

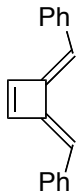


7(*in,in*) → **8**(*in,in*), 95%:

¹H NMR (400 MHz, CDCl₃): 7.03 (s, 1H), 6.91 (d, *J*=7.2 Hz, 2H), 6.88 (app t, *J*=7.4 Hz, 1H), 6.77 (app t, *J*=7.6 Hz, 2H), 6.24 (s, 1H)

¹³C NMR (100 MHz, CDCl₃): 146.0, 143.4, 136.6, 129.4, 127.2, 126.5, 115.8

IR (ν_{\max} , cm⁻¹, KBr): 694 (s), 748 (s), 913 (s), 1027 (w), 1076 (w), 1155 (w), 1179 (w), 1446 (m), 1493 (m), 1596 (w), 1736 (w), 2927 (w), 3023 (m), 3055 (w)

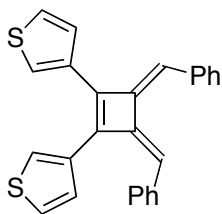


7(*out,out*) → **8**(*out,out*), 87%:

¹H NMR (400 MHz, CDCl₃): 7.50 (s, 1H), 7.46 (d, *J*=7.4 Hz, 2H), 7.37 (app t, *J*=7.4 Hz, 2H), 7.24 (app t, *J*=7.4 Hz, 1H), 6.24 (s, 1H)

¹³C NMR (100 MHz, CDCl₃): 146.0, 143.4, 137.2, 128.8, 127.9, 127.0, 110.3

IR (*v*_{max}, cm⁻¹, KBr): 525 (m) 688 (s), 741 (m), 769 (s), 866 (w), 910 (m), 1027 (w), 1074 (w), 1259 (w), 1448 (m), 1493 (w), 1736 (w), 2928 (w), 3022 (w), 3050 (w), 3082 (w)



Compound 9(*in,out*): To a solution of **7**(*in,out*) (482 mg, 1.2 mmols) in toluene (PhCH₃, 11 mL) was added 3-thiopheneboronic acid (350 mg, 2.7 mmols), EtOH (3 mL), and H₂O (3 mL). The system was bubbled with argon for 60 minutes before adding Pd(PPh₃)₄ (80 mg, 2.5 mol%) followed by flushing with argon for an additional 10 minutes. The reaction mixture was heated to reflux overnight. After cooling to room temperature, the reaction was diluted with CH₂Cl₂ (50 mL) and filtered through celite. The solvent was removed under reduced pressure to give a pale brown solid. The crude material was purified by flash column chromatography (SiO₂, 1:9 benzene:hexanes) to give 436 mg (89%) of pure **10**(*in,out*) as a pale yellow solid.

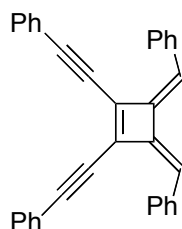
¹H NMR (400 MHz, CDCl₃): 7.65 (dd, *J*=2.8 Hz, 1.2 Hz, 1H), 7.57 (d, *J*=7.4 Hz, 2H), 7.40 (app t, *J*=7.8 Hz, 2H), 7.36 (dd, *J*=5.0 Hz, 3.4 Hz, 1H), 7.30 (d, *J*=5.2 Hz, 2H), 7.17 (dd, *J*=4.9 Hz,

2.9 Hz, 1H), 7.05 (m, 3H), 7.01 (m, 2H), 6.87 (m, 2H), 6.65 (s, 1H), 6.60 (s, 1H)

¹³C NMR (100 MHz, CDCl₃): 146.3, 144.5, 142.7, 141.4, 136.8, 136.2, 133.9, 133.1, 129.7, 129.6, 128.3, 128.0, 127.7, 127.0, 126.9, 126.7, 126.0, 125.4, 125.0, 124.9, 116.1, 113.3

HRMS (ESI): Calc for C₂₆H₁₈S₂ [M+H]⁺ 395.0923, found 395.0936

Melting point (C₆H₆/Hexanes): 124-130 °C



Compound 10(out,out): Compound *7(out,out)* (50 mg, 0.13 mmols), phenylacetylene (50 μL, 0.31 mmols), (PPh₃)₂PdCl₂ (5 mg, 5 mol%), and copper(I) iodide (CuI, 2 mg, 10 mol%) were suspended in triethylamine (Et₃N, 1.5 mL) that had been degassed using the freeze-pump-thaw method. Argon was bubbled through the suspension for 30 minutes. The reaction mixture was heated to 35 °C overnight. After cooling to room temperature, the reaction mixture was diluted with CH₂Cl₂ (25 mL) and filtered through a pad of celite. The solvent was removed under reduced pressure. The crude residue was flushed through a silica plug (25% CH₂Cl₂/hexanes) then recrystallized from hot CH₂Cl₂/MeOH to give 33 mg (59%) of *11(out,out)* as yellow crystals.

¹H NMR (500 MHz, CDCl₃): 7.83 (d, *J*=7.5 Hz, 2H), 7.56 (2H, m), 7.42-7.39 (5H, m), 7.31 (app t, *J*=7.5 Hz, 1H), 6.51 (s, 1H)

¹³C NMR (125 MHz, CDCl₃): 141.0, 138.7, 135.9, 132.0, 129.6, 129.5, 128.7, 128.5, 127.6, 122.7, 113.9, 105.6, 84.3

HRMS (DART): calc for C₃₄H₂₂ [M+H]⁺ 431.1794, found 431.1797

Melting point (CH₂Cl₂/MeOH): 160-163 °C with decomposition

Absorbance (CHCl₃): λ_{max} = 304 nm, 402 nm

Emission (CHCl₃): λ_{em} = 485 nm, Φ_{em} = 0.63, t = 5.77 ns

Photolysis Experiments: A single isomer of compound **7** (10 mg, 0.026 mmols) was dissolved in hexanes (2.6 mL) that had previously been degassed by bubbling with Argon for 30 minutes. The reaction mixture was flushed with Argon for an additional 10 minutes. After 1.5 hours of irradiation with an Hg-pen lamp (no optical filters), the solvent was removed and the isomerization monitored by ¹H NMR. Each isomer was then resubjected to the reaction conditions and irradiated for 15.5 additional hours after which ¹H NMR indicated the isomerization had reached a photostationary state.

2.7 References

- (1) Blomquist, A. T.; Maitlis, P. M. *Proc. Chem. Soc. (London)* **1961**, 332.
- (2) (a) Huntsman, W. D.; Wristers, H. J. *J. Am. Chem. Soc.* **1963**, *85*, 3308. (b) Huntsman, W. D.; Wristers, H. J. *J. Am. Chem. Soc.* **1965**, *89*, 342. (c) Coller, B. A. W.; Heffernan, M. L.; Jones, A. J. *Aust. J. Chem.* **1968**, *21*, 1807. (d) Hopf, H. *Angew. Chem., Int. Ed. Engl.* **1970**, *9*, 732.
- (3) Toda, F.; Garratt, P. *Chem. Rev.* **1992**, *92*, 1685.
- (4) Braverman, S.; Suresh Kumar, E. V. K.; Cherkinsky, M.; Sprecher, M.; Goldberg, I. *Tetrahedron* **2005**, *61*, 3547.
- (5) For examples of the use of **2**, see: (a) Toda, F.; Akagi, K. *J. Chem. Soc., Chem. Commun.* **1970**, 764. (b) Toda, F.; Akagi, K. *Tetrahedron* **1971**, *27*, 2801. (c) Iyoda, M.; Kuwatani, Y.; Oda, M. *J. Am. Chem. Soc.* **1989**, *111*, 3761. (d) Toda, F.; Tanaka, K.; Sano, I.; Isozaki, T. *Angew. Chem.* **1994**, *106*, 1856. (e) Kuwatani, Y.; Yamamoto, G.; Iyoda, M. *Org. Lett.* **2003**, *5*, 3371. (f) Kuwatani, Y.; Yamamoto, G.; Oda, M.; Iyoda, M. *Bull. Chem. Soc. Jpn.* **2003**, *5*, 2188.
- (6) Toda, F.; Kumada, K.; Ishiguro, N.; Akagi, K. *Bull. Chem. Soc. Jpn.* **1970**, *43*, 3535.

-
- (7) Toda, F. *J. Chem. Soc., Chem. Commun.* **1969**, 1219.
- (8) Brandsma, L. *Synthesis of Acetylenes, Allenes and Cumulenes*; Elsevier: Oxford, **2004**, 235–265.
- (9) (a) Ulman, A.; Manassen, J. *J. Am. Chem. Soc.* **1975**, *97*, 6540. (b) Smith, C. D.; Tchabanenko, K.; Adlington, R. M.; Baldwin, J. E. *Tetrahedron Lett.* **2006**, *47*, 3209.
- (10) Landor, S. R.; Demetriou, B.; Evans, R. J.; Grzeskowiak, R.; Devey, P. *J. Chem. Soc., Perkin Trans. 2* **1972**, 1995.
- (11) Jacobs, T. L.; Brill, W. F. *J. Am. Chem. Soc.* **1953**, *75*, 1314.
- (12) (a) Kleveland, K.; Skattebøl, L. *J. Chem. Soc., Chem. Commun.* **1973**, 432. (b) Hopf, H.; Lenich, F. Th. *Chem. Ber.* **1973**, *106*, 3461. (c) Pasto, D. J.; Yang, S.-H. *J. Org. Chem.* **1989**, *54*, 3544.
- (13) Toda, F.; Tanaka, K.; Tamashima, T.; Kato, M. *Angew. Chem. Int. Ed.* **1998**, *37*, 2724.
- (14) Pasto, D. J.; Kong, W. *J. Org. Chem.* **1989**, *54*, 4028.
- (15) (a) Saito, S.; Hirayama, K.; Kabuto, C.; Yamamoto, Y. *J. Am. Chem. Soc.* **2000**, *122*, 10776. (b) Bouwkamp, M. W.; Bowman, A. C.; Lobkovsky, E.; Chirik, P. J. *J. Am. Chem. Soc.* **2006**, *128*, 13340. (c) Alcaide, B.; Almendros, P.; Aragoncillo, C. *Chem. Eur. J.* **2009**, *15*, 9987. (d) Alcaide, B.; Almendros, P.; Aragoncillo, C. *Chem. Soc. Rev.* **2010**, *39*, 783. (e) Kitagaki, S.; Kajita, M.; *Org. Lett.* **2012**, *14*, 1366.
- (16) Roberts, B. W.; Wissner, A. *J. Am. Chem. Soc.* **1972**, *94*, 7168.
- (17) For examples of this methodology in the synthesis of polycyclic aromatic compounds, see: (a) Tovar, J. D.; Swager, T. M. *Adv. Mater.* **2001**, *13*, 1775. (b) Tovar, J. D.; Rose, A.; Swager, T. M. *J. Am. Chem. Soc.* **2002**, *124*, 7762.

Chapter 2 Appendix
**¹H-NMR and ¹³C-NMR Spectra
And Additional Figures**

Adapted from: Parkhurst, R. R.; Swager, T. M. "Synthesis of 3,4-Bis(benzylidene)cyclobutenes," *Synlett*, **2011**, 1519.

Table A2.1. X-ray crystallographic data.

	7 (<i>in,out</i>)	7 (<i>in,in</i>)	7 (<i>out,out</i>)
Empirical formula	C ₁₈ H ₁₂ Br ₂	C ₁₈ H ₁₂ Br ₂	C ₁₈ H ₁₂ Br ₂
Formula weight (g mol ⁻¹)	388.101	388.101	388.101
a (Å)	11.760	7.715	13.470
b (Å)	17.231	9.781	5.621
c (Å)	7.449	11.105	20.515
α (°)	90.00	69.84	90.00
β (°)	104.63	81.16	104.08
γ (°)	90.00	71.65	90.00
Volume (Å ³)	1460.50	745.69	1506.63
Space group	<i>P</i> 2 ₁ / <i>c</i>	<i>P</i> -1	<i>P</i> 2/ <i>n</i>
Calculated density (g cm ⁻³)	1.765	1.728	1.711
<i>Z</i>	4	2	4
Temperature (°C)	-173.0	-173.0	-173.0
R(<i>F</i>)	0.0228	0.0289	0.0725
R _w (<i>F</i> ²)	0.0589	0.0737	0.2136

^aX-ray crystal structure data collected and solved by Dr. Peter Müller.

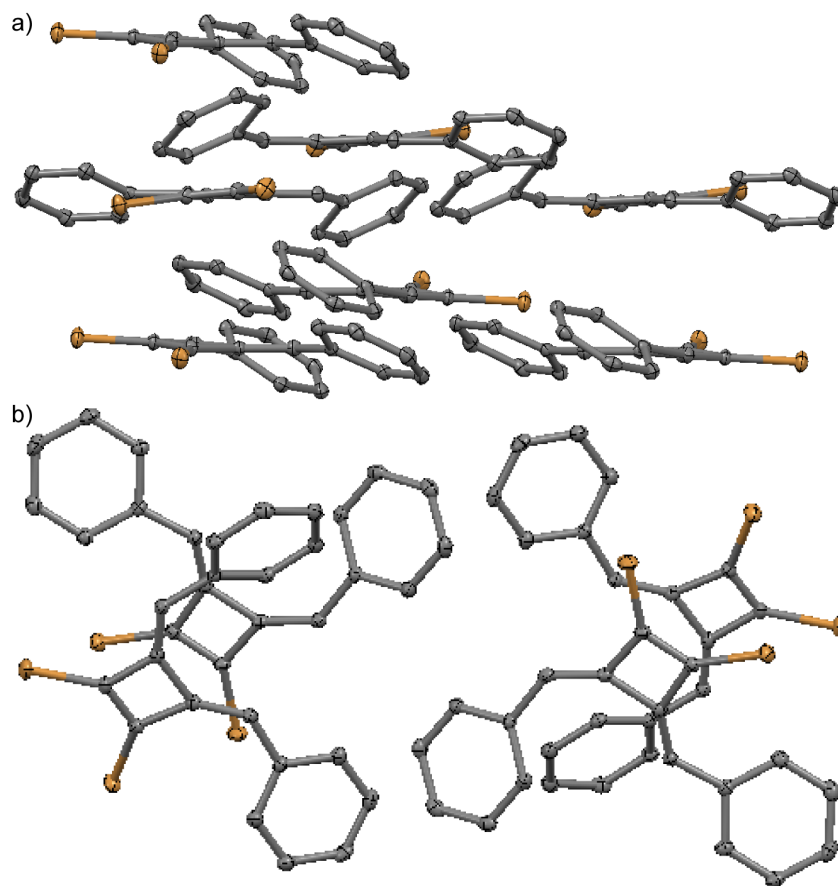


Figure A2.1. Crystal packing in the X-ray crystal structure of **7**(*in,out*). X-ray quality crystals were grown from slow evaporation of a solution **7**(*in,out*) in CH₂Cl₂/MeOH. Anisotropic thermal ellipsoids set at 50% probability.

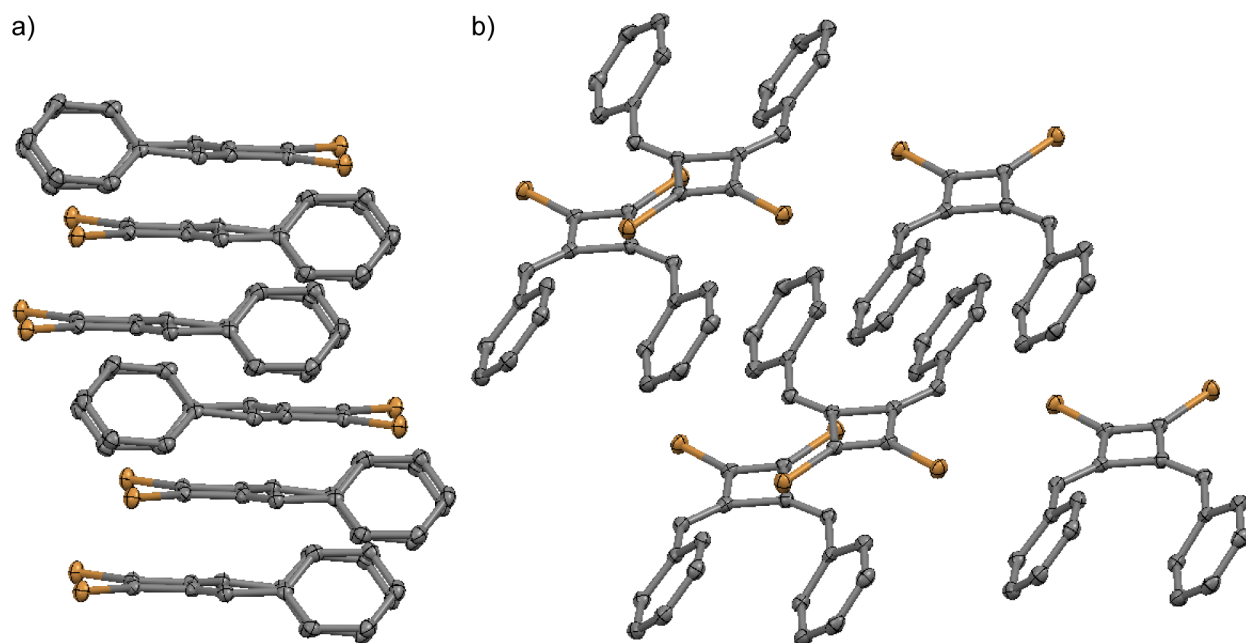


Figure A2.2. Crystal packing in the X-ray crystal structure of **7**(*in,in*). X-ray quality crystals were grown from slow evaporation of a solution **7**(*out,out*) in CH₂Cl₂/MeOH. Anisotropic thermal ellipsoids set at 50% probability.

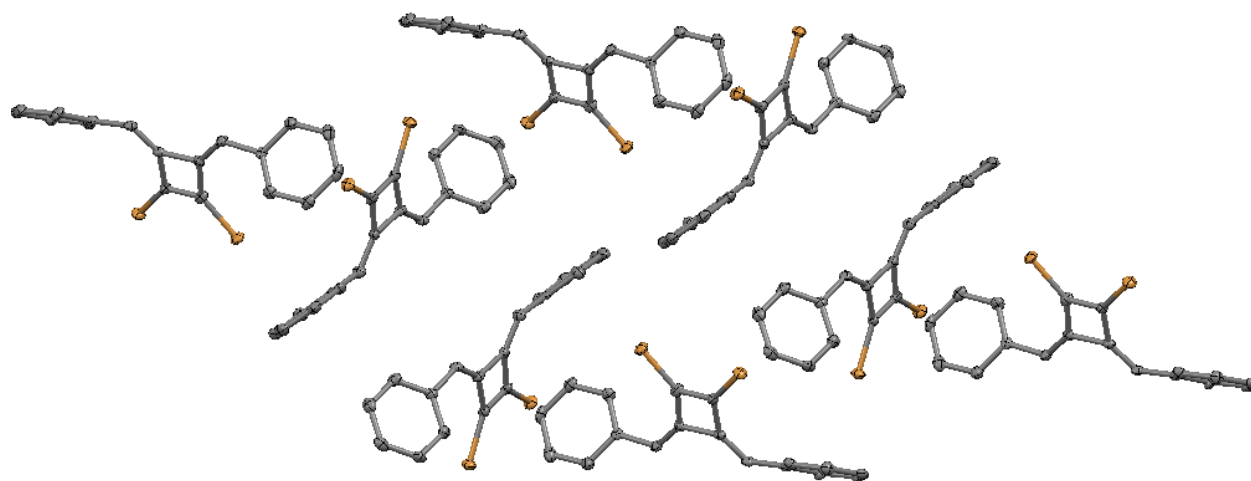
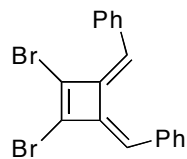
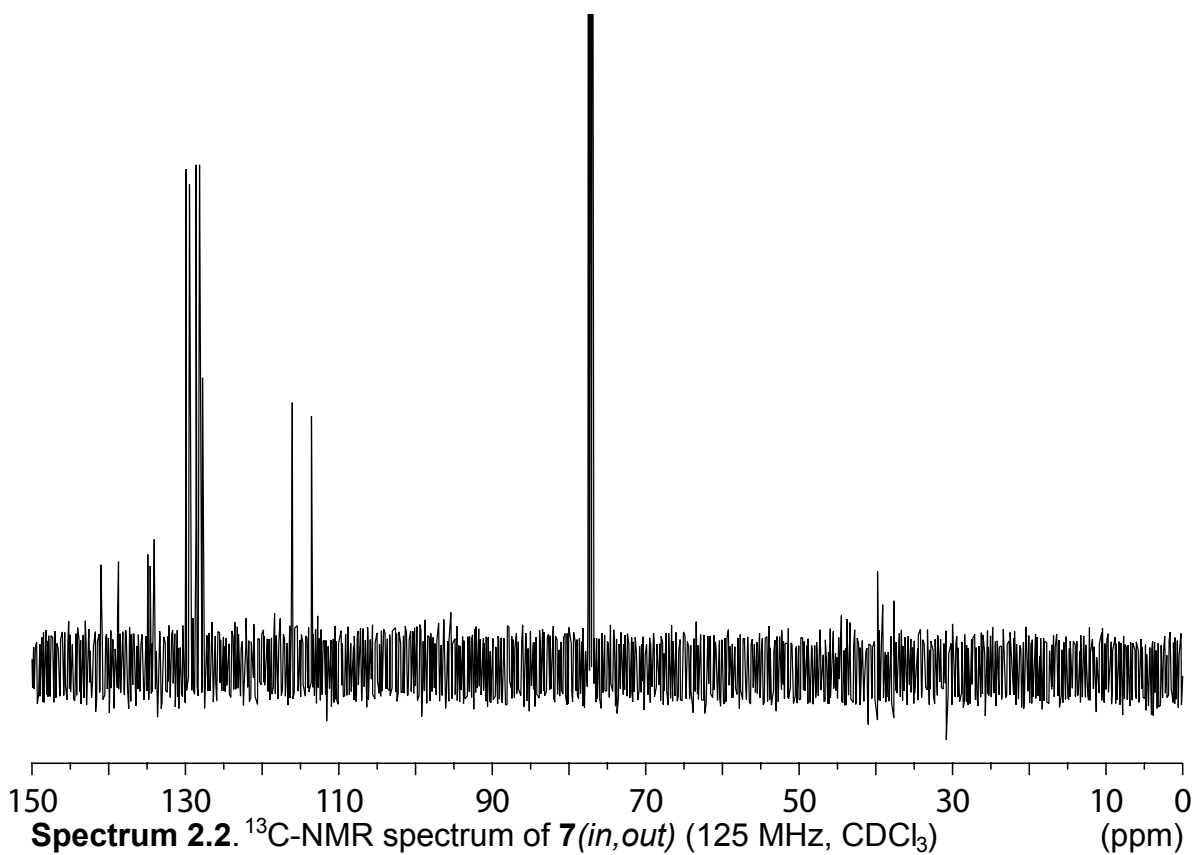
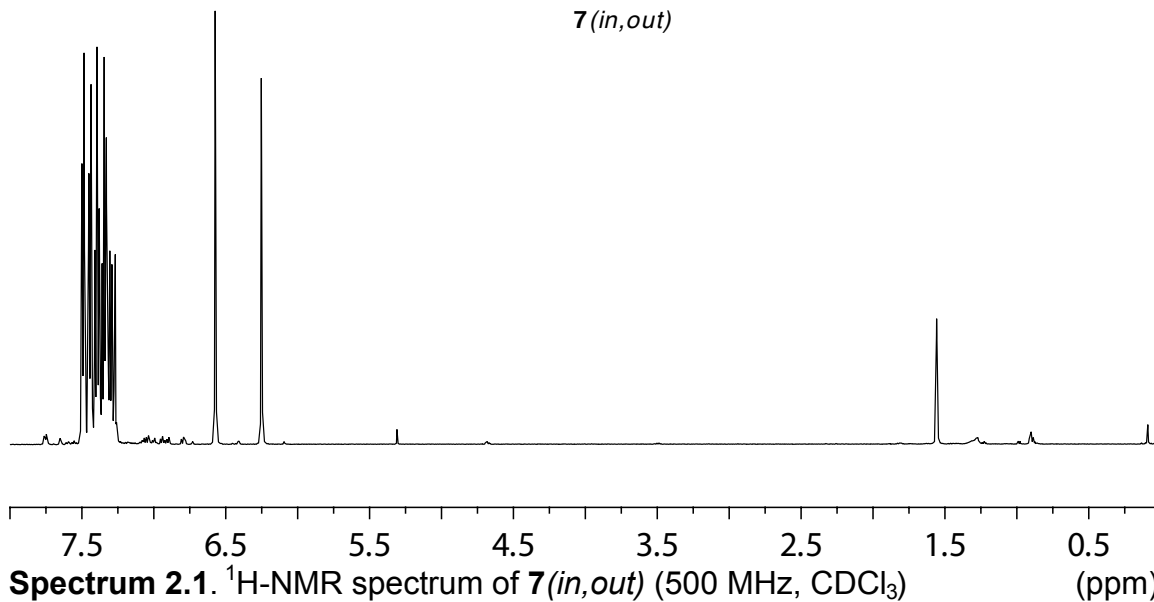
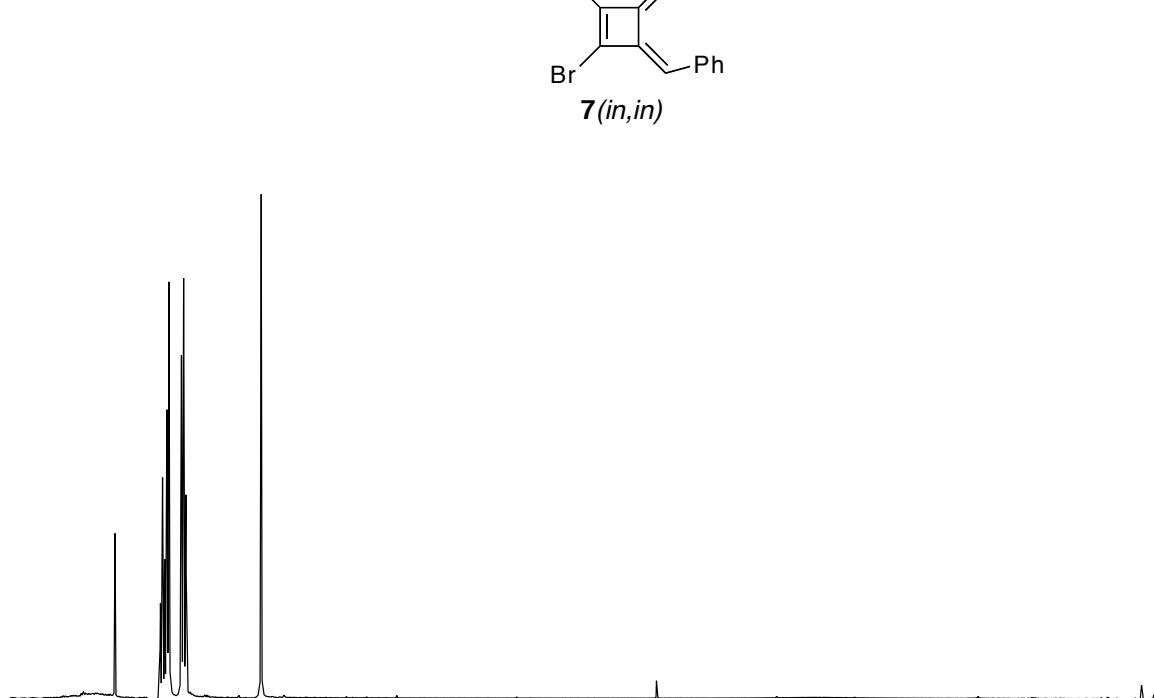
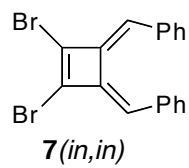


Figure A2.3 Crystal packing in the X-ray crystal structure of **7**(*out,out*). X-ray quality crystals were grown from slow vapor diffusion of MeOH into a solution **7**(*out,out*) in CHCl₃. Anisotropic thermal ellipsoids set at 50% probability.

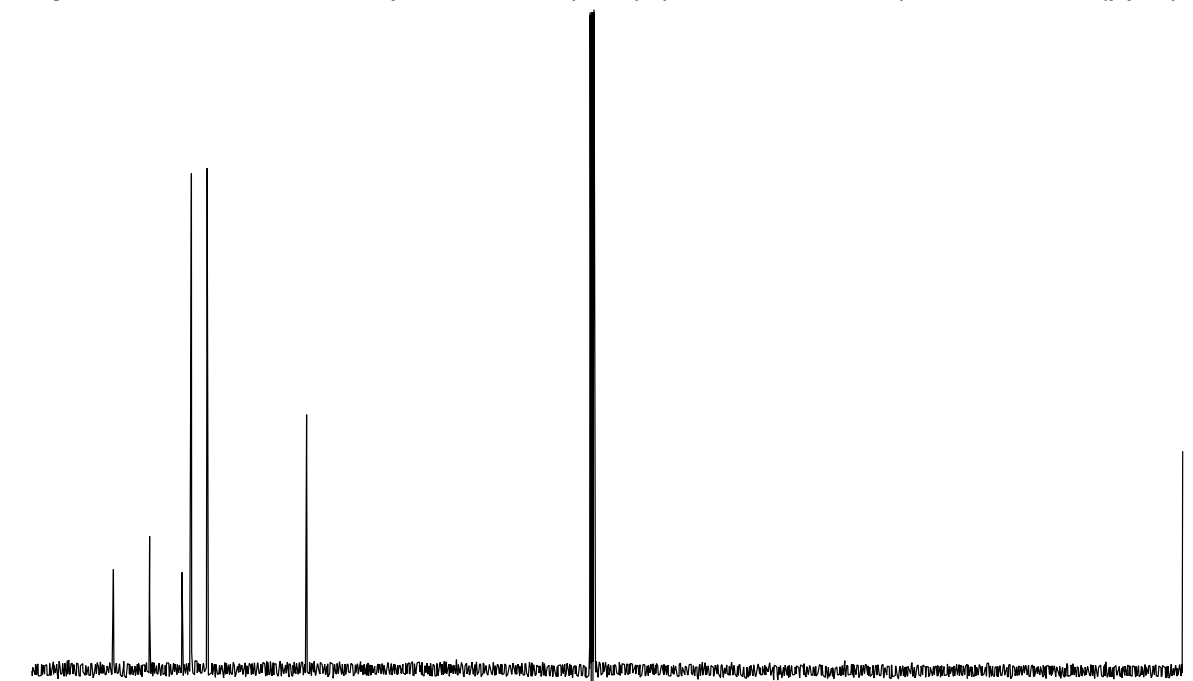


7(*in,out*)

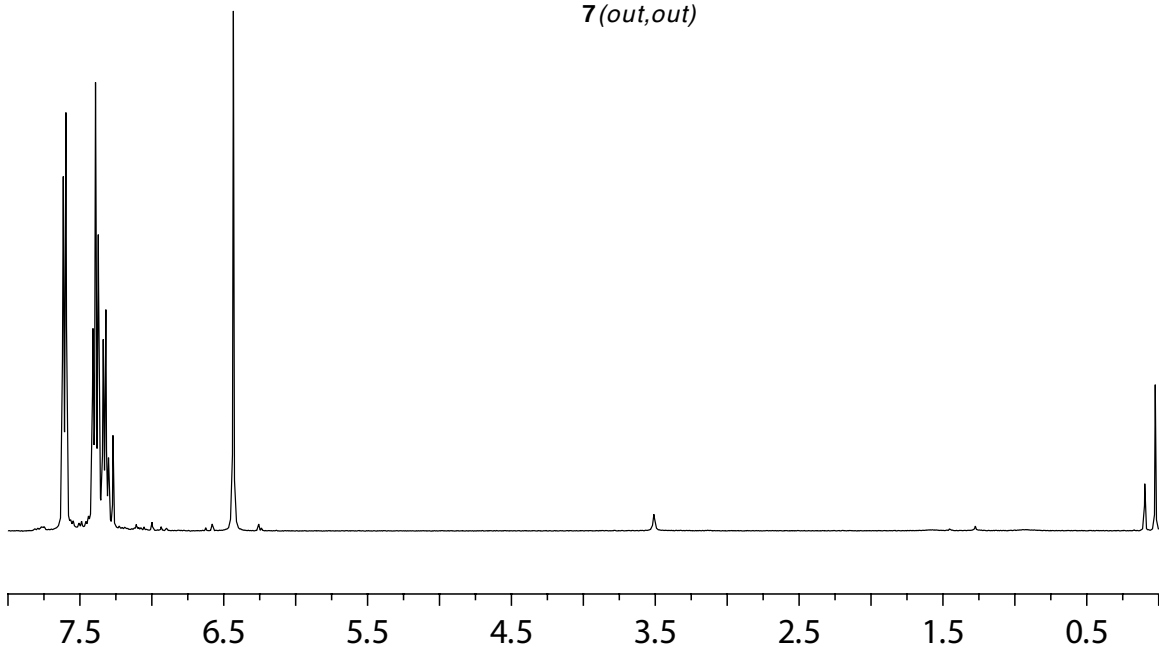
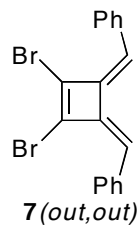




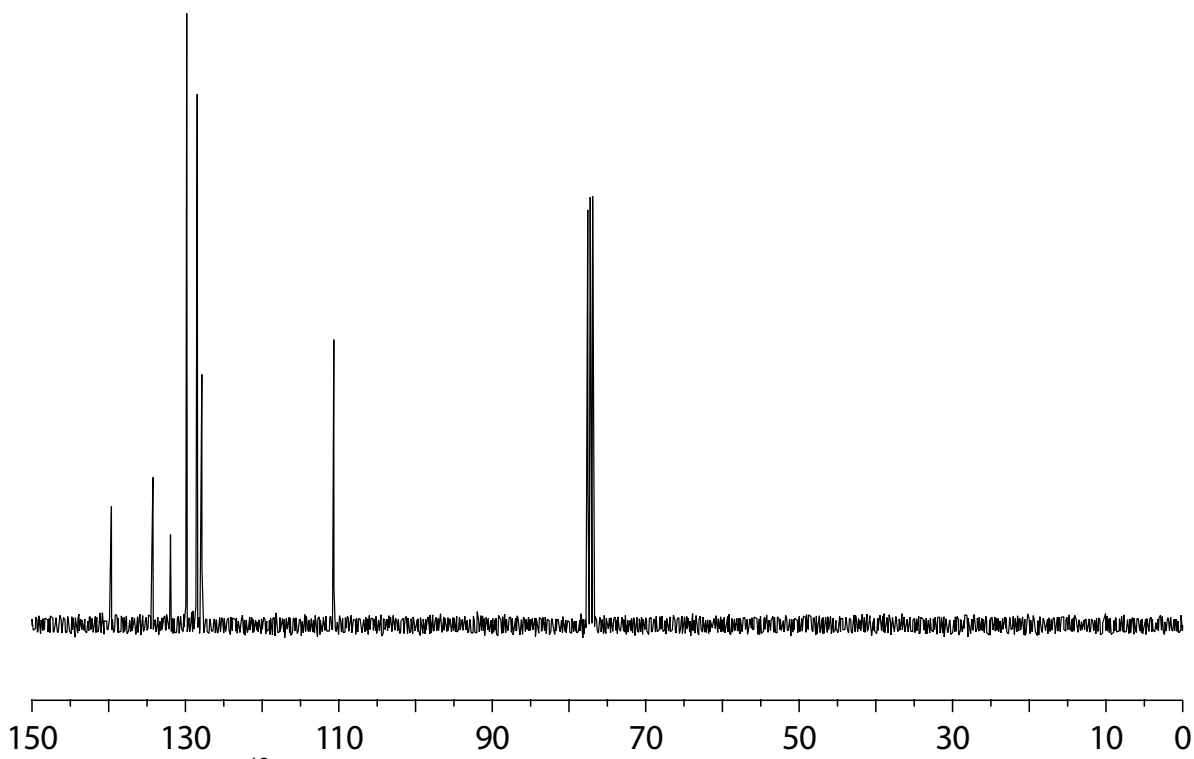
Spectrum 2.3. ¹H-NMR spectrum of **7** (*in, in*) (500 MHz, CDCl₃) (ppm)



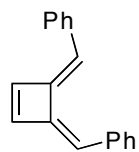
Spectrum 2.4. ¹³C-NMR spectrum of **7** (*in, in*) (125 MHz, CDCl₃) (ppm)



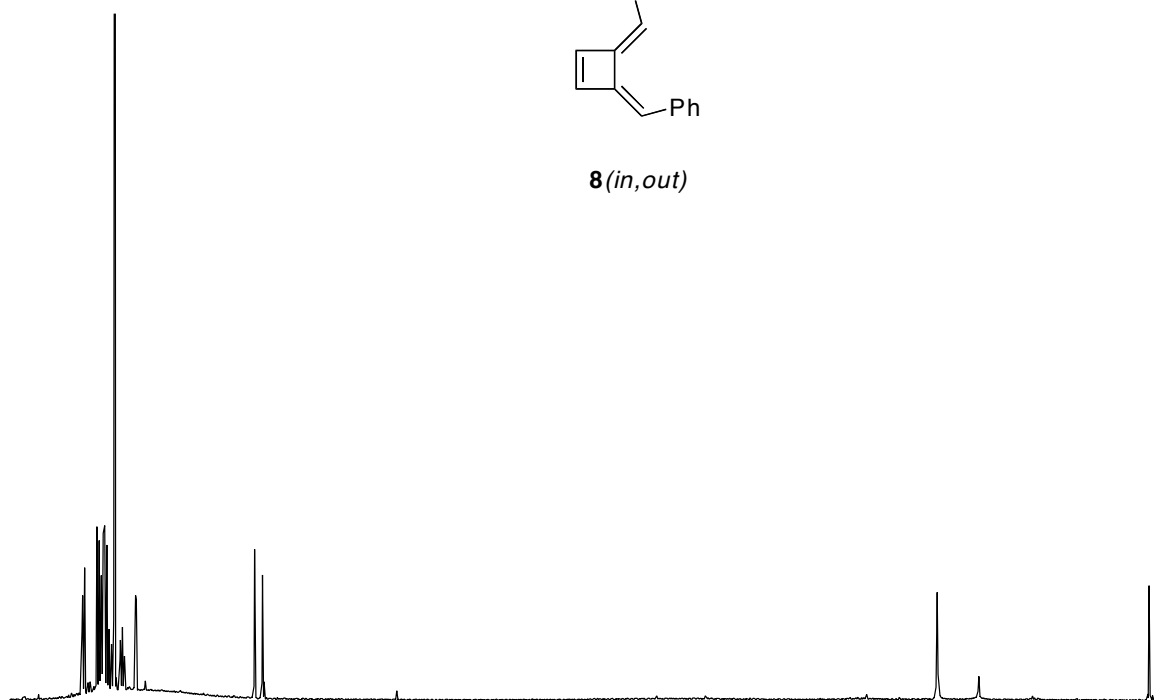
Spectrum 2.5. ¹H-NMR spectrum of *7(out,out)* (400 MHz, CDCl₃) (ppm)



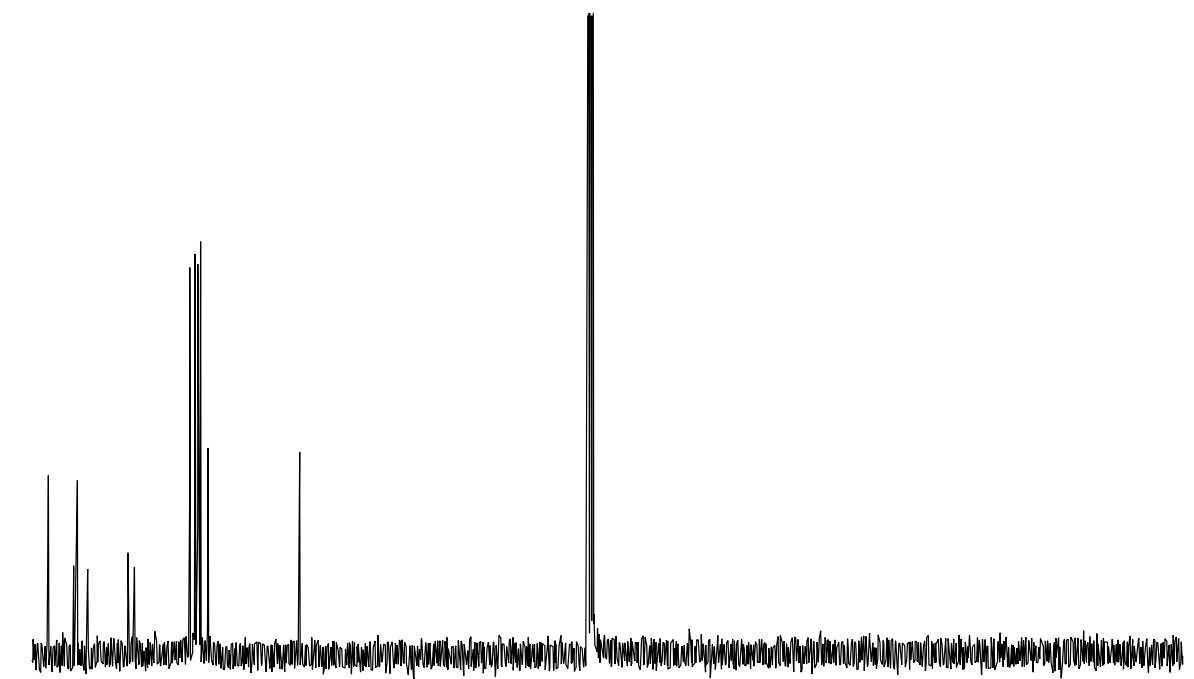
Spectrum 2.6. ¹³C-NMR spectrum of *7(out,out)* (100 MHz, CDCl₃) (ppm)



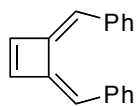
8(*in,out*)



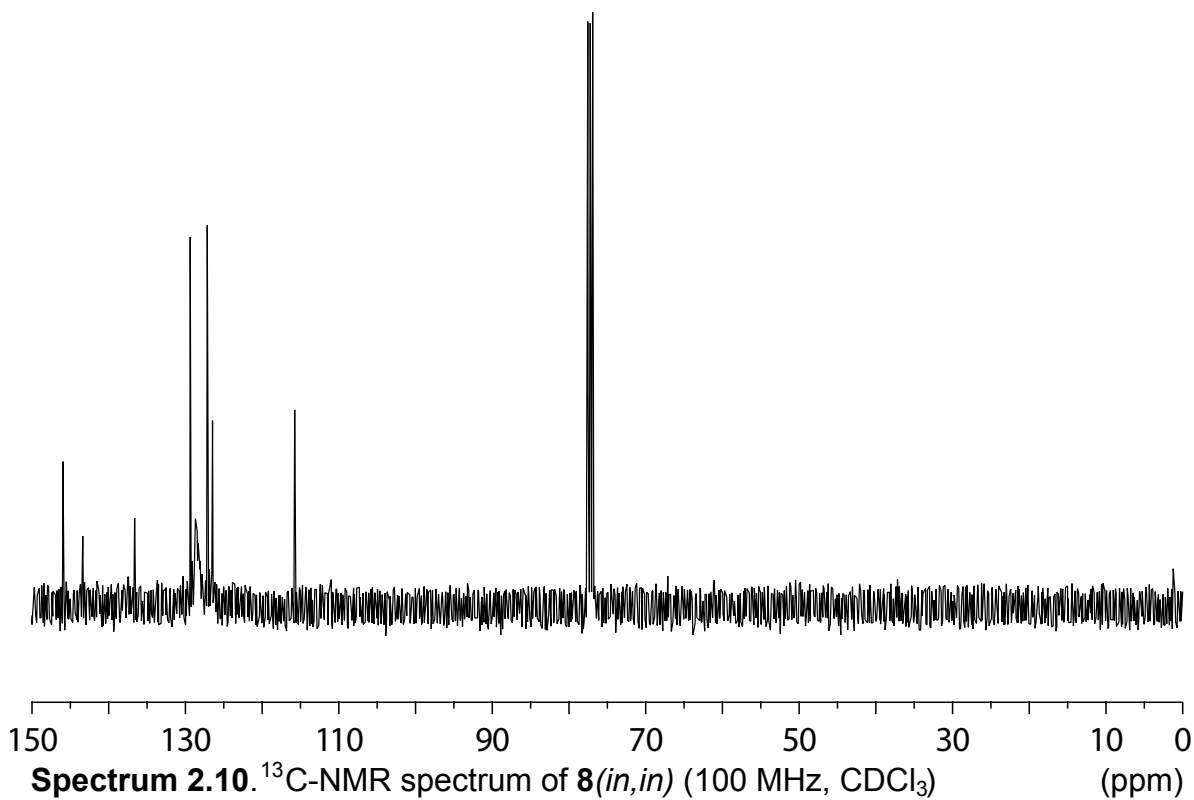
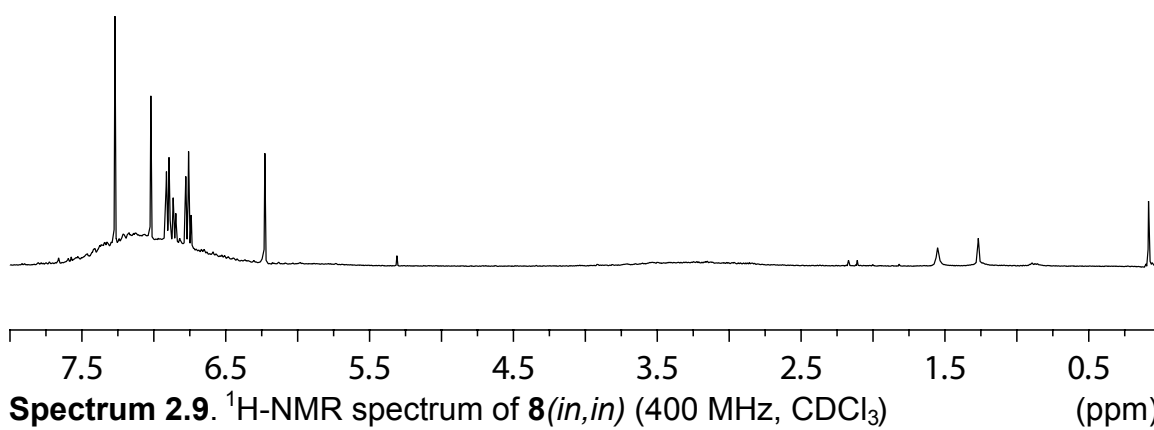
Spectrum 2.7. ¹H-NMR spectrum of **8**(*in,out*) (400 MHz, CDCl₃) (ppm)

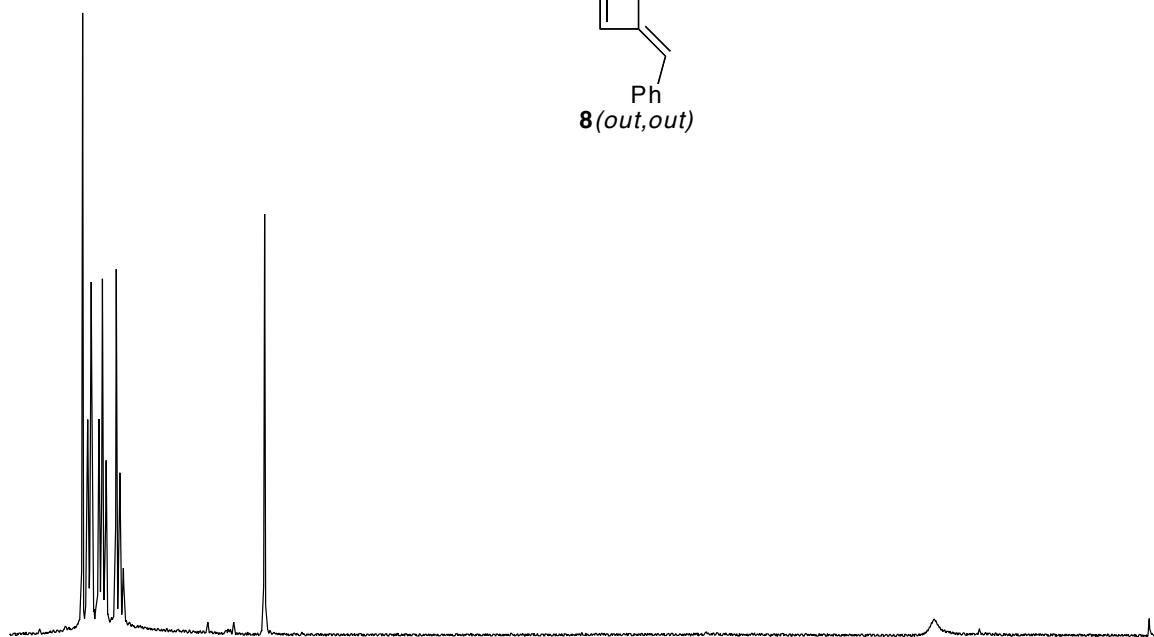
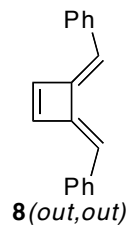


Spectrum 2.8. ¹³C-NMR spectrum of **8**(*in,out*) (100 MHz, CDCl₃) (ppm)

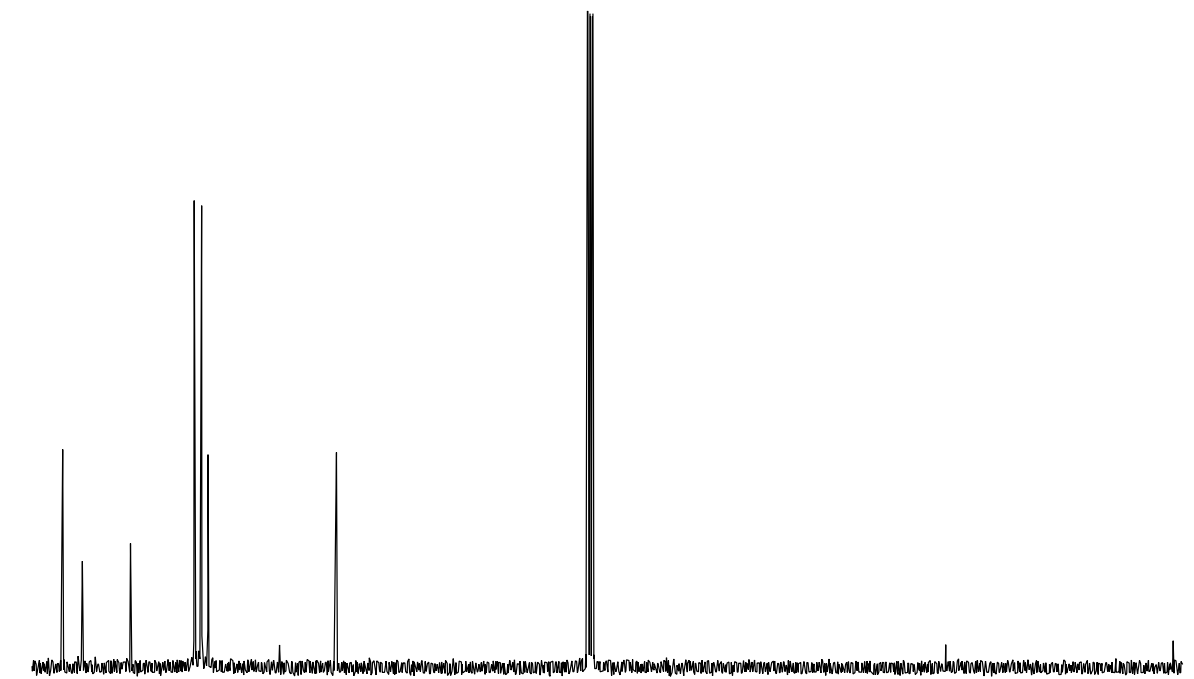


8 (*in, in*)



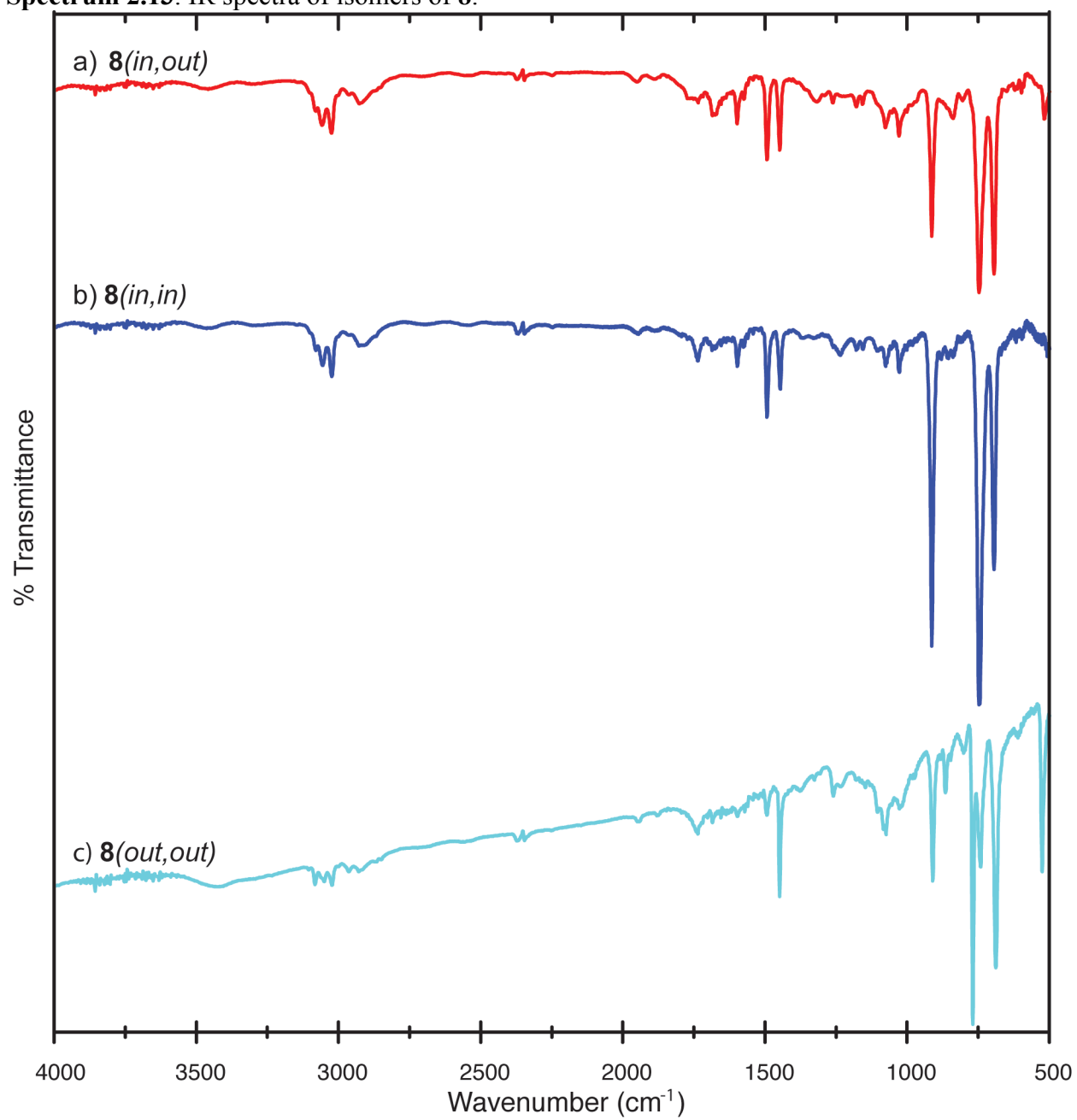


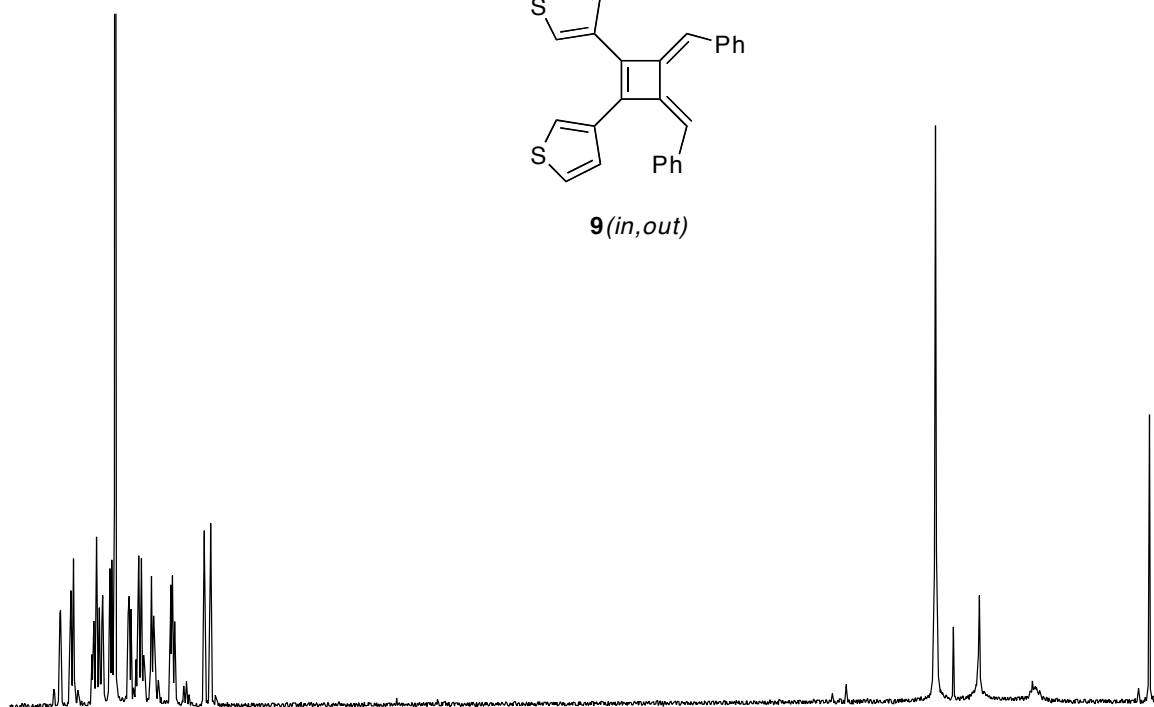
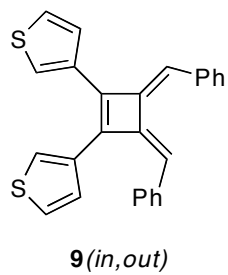
Spectrum 2.11. ¹H-NMR spectrum of **8(out,out)** (400 MHz, CDCl₃) (ppm)



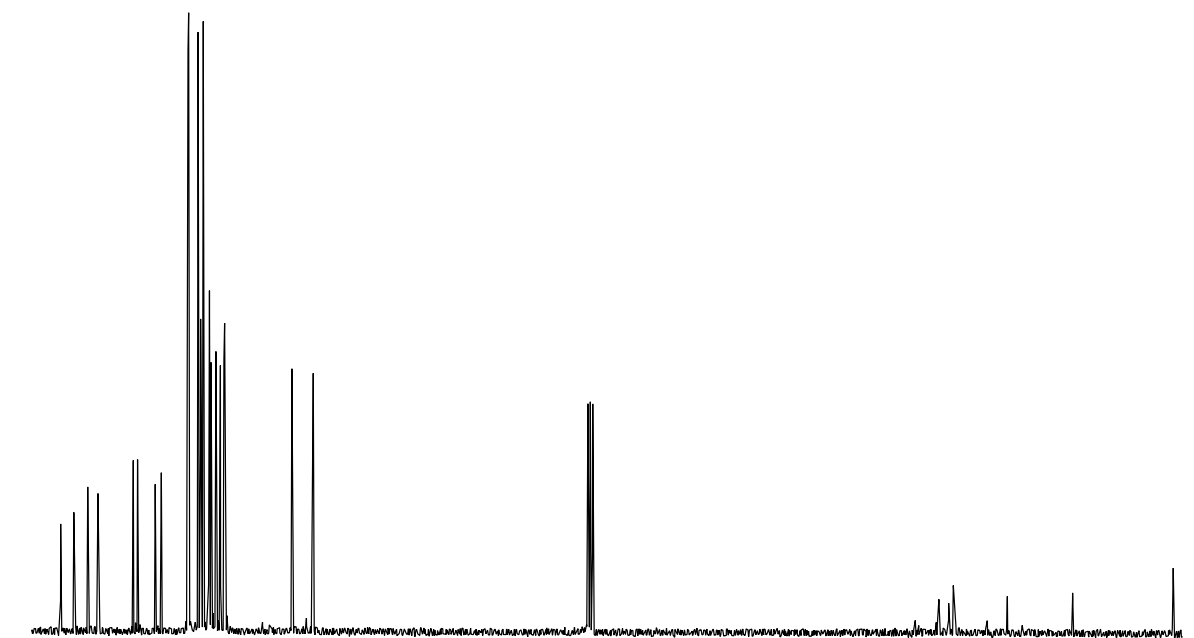
Spectrum 2.12. ¹³C-NMR spectrum of **8(out,out)** (100 MHz, CDCl₃) (ppm)

Spectrum 2.13. IR spectra of isomers of **8**.

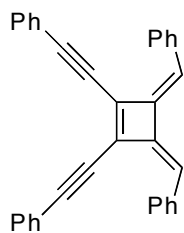




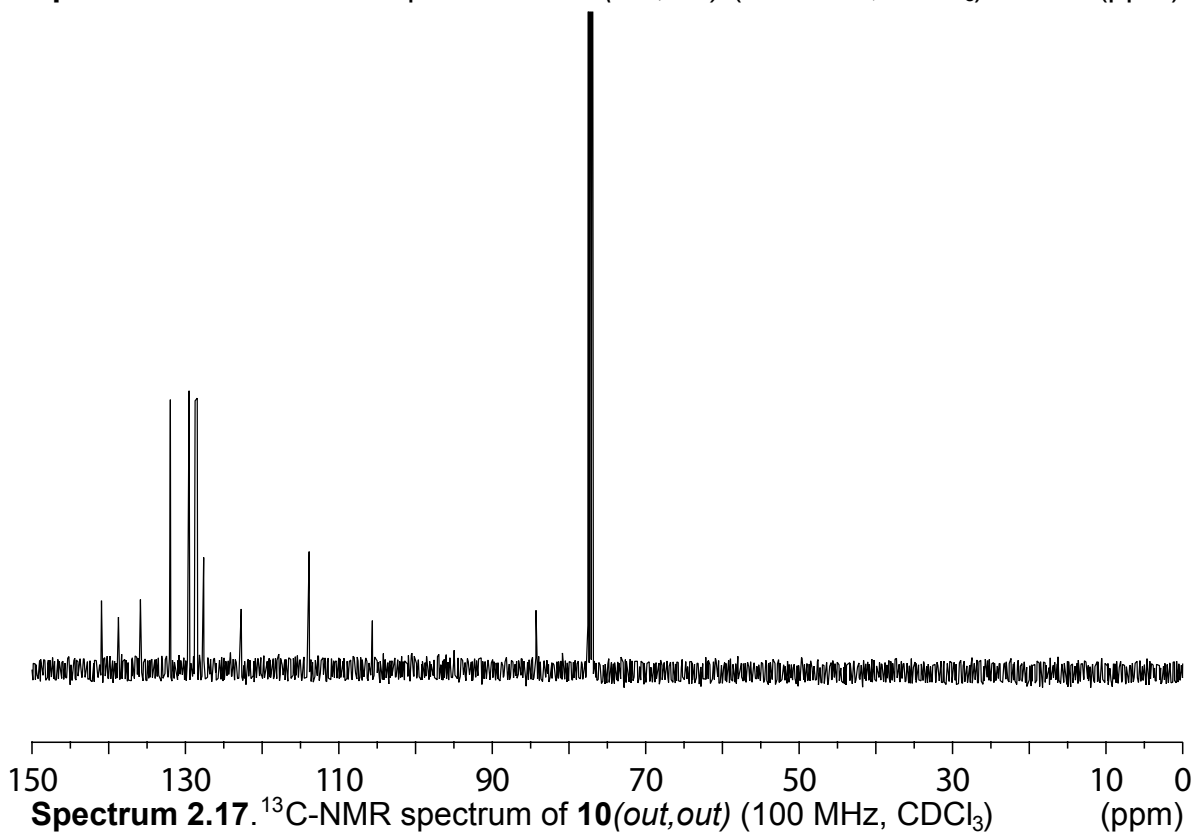
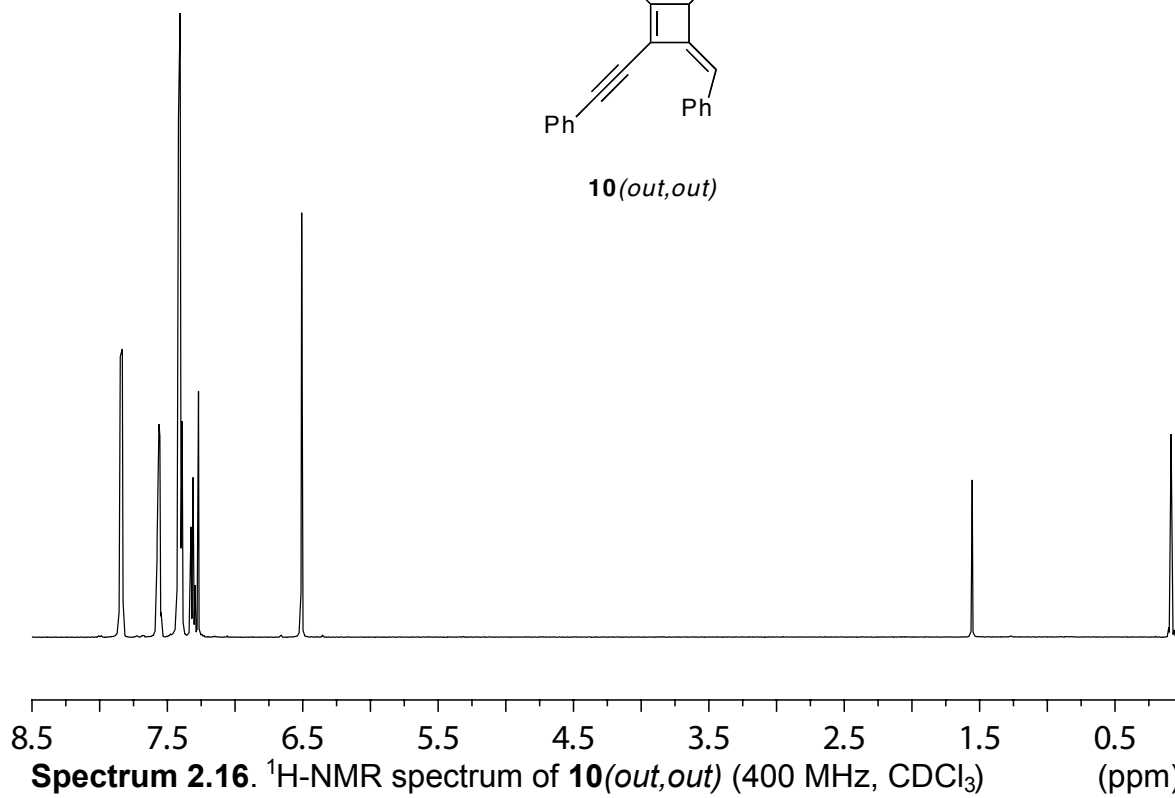
Spectrum 2.14. ¹H-NMR spectrum of **9**(*in,out*) (400 MHz, CDCl₃) (ppm)



Spectrum 2.15. ¹³C-NMR spectrum of **9**(*in,out*) (100 MHz, CDCl₃) (ppm)



10(out,out)



Chapter 3

Synthesis and Optical Properties of Phenylene-Containing Oligoacenes (POAs)

Adapted from: Parkhurst, R. R.; Swager, T. M. "Synthesis and Optical Properties of Phenylene-Containing Oligoacenes (POAs)," **2012**, *submitted*.

3.1 Introduction

The promise of organic electronics to enable the creation of inexpensive, flexible, and multifunctional devices¹ is presently limited by access to stable high performance materials. One strategy to develop high performance materials is to create extended rigid aromatic systems that have a fixed conformation to promote delocalization and minimize energetic disorder in the electronic states. Among the polycyclic aromatic hydrocarbons (PAHs), acenes, defined as linearly annelated arenes with the fewest number of rings containing Clar sextets,² are considered one of the most important candidates for high performance organic semiconductors (Figure 3.3a).

A natural strategy to create higher charge mobilities in an organic material is to increase the spatial electronic delocalization in the constituent molecular building blocks. However, as the length of the acene increases, the reduction in aromaticity also gives to a rapid decrease in the HOMO-LUMO gap, and the chemical stability of these materials becomes problematic (Figure 3.1). The higher acene homologs do appear to have improved electronic properties such as increasing charge mobility, decreasing reorganization energy, and a predicted decrease in exciton binding energy. This final property is appealing for solar cell applications, where recently the unique ability of acenes to undergo singlet fission has been of interest as method of creating two dissociated charge carriers from a single photon.³

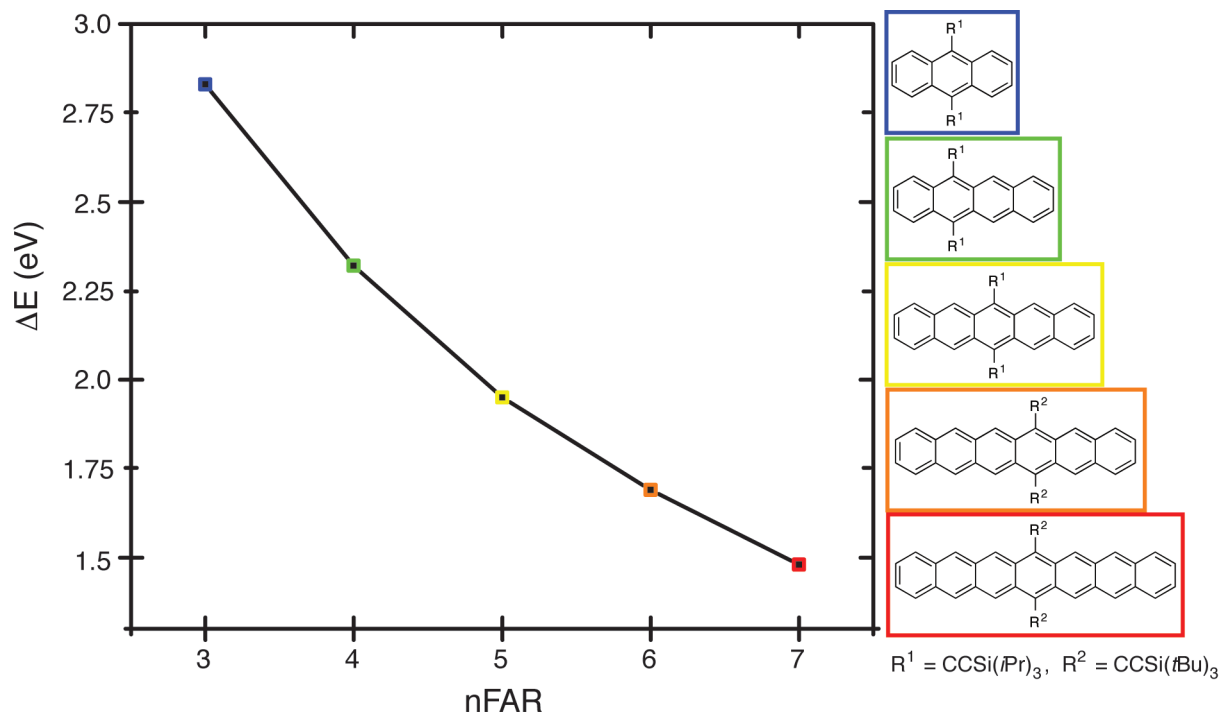
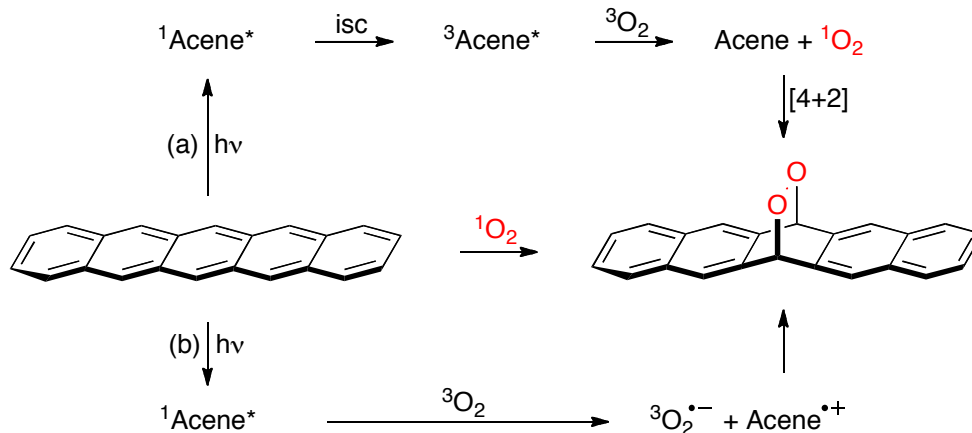


Figure 3.1. Rapidly decreasing band gap (E_g (eV), estimated from lowest energy λ_{\max}) versus number of fused aromatic rings (nFAR) of the trialkylsilylethynyl-substituted acenes.⁴

The main source of instability in the higher acenes is susceptibility to photo-oxidation or photo-dimerization. The oxidation occurs *via* interaction with singlet oxygen (1O_2) and is believed to pass through one of two pathways (Scheme 3.1).⁵ A number of methods have been proposed in the literature to synthesize stable analogs of the higher acenes. One of the most successful of these methods, developed by Anthony and coworkers, is the installation of bulky (trialkylsilyl)ethynyl groups.⁴ The advantages of this functional group are threefold as exemplified by (triisopropylsilyl)ethynyl-substituted pentacene (TIPS-pentacene)^{4a}: the steric bulk of the TIPS group prevents interaction between the central, most reactive ring of pentacene and oxygen. The TIPS-ethynyl groups also encourage brick-like stacking in the solid state as opposed to the herringbone packing of unsubstituted pentacene (Figure 3.2),^{6,7} which improves π -interactions between molecules. Finally, the bulky substituents improve solubility, and therefore processability, of the material.



Scheme 3.1. Proposed pathways of photo-oxidation of pentacene; (a) [4+2] cycloaddition with singlet oxygen, or (b) charge transfer to oxygen followed by recombination.

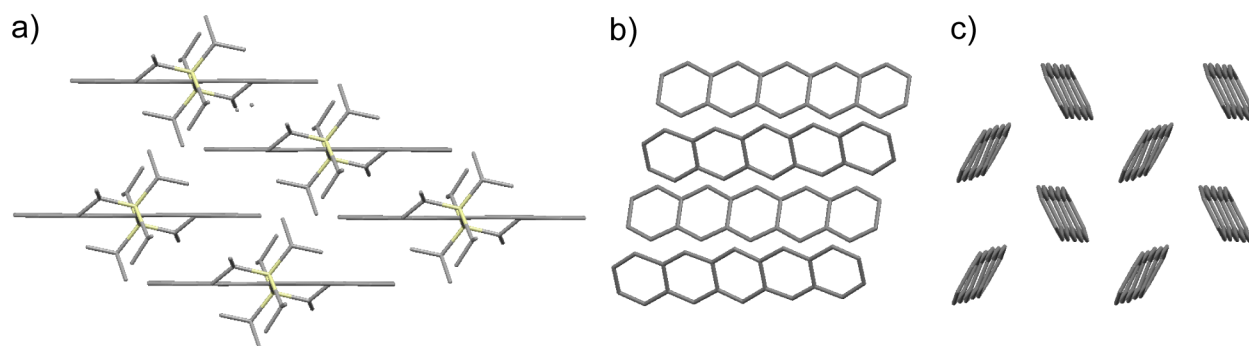


Figure 3.2. (a) Brick-like crystal packing of TIPS-Pentacene. (b) Front and (c) side views of herringbone crystal packing of pentacene. Crystal structure data from (a) ref. 4a, (b,c) ref. 7 gathered from the Cambridge Structural Database (CSD).

A close relative to the acenes are the [N]phenylenes, a family of PAHs wherein benzene rings are fused together by four-member rings, resulting in a ladder structure with alternating aromatic and antiaromatic character (Figure 3.3b).⁸ Molecules of this family are most often synthesized *via* the [2 + 2 + 2] cycloaddition methodology developed largely by Vollhardt *et al.* It has been demonstrated both experimentally and theoretically that the π -bonds in these systems tend to localize within the six-membered rings so as to minimize the 4π antiaromatic character of the cyclobutadiene linkage.⁹ We report herein that antiaromatic phenylene-linkages can be used

in conjunction with oligoacene units to create high stability extended, shape-persistent phenylene-containing oligoacenes (POAs) with interesting electronic properties.

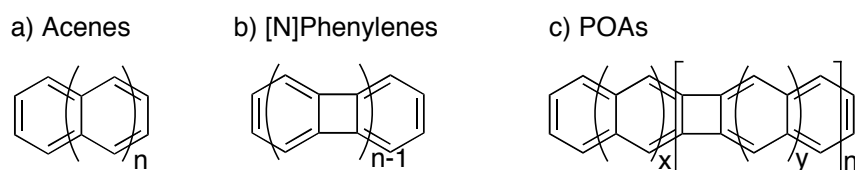
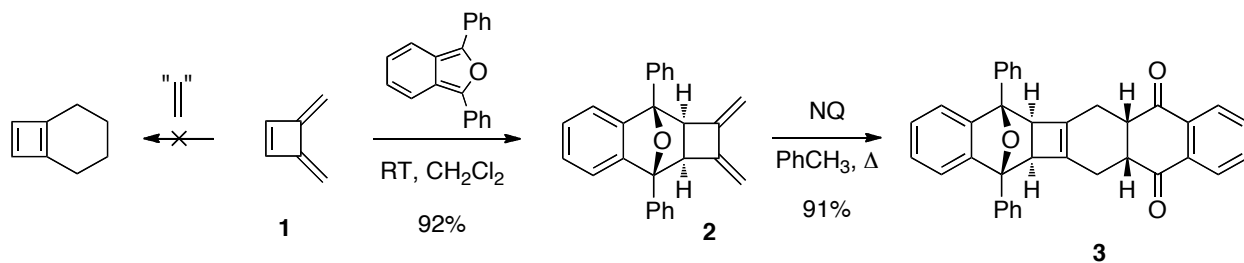


Figure 3.3. General structures of (a) acenes, (b) [N]phenylenes, and (c) phenylene-containing oligoacenes (POAs).

3.2 Diels-Alder Reactivity of 3,4-Bis(methylene)cyclobutene

The synthesis reported herein relies on the unique Diels-Alder reactivity of 3,4-bis(methylene)cyclobutene (**1**) (Scheme 3.1).¹⁰ Although the exocyclic methylene groups are locked in the desired *s-cis* conformation, **1** is not reactive as a Diels-Alder diene as the resulting product would contain cyclobutadiene. However, we have shown that initial reaction of the endocyclic double bond with a diene such as 1,3-diphenylisobenzofuran (Scheme 3.2) is facile and selective. This reaction, in turn, generates a single isomer of **2**, which is reactive as a Diels-Alder diene. A second Diels-Alder reaction with 1,4-naphthoquinone (NQ) yields a single isomer of polycyclic **3**.



Scheme 3.2. Sequential Diels-Alder reactions to yield **3** (NQ = naphthoquinone).

The stereoselectivity of each Diels-Alder reaction has been confirmed by both 2D NMR of compound **2** (Figure 3.4) and an X-ray crystal structure of compound **3** (Figure 3.5a). The Heteronuclear Single Quantum Coherence (HSQC) and Heteronuclear Multiple Bond Correlation (HMBC) spectra of compound **2a** are shown in Figure 3.4. The significant difference between the two potential isomers is the long range coupling (J^3) between proton H^a and quaternary C1 and C2. In the energy-minimized structure of the *endo* product the torsion angles between H^a and C1 or C2 are 31° and 167° , respectively, whereas in the *exo* product these values are 77° and 57° , respectively. According to the Karplus equation,¹¹ 3J -coupling constants should be close to 0 Hz with torsion angles around 90° , and reaching local maxima of approximately 8 Hz at 0° and 10 Hz at 180° . Therefore, the lack of cross-peaks between H^a and either of the above quaternary carbons in the HMBC of **2a** indicates formation of the *exo* product.

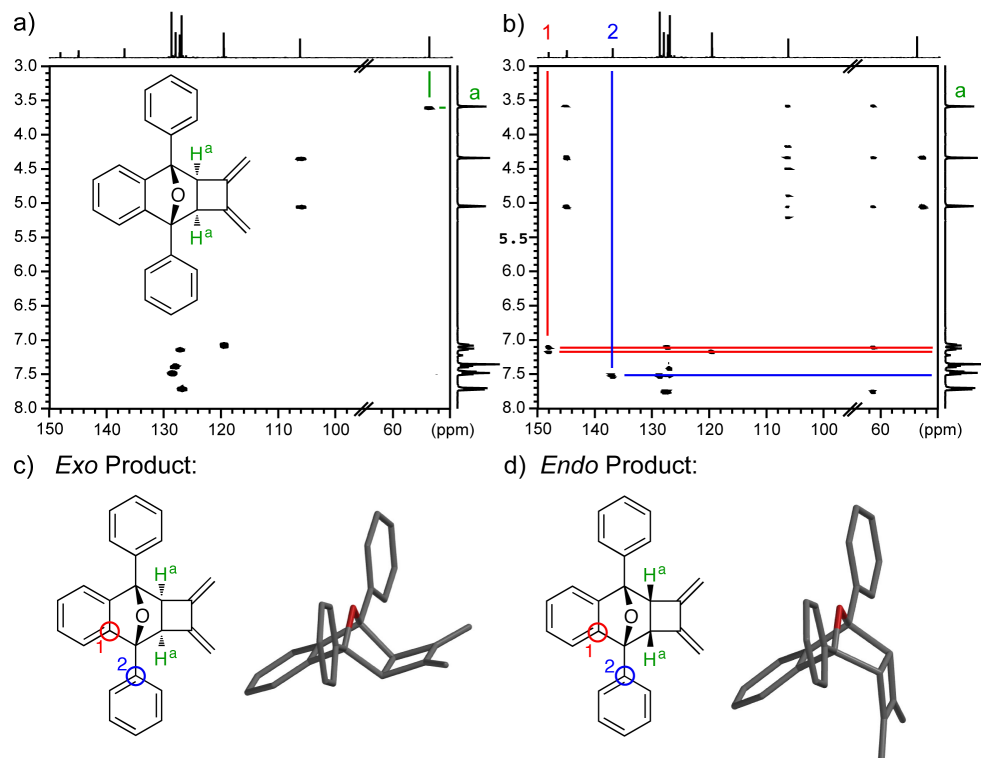


Figure 3.4. Determination of the stereochemistry of **2a**. (a) HSQC-NMR, (b) HMBC-NMR, (c) *exo*-product, and (d) *endo*-product.

Although Diels-Alder reactions of isobenzofurans tend to result in a mixture of isomers,¹² the initial reaction in this case is selective for the *exo* product, consistent with previous reports by Kaupp *et al.*¹³ Examining the LUMO of **1** (B3LYP/6-31g**, Figure 3.5b), secondary orbital interactions (SOIs) of the orbitals on C3/4 with the diene HOMO would favor the *endo* transition state, however the coefficients at this position are significantly smaller than those at C5/C6.¹⁴ The geometry of the highly strained ring brings the C5/C6 molecular orbitals closer to the reaction site, causing instead an anti-bonding interaction in the *endo* transition state. In the second Diels-Alder reaction, the product results from approach of the dienophile to the less hindered side of diene **2**.

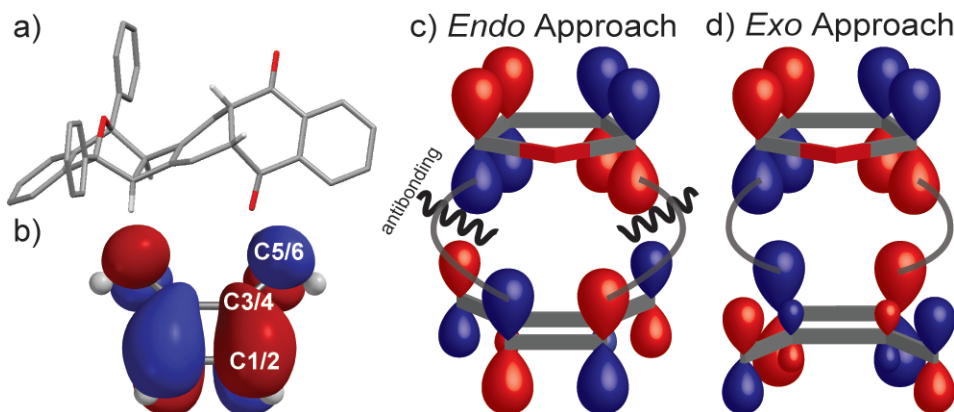
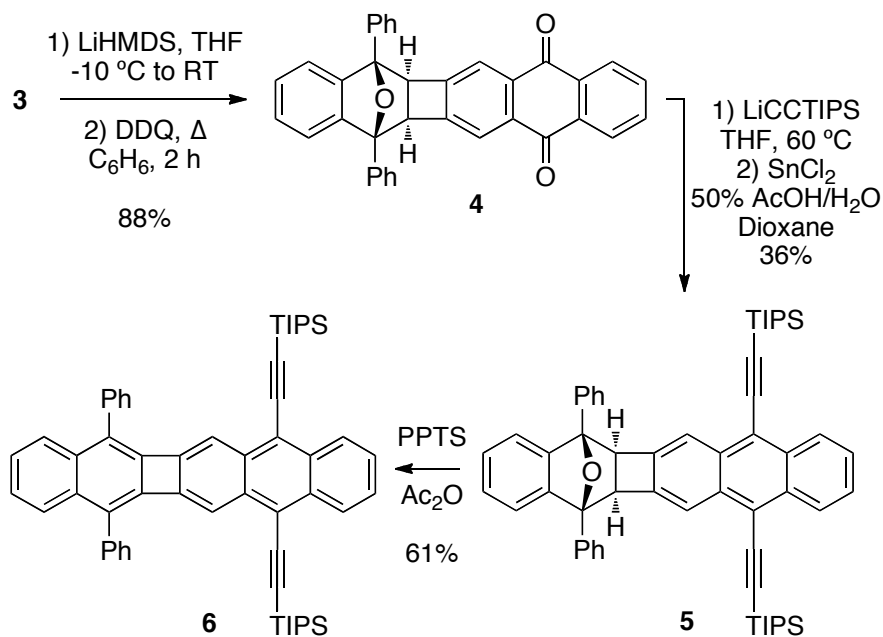


Figure 3.5. (a) X-Ray crystal structure of **3**, (b) LUMO of **1** (B3LYP/6-31g**), (c) *endo* and (d) *exo* approaches of **1** to a furan diene.

3.3 Synthesis of [2-3]Phenylene-Containing Oligoacene

With **3** in hand, its fully-unsaturated counterpart, compound **6**, is readily available through a series of synthetic transformations (Scheme 3.3). Addition of a strong base such as lithium hexamethyldisilazide (LiHMDS) generates the high-energy bis-enolate, which then

oxidizes to the 1,4-quinone, presumably by action of air introduced during the work-up. However, attempts to trap the bisenolate *in situ* with electrophiles such as bromoalkanes and triflic anhydrides were unsuccessful. DDQ is then used to aromatize the neighboring ring giving compound **4** in an 88% yield over two steps (for X-ray crystal structure of **4** see Figure A2.1, Appendix). Nucleophilic addition of TIPS-protected lithium acetylide followed by reductive deoxygenation yields the TIPS-anthracene containing compound **5**. Finally, **5** is dehydrated to give **6**. Analysis by differential scanning calorimetry (DSC) indicates the high thermal stability of POA **6** (Figure 3.6).



Scheme 3.3. Synthesis of POA **6** from compound **3**.

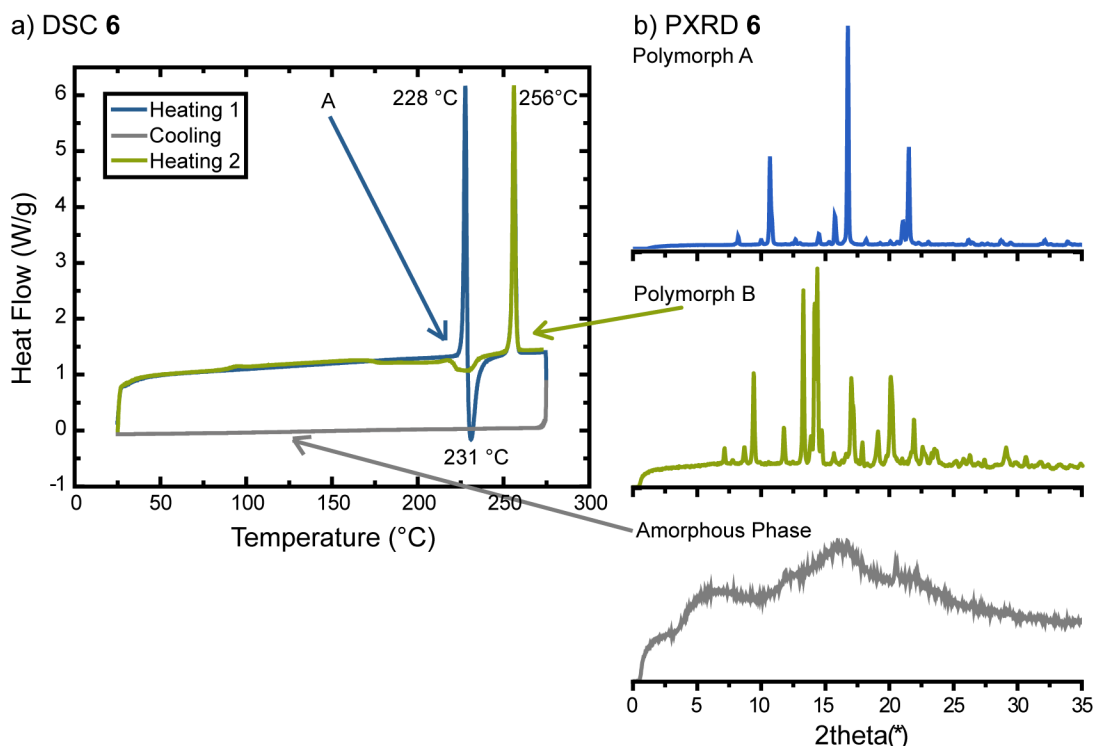
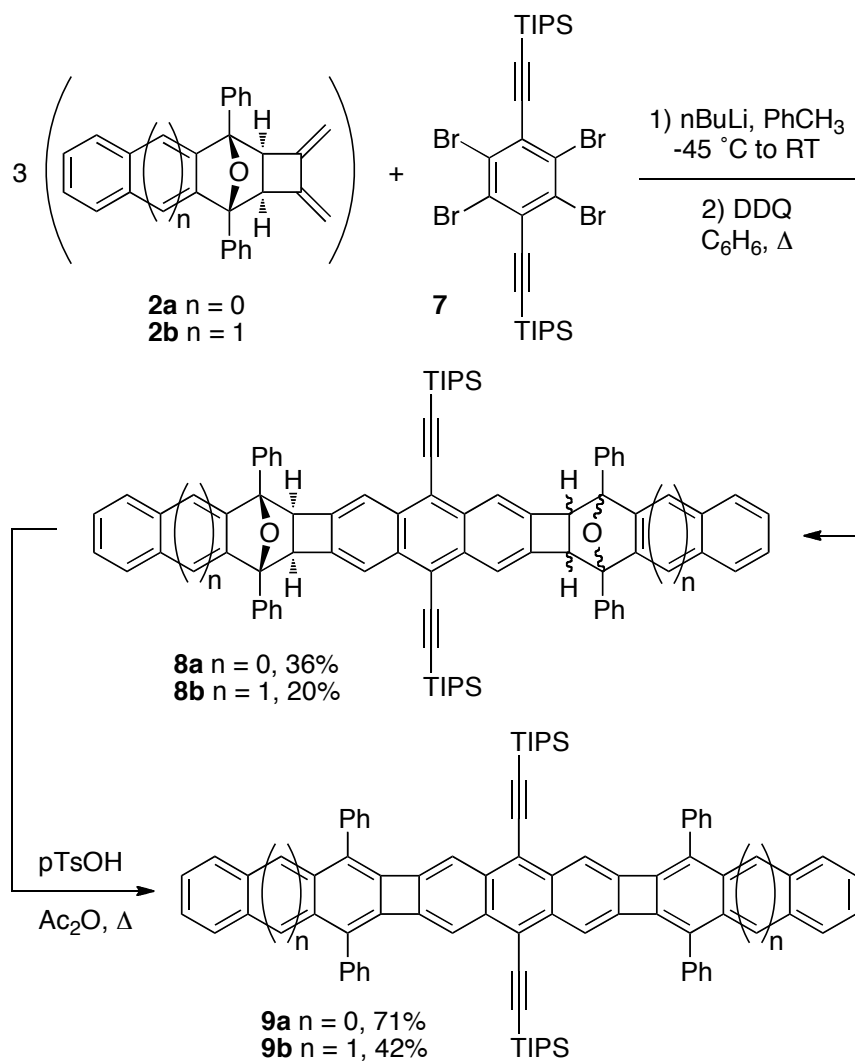


Figure 3.6. (a) DSC of POA **6** recrystallized from EtOAc to give kinetic polymorph A, which reorganizes to thermodynamic polymorph B after heating. (b) PXRD of POA **6** taken at various points during the DSC heating/cooling cycle.

3.4 Synthesis of [2-3-2] and [3-3-3]Phenylene-Containing Oligoacene

Based on the synthetic methodology demonstrated above, molecules of this family can be extended into even larger structures (Scheme 3.4). 1,3-Diphenylisobenzofuran¹⁵ can be used to generate diene **2b**. Reacting a bisfunctionalized dienophile with **2** results in symmetrical structures. As a bisaryne precursor, we chose to use 1,2,4,5-tetrabromo-1,6-bis(triisopropylsilyl)ethynylbenzene (**7**), synthesized *via* the procedure previously reported by our laboratory.¹⁶ Products from the bisaryne Diels-Alder addition of **2** with **7** were taken on to aromatization step without further purification to yield isomeric mixtures of precursors **8a/b**. Dehydration was then carried out with *p*-toluenesulfonic acid (*p*TsOH) in acetic anhydride (Ac₂O) to give the desired POAs **9a/b**.



Scheme 3.4. Bisaryne Diels-Alder reaction and aromatization to yield POAs **9a/b**.

3.5 Optical and Electrochemical Properties of POAs

Analysis of the optical properties of **6** and **9a/b** as compared to those of TIPS-anthracene (**TIPS-Anth**)¹⁷ is shown in Figures 3.7 and 3.8. The absorbance curve of compound **5** is almost identical to that of **TIPS-Anth** with the exception of a slightly lower energy absorption around 260 nm corresponding to the phenyl substituents (Figure 3.7). In the case of **6**, there are two distinct absorbances; a higher energy absorption due to the diphenylnaphthalene chromophore and lower energy absorption ($\lambda_{\text{max}} = 464\text{ nm}$) due to the diethynylanthracene chromophore. The

21 nm bathochromic shift that takes place between **TIPS-Anth** and compound **6** demonstrates that although the phenylene-linkage limits delocalization between the two chromophores there is still sufficient communication to cause a reduction in the bandgap of about 0.17 eV. A similar pattern is evident in the absorbance curves **9a/b**, with a reduction in the band gap with each increase in the length of the POA.

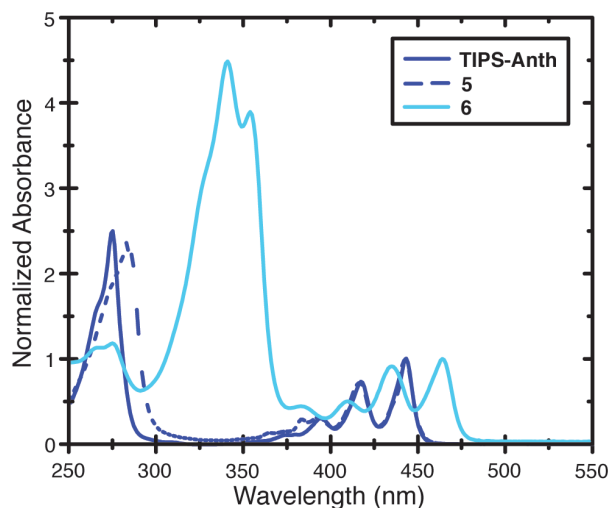


Figure 3.7. Absorbance overlay of **TIPS-Anth**, compound **5**, and compound **6** in CHCl_3 .

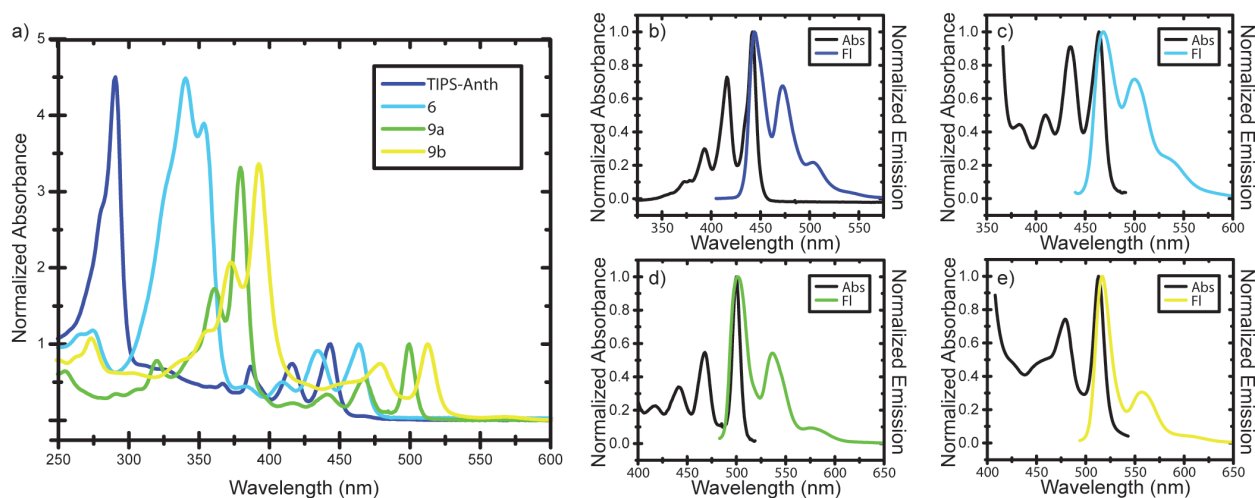


Figure 3.8. (a) Overlay of the absorbance curves of **TIPS-Anth**, **6**, and **9a/b**. Absorbance and Emission of (b) **TIPS-Anth**, $\lambda_{\text{max}} = 442 \text{ nm}$, $\lambda_{\text{em}} = 444 \text{ nm}$, $\phi_{\text{em}} = 0.97$, $\tau = 5.04 \text{ ns}$; (c) **6**, $\lambda_{\text{max}} = 464 \text{ nm}$, $\lambda_{\text{em}} = 469 \text{ nm}$, $\phi_{\text{em}} = 0.69$, $\tau = 7.72 \text{ ns}$ (d) **9a**, $\lambda_{\text{max}} = 500 \text{ nm}$, $\lambda_{\text{em}} = 502 \text{ nm}$, $\phi_{\text{em}} = 0.45$, $\tau = 5.60 \text{ ns}$, and (e) **9b**, $\lambda_{\text{max}} = 513 \text{ nm}$, $\lambda_{\text{em}} = 517 \text{ nm}$, $\phi_{\text{em}} = 0.26$, $\tau = 6.71 \text{ ns}$. All experiments were performed in CHCl_3 .

There is a corresponding bathochromic shift in the emission curve of each POA. The emission quantum yields decrease within the series from **TIPS-Anth** ($\phi_{em} = 0.94$) to **9b** ($\phi_{em} = 0.26$). In each case the Stokes shift is small, ranging from 2-5 nm, and are consistent with rigid, shape-persistent nature of these materials.

Additionally, the ionization potential and stability of the oxidized forms of the compounds were analyzed by cyclic voltammetry (CV) (Table 3.1 and Figure 3.9). The difference in the potential of the first oxidation peak (E_{ox} vs. Fc/Fc^+) of **TIPS-Anth**, **6**, and **9a** is quite small decreasing from 710 mV for **TIPS-Anth** to 678 mV for **9a**. Therefore, the reduction in the band gap for these three species can primarily be attributed to a decreasing LUMO level, confirming the oxidative stability. Although **TIPS-Anth** and **6** both undergo only one reversible oxidation, compound **9a** displays a second oxidation peak within the window studied (Figure 3.9c). Compound **9b**, alternatively, exhibits three reversible oxidation peaks, with the first two shifted to significantly lower potentials than those previously discussed (Figure 3.9d). Consistent with these findings, **9b** appears to be susceptible to oxidative degradation in the solution state (although this process is slow).

Table 3.1. Electrochemical Data for POAs.

Compound	E_{ox} (mV) ^a vs. Fc/Fc^+	HOMO (eV)	LUMO (eV)	E_g (optical) ^b (eV)
TIPS-Anth	710	-5.42	-2.68	2.74
6	702	-5.41	-2.84	2.57
9a	678	-5.39	-2.96	2.43
9b	527	-5.24	-2.87	2.37

^aPerformed in a 0.1 M solution of TBAPF₆, in CH₂Cl₂, Pt button electrode, scan rate 150 mV/s, ferrocene as an external standard. ^bDetermined from λ_{onset} in CHCl₃.

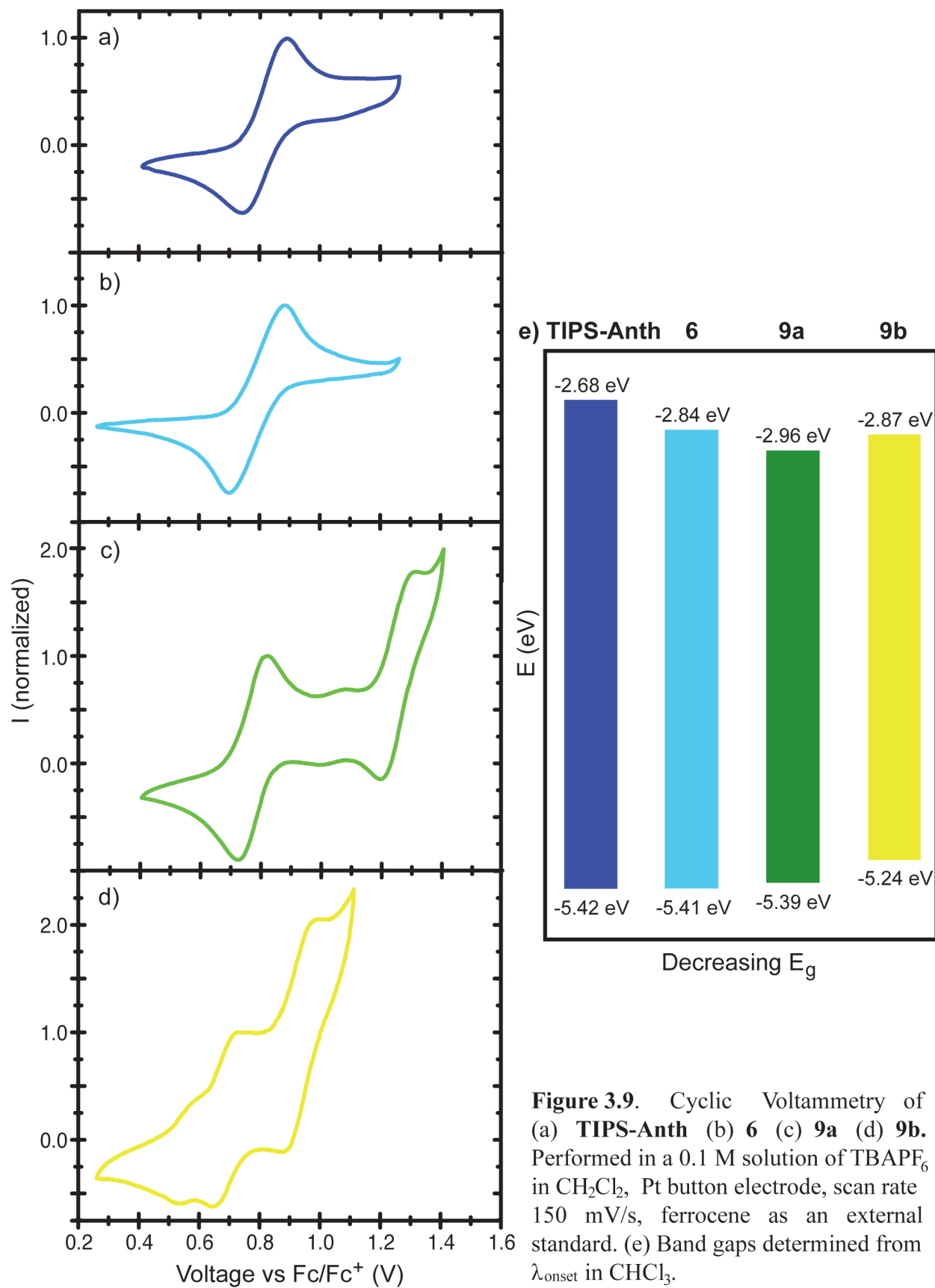


Figure 3.9. Cyclic Voltammetry of (a) TIPS-Anth (b) **6** (c) **9a** (d) **9b**. Performed in a 0.1 M solution of TBAPF₆ in CH₂Cl₂, Pt button electrode, scan rate 150 mV/s, ferrocene as an external standard. (e) Band gaps determined from λ_{onset} in CHCl₃.

3.6 X-Ray crystallography of POAs

Compounds **6** and **9a** were both analyzed by X-ray crystallography (Figure 3.10). Examination of the bond lengths around the phenylene-linkage confirms the increased localization of π -bonds, with bond lengths alternating between 1.46 Å exocyclic and 1.34 Å endocyclic to the four-membered ring. Although theoretical studies have shown [N]phenylenes to be planar in the lowest energy conformation, strain and antiaromaticity are also known to impart additional flexibility to [N]phenylenes in the solid state.⁷ In the case of **6** and **9a** there are small torsion angles around the phenylene-linkage ($5.60^\circ/1.31^\circ$ and $1.58^\circ/0.05^\circ$, respectively), however the molecules are very close to planar.

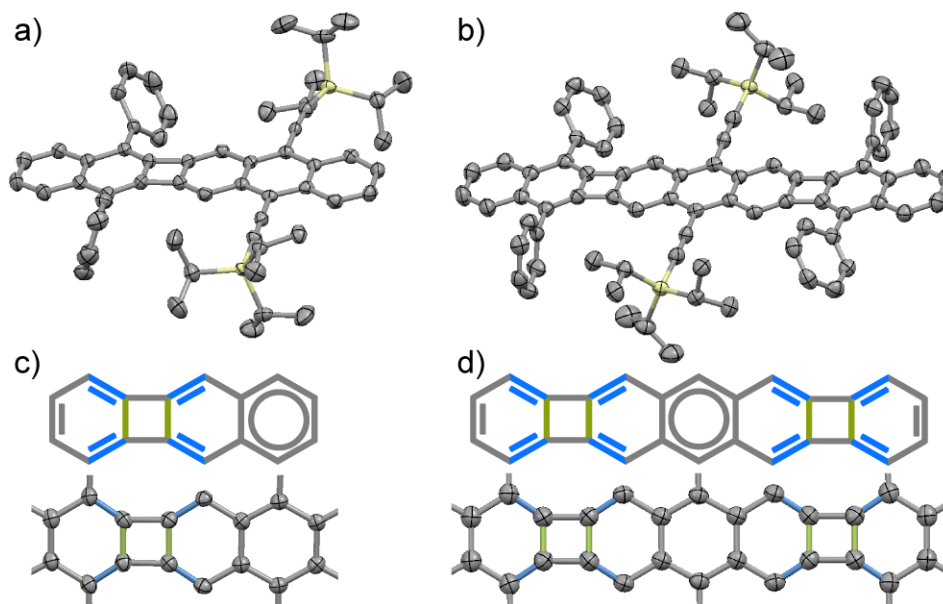


Figure 3.10. Crystal structures of (a) **6** and (b) **9a**. Localization of π -bonds in (c) **6** and (d) **9a**.

3.7 Conclusions

In conclusion, we have reported the design and synthesis of new class of non-benzenoid PAHs, Phenylene-Containing Oligoacenes. The unique reactivity of 3,4-Bismethylene-

cyclobutene was exploited to build ladder structures *via* sequential Diels-Alder reactions. The resulting POAs represent stable, shape-persistent chromophores, with band gap and quantum efficiencies that decrease as length increases. Studies on the ability of this class of molecules to exhibit singlet fission are underway.

3.8 Experimental

Materials: All reactions were carried out under argon using standard Schlenk techniques unless otherwise noted. All solvents were of ACS reagent grade or better unless otherwise noted. Anhydrous tetrahydrofuran (THF), diethyl ether (Et₂O), dichloromethane (CH₂Cl₂) and toluene (PhCH₃) were obtained from J. T. Baker and dried on a solvent column purification system. Silica gel (40 μm) was purchased from SiliCycle Inc. All reagent grade materials were purchased from Alfa Aesar or Sigma-Aldrich and used without further purification. Compound **1** was prepared quantitatively *via* Flash Vacuum Pyrolysis (FVP) of 50% solution of 1,5-hexadiyne in pentane at 375 °C according to the procedure described in the literature.¹⁰ Compound **1** can be stored for extended periods of time under inert atmosphere at cold temperatures. TIPS-anthracene was prepared *via* two-fold Sonogashira coupling of 9,10-dibromoanthracene with TIPS-acetylene as described in the literature.¹⁷ 1,3-Diphenylnaphthofuran was prepared according to the procedure originally developed by Cava *et al.* and modified by Neckers *et al.*¹⁵ and used immediately. Compound **7** was prepared according to the procedure described earlier by our group.¹⁶

NMR Spectroscopy: ¹H and ¹³C NMR spectra for all compounds were acquired in CDCl₃ on a Bruker Avance Spectrometer operating at (400 MHz and 100 MHz, respectively), or on a Varian

Inova Spectrometer (500 MHz or 125 MHz, respectively). Chemical shifts (δ) are reported in parts per million (ppm) and referenced with residual CHCl_3 (7.27 ppm). Where noted, small volumes (< 0.1 mL) of carbon disulfide (CS_2) were used to increase solubility.

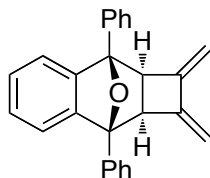
Mass Spectrometry: High-resolution mass spectra (HRMS) were obtained at the MIT Department of Chemistry Instrumentation Facility employing either electrospray (ESI) or Direct Analysis in Real Time (DART) as the ionization technique. Additional mass spectra were obtained using Matrix-Assisted Laser Desorption/Ionization-Time of Flight (MALDI-TOF, Bruker Omnicflex), by depositing samples directly onto the target without a matrix.

Absorption and Emission Spectroscopy: Ultraviolet-visible absorption spectra were measured with an Agilent 8453 diode array spectrophotometer and corrected for background signal with a solvent-filled cuvette. Fluorescence spectra were measured on a SPEX Fluorolog- τ 3 fluorimeter (model FL- 321, 450 W Xenon lamp) using right-angle detection. Fluorescence quantum yields in chloroform (CHCl_3) were determined relative to perylene in ethanol (EtOH), Coumarin 6 in EtOH, or 9,10-diphenylanthracene in cyclohexane as indicated, and are corrected for solvent refractive index and absorption differences at the excitation wavelength. Fluorescence lifetimes were measured *via* frequency modulation using a Horiba-Jobin-Yvon MF2 lifetime spectrometer equipped with a 365 nm laser diode and using the modulation of POPOP (1,4-bis(5-phenyloxazol-2-yl)benzene) as a calibration reference.

Electrochemistry: Cyclic voltammetry (CV) was performed on an Autolab PGState 20 potentiostat (Eco Chemie), using a silver (Ag) wire reference electrode submersed in 0.01 M

AgNO₃ in acetonitrile (MeCN), under a nitrogen atmosphere in a glovebox. A platinum (Pt) button electrode was used as the working electrode and a Pt coil as the counter electrode. The Ferrocene/Ferrocinium redox couple served as an external reference at a scan rate of 150 mV/s.

Synthetic Procedures:

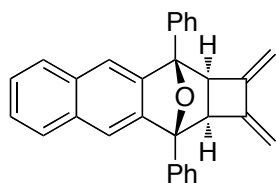


Compound 2a: The concentration of **1** in pentane was determined *via* ¹H NMR using 25 μL of THF as an internal standard in benzene-d₆ prior to use. 1,3-Diphenylisobenzofuran (2.000g, 7.40 mmols) and **1** (1.20 mL, 7.40 mmols) were dissolved in anhydrous CH₂Cl₂ (40 mL) in a Schlenk flask under N₂ in a glovebox. The reaction flask was sealed, removed from the glovebox, and allowed to stir at room temperature overnight. The solvent was removed under reduced pressure to give an off-white solid. Flash column chromatography (SiO₂, 25% CH₂Cl₂/hexanes) yielded 2.430g (92%) of a white solid, which was stored at cold temperatures.

¹H NMR (400 MHz, CDCl₃): 7.71 (d, *J*=8.3 Hz, 4H), 7.48 (app t, *J*=7.7 Hz, 4H), 7.39 (app t, *J*=7.6 Hz, 2H), 7.13 (dd, *J*=3.1 Hz, 5.7 Hz, 2H), 7.07 (dd, *J*=3.4 Hz, 5.3 Hz, 2H), 5.05 (s, 2H), 4.35 (s, 2H), 3.60 (s, 2H)

¹³C NMR (100 MHz CDCl₃): 147.8, 144.7, 136.7, 128.5, 127.8, 127.0, 126.7, 119.3, 106.0, 91.1, 53.5

HRMS (ESI): calc for C₂₆H₂₀O [M+H]⁺ 349.1587, found 349.1587

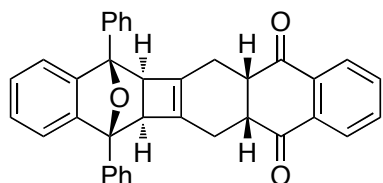


Compound 2b: The concentration of **1** in pentane was determined *via* ^1H NMR using 25 μL of THF as an internal standard in benzene- d_6 prior to use. 1,3-Diphenylisnaphthofuran (442 mg, 1.40 mmols) and **1** (0.46 mL, 1.40 mmols) were dissolved in anhydrous CH_2Cl_2 (10 mL) following the same procedure as described above and allowed to stir overnight. The solvent was removed under reduced pressure to give an off-white solid. Flash column chromatography (SiO_2 , 25% CH_2Cl_2 /hexanes) yielded 467 mg (85%) of a white solid, which was stored at cold temperatures.

^1H NMR (500 MHz, CDCl_3): 7.83 (d, $J=7.7$ Hz, 2H), 7.76 (dd, $J=6.2$ Hz, 7.7 Hz, 1H), 7.58 (app t, $J=7.7$ Hz, 2H), 7.49-7.43 (m, 3H), 5.12 (s, 1H), 4.43 (s, 1H), 3.75 (s, 1H)

^{13}C NMR (125 MHz, CDCl_3): 146.2, 145.2, 136.8, 133.0, 128.7, 128.4, 128.0, 126.9, 126.2, 118.0, 106.3, 91.1, 53.8

HRMS (DART): calc for $\text{C}_{30}\text{H}_{22}\text{O}$ $[\text{M}+\text{H}]^+$ 399.1743, found 399.1743



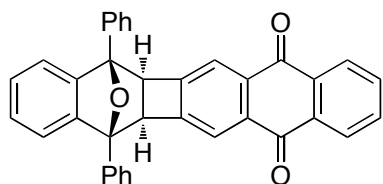
Compound 3: Compound **2a** (200 mg, 0.57 mmols) and **NQ** (91 mg, 0.57 mmols) were combined in PhCH_3 (3.0 mL) in a pressure tube. Argon was bubbled through the solution for 10 minutes before sealing the tube and heating the reaction to 110 $^\circ\text{C}$ overnight. The solution was loaded directly onto SiO_2 and purified *via* flash column chromatography (1-5% EtOAc/hexanes) to yield 262 mg (91%) of a colorless solid.

¹H NMR (400 MHz, CDCl₃): 7.99 (dd, *J*=3.3 Hz, 5.8 Hz, 2H), 7.72 (dd, *J*=3.6 Hz 6.9 Hz, 2H), 7.67 (d, *J*=3.3 Hz, 4H), 7.46 (app t, *J*=8.4 Hz, 4H), 7.39 (app t, *J*=7.3 Hz, 2H), 7.12 (dd, *J*=3.0 Hz, 5.3 Hz, 2H), 6.95 (dd, *J*=3.0 Hz, 5.3 Hz, 2H), 3.46 (s, 2H), 3.33 (app t, *J*=4.6 Hz, 2H), 2.37 (broad d, *J*=15.9 Hz, 2H), 1.82 (broad d, *J*=16.6 Hz, 2H)

¹³C NMR (100 MHz, CDCl₃): 197.8, 148.1, 140.3, 137.2, 134.2, 134.0, 128.4, 127.8, 126.8, 126.7, 126.6, 119.2, 86.1, 53.8, 47.0, 23.7

HRMS (DART): calc for C₃₆H₂₆O₃ [M-H]⁻ 505.1798, found 505.1801

MP (C₆H₆/MeOH): Decomposition



Compound 4: Compound **3** (315 mg, 0.62 mmols) was dissolved in anhydrous THF (8.0 mL) and flushed with argon for 10 minutes. The solution was cooled to -10 °C in an ice/brine bath and freshly prepared lithium hexamethyldisilazide (LiHMDS, 1.93 mmols) in THF (4.0 mL) was added. The reaction mixture was allowed to warm to room temperature overnight. The reaction mixture was poured into water (25 mL) and extracted with CH₂Cl₂ (2 × 25 mL). The combined organics were washed with brine (25 mL), dried over anhydrous magnesium sulfate (MgSO₄), and concentrated under reduced pressure. The crude solid was then taken up in benzene (C₆H₆, 2.0 mL) and 2,3-dichloro-5,6-dicyano-1,5-benzoquinone (DDQ, 169 mg, 0.74 mmols) was added. The reaction mixture was heated to reflux for 2 hours. After cooling to room temperature, the reaction mixture was loaded directly on to SiO₂. Flash column chromatography (10%

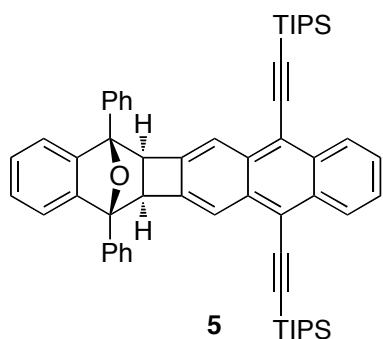
EtOAc/hexanes) yielded 275 mg (88%) of a pale yellow solid. X-ray quality crystals were grown from slow evaporation of CHCl₃.

¹H NMR (400 MHz, CDCl₃): 8.19 (dd, *J*=3.4 Hz, 5.8 Hz, 2H), 7.76-7.71 (m, 4H), 7.56-7.46 (m, 6H), 7.22 (dd, *J*=3.0 Hz, 5.5 Hz, 2H), 7.11 (dd, *J*=3.0 Hz, 5.4 Hz, 2H), 4.30 (s, 1H)

¹³C NMR (100 MHz, CDCl₃): 183.2, 150.2, 147.5, 135.6, 134.5, 133.8, 133.2, 128.7, 128.4, 127.3, 127.0, 126.7, 121.4, 119.5, 88.8, 55.5

HRMS (DART): calc for C₃₆H₂₂O₃ [M+H]⁺ 503.1642, found 503.1649

MP (CHCl₃): 295.5-300.0 °C



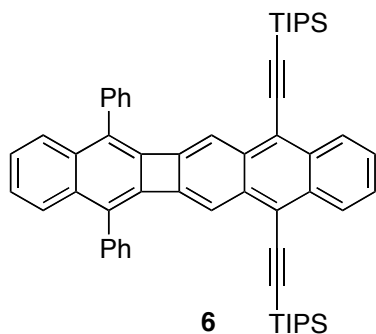
Compound 5: TIPS-acetylene (100 μL, 0.45 mmols) was dissolved in dry THF (2.0 mL) and flushed with argon for 10 minutes. Next, *n*BuLi (1.6 M in hexanes, 0.29 mL) was added dropwise at room temperature and the reaction mixture was stirred for 30 minutes. Compound 4 (100 mg, 0.20 mmols) in dry THF (1.0 mL) was transferred to the reaction flask *via* cannula, followed by heating to 60 °C for 30 minutes. After cooling to room temperature, the reaction was quenched with a saturated aqueous solution of ammonium chloride (NH₄Cl_(aq), 25 mL) and extracted with CH₂Cl₂ (2 × 25 mL). The combined organics were dried over MgSO₄, filtered, and the solvent was removed under reduced pressure. The crude residue was then taken up in a *p*-dioxane (1.6 mL) and tin(II) chloride (SnCl₂, 180 mg, 0.80 mmols) in 50% AcOH (0.8 mL)

was added dropwise. After stirring at room temperature for 4 hours, the precipitate was collected by filtration and washed with cold methanol to give 25 mg (15%) of compound **5** as a yellow solid. The filtrate was then diluted with CH₂Cl₂ (25 mL) and washed with 1 N HCl, water, and brine (25 mL each), dried over anhydrous sodium sulfate (Na₂SO₄) and the solvent was removed under reduced pressure. Flash column chromatography (SiO₂, 0-15% CH₂Cl₂/hexanes) yielded an additional 35 mg (21%) of compound **5**.

¹H NMR (400 MHz, CDCl₃): 8.52 (dd, *J*=3.2, 6.6 Hz), 7.98 (s, 2H), 7.79 (d, *J*=7.6 Hz, 4H), 7.52-7.49 (m, 6H), 7.42 (app t, *J*=7.6 Hz, 2H), 7.22 (dd, *J*=3.0, 5.4 Hz, 2H), 7.15 (dd, *J*=3.0, 5.3 Hz, 2H), 4.44 (s, 2H), 1.22-1.20 (m, 42H)

¹³C NMR (100 MHz, CDCl₃): 148.0, 142.0, 136.3, 133.6, 131.8, 128.5, 127.9, 127.1, 127.0, 126.6, 126.4, 120.0, 119.4, 118.8, 103.7, 103.6, 89.7, 55.4, 18.9, 11.4

HRMS (DART): calc for C₅₈H₆₄OSi₂ [M+H]⁺ 833.4568, found 833.4544



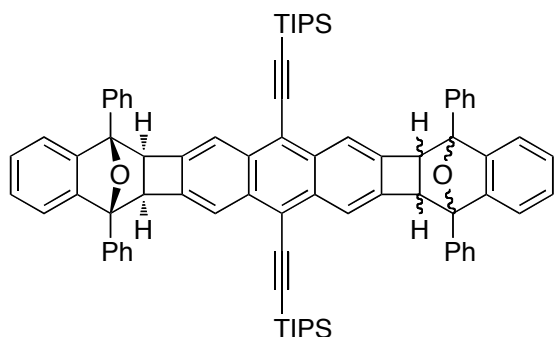
Compound 6: Compound **5** (50 mg, 0.059 mmols) and pyridinium *p*-toluenesulfonate (PPTS, 150 mg, 0.59 mmols) were combined in acetic anhydride (Ac₂O, 1.5 mL). The reaction mixture was flushed with argon for 10 minutes. After heating to 120 °C overnight, the reaction mixture was cooled in a refrigerator. The yellow precipitate was collected by filtration and washed with cold MeOH to yield 29 mg of compound **6** (61%).

¹H NMR (500 MHz, CDCl₃): 8.48 (dd, *J*=6.5, 3.2 Hz, 2H), 7.89 (dd, *J*=6.4, 3.4 Hz, 2H), 7.82 (s, 2H), 7.69 (d, *J*=7.0 Hz, 4H), 7.59 (app t, *J*=7.4 Hz, 4H), 7.54-7.48 (m, 4H), 7.37 (dd, *J*=6.4, 3.3 Hz), 1.19-1.17 (m, 42 H)

¹³C NMR (125 MHz, CDCl₃): 146.5, 143.4, 136.4, 134.85, 134.82, 132.4, 131.0, 129.5, 128.7, 127.8, 127.01, 126.95, 126.89, 126.4, 119.3, 115.0, 104.0, 103.2, 18.9, 11.4

HRMS (DART): calc for C₅₈H₆₂Si₂ [M+H]⁺ 815.4463, found 815.4483

MP (EtOAc): 224.3-227.8 °C, 253.1-258.4 °C



Compound 8a: Compound **2a** (643 mg, 1.85 mmols) and compound **7** (460 mg, 0.61 mmols) were dissolved in anhydrous PhCH₃ (18.0 mL) in a flame-dried Schlenk flask and flushed with argon for 30 minutes. The solution was then cooled to -40 °C in an MeCN/dry ice bath. *n*BuLi (0.94 mL, 1.5 mmols) was diluted with dry hexanes (7.0 mL) and added to reaction mixture over 90 minutes *via* syringe pump. The reaction was allowed to warm to room temperature overnight. The reaction was quenched with H₂O (50 mL), extracted with CH₂Cl₂ (3 × 75 mL), and the combined extracts were washed with brine (50 mL). The organic layer was dried over MgSO₄, filtered and the solvent removed under reduced pressure. The crude residue was taken up in C₆H₆ (18.0 mL) and DDQ (346 mg, 1.5 mmols) was added. The reaction mixture was flushed with Argon for 10 minutes before heating to reflux over night. After cooling to room temperature the

suspension was adsorbed onto SiO₂ and flash column chromatography (10-30% CH₂Cl₂/hexanes) yield 241 mg (36%) of **8a** as a mixture of *syn*- and *anti*- isomers. The isomers are separable by column chromatography (although separation is unnecessary in this case), and the *anti*- isomer is assumed to be the less polar of the two.

Anti-8a:

¹H NMR (500 MHz, CDCl₃): 7.87 (s, 4H), 7.74 (d, *J*=8.1 Hz, 8H), 7.47 (app t, *J*=7.7 Hz, 8H), 7.38 (app t, *J*=7.1 Hz, 4H), 7.19 (dd, *J*=3.0 Hz, 5.1 Hz, 4H), 7.10 (dd, *J*=3.0 Hz, 4.4 Hz, 4H), 4.37 (s, 4H), 1.14-1.10 (m, 42H)

¹³C NMR (125 MHz, CDCl₃): 148.1, 141.5, 136.3, 133.0, 128.4, 127.8, 127.0, 126.5, 119.9, 119.4, 118.9, 104.0, 102.8, 89.6, 55.4, 19.0, 11.4

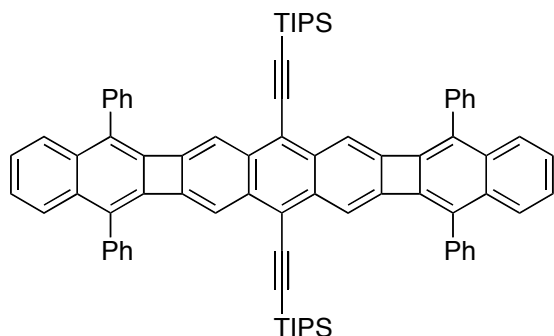
HRMS (ESI): calc for C₈₀H₇₈O₂Si₂ [M+H]⁺ 1127.5613, found 1127.5607

Syn-8a:

¹H NMR (500 MHz, CDCl₃): 7.87 (s, 4H), 7.74 (d, *J*=8.7 Hz, 8H), 7.47 (app t, *J*=7.7 Hz, 8H), 7.38 (app t, *J*=7.4 Hz, 4H), 7.19 (dd, *J*=3.0 Hz, 5.4 Hz, 4H), 7.12 (dd, *J*=3.0 Hz, 5.3 Hz, 4H), 4.36 (s, 4H), 1.14 (m, 42H)

¹³C NMR (125 MHz, CDCl₃): 148.0, 141.4, 136.3, 133.0, 128.5, 127.8, 127.0, 126.5, 119.9, 119.4, 119.1, 112.6, 104.0, 89.6, 55.3, 19.0, 11.4

HRMS (ESI): calc for C₈₀H₇₈O₂Si₂ [M+H]⁺ 1127.5613, found 1127.5610

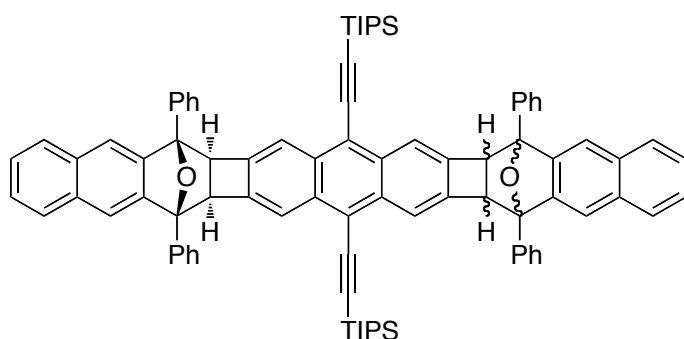


Compound 9a: Compound **8a** (25 mg, 0.020 mmols) and *p*-toluenesulfonic acid (pTsOH, 584 mg, 0.44 mmols) were combined in Ac₂O (2.2 mL). The reaction mixture was flushed with argon for 10 minutes. After heating to 120 °C overnight, the reaction mixture was cooled in a refrigerator. A dark solid precipitated and was collected by filtration and washed with cold MeOH to yield 17 mg of compound **9a** (71%).

¹H NMR (500 MHz, CDCl₃): 7.83 (dd, *J*=3.4, 6.3 Hz, 4H), 7.67 (s, 4H), 7.64 (d, *J*=7.1 Hz, 8H), 7.56 (app t, *J*=7.3 Hz, 8H), 7.48 (app t, *J*=7.4 Hz, 4H), 7.34 (dd, *J*=3.3, 6.4 Hz), 1.07 (m, 42H)

¹³C NMR (100 MHz, CDCl₃): 146.9, 143.4, 136.4, 134.92, 134.88, 130.6, 129.5, 128.7, 127.8, 126.9, 126.4, 120.0, 115.2, 103.5, 103.2, 18.8, 11.3

HRMS (DART): calc for C₈₀H₇₄Si₂ [M+H]⁺ 1091.5402, found 1091.5389



Compound 8b: Compound **2b** (200 mg, 0.50 mmols) and compound **7** (125 mg, 0.17 mmols) were dissolved in anhydrous PhCH₃ (5.0 mL) in a flame-dried Schlenk flask and flushed with

argon for 30 minutes. The reaction mixture was then cooled to $-40\text{ }^{\circ}\text{C}$ in an MeCN/dry ice bath. *n*BuLi (0.26 mL, 0.42 mmols) diluted with dry hexanes (2.2 mL) was added to the reaction mixture over 90 minutes *via* syringe pump. The reaction was allowed to warm to room temperature overnight. The reaction was quenched with H₂O (50 mL), extracted with CH₂Cl₂ (3 × 50 mL), and the combined extracts were washed with brine (50 mL). The organic layer was dried over MgSO₄, filtered and the solvent removed under reduced pressure. The crude residue was taken up in C₆H₆ (5 mL) and DDQ (84 mg, 0.37 mmols) was added. The reaction mixture was flushed with argon for 10 minutes before heating to reflux over night. After cooling to room temperature the suspension was adsorbed onto SiO₂ and flash column chromatography (10-60% CH₂Cl₂/hexanes) yield 39 mg (20%) of **8b** as a mixture of *syn*- and *anti*- isomers. The isomers are separable by column chromatography (although separation is unnecessary in this case), and the *anti*- isomer is assumed to be the less polar of the two.

Anti-8b:

¹H NMR (500 MHz, CDCl₃): 7.91 (s, 4H), 7.82 (d, *J*=7.0 Hz, 8H), 7.76 (dd, *J*=3.4 Hz, 6.2 Hz, 4H), 7.52 (app t, *J*=7.4 Hz, 8H), 7.46-7.41 (m, 12H), 4.48 (s, 4H), 1.18-1.13 (m, 42H)

¹³C NMR (125 MHz, CDCl₃): 146.2, 141.5, 136.4, 133.0, 132.8, 128.6, 128.1, 127.9, 126.6, 126.0, 120.0, 118.0, 104.0, 102.9, 89.5, 55.6, 19.0, 11.4

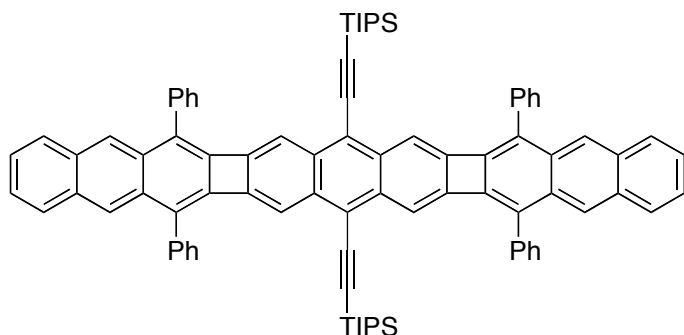
HRMS (ESI): calc for C₃₈H₈₂O₂Si₂ [M+Na]⁺ 1249.5746, found 1249.5796

Syn-8b:

¹H NMR (500 MHz, CDCl₃): 7.91 (s, 4H), 7.82 (d, *J*=8.6 Hz, 8H), 7.77 (dd, *J*=3.2 Hz, 6.0 Hz, 4H), 7.53 (app t, *J*=7.6 Hz, 8H), 7.47 (s, 4H) 7.46-7.42 (m, 8H), 4.46 (s, 4H), 1.17 (m, 42H)

^{13}C NMR (125 MHz, CDCl_3): 146.3, 141.6, 136.4, 133.1, 132.8, 128.6, 128.2, 128.0, 126.6, 126.0, 120.0, 119.0, 104.0, 102.8, 89.4, 55.7, 19.0, 11.4

HRMS (ESI): calc for calc for $\text{C}_{88}\text{H}_{82}\text{O}_2\text{Si}_2$ $[\text{M}+\text{Na}]^+$ 1249.5746, found 1249.5708



Compound 9b: Compound **8b** (25 mg, 0.020 mmols) and pTsOH (50 mg, 0.25 mmols) were combined in Ac_2O . The reaction mixture was flushed with argon for 10 minutes. After heating to 120°C overnight, the reaction mixture was cooled in a refrigerator. A dark solid precipitated and was collected by filtration and washed with cold MeOH to yield 10 mg of compound **9b** (42%).

^1H NMR (500 MHz, CDCl_3): 8.31 (s, 4H), 7.84 (s, 4H), 7.80 (dd, $J=3.2$ Hz, 6.4 Hz, 4H), 7.75 (d, $J=6.8$ Hz, 8H), 7.63 (app t, $J=7.2$ Hz, 8H), 7.54 (app t, $J=6.0$ Hz, 4H), 7.41 (dd, $J=3.2$, 6.4 Hz, 4H), 1.14-1.08 (m, 42H)

^{13}C NMR (125 MHz, $\text{CDCl}_3/\text{CS}_2$): 146.6, 142.0, 136.5, 134.9, 133.1, 131.8, 129.9, 129.6, 128.8, 128.0, 127.8, 125.9, 120.1, 115.8, 103.8, 103.3, 18.8, 11.3

MS (MALDI): Calc for $\text{C}_{88}\text{H}_{78}\text{Si}_2$ $[\text{M}]^+$ 1191.57, found 1191.63

3.9 References

- (1) Anthony, J. E. *Angew. Chem. Int. Ed.* **2008**, 47, 452.
- (2) Ruiz-Morales, Y. J. *Phys. Chem. A*, **2002**, 106, 11283.

-
- (3) (a) Smith, M. B.; Michl, J. *Chem. Rev.* **2010**, 110, 6891 and references within. (b) Siebbeles, L. D. A. *Nature Chem.* **2010**, 2, 608. (c) Jadhav, P. J.; Mohanty, A.; Sussman, J.; Lee, J.; Baldo, M. A. *Nano Lett.* **2011**, 11, 1495. (d) Ramanan, C.; Smeigh, A. L.; Anthony, J. E.; Marks, T. J.; Wasielewski, M. R. *J. Am. Chem. Soc.* **2011**, 134, 386.
- (4) (a) Anthony, J. E.; Brooks, J. S.; Eaton, D. L.; Parkin, S. R. *J. Am. Chem. Soc.* **2001**, 123, 9482. (b) Odom, S. A.; Parkin, S. R.; Anthony, J. E. *Org. Lett.* **2003**, 5, 4245. (b) Payne, M. M.; Parkin, S. R.; Anthony, J. E. *J. Am. Chem. Soc.* **2005**, 127, 8028.
- (5) Kaur, I.; Jia, W.; Kopreski, R. P.; Selvarasah, S.; Dokmeci, M. R.; Pramanik, C.; McGruer, N. E.; Miller, G. P. *J. Am. Chem. Soc.* **2008**, 130, 16274.
- (6) (a) Campbell, R.B.; Robertson, J. M.; Trotter, J. *Acta Crystallogr.* **1961**, 14, 705. (b) Campbell, R.B.; Robertson, J. M.; Trotter, J. *Acta Crystallogr.* **1962**, 15, 289. (c) Mattheus, C. C.; Dros, A. B.; Baas, J.; Meetsma, A.; de Boer, J. L.; Palstra, T. T. M. *Acta Crystallogr. Sect. C*, **2001**, 57, 939.
- (7) Holmes, D.; Kumaraswamy, S.; Matzger, A. J.; Vollhardt, K. P. C. *Chem. Eur. J.* **1999**, 5, 3399.
- (8) For a review on [N]Phenylenes see: Miljanić, O. Š.; Vollhardt, K. P. C. in *Carbon-Rich Compounds: From Molecules to Materials*, Eds. Haley, M. M.; Tykwinski, R. R. Wiley-VCH, Weinheim, **2006**, pp 140-197.
- (9) Schleifenbam, A.; Feeder, N.; Vollhardt, K. P. C. *Tetrahedron Lett.* **2001**, 42, 7329.
- (10) (a) Blomquist, A. T.; Maitlis, P. M. *Proc. Chem. Soc. (London)* **1961**, 332. (b) Huntsman, W. D.; Wristers, H. J. *J. Am. Chem. Soc.* **1963**, 85, 3308. (c) Huntsman, W. D.; Wristers, H. J. *J. Am. Chem. Soc.* **1965**, 89, 342. (d) Coller, B. A. W.; Heffernan, M. L.; Jones, A. J. *Aust. J. Chem.* **1968**, 21, 1807. (e) Hopf, H. *Angew. Chem. Int. Ed.* **1970**, 9, 732. (f) Toda, F.; Garratt, P. *Chem. Rev.* **1992**, 92, 1685.
- (11) Simpson, J. H. *Organic Structure Determination Using 2-D NMR Spectroscopy*, 2nd Ed. Elsevier: Oxford, 2012, pp 137-139.
- (12) (a) Fier, S.; Sullivan, R. W.; Rickborn, B. *J. Org. Chem.* **1988**, 53, 2353. (b) Rainbolt, J. E.; Miller, G. P.. *J. Org. Chem.* **2007**, 72, 3020
- (13) Kaupp, G.; Gruter, H.-W.; Teufel, E. *Chem. Ber.* **1983**, 116, 618.
- (14) Sauer, J.; Sustmann, R. *Angew. Chem. Int. Ed.* **1980**, 19, 779

(15) (a) Cava, M. P.; VanMeter, J. P. *J. Am. Chem. Soc.* **1962**, *84*, 2008. (b) Cava, M. P.; VanMeter, J. P., *J. Org. Chem.* **1969**, *34*, 538. (c) Mondal, R.; Shah, B. K.; Neckers, D. C. *J. Org. Chem.* **2006**, *71*, 4085.

(16) (a) VanVeller, B.; Miki, K.; Swager, T. M.; *Org. Lett.* **2010**, *12*, 1292. (b) Bowles, D. M.; Palmer, G. J.; Landis, C. A.; Scott, J. L.; Anthony, J. E. *Tetrahedron.* **2001**, *57*, 3753.

(17) TIPS-anthracene was synthesized according to the procedure of Wasielewski, *et al.*: Goldsmith, R. H.; Vura-Weis, J.; Scott, A. M.; Borkar, S.; Sen, A.; Ratner, M. A.; Wasielewski, M. R. *J. Am. Chem. Soc.* **2008**, *130*, 7659.

Chapter 3 Appendix
 **$^1\text{H-NMR}$ and $^{13}\text{C-NMR}$ Spectra
And Additional Figures**

Adapted from: Parkhurst, R. R.; Swager, T. M. "Synthesis and Optical Properties of Phenylene-Containing Oligoacenes (POAs)," **2012**, *submitted*.

Table A3.1. X-ray crystallographic data.^a

	3	4	6	9a
Empirical formula	C ₇₅ H ₅₅ O ₆	C ₃₆ H ₂₂ O ₃	C ₅₈ H ₆₂ Si ₂	C ₈₀ H ₇₄ Si ₂
Formula weight (g mol ⁻¹)	1052.258	502.569	815.301	1091.639
a (Å)	10.075	8.551	16.721	19.445
b (Å)	16.278	17.999	8.106	8.080
c (Å)	17.943	16.570	36.398	20.584
α (°)	107.58	90.00	90.00	90.00
β (°)	96.79	100.06	102.94	109.92
γ (°)	102.58	90.00	90.00	90.00
Volume (Å ³)	2683.81	2511.07	4808.12	3040.57
Space group	<i>P</i> -1	<i>P</i> 2 ₁ / <i>n</i>	<i>P</i> 2 ₁	<i>P</i> 2 ₁ / <i>n</i>
Calculated density (g cm ⁻³)	1.302	1.329	1.126	1.192
<i>Z</i>	2	4	4	2
Temperature (°C)	-173.0	-173.0	-173.0	-173.0
R(F)	0.0412	0.0384	0.0310	0.0447
R _w (F ²)	0.1099	0.0979	0.0828	0.1238

^aX-ray crystal structure data collected and solved by Dr. Michael Takase.

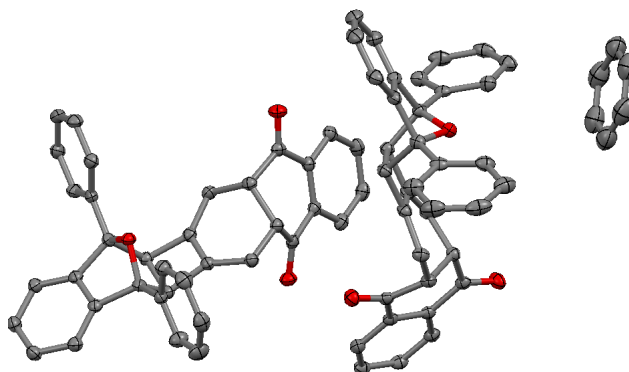


Figure A3.1. X-ray crystal structure of **3**. Hydrogens are omitted for clarity. X-ray quality crystals were grown *via* slow vapor diffusion of MeOH into a C₆H₆ solution of **3**. Two molecules of **3** crystallized per asymmetric unit with half an equivalent of C₆H₆. Anisotropic thermal ellipsoids set at 50% probability.

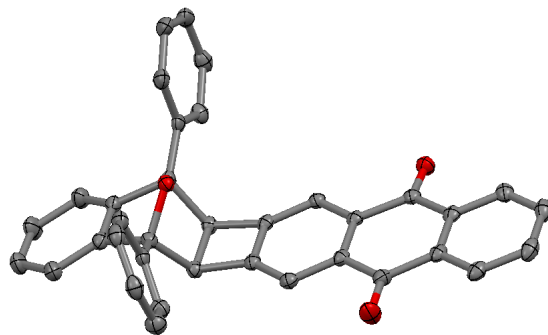


Figure A3.2. X-ray crystal structure of **4**. Hydrogens are omitted for clarity. X-ray quality crystals were grown *via* slow evaporation of CHCl_3 . Anisotropic thermal ellipsoids set at 50% probability.

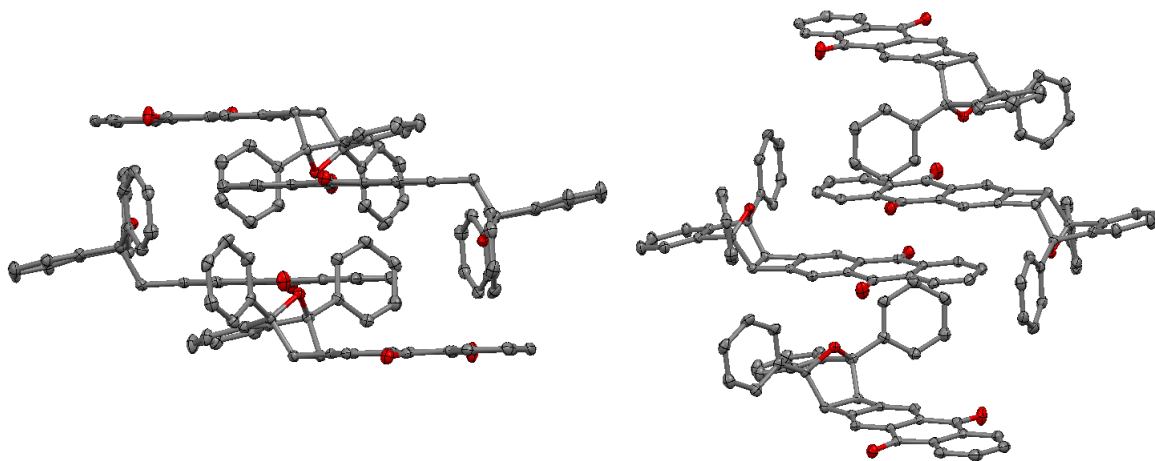


Figure A3.3. Two views (left and right) of the crystal packing of **4**.

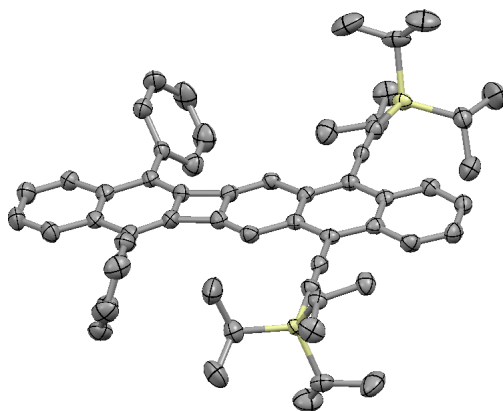


Figure A3.4. X-ray structure of **6**. X-ray quality crystals were grown *via* slow evaporation of a solution of **6** in CH₂Cl₂/MeOH. Anisotropic thermal ellipsoids set at 50% probability.

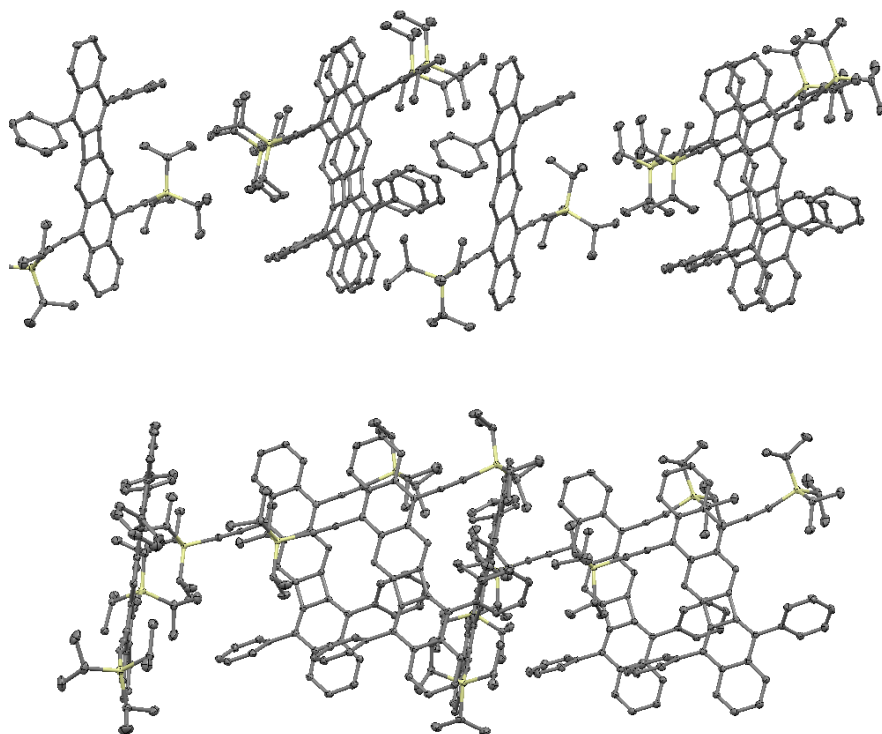


Figure A3.5. Two views (top and bottom, rotated about the y-axis) of crystal packing of **6**. π - π distance: 6.382 Å.

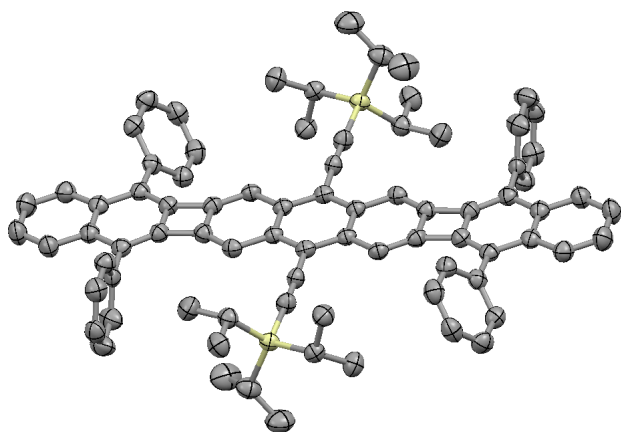


Figure A3.6. X-ray structure of **9a**. X-ray quality crystals were grown *via* slow vapor diffusion of MeOH into a solution of **6** in CHCl₃. Anisotropic thermal ellipsoids set at 50% probability.

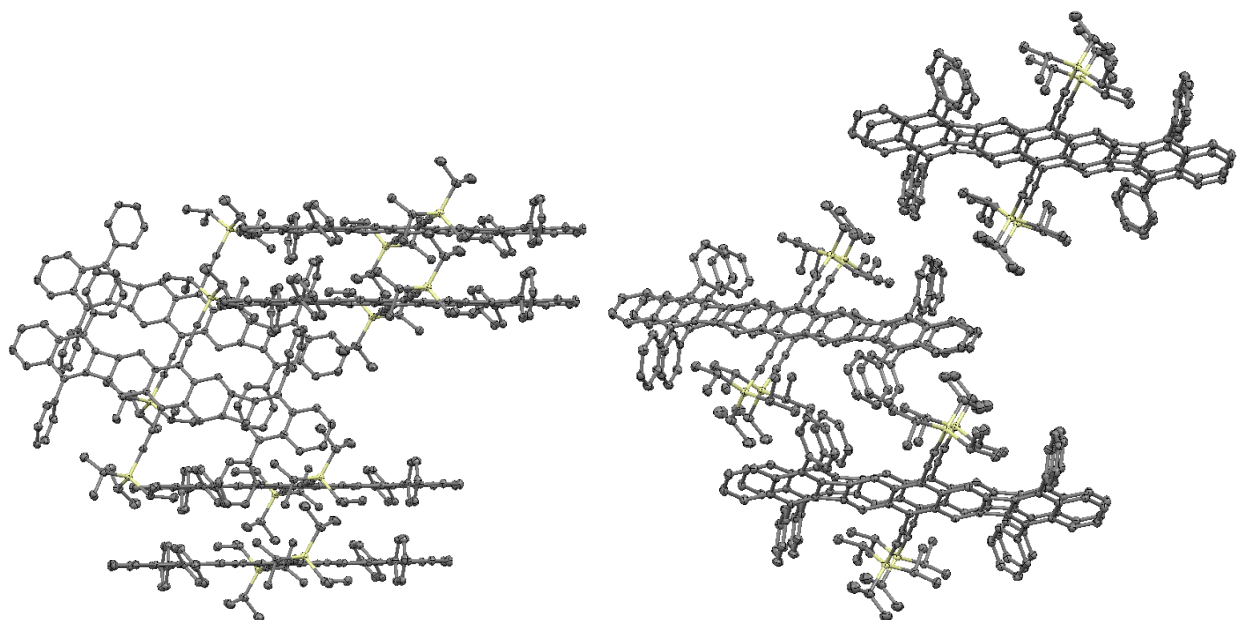
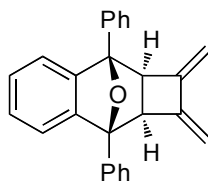
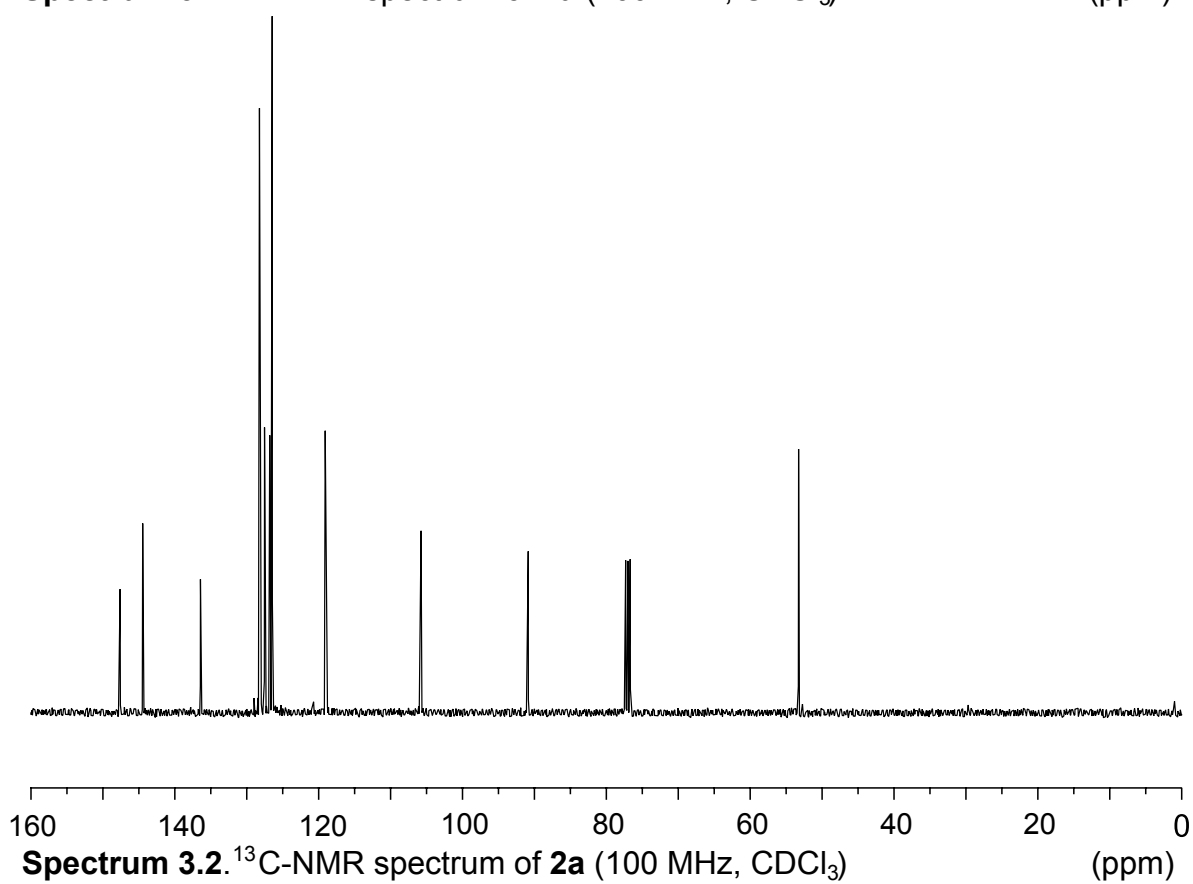
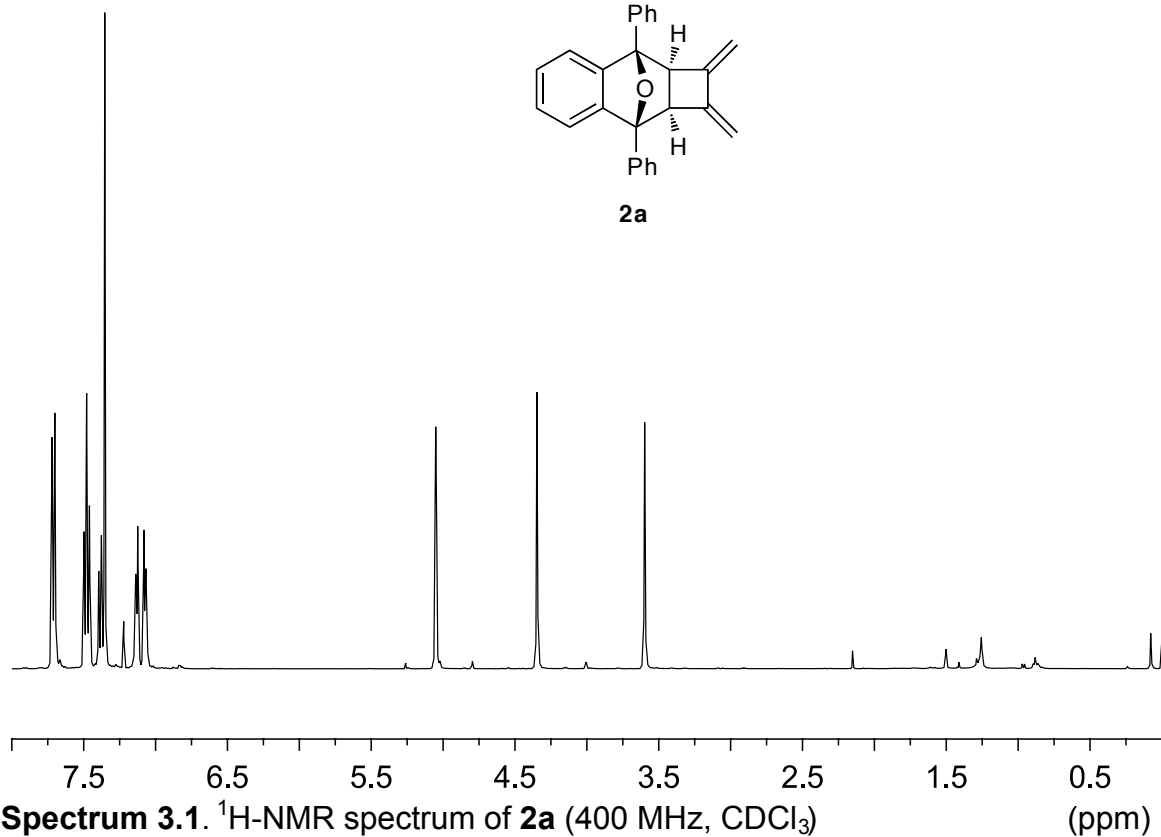
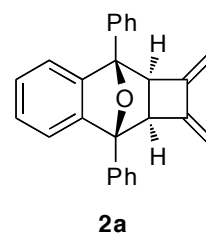
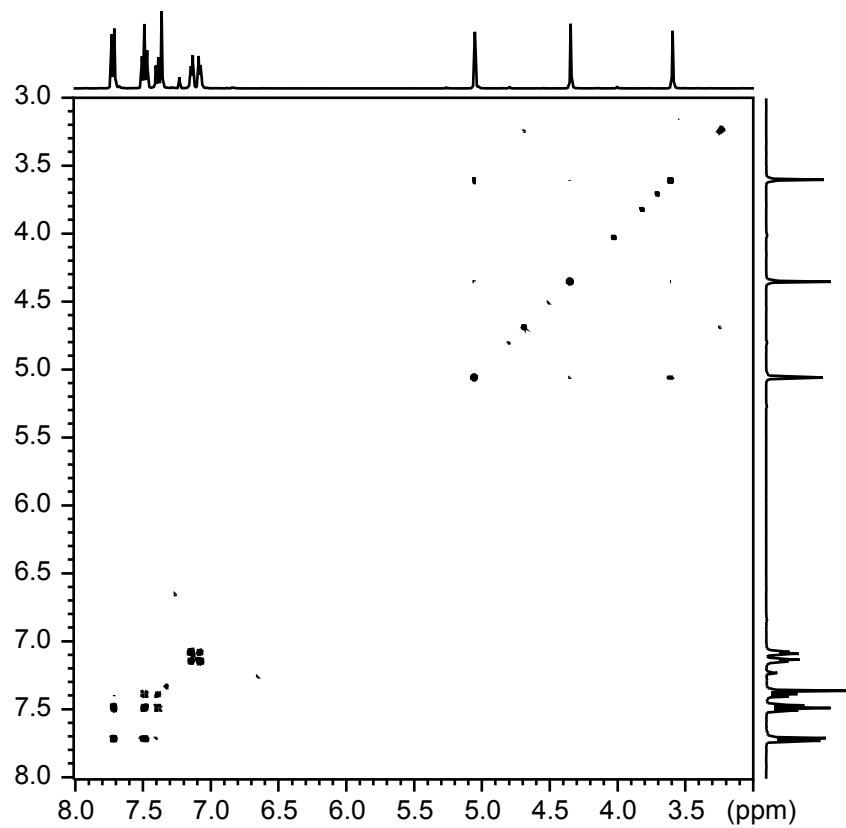


Figure A3.7. Two views (left and right, rotated about the x-axis) of crystal packing of **9a**. π - π distance: 8.080 Å.

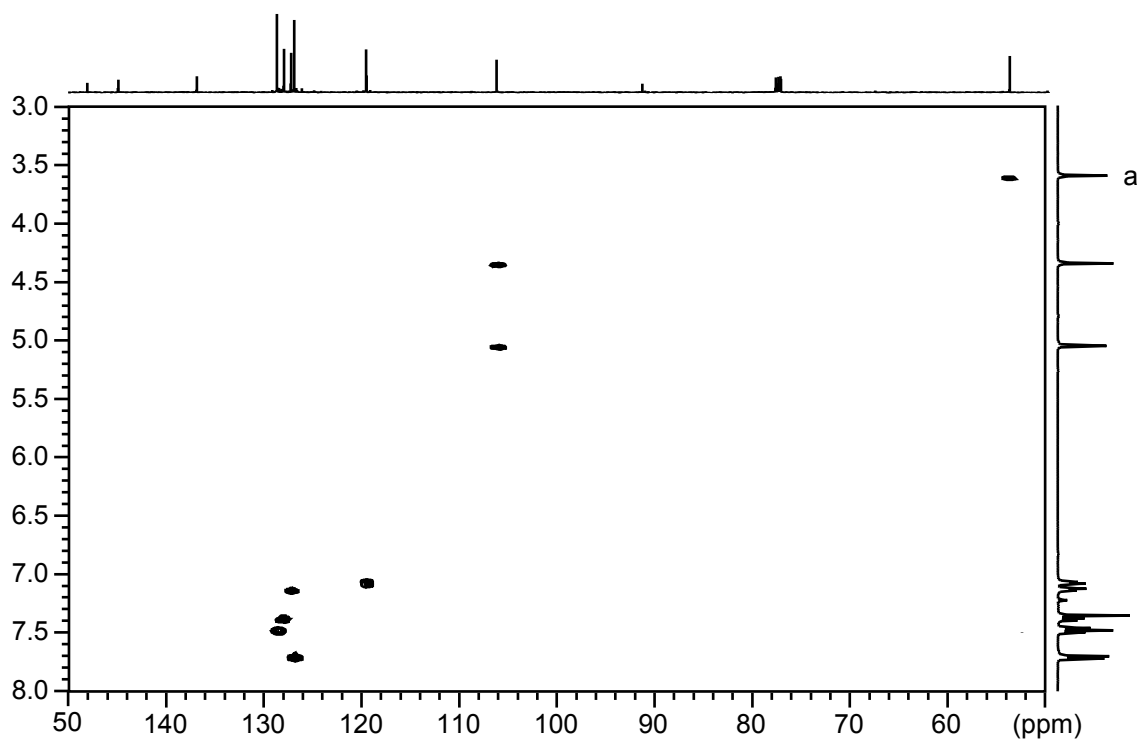


2a

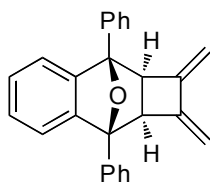




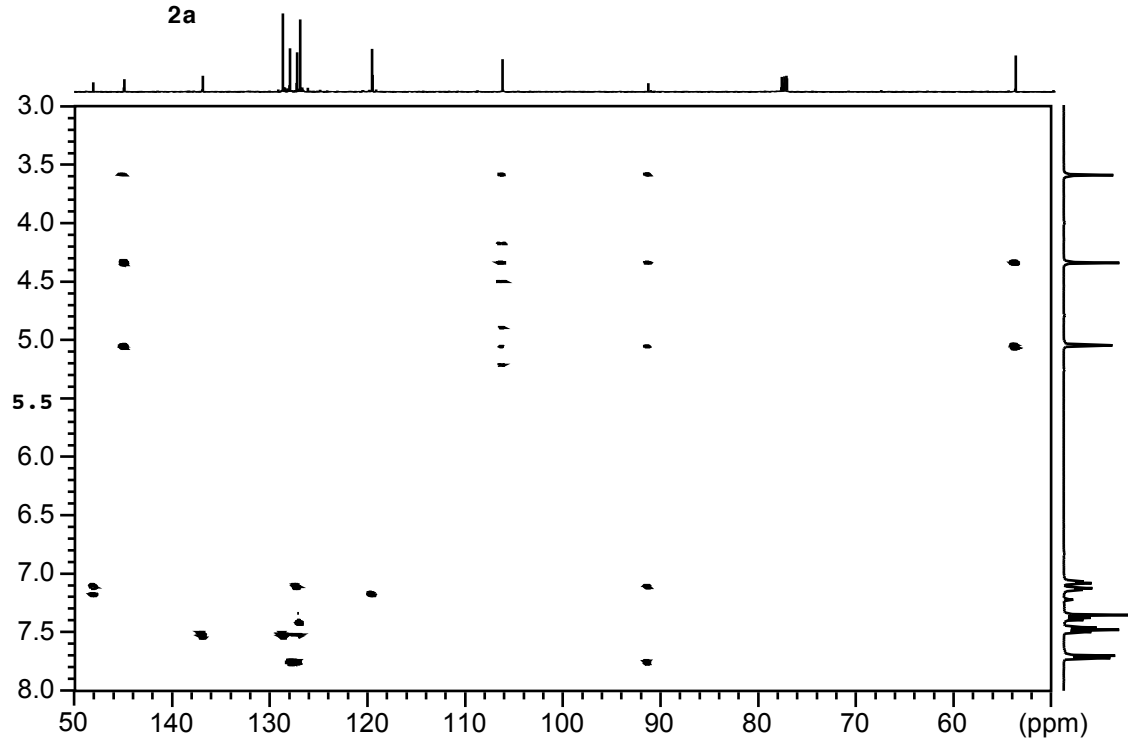
Spectrum 3.3. GCOSY spectrum of **2a** (500 MHz, CDCl₃)



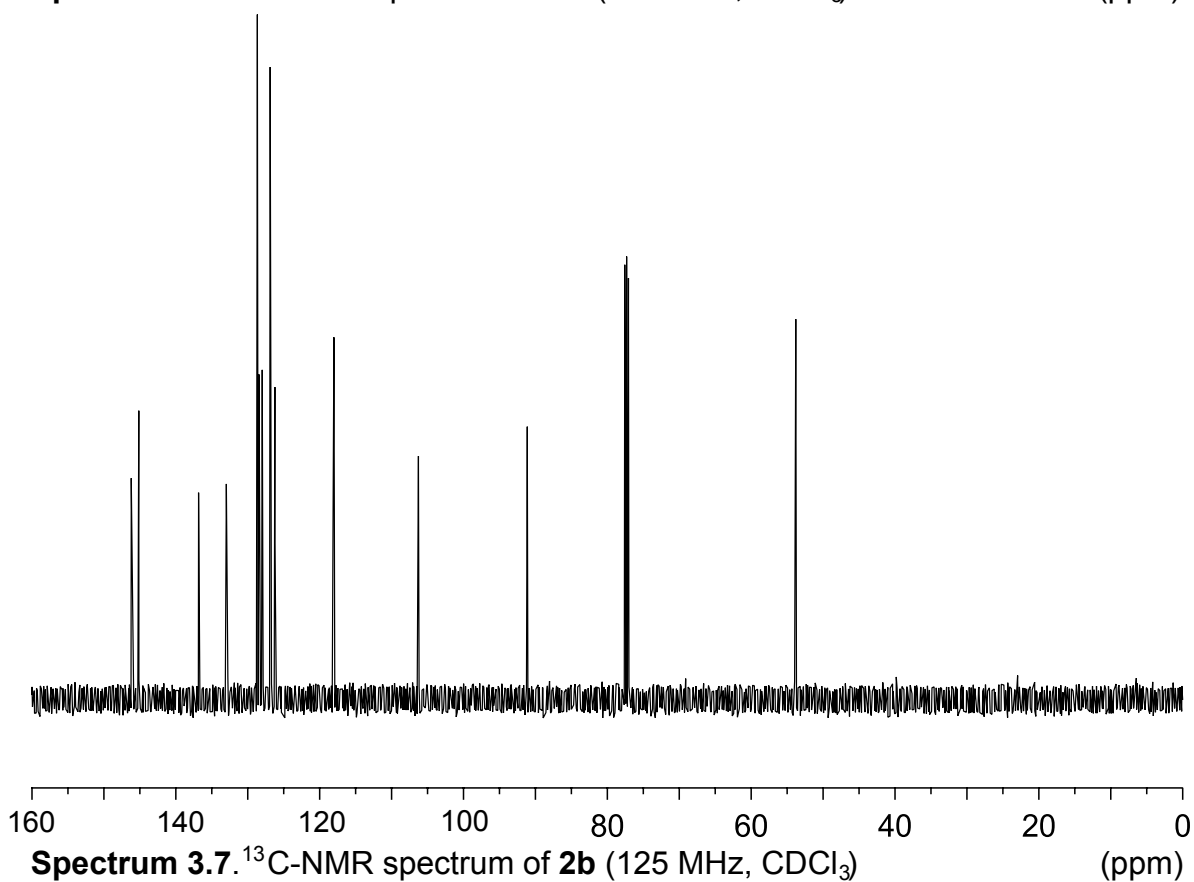
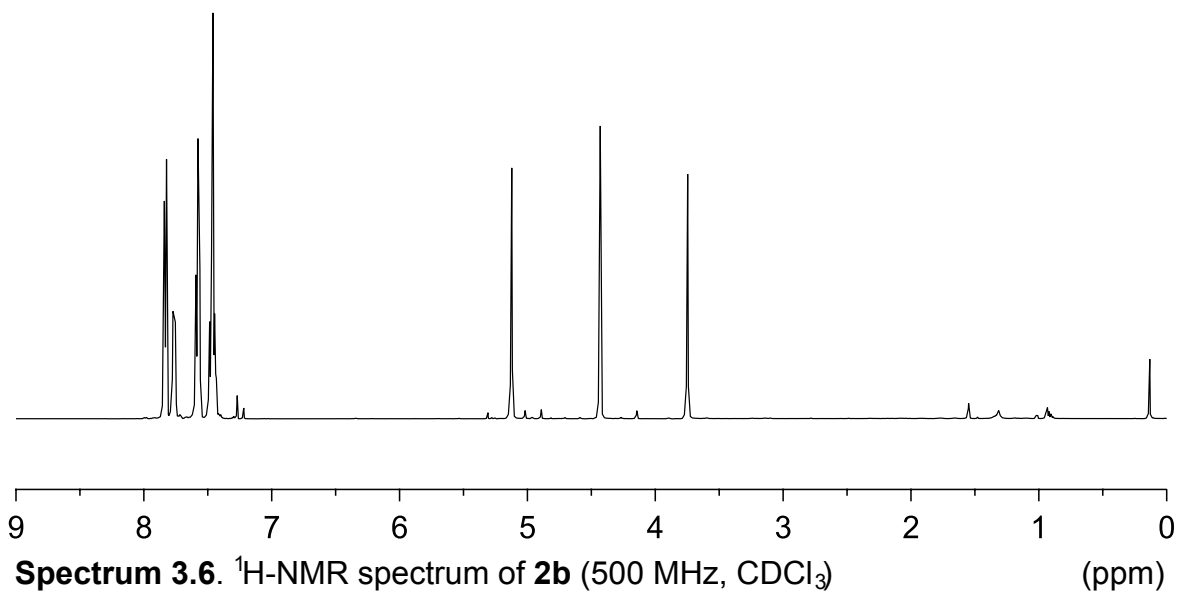
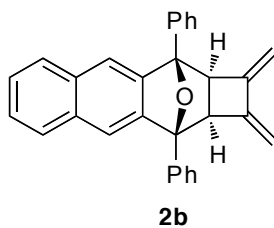
Spectrum 3.4. HSQC spectrum of **2a** (500 MHz, CDCl₃)

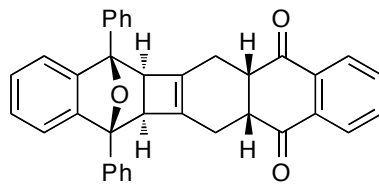


2a

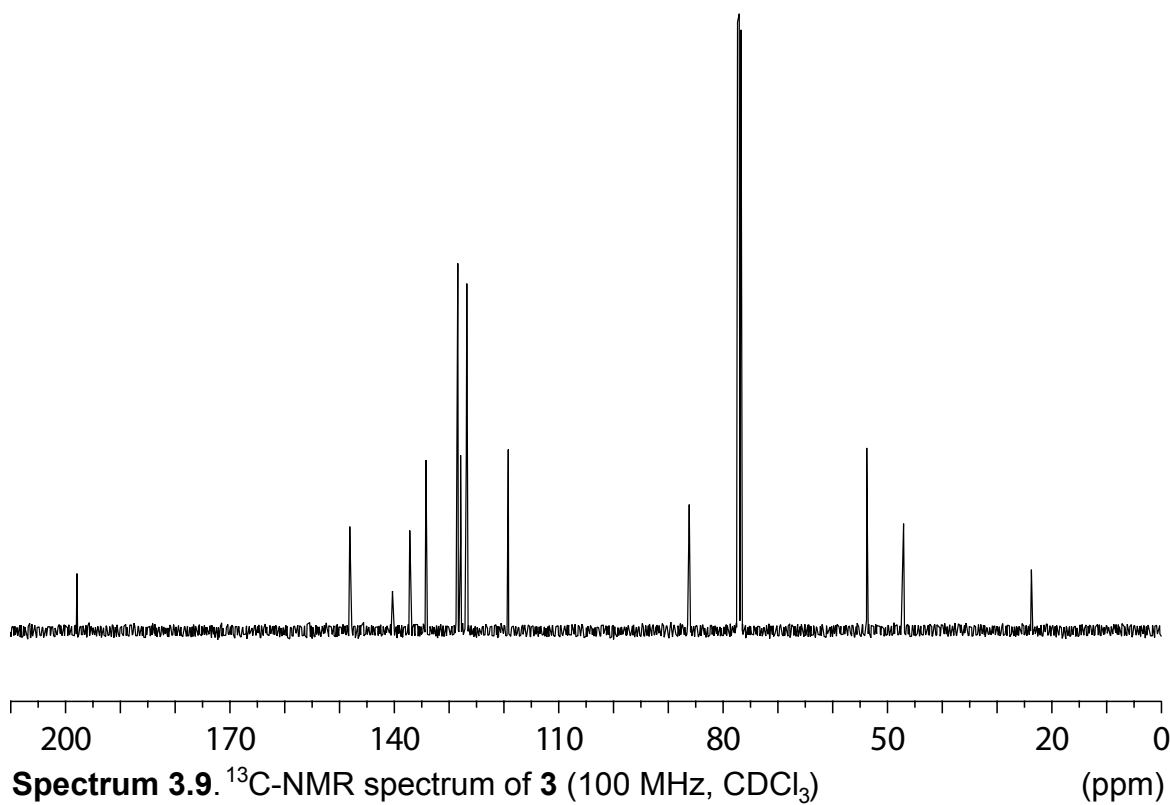
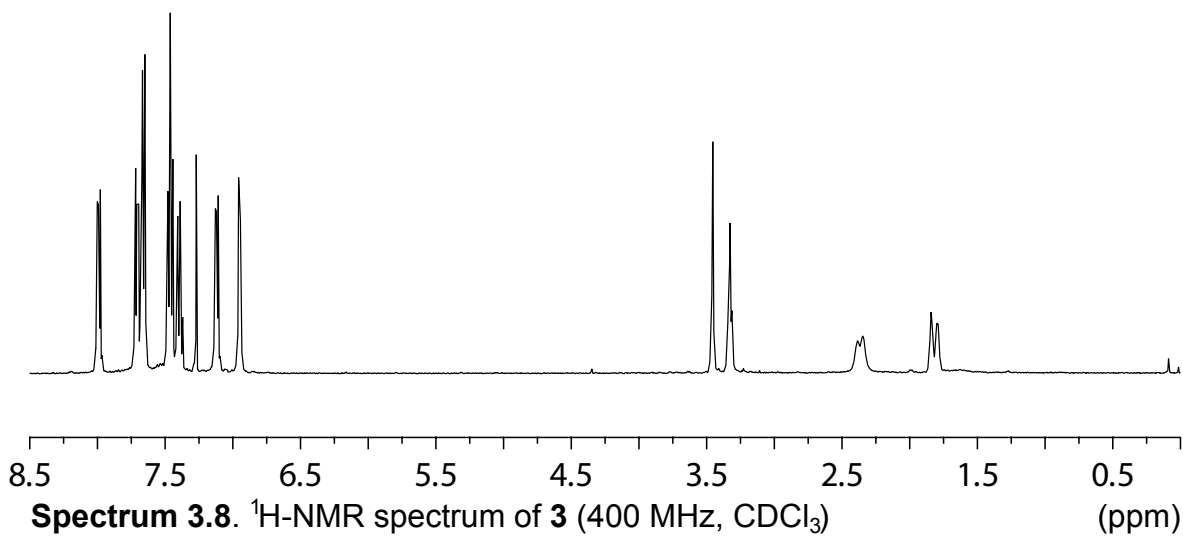


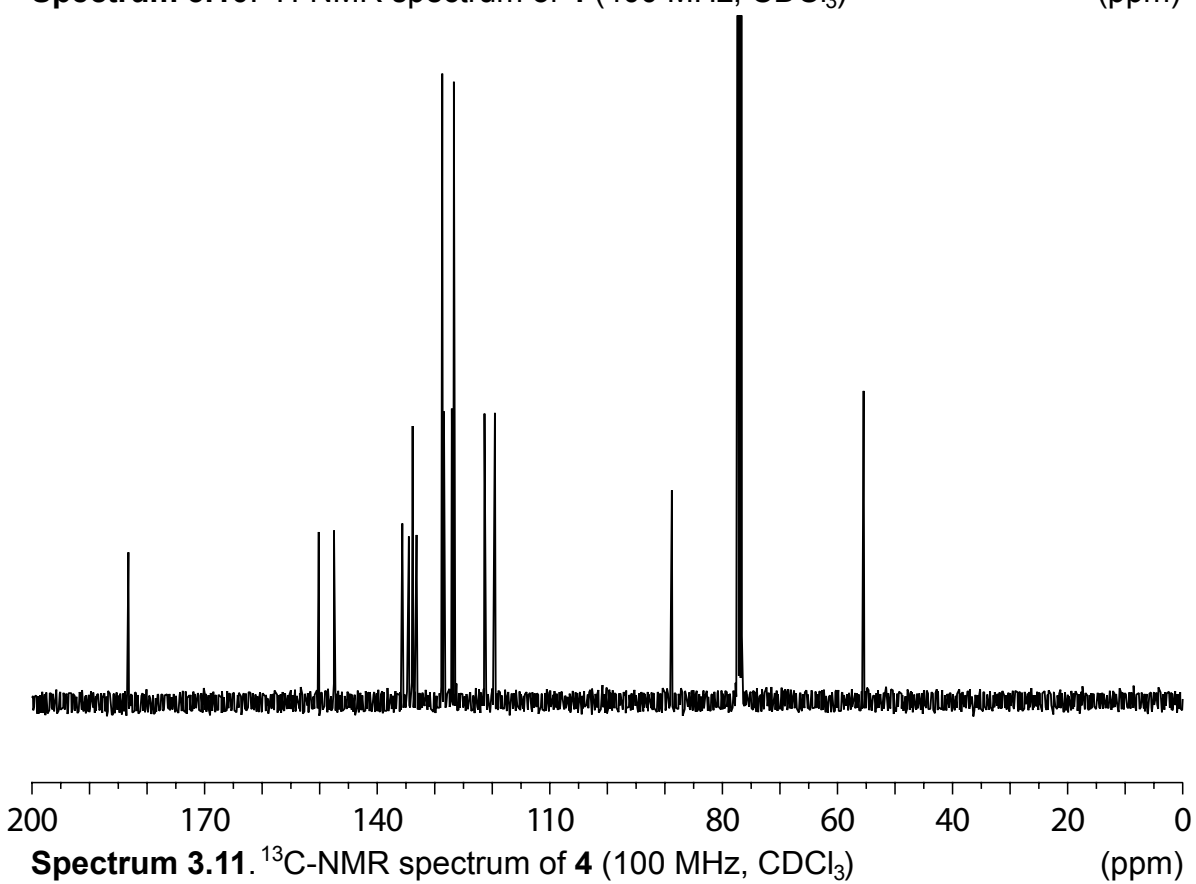
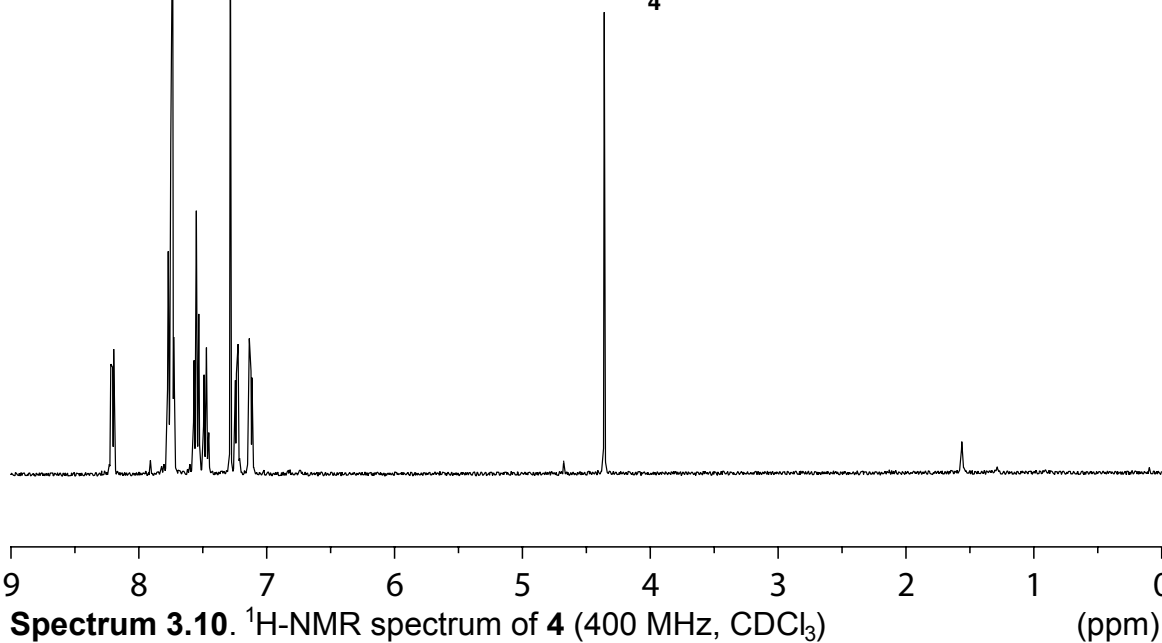
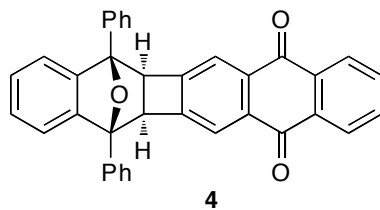
Spectrum 3.5. HMBC spectrum of **2a** (500 MHz, CDCl₃)

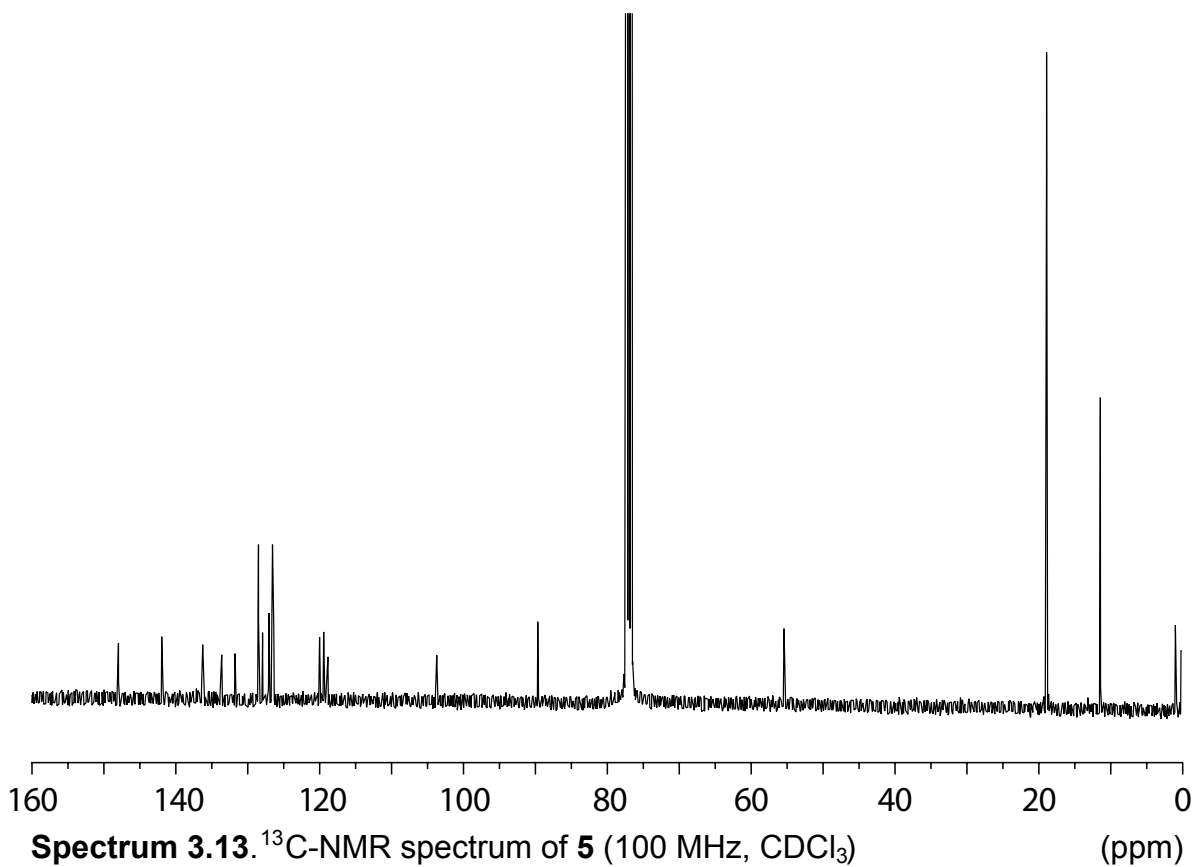
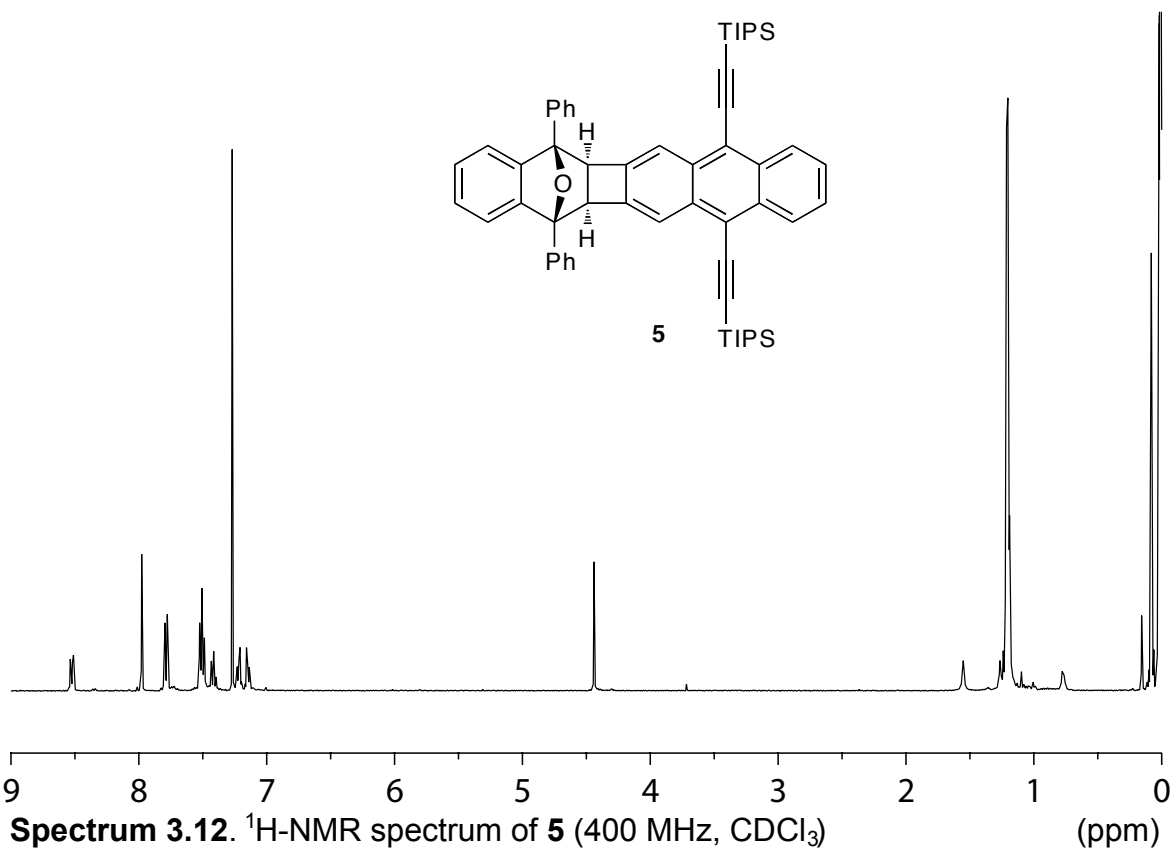


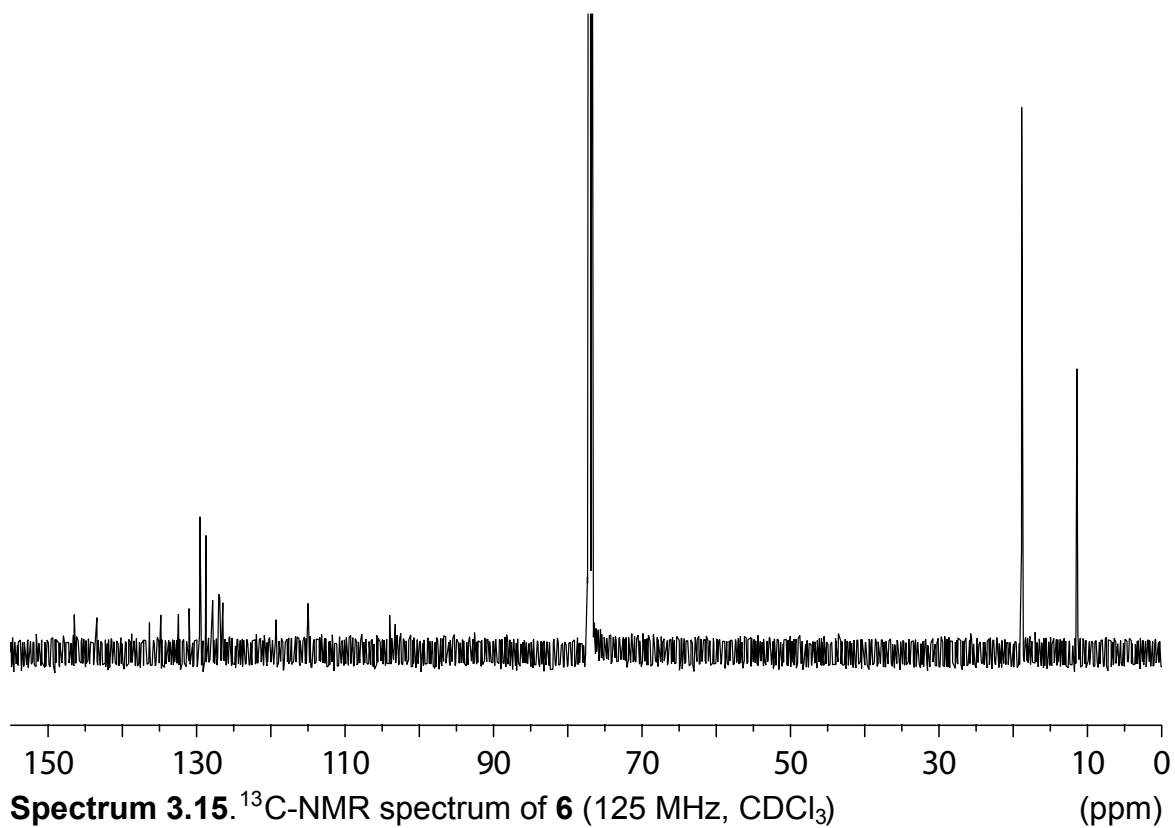
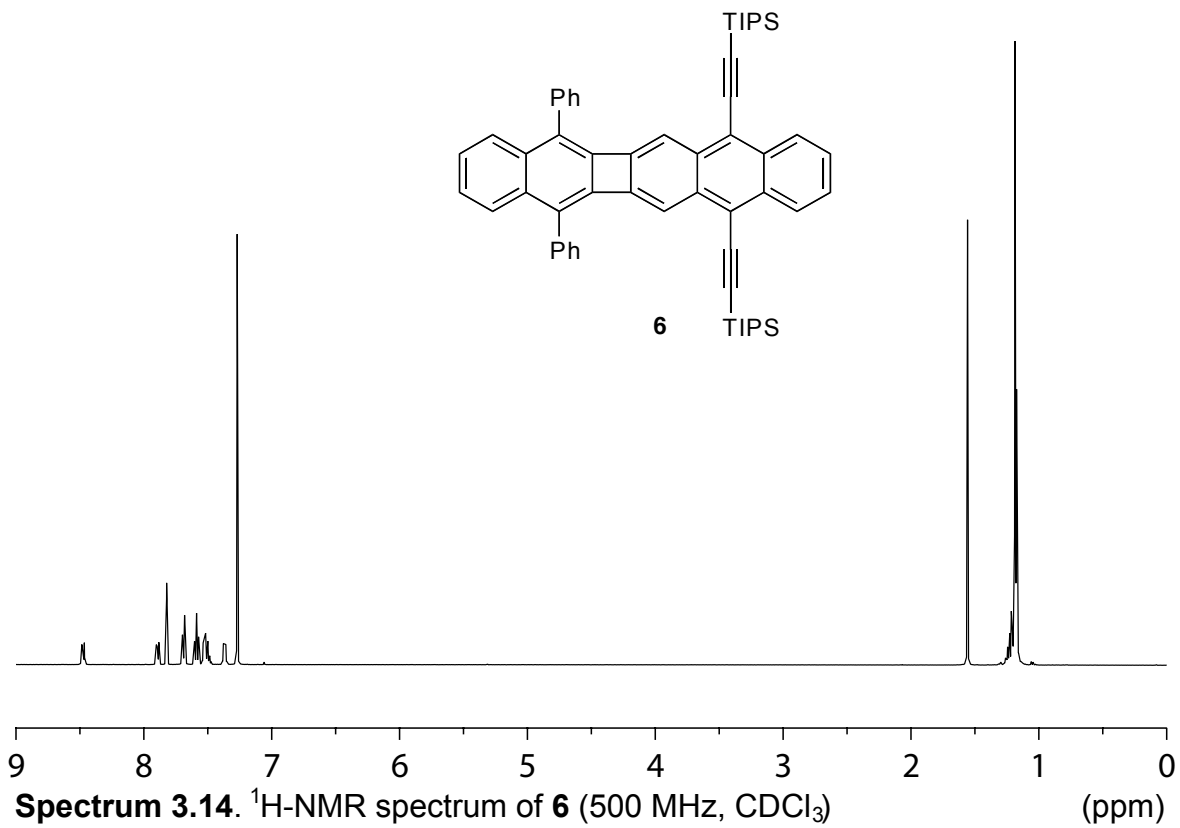


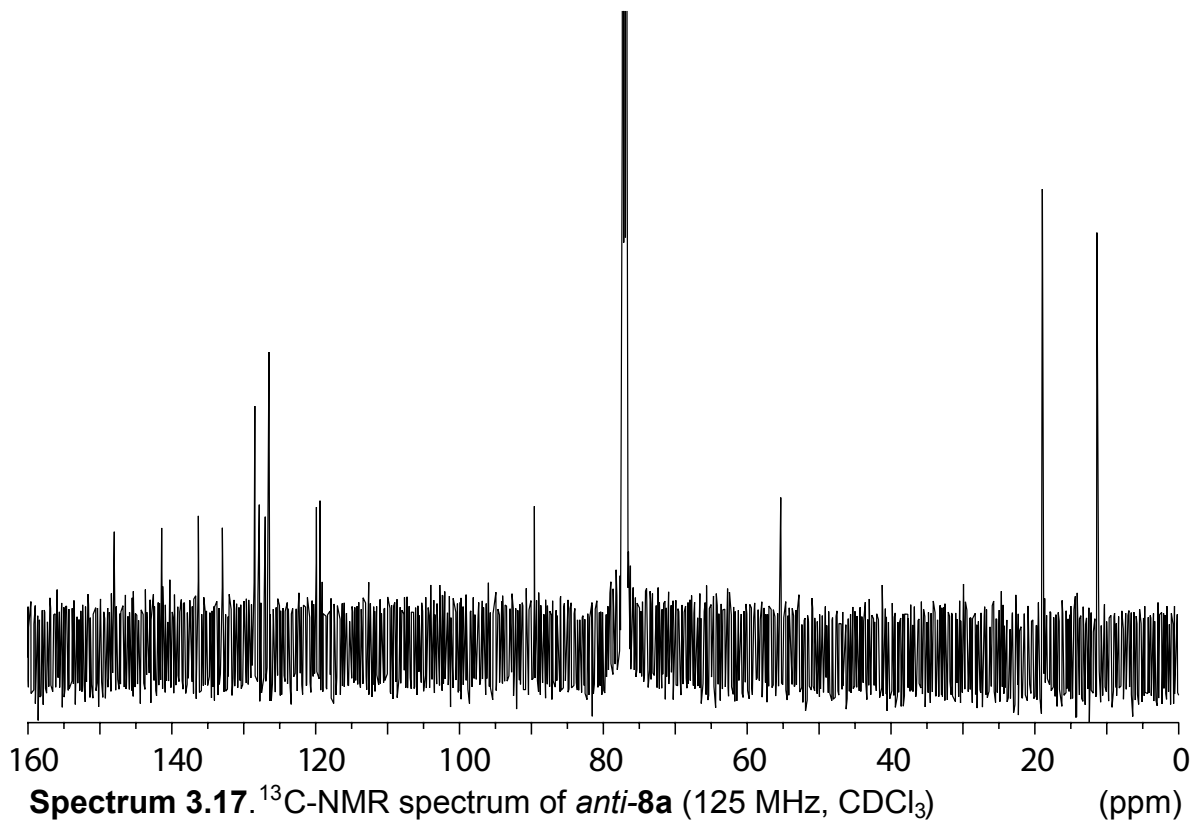
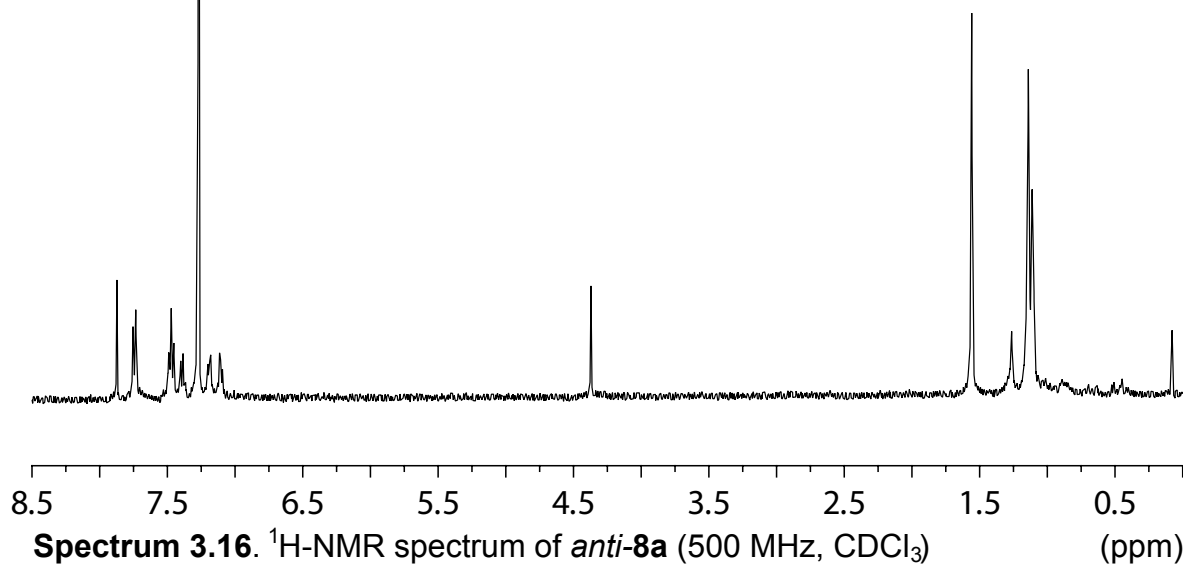
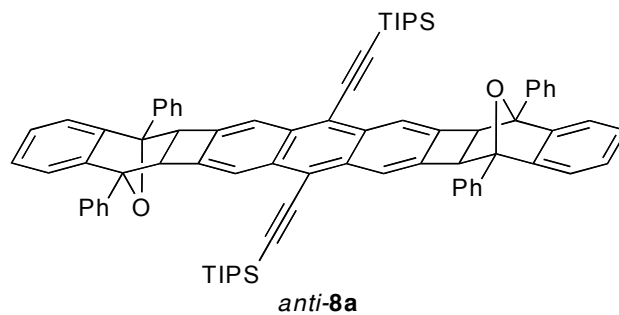
3

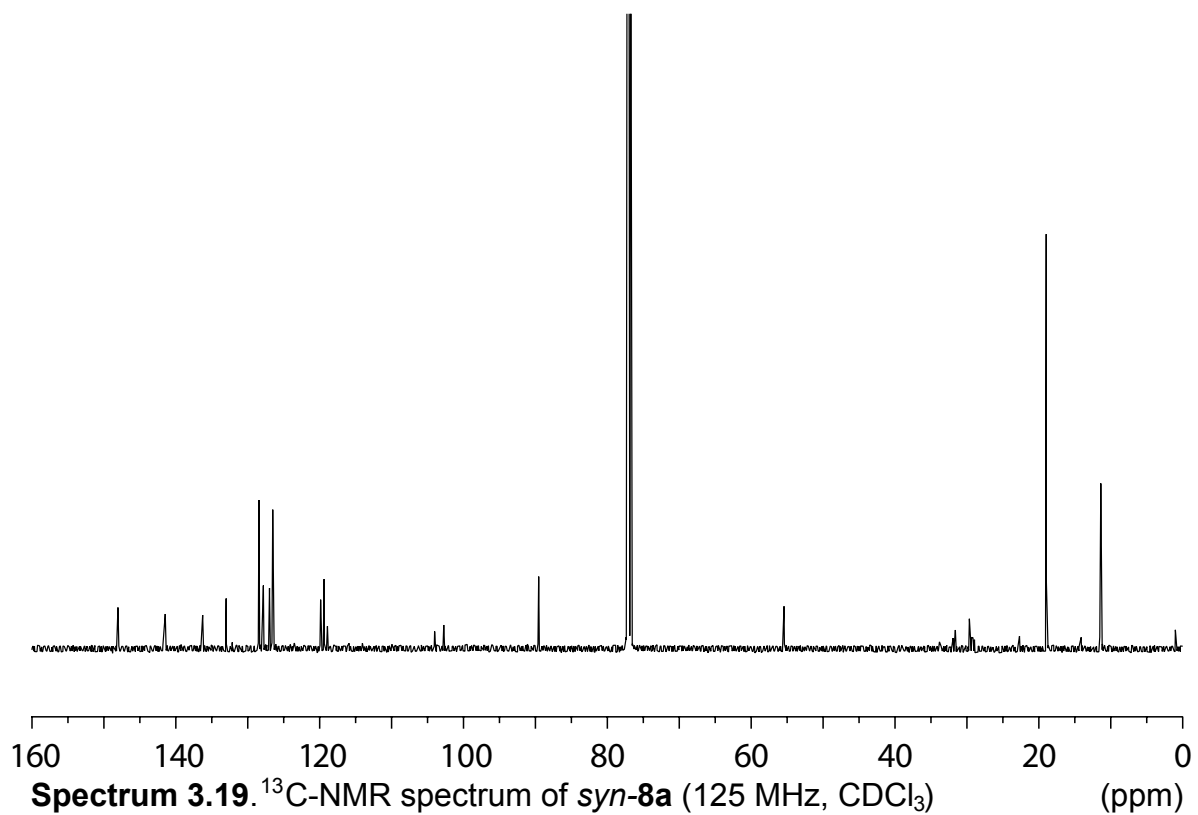
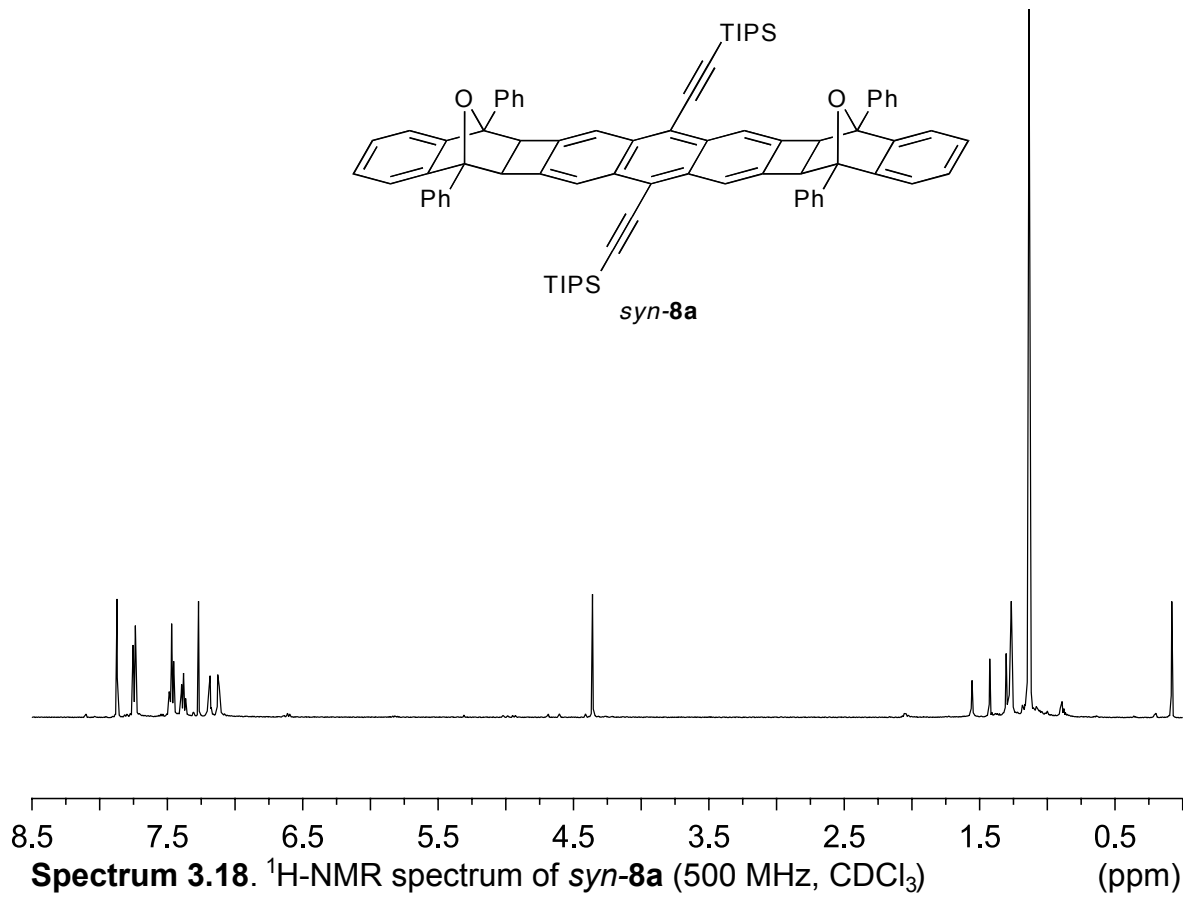
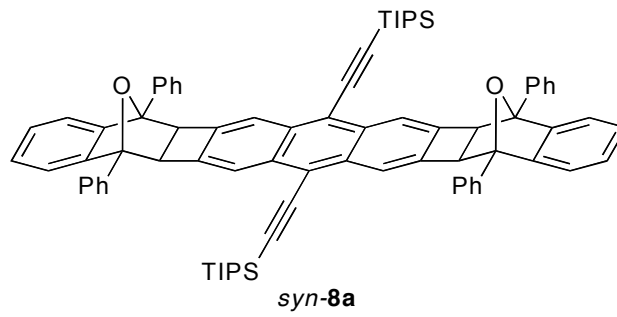


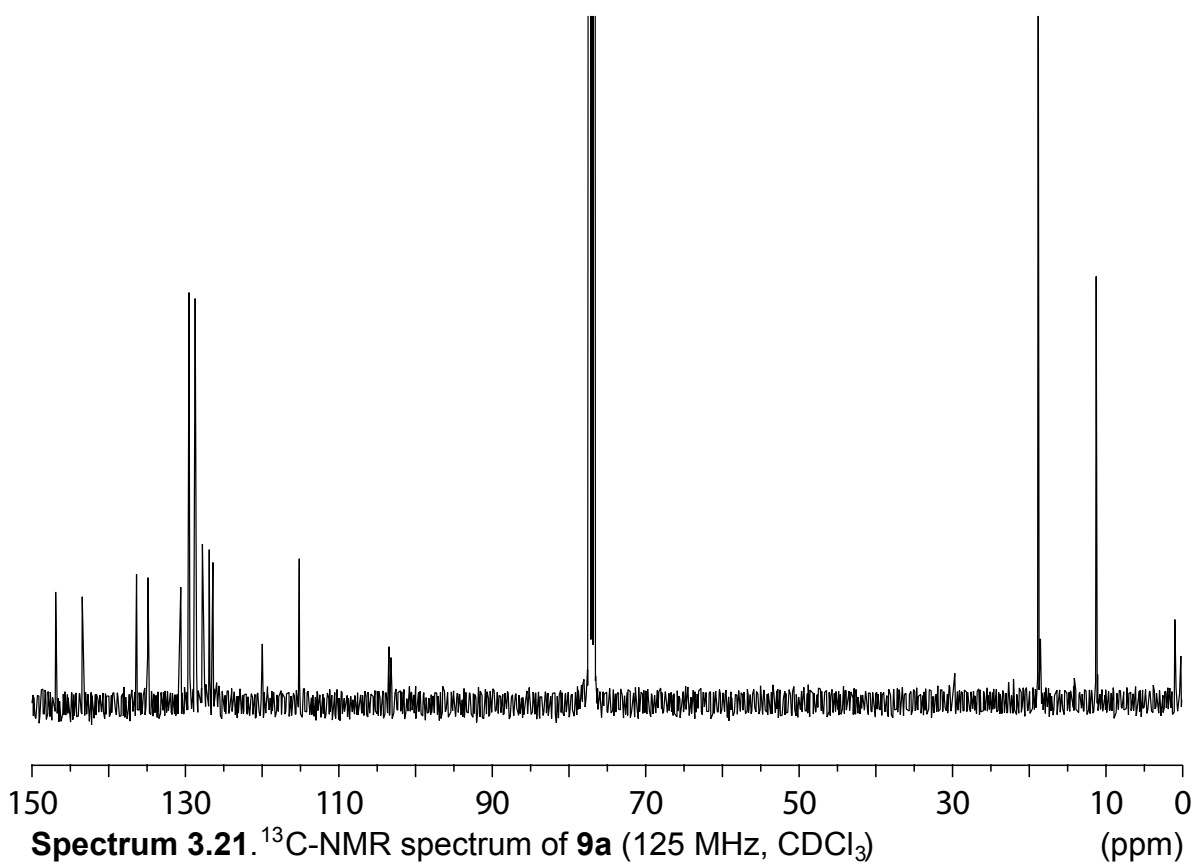
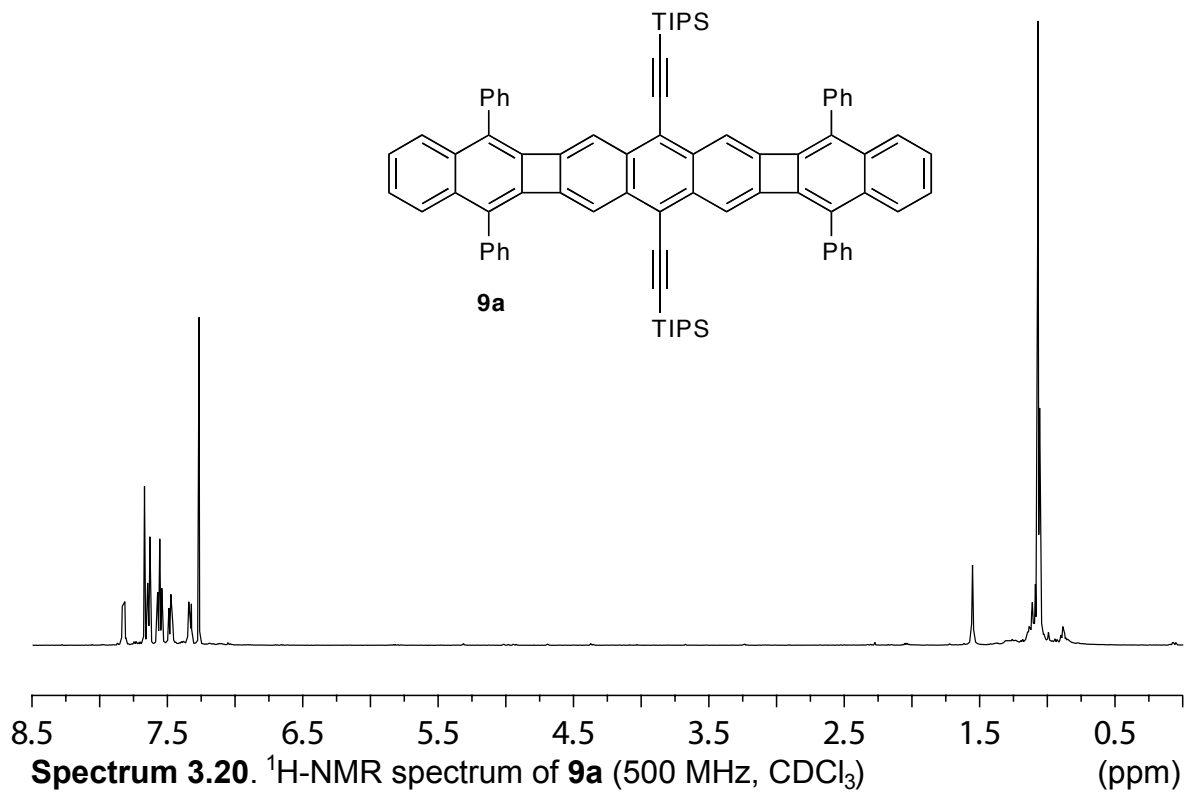


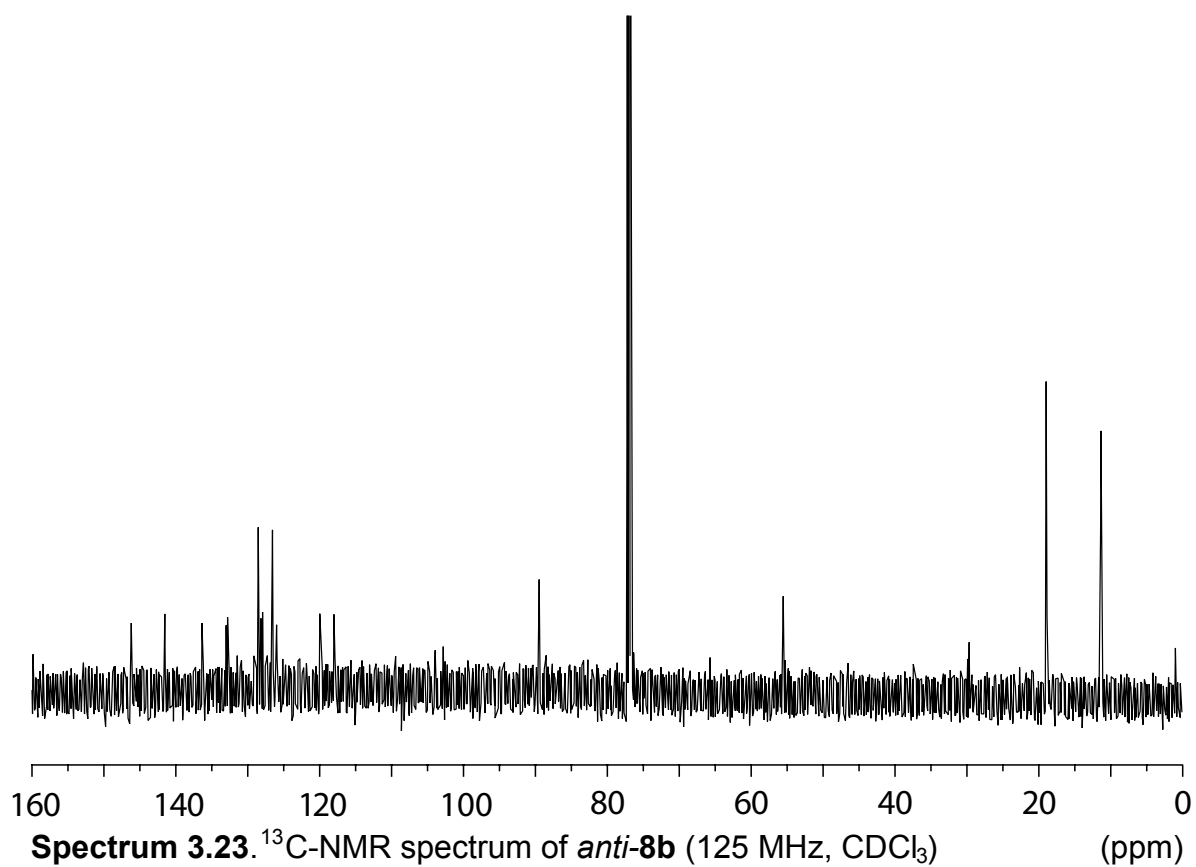
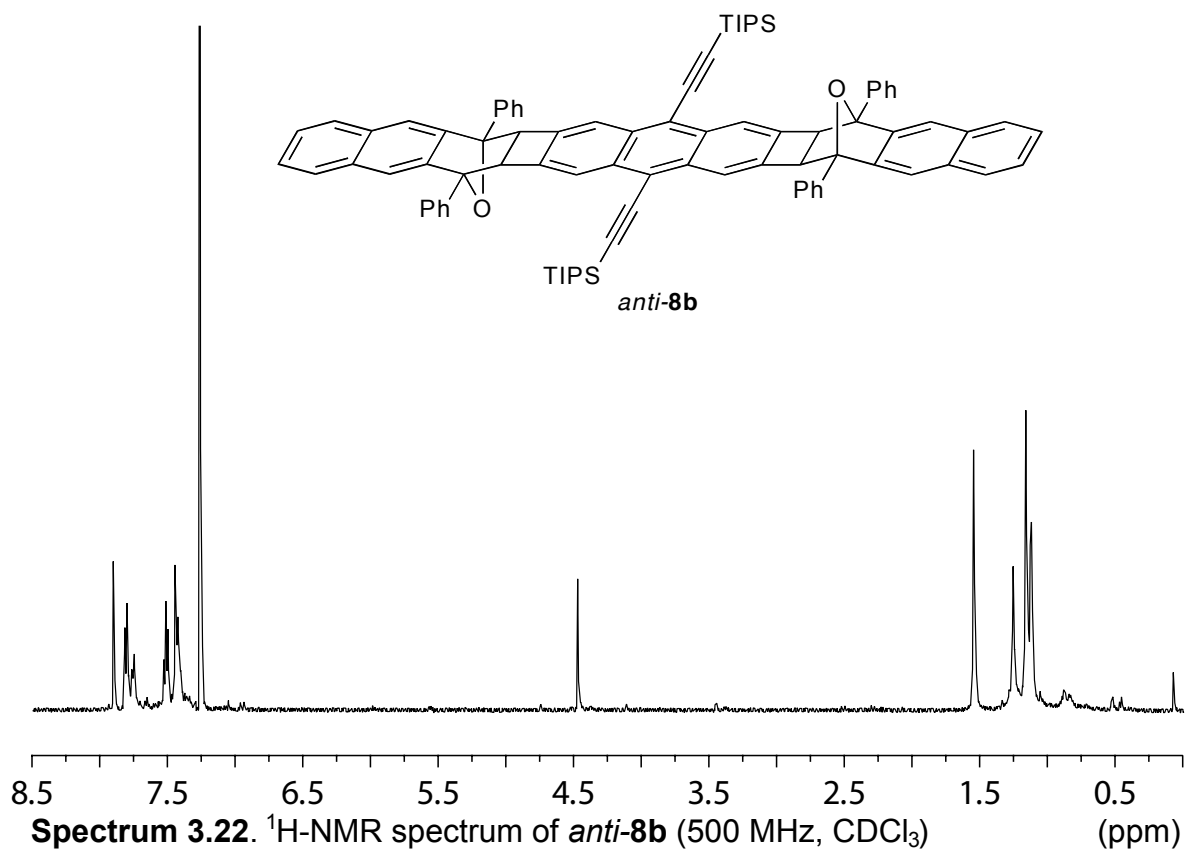


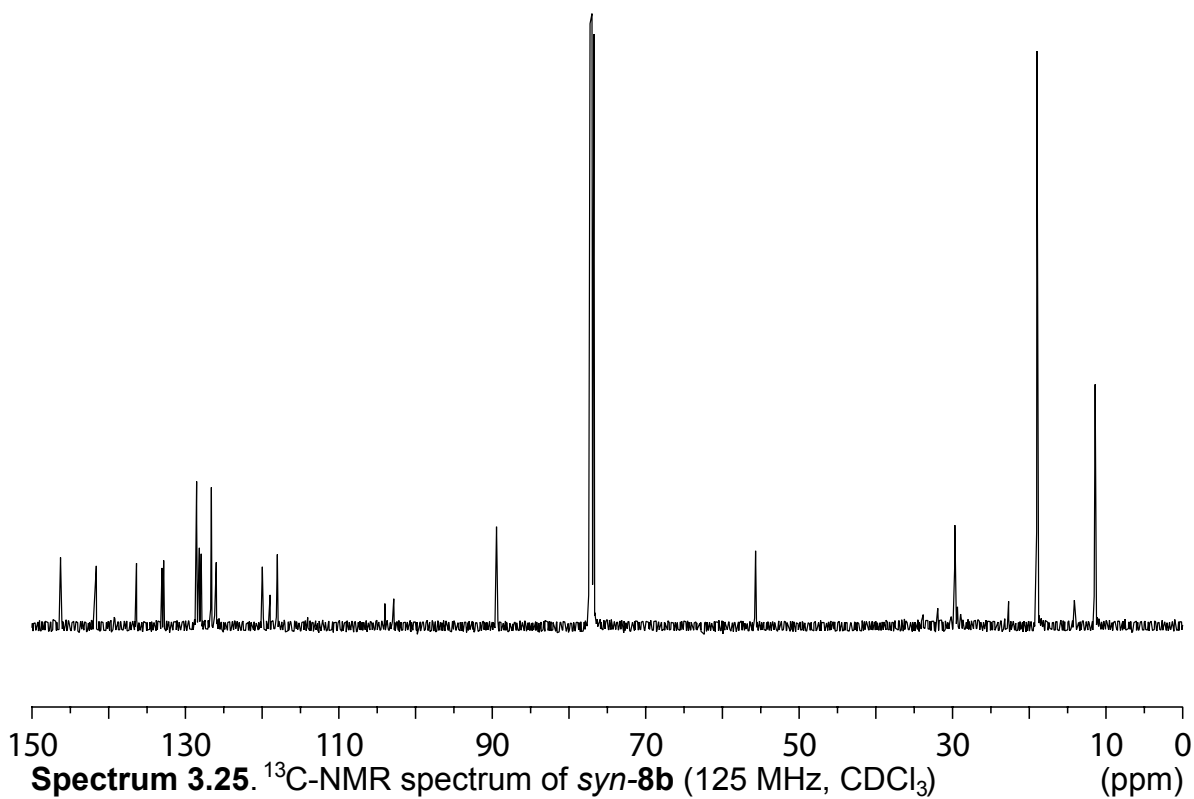
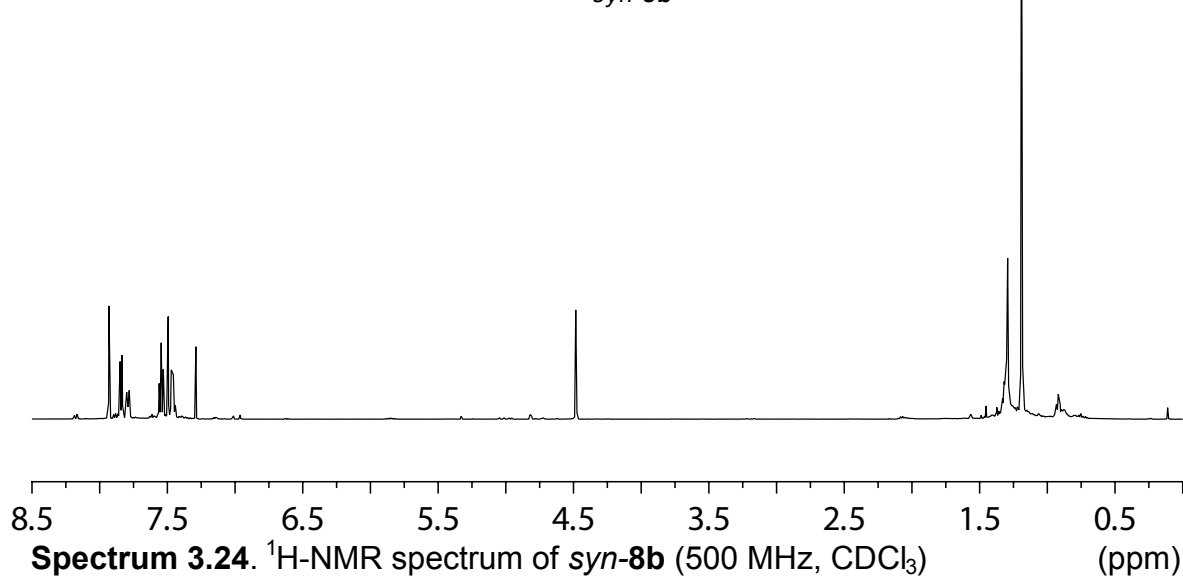
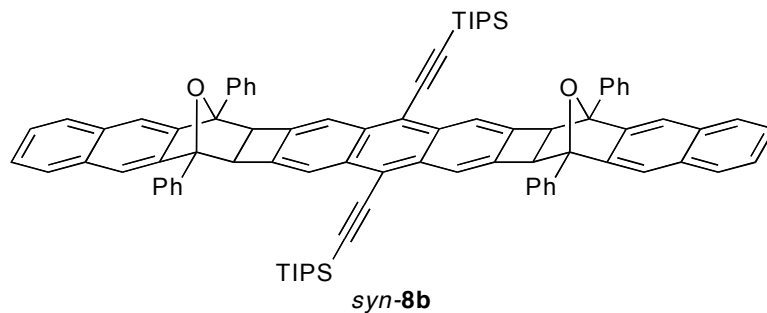


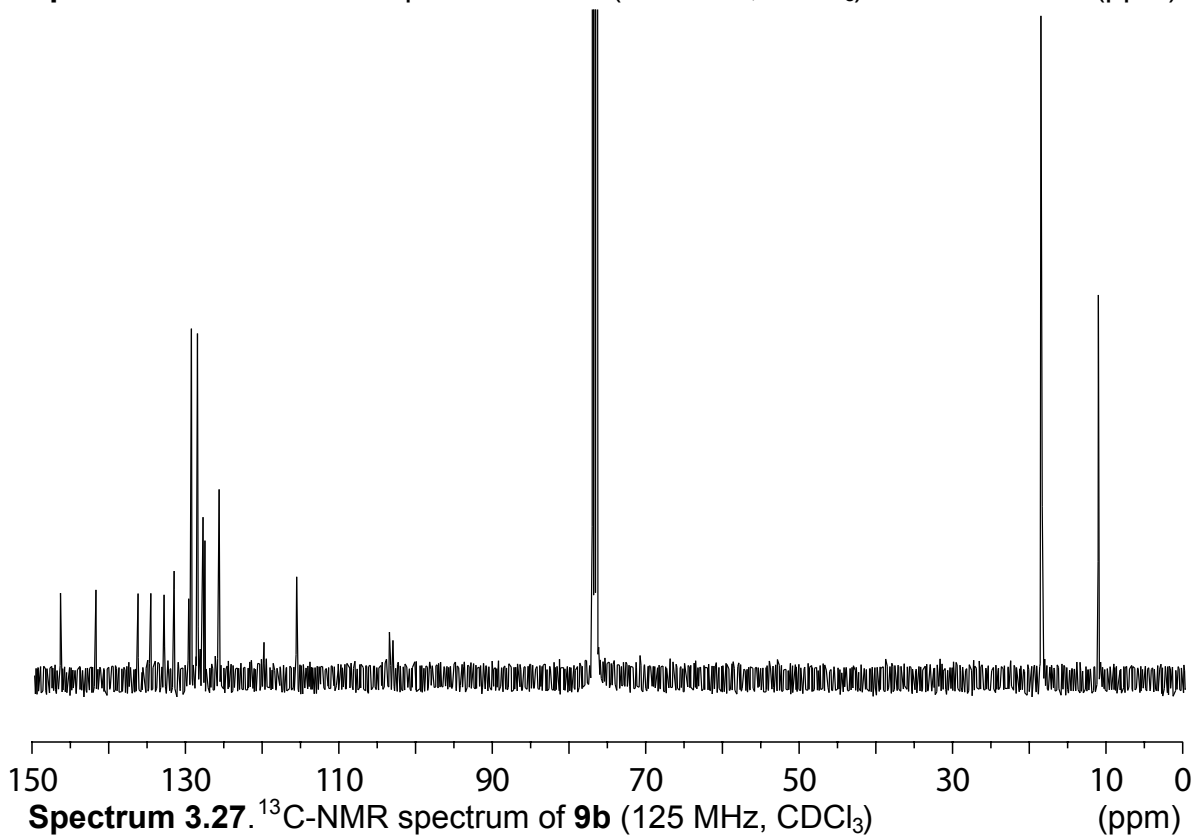
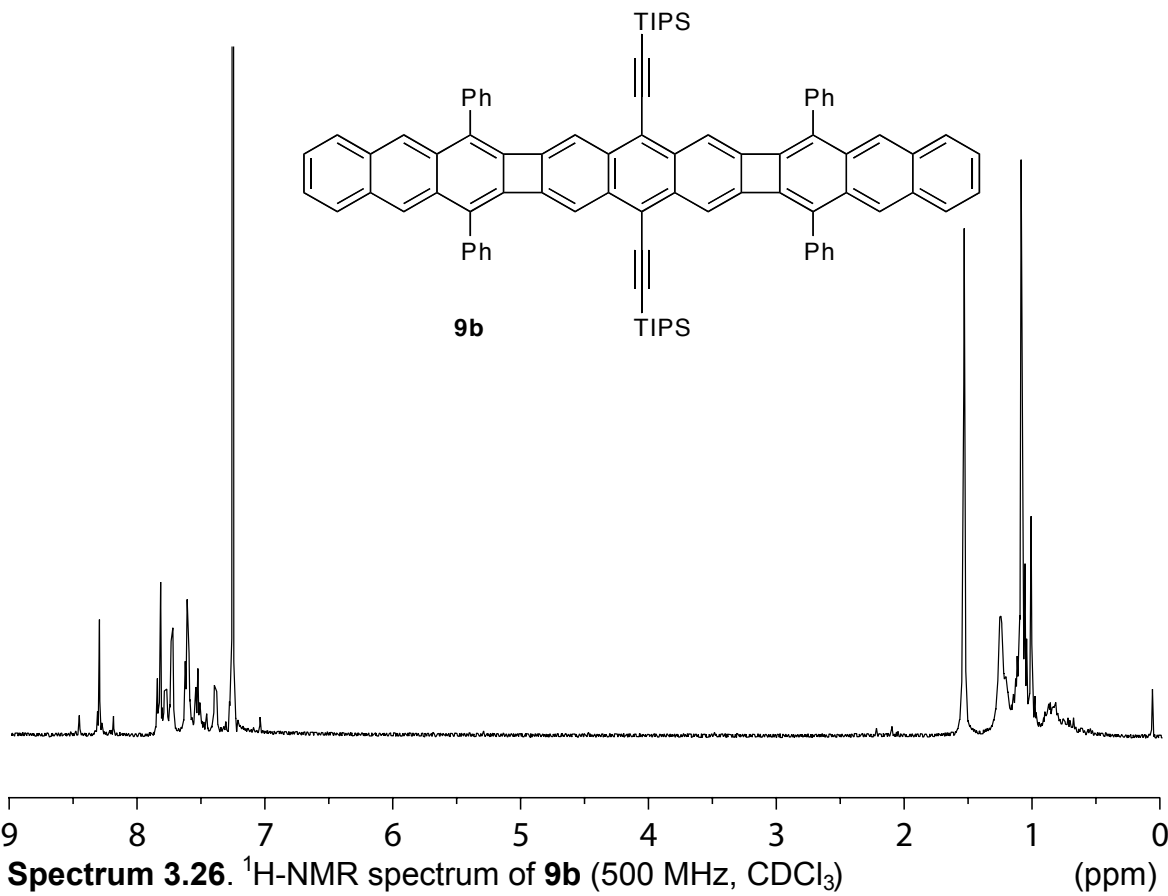


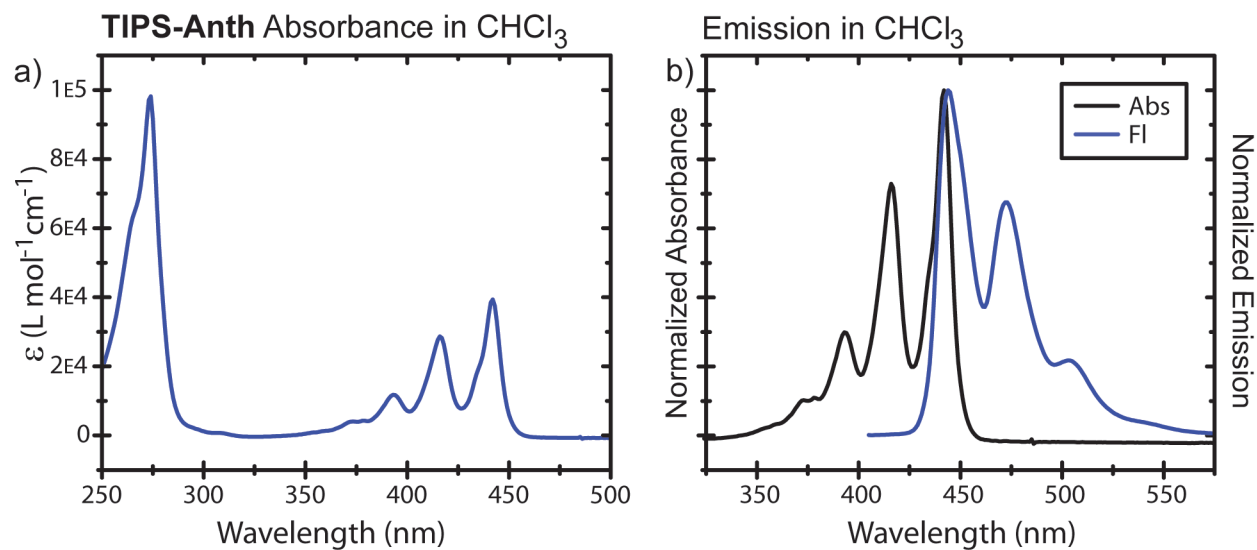




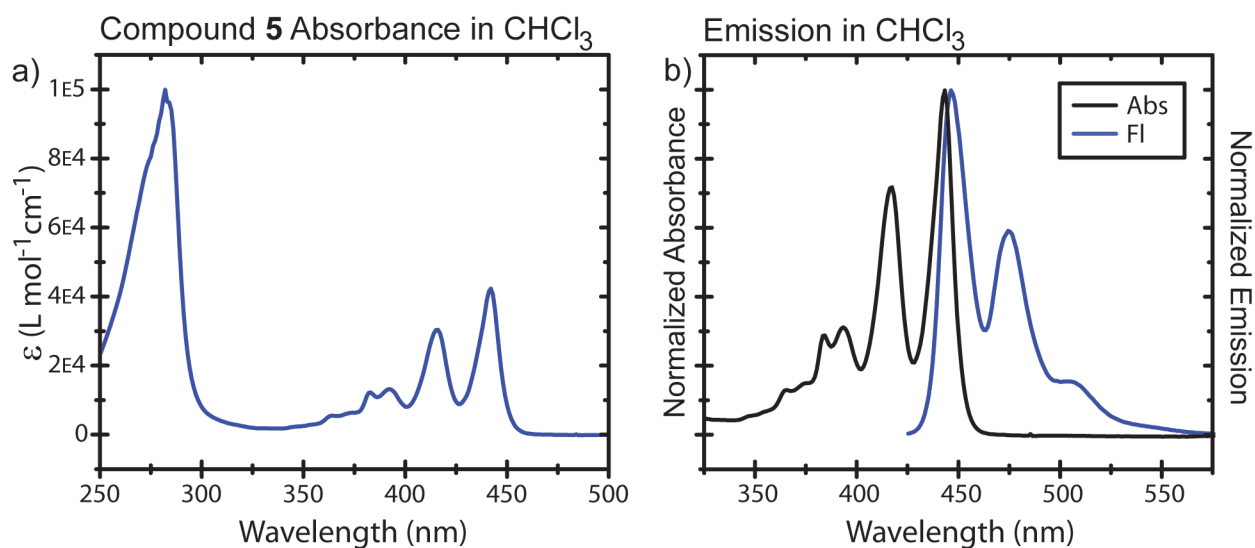




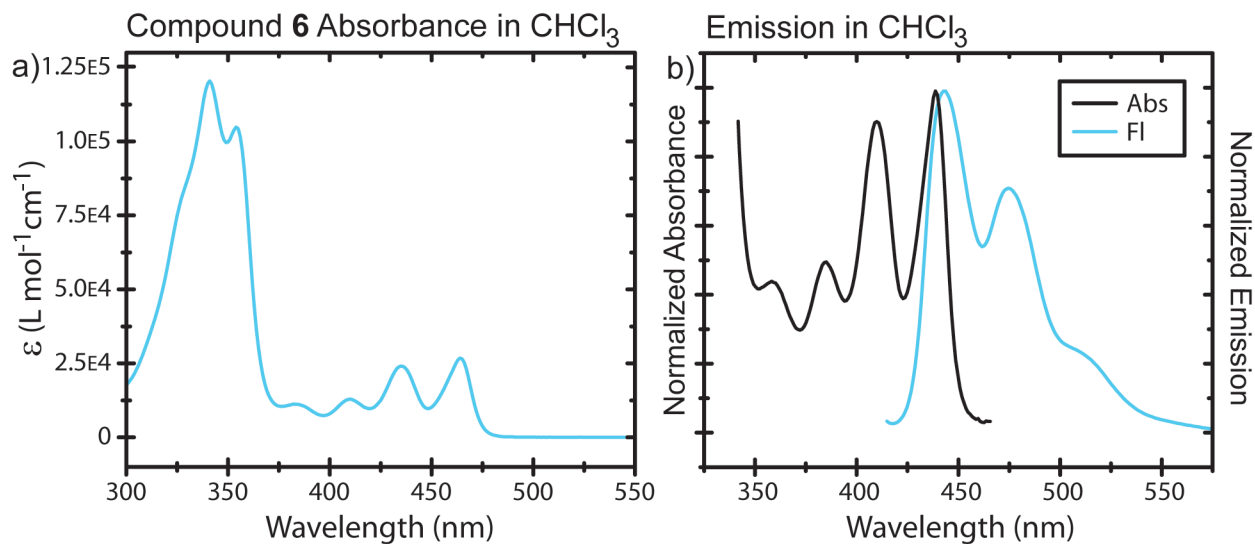




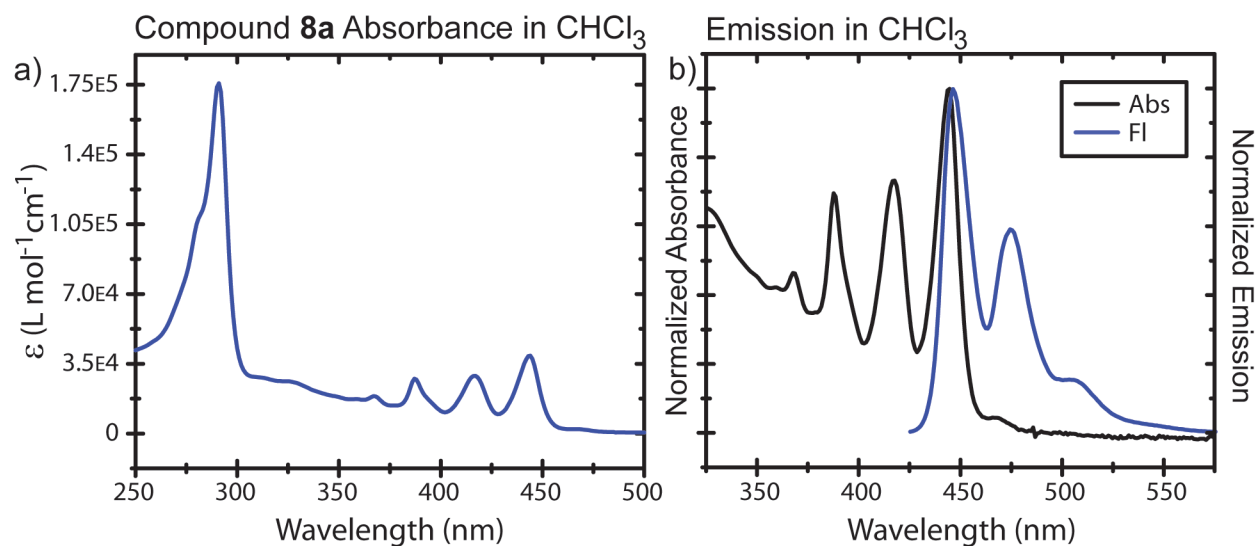
Spectrum 3.28. (a) Absorbance of **TIPS-Anth** in CHCl₃ (b) Emission of **TIPS-Anth** in CHCl₃, $\lambda_{\text{max}} = 442$ nm, $\lambda_{\text{em}} = 444$ nm, $\phi_{\text{em}} = 0.97$ (std: 9,10-diphenylanthracene/cyclohexane), $\tau = 5.04$ ns.



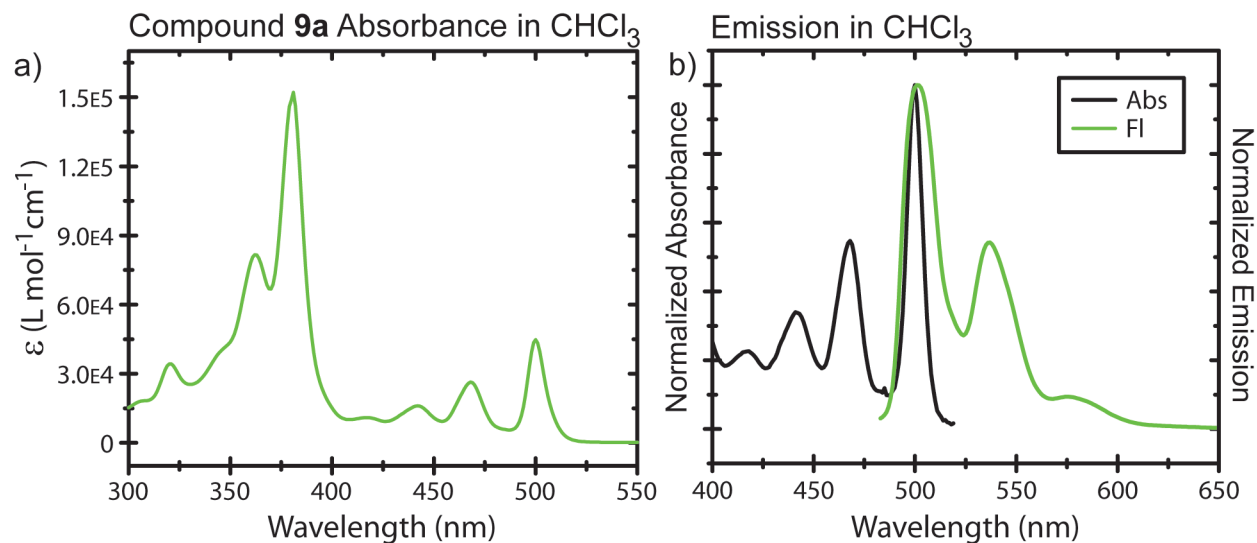
Spectrum 3.29. (a) Absorbance of **5** in CHCl_3 (b) Emission of **5** in CHCl_3 , $\lambda_{\text{max}} = 443 \text{ nm}$, $\lambda_{\text{em}} = 446 \text{ nm}$.



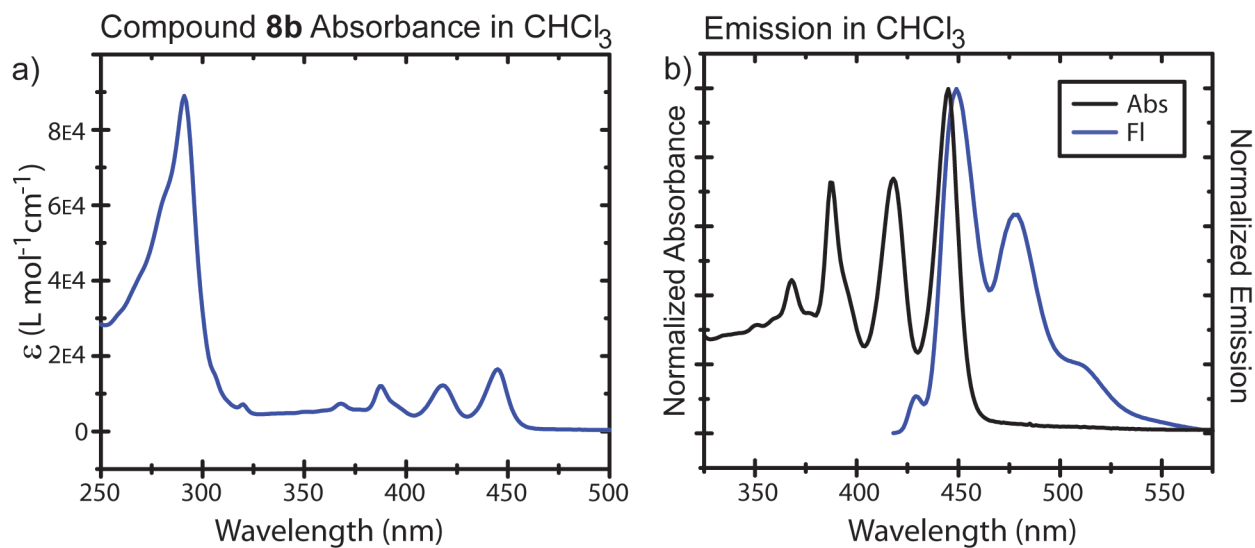
Spectrum 3.30. (a) Absorbance of **6** in CHCl_3 (b) Emission of **6** in CHCl_3 , $\lambda_{\text{max}} = 464 \text{ nm}$, $\lambda_{\text{em}} = 469 \text{ nm}$, $\phi_{\text{em}} = 0.69$ (std: perylene/EtOH), $\tau = 7.72 \text{ ns}$.



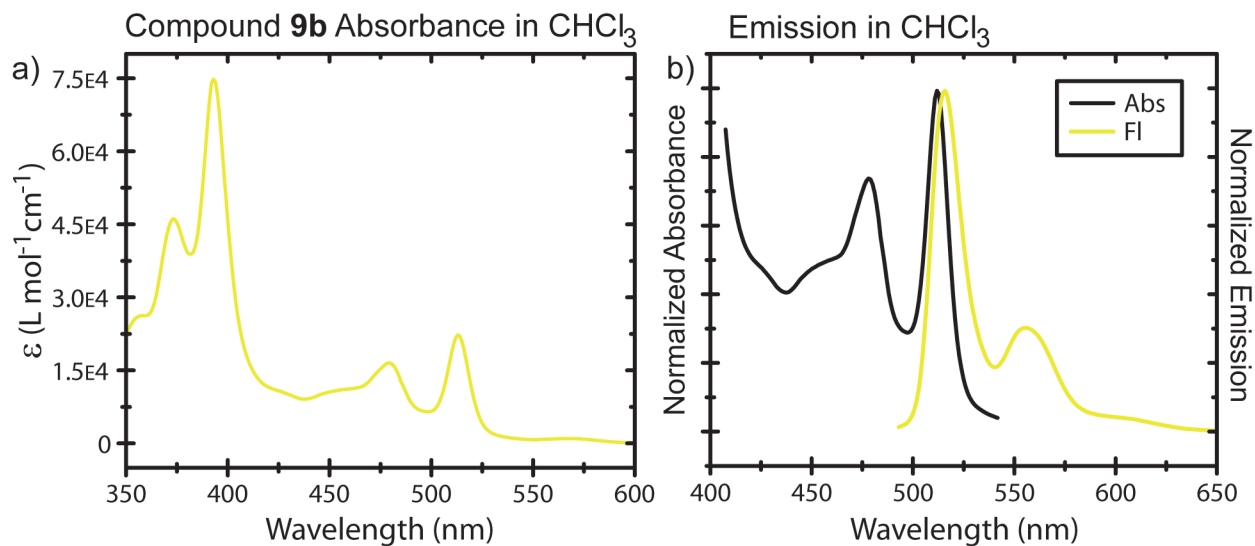
Spectrum 3.31. (a) Absorbance of **8a** in CHCl_3 (b) Emission of **8a** in CHCl_3 , $\lambda_{\text{max}} = 444 \text{ nm}$, $\lambda_{\text{em}} = 447 \text{ nm}$.



Spectrum 3.32. (a) Absorbance of **9a** in CHCl_3 (b) Emission of **9a** in CHCl_3 , $\lambda_{\text{max}} = 500 \text{ nm}$, $\lambda_{\text{em}} = 502 \text{ nm}$, $\phi_{\text{em}} = 0.45$ (std: coumarin 6/EtOH), $\tau = 5.60 \text{ ns}$.



Spectrum 3.33. (a) Absorbance of **8b** in CHCl_3 (b) Emission of **8b** in CHCl_3 , $\lambda_{\text{max}} = 445 \text{ nm}$, $\lambda_{\text{em}} = 449 \text{ nm}$.



Spectrum 3.34. (a) Absorbance of **9b** in CHCl_3 (b) Emission of **9b** in CHCl_3 , $\lambda_{\text{max}} = 513 \text{ nm}$, $\lambda_{\text{em}} = 517 \text{ nm}$, $\phi_{\text{em}} = 0.26$ (std: coumarin 6/EtOH), $\tau = 6.71 \text{ ns}$.

Chapter 4

Acenoid Derivatives for Singlet Fission in Organic Solar Cells

This chapter is the result of collaborative efforts between the author and Nicholas Thompson of the Baldo research group. Mr. Thompson is responsible for the data in Figures 4.5 and 4.6.

4.1 Introduction

Replacement of inorganic active layers in solar cells with organic materials has the potential to decrease manufacturing costs with increased ease of processability as well as compatibility with flexible substrates.¹ Singlet fission is a photophysical phenomenon first detected in anthracene crystals in 1965,² in which there has recently been a resurgence in interest due to its potential for improving the efficiency of organic solar cells.³ In this spin-allowed process, an incoming photon excites a chromophore in the ground state (S_0 , Figure 4.1) to its first singlet excited state (S_1).⁴ The resulting exciton then interacts with a neighboring chromophore in the ground state, transferring energy and generating two excitons in the first triplet excited state (T_1). This phenomenon generally occurs in chromophores in which the energy of S_1 ($E(S_1)$) is approximately twice that of T_1 ($E(S_1) \approx 2E(T_1)$).

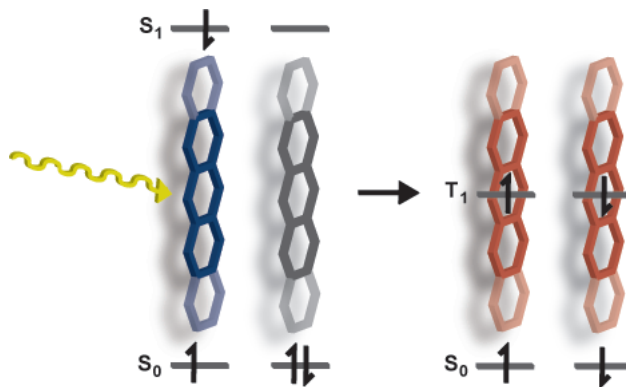


Figure 4.1. Singlet Fission to produce two triplet excitons.

The theoretical limit of efficiency in organic solar cells, known as the Shockley-Queisser limit,⁵ is approximately 31%. Calculations have shown that this value could be increased to approximately 44% in a photovoltaic device in which singlet fission occurs quantitatively, generating two charge carriers for each incoming photon (Figure 4.2).⁶ The potential of singlet fission has already been successfully exploited by Baldo and coworkers in pentacene-based

photodetectors with quantum efficiencies greater than 100%,⁷ and by improving the performance of tetracene-based solar cells.^{3b} Other potential advantages to triplets as charge carriers include a decrease in back electron transfer to the ground state, as this process would be spin-forbidden, longer exciton diffusion, and longer exciton lifetimes to allow for charge separation (however, this also increases susceptibility to quenching).⁴

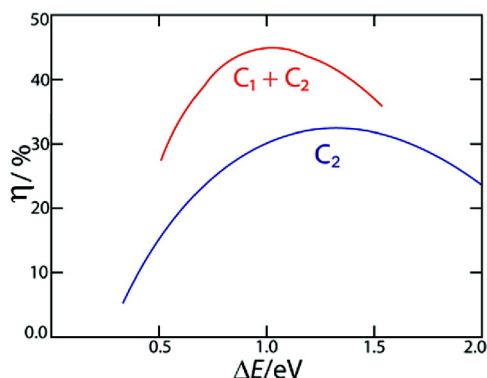


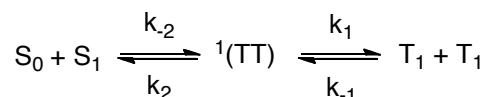
Figure 4.2. Schematic representation of the theoretical efficiency as a function of the S_0 - T_1 energy difference (ΔE) of a standard organic photovoltaic cell (OPV, blue) and a singlet fission OPV (red). Reproduced with permission from ref. 4. Copyright 2010 American Chemical Society.

Singlet fission has been observed in a variety of chromophores including polythiophenes,⁸ polydiacetylenes,⁹ and carotenoids,¹⁰ but it has classically and most often been associated with oligoacenes, such as anthracene, as mentioned above. The values associated with $E(S_1)$ and $E(T_1)$ of anthracene, tetracene, and pentacene are summarized in Table 4.1. In the case of tetracene the singlet fission process is slightly endoergic [$2E(T_1) > E(S_1)$] and therefore requires thermal activation,¹¹ whereas in pentacene it is slightly exoergic [$2E(T_1) < E(S_1)$].^{10c}

Table 4.1. Literature values for E(S₁) and 2E(T₁) for acenes n = 3-5.

Compound	E(S ₁) (eV)	2 × E(T ₁) (eV)
Anthracene (n = 3) ¹²	3.13	3.66
Tetracene (n = 4) ¹³	2.32	2.50
Pentacene (n = 5) ¹⁴	1.83	1.72

It has been demonstrated in the literature that the rates of singlet fission and the reverse process, triplet-triplet annihilation to give a singlet, are both magnetic field dependent, with singlet fission decreasing with increasing applied magnetic field.¹⁵ A very simplified model for understanding this result is the mechanism displayed in Scheme 4.1.⁴ In this scheme the two chromophores pass through a spin-paired correlated triplet-triplet state [¹(TT)]. The rate of singlet fission (k₁) is proportional to the singlet character of the ¹(TT) state, which decreases with increased magnetic field.⁷ As stated previously, this is a simplified model that does not account for all of the experimental observations associated with singlet fission, however it predicts this particular phenomenon accurately.



Scheme 4.1. Simplified mechanism of singlet fission (forward direction) and triplet-triplet annihilation (reverse direction).

Although the study of singlet fission has become increasingly prevalent in the literature during the last decade, there is still much to be understood. If it is to be employed in organic photovoltaics, it is necessary to find a chromophore that meets several criteria: singlet fission must occur at a very fast rate and the reverse process at a slow rate, and there should be coupling

interactions between neighboring chromophores in the solid state that are strong enough for fission to occur but weak enough to allow the resulting triplets to become independent.⁴

4.2 Singlet Fission in Dithienyl-Acenes

The first synthesis of 6,13-di(thien-2-yl)pentacene **1** was reported independently by two groups in 2005 and 2006.¹⁶ Nuckolls and coworkers^{16b} were interested in studying the solid-state properties of aryl-substituted acenes in search of stable acenes with high charge mobilities. As predicted, thiophene-substitution forces **1** to stack in an organized, cofacial manner with a distance of 3.6 Å between acene cores (Figure 4.3). Due in part to this solid-state arrangement, thin film field effect transistors (FETs) of **1** were shown to have very high charge mobilities of $0.1 \text{ cm}^2 \text{ V}^{-1} \text{ s}^{-1}$. Although there did not appear to be any long-range ordering in the thin films *via* X-ray scattering, a large bathochromic shift (73 nm) in the thin film absorption spectrum indicated significant π -stacking.

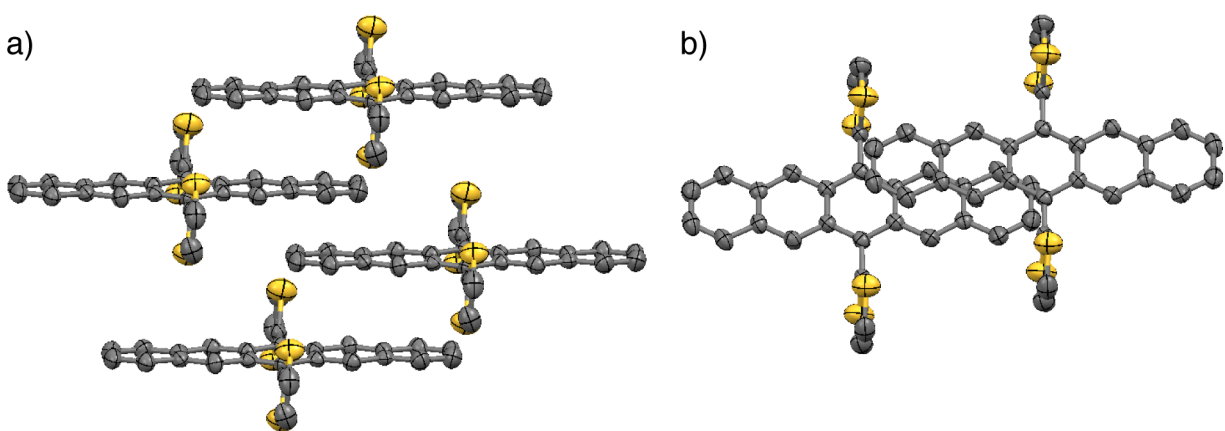
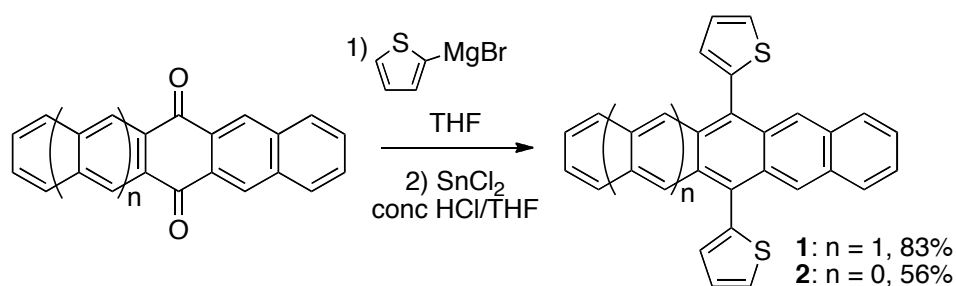


Figure 4.3. Two views of the crystal packing of **1**. The position of the sulfur atoms (yellow) is disordered in the crystal with a mixture of *syn* and *anti* configurations. Crystal structure data from ref. 16b gathered from the American Chemical Society.

Inspired by the promising electronic properties of **1**, we chose to investigate its singlet fission ability, as well as that of the previously unknown 5,12-di(thien-2-yl)tetracene (**2**). Compounds **1** and **2** were synthesized from the corresponding acenequinone using a modification of the procedure reported by Nuckolls (Scheme 4.1). Compound **2** is a bright red-orange solid that emits green with a fluorescence quantum yield of 17% (Figure 4.4a).



Scheme 4.2 Synthesis of thienyl-substituted acenes **1** and **2**.

The overlay of the absorbance of compound **2** in both solution and in the solid state is shown in Figure 4.4b. Nuckolls *et al.* observed a large bathochromic shift (73 nm) and change in the vibrational structure in the absorbance spectrum of **1** in going from solution to thin film, which they attributed to ordering in the films and Davydov splitting.^{16b} For **2**, however, there is only a small bathochromic shift of 15 nm between the solution and solid state absorbance spectra and the vibronic progression is relatively unchanged, indicating that coupling in the solid state may not be as effective. The same pattern was observed in 5,12-diphenyltetracene in work published in 2012.¹⁷ Fortunately in that case, singlet fission efficiencies upwards of 61% were observed in the largely amorphous thin films.

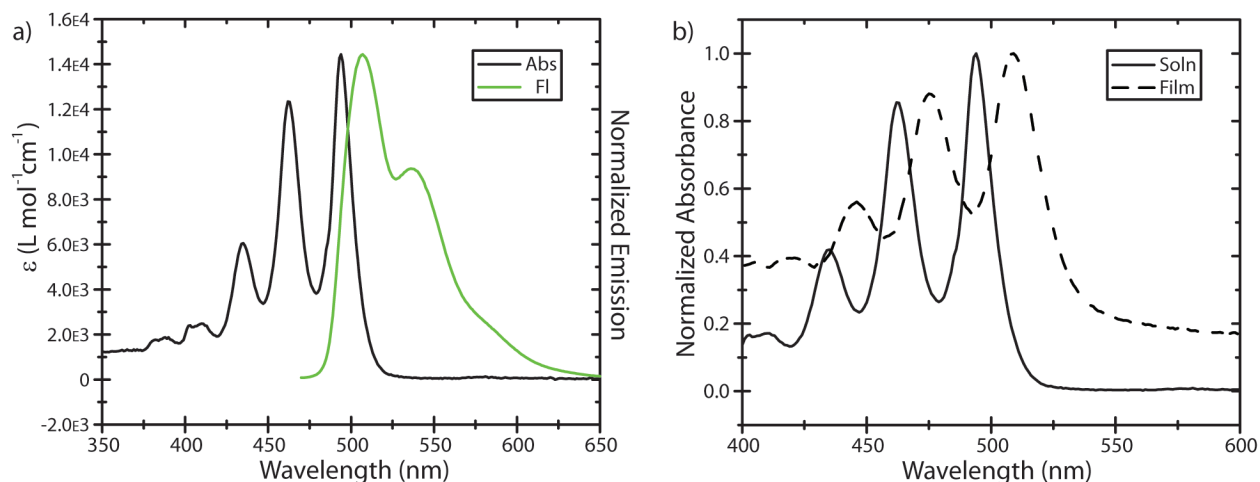


Figure 4.4. (a) Absorbance and emission of **2** in methylcyclohexane, $\lambda_{\max} = 494$ nm, $\lambda_{\text{em}} = 507$ nm, $\phi_{\text{em}} = 0.17$, $\tau = 3.792$ ns. (b) Absorbance of **2** in solution state and thin film (thin film $\lambda_{\max} = 509$ nm). Thin films were prepared by spin-coating a solution of **2** in PhCH₃.

The occurrence of singlet fission in a powder sample of **2** was investigated by recording the change in fluorescence under an applied magnetic field (Figure 4.5). The resulting curve is typical of singlet fission systems, with a small decrease in fluorescence at low field, followed by an increase at higher field. An increase of approximately 8% is reached at 0.5 T. In their seminal work on tetracene, Merrifield and coworkers measured this effect on single crystals using a specific orientation of the magnetic field relative to the axes of the crystal.^{15b} Since the measurements reported here were performed on a powder of **2**, singlet fission is likely even more efficient than the plot indicates.

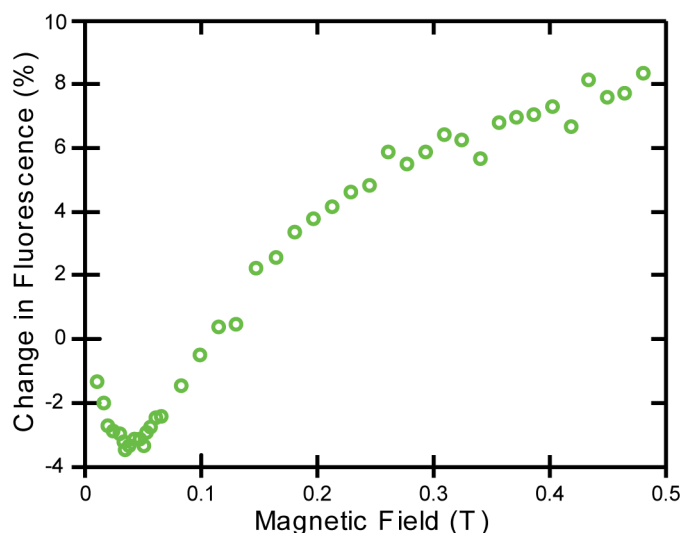


Figure 4.5. Percent change in instant fluorescence of **1** with increasing magnetic field.

Photovoltaic devices using **1** as the donor layer were also investigated. In 2009, Nuckolls and coworkers demonstrated the use of **1** as a hole-transporting layer in a bilayer solar cell.¹⁸ They observed efficiencies comparable to those previously reported in solar cells composed of unsubstituted pentacene with improved stability,¹⁹ however they did not consider any potential effects of singlet fission. In the present work, a solar cell was constructed using dicyano-perylene diimide (**PDI-CN2**, Figure 4.7) as the acceptor layer to ensure that the triplets are dissociated at the donor/acceptor interface. The band diagrams and device architecture for these measurements are shown in Figure 4.6a.

The bilayer junction acted as a rectifying diode and photocurrent was only observed under illumination. The plot of the external quantum efficiency of three devices (EQE, Figure 4.6c) indicates that the current in the devices is generated by **1**, since its shape overlaps well with that of the absorbance spectrum. The photocurrent decreases with increasing magnetic field, indicating both that singlet fission is occurring and that the triplets are able to dissociate at the interface (Figure 4.6d).

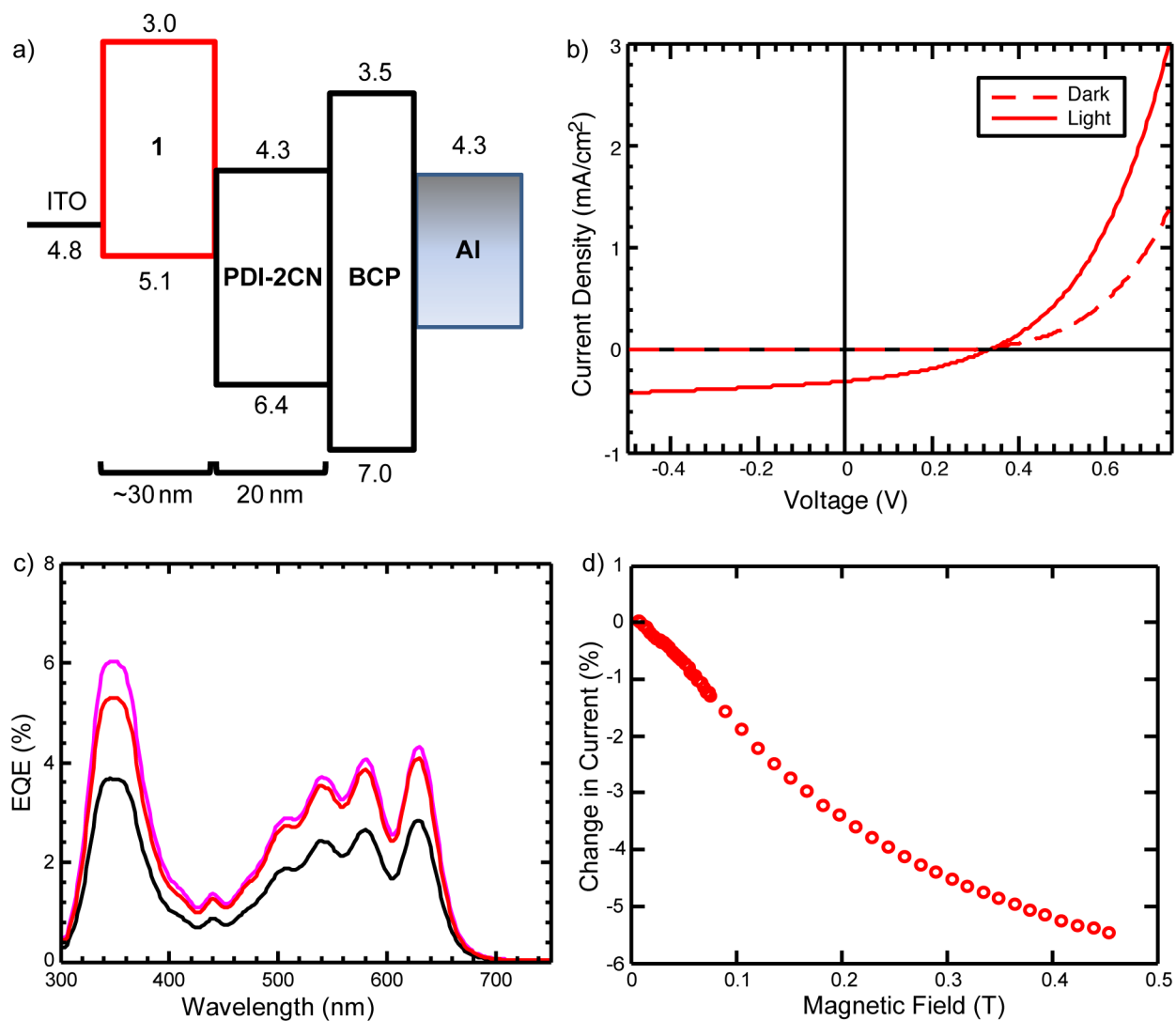


Figure 4.6. (a) Device architecture, (b) $J-V$ curve, $V_{OC} = 0.33$ V, (b) plot of external quantum efficiency (EQE), and (d) plot of magnetic field dependence of photocurrent.

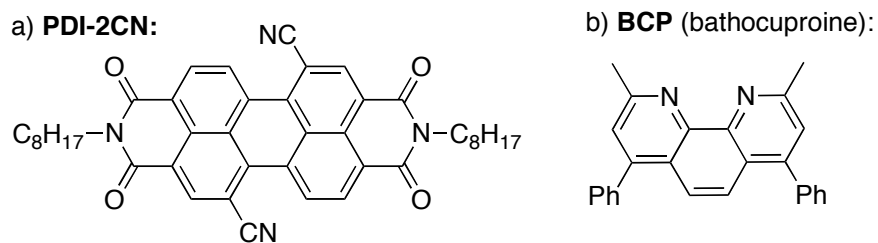
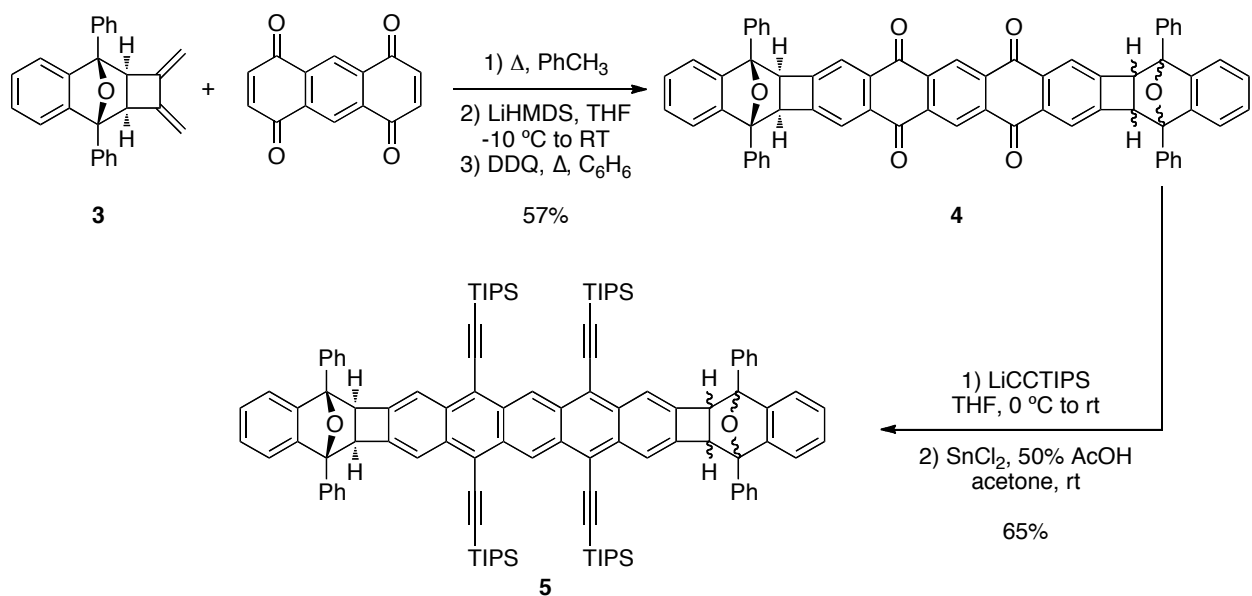


Figure 4.7. Chemical structure of (a) PDI-2CN, and (b) BCP (bathocuproine).

4.3 Towards Phenylene-Containing Oligoacenes (POAs) for Singlet Fission

Inspired by the renewed interest in oligoacenes for organic photovoltaic applications, we sought to investigate the phenomenon of singlet fission in phenylene-containing oligoacenes (POAs, cf. chapter 3). POAs are a new class of polycyclic aromatic hydrocarbons (PAHs) that combine the properties of acenes and [N]phenylenes, resulting in stable, extended ladder structures. Unfortunately singlet fission is not very efficient in anthracenes, such as the POAs reported previously, due to the relatively high endoergicity of the process ($2E(T_1) - (S_1) = 0.53$ eV in unsubstituted anthracene). Therefore, the synthesis of POA containing pentacene was undertaken.

Diene **3** was synthesized according to the procedure described in chapter 3 of this thesis and reacted with bis-dienophile 1,4,5,8-anthraquinone (Scheme 4.3).²⁰ The resulting double Diels-Alder adduct was taken on to the next step without further purification. Deprotonation with lithium hexamethyldisilazide (LiHMDS) followed by oxidation to the quinone, and aromatization with 2,3-dichloro-5,6-dicyano-1,4-benzoquinone (DDQ) yielded compound **4** in a 57% yield over three steps. Nucleophilic addition of TIPS-protected lithium acetylide and tin(II) chloride mediated reductive deoxygenation cleanly yielded pentacene-containing compound **5**. The absorbance spectrum for **5** is expectedly similar to that of TIPS-pentacene ($\lambda_{\text{max}} = 644$ nm)²¹ with a small bathochromic shift ($\lambda_{\text{max}} = 662$ nm) due to the two additional ethynyl substituents (Figure 4.8).



Scheme 4.3. Synthesis of pentacene-containing **5**.

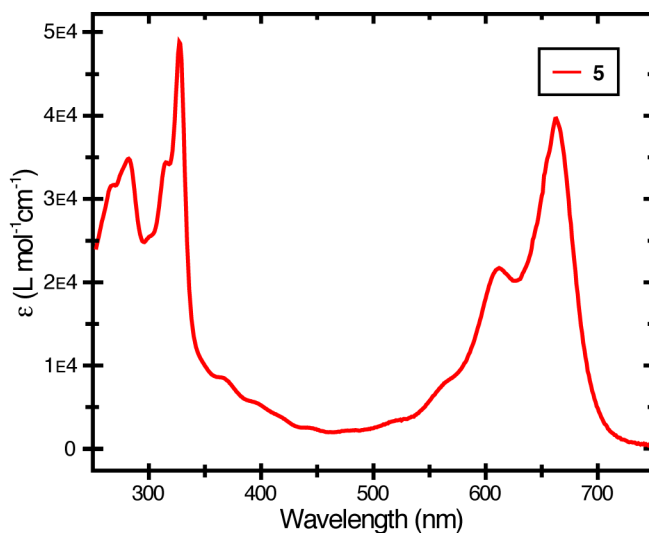
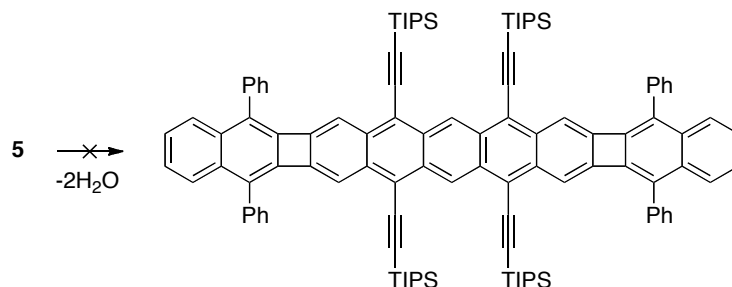


Figure 4.8. Absorbance spectrum of compound **5**, $\lambda_{\text{max}} = 662$ nm.

Surprisingly, the final dehydration step to yield the desired pentacene-containing POA was found to be non-trivial and successful conditions have yet to be found (Scheme 4.4). The conditions investigated thus far are summarized in Table 4.2. Using the dehydration conditions that were successful in the synthesis of [2-3-2] and [3-3-3]POA (cf. chapter 3), *p*-toluenesulfonic acid (pTsOH) in acetic anhydride (Ac₂O), a red-emitting product was obtained with a

desymmetrized ^1H NMR spectrum indicative of monodehydration (Figure 4.9). However, this product rapidly decomposed in the presence of air precluding further characterization.



Scheme 4.4. Attempted dehydration of **5** to pentacene-containing POA.

Table 4.2. Dehydration conditions screened for compound **5**.

Reagent ^a	Solvent ^b	Temp.	Time	Results
AlCl_3	THF	60 °C	2h	Decomposition
P_2S_5	CS_2	r.t.	2h	Decomposition
PPTS	Ac_2O	120 °C	Overnight	Decomposition
LiHMDS	THF	-78 °C to 0 °C to 60 °C	2h	No reaction
HClO_4	EtOH	Reflux	2d	No reaction
pTsOH	PhCH_3	Reflux	24h	No reaction
HCl	Dioxane/ Ac_2O	120 °C	Overnight	No reaction
pTsOH	Ac_2O	Reflux	Overnight	Monodehydration

Abbreviations: ^aAluminum trichloride (AlCl_3), phosphorous pentasulfide (P_2S_5), pyridinium *p*-toluenesulfonate (PPTS), perchloric acid (HClO_4). ^bTetrahydrofuran (THF), carbon disulfide (CS_2), ethanol (EtOH), toluene (PhCH_3).

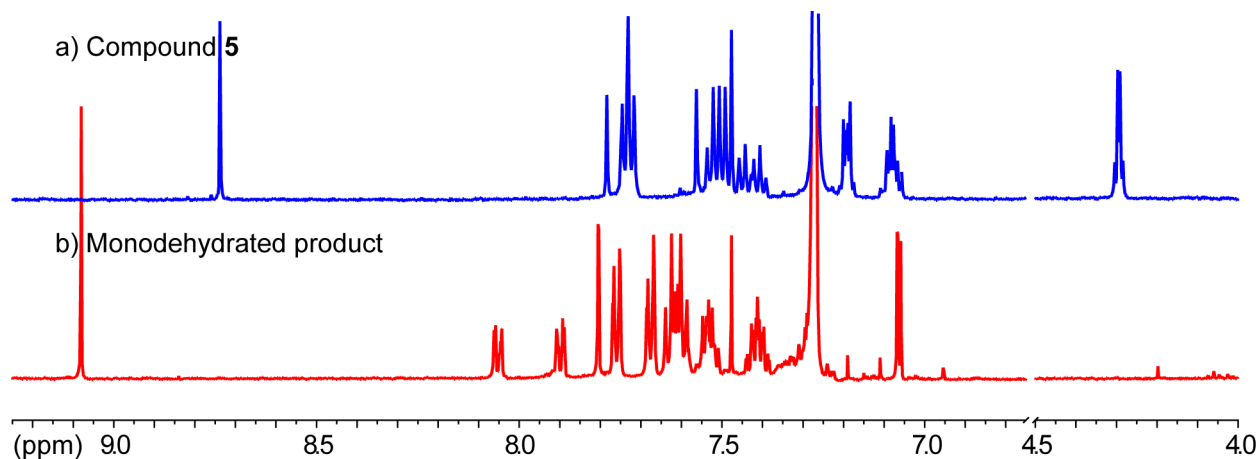


Figure 4.9. (a) ^1H NMR spectrum of compound **5** in CDCl_3 , and (b) ^1H NMR spectrum of the short-lived presumed monodehydration product.

The susceptibility of the monodehydrated precursor to oxidative degradation likely indicates that the four TIPS-ethynyl substituents are not protecting the acene core effectively. Unlike the disubstituted TIPS-pentacene, tetraethynyl-substituted pentacenes have not been well studied in the past. However, as the central ring in pentacene is the most reactive, it has been shown in derivatives bearing other substituents that 6,13-disubstitution is much more effective at extending the half-life of the acene than 5,7,12,14-tetrasubstitution.²² For phenyl- and 2',6'-dimethylphenyl-substituted pentacene for example, the half-life is two to three times longer for the disubstituted compound. Therefore, in order to achieve a pentacene-containing POA it would be necessary redesign a synthetic route employing a bis-dienophile other than 1,4,5,8-anthraquinone that would result in substitution on the central ring.

4.4 Conclusions

With the appropriate chromophore and device architecture, the process of singlet fission holds great promise for increasing the efficiency of organic solar cells. Two acenoid chromophores capable of singlet fission are reported. The previously unknown 5,12-di(thien-2-

yl)tetracene (**2**) was synthesized from 5,12-tetracenequinone *via* a modified procedure from that in the literature. The magnetic field dependence of the fluorescence of **2** indicates that singlet fission is able to occur even in an amorphous powder. Solar cell devices employing 6,13-di(thien-2-yl)pentacene (**1**) as the donor layer and **PDI-2CN** as the acceptor layer were constructed. The decreasing photocurrent generated by the solar cell with increasing magnetic field confirms that triplets are generated by singlet fission in **1**, and that they are then able to dissociate at the donor/acceptor interface.

Preliminary investigation on the synthesis of a pentacene-containing POA as a potential singlet fission material was also undertaken. The synthesis of precursor **5** proved to be quite facile. However, the dehydration step provided an obstacle, likely due to the high reactivity of the desired product.

4.5 Experimental

Materials: All reactions were carried out under argon using standard Schlenk techniques unless otherwise noted. All solvents were of ACS reagent grade or better unless otherwise noted. Anhydrous tetrahydrofuran (THF), diethyl ether (Et₂O), and toluene (PhCH₃) were obtained from J. T. Baker and dried on a solvent column purification system. Silica gel (40 μm) was purchased from SiliCycle Inc. All reagent grade materials were purchased from Alfa Aesar or Sigma-Aldrich and used without further purification. Compound **1** was synthesized using a modification of the procedure reported by Nuckolls *et al.* and the spectral data matched that which was reported.¹⁶ The modified procedure is the same as reported for compound **2** below, starting from 6,13-pentacenequinone. Compound **3** was prepared according to the procedure described previously in this thesis (*cf.* compound **2a**, chapter 3). 1,4,5,8-anthraquinone was

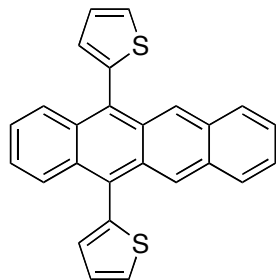
synthesized in two steps according to the procedure described in the literature.²⁰

NMR Spectroscopy: ¹H and ¹³C NMR spectra for all compounds were acquired in CDCl₃ on a Varian Inova Spectrometer (500 MHz or 125 MHz, respectively). Chemical shifts (δ) are reported in parts per million (ppm) and referenced with residual CHCl₃ (7.27 ppm).

Mass Spectrometry: High-resolution mass spectra (HRMS) were obtained at the MIT Department of Chemistry Instrumentation Facility employing either electrospray (ESI) or Direct Analysis in Real Time (DART) as the ionization technique.

Absorption and Emission Spectroscopy: Ultraviolet-visible absorption spectra were measured with an Agilent 8453 diode array spectrophotometer and corrected for background signal with a solvent-filled cuvette. Fluorescence spectra were measured on a SPEX Fluorolog-τ3 fluorimeter (model FL- 321, 450 W Xenon lamp) using right-angle detection. Fluorescence quantum yields in methylcyclohexane were determined relative to perylene in ethanol (EtOH), and are corrected for solvent refractive index and absorption differences at the excitation wavelength. Fluorescence lifetimes were measured *via* frequency modulation using a Horiba-Jobin-Yvon MF2 lifetime spectrometer equipped with a 365 nm laser diode and using the modulation of POPOP (1,4-bis(5-phenyloxazol-2-yl)benzene) as a calibration reference.

Synthetic Procedures:

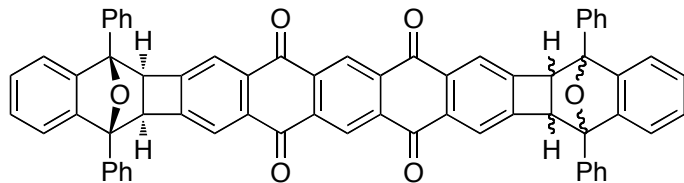


Compound 2: Activated magnesium turnings (Mg, 188 mg, 7.74 mmols) were suspended in anhydrous Et₂O (12 mL) in a round-bottom flask fitted with a reflux condenser. After adding 2-bromothiophene (0.75 mL, 7.74 mmols) the reaction mixture was allowed to stir without heating until all the Mg had dissolved (about 45 minutes) resulting in a cloudy, yellow solution. The freshly prepared Grignard reagent was then added *via* cannula to a suspension of 5,12-tetracenequinone in anhydrous THF (48 mL), and the reaction was heated to reflux for 1 hour. After cooling to room temperature, the reaction was poured into a saturated aqueous solution of ammonium chloride (NH₄Cl_(aq), 50 mL), and extracted with Et₂O (2 × 50 mL). The combined extracts were dried over anhydrous magnesium sulfate (MgSO₄) and the solvent removed under reduced pressure. The crude residue was then taken up in THF (20 mL). A saturated solution of tin(II) chloride (SnCl₂) in concentrated HCl (4 mL) was added and the reaction was stirred at room temperature for 30 minutes. The orange-red solid was collected by filtration and washed with 1 N HCl to give 429 mg (56 %) of **2**.

¹H NMR (500 MHz, CDCl₃): 8.50 (s, 2H), 7.87 (m, 4H), 7.11 (d, *J*=5.2 Hz, 2H), 7.40 (dd, *J*=5.2, 3.4 Hz, 2H), 7.35 (m, 4H), 7.32 (d, *J*=3.3 Hz, 2H)

¹³C NMR (125 MHz, CDCl₃): 139.1, 131.3, 131.1, 130.3, 130.1, 129.7, 128.4, 127.3, 126.9, 126.7, 125.52, 125.49, 125.4

HRMS (DART): Calc for C₂₆H₁₆S₂ [M+H]⁺ 393.0766, found 393.0765



Compound 4, step 1: Compound **3** (350 mg, 1.00 mmols) and 1,4,5,8-anthraquinone (107 mg, 0.45 mmols) were combined in PhCH₃ (7.0 mL) in a pressure tube. The suspension was bubbled with argon for 10 minutes. The tube was then sealed and heated to 120 °C overnight. After cooling to room temperature the reaction was precipitated into hexanes, and an off-white solid (280 mg, 66% crude yield) was collected by filtration and used without further purification.

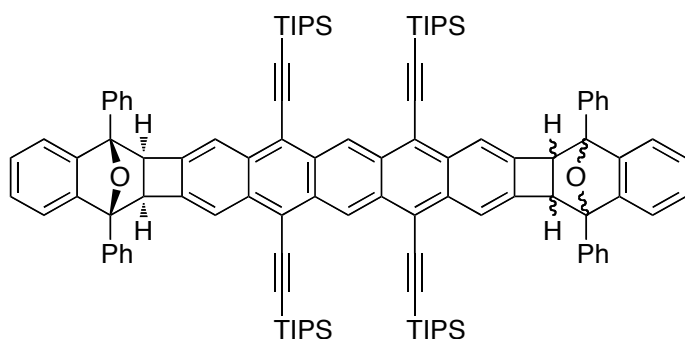
Step 2: The crude Diels-Alder product (280 mg, 0.30 mmols) was suspended in dry THF (6.0 mL), flushed with argon for 10 minutes, and cooled to 0 °C in an ice/water bath. A freshly prepared solution of lithium hexamethyldisilazide (LiHMDS) in dry THF (1.83 mmols) was then added to the suspension *via* cannula. The reaction mixture was allowed to warm to room temperature overnight. The reaction mixture was poured into water (50 mL) and extracted with dichloromethane (CH₂Cl₂, 2 × 50 mL). The combined organics were washed with brine (50 mL), dried over MgSO₄, and concentrated under reduced pressure.

Step 3: The crude solid was then taken up in benzene (C₆H₆, 10.0 mL) and 2,3-dichloro-5,6-dicyano-1,5-benzoquinone (DDQ, 150 mg, 0.66 mmols) was added. The reaction mixture was heated to reflux overnight. After cooling to room temperature, the reaction mixture was loaded directly on to SiO₂. Flash column chromatography (90% CH₂Cl₂/hexanes) yielded 242 mg (57% over 3 steps) of **3** as pale yellow solid.

¹H NMR (500 MHz, CDCl₃): 8.982/8.978 (s, 1H), 7.73 (m, *J*=5.4 Hz, 12H), 7.53 (app t, *J*=7.4 Hz, 8H), 7.46 (app t, *J*=5.2 Hz, 4H), 7.22 (dd, *J*=5.4 Hz, 2.9 Hz, 4H), 7.12 (dd, *J*=5.4 Hz, 3.2 Hz, 4H), 4.36/4.35 (s, 2H)

¹³C NMR (125 MHz, CDCl₃): 182.0, 151.3, 147.6, 136.4, 135.7, 134.6, 129.0, 128.7, 127.6, 127.1, 126.8, 121.9, 119.8, 89.0, 55.9

HRMS (ESI): calc for C₆₆H₃₈O₆ [M+H]⁺ 928.2741, found 928.3093



Compound 5: TIPS-acetylene (130 μ L, 0.57 mmols) was dissolved in dry THF (3.0 mL) and flushed with argon for 10 minutes. The solution was cooled to 0 $^{\circ}$ C in an ice/water bath. *n*BuLi (1.6 M in hexanes, 0.35 mL) was then added dropwise and the reaction mixture stirred for 50 minutes. Compound 4 (105 mg, 0.11 mmols) in dry THF (3.0 mL) was transferred to the reaction flask *via* cannula, and the reaction allowed to warm to room temperature overnight. The reaction was quenched with NH₄Cl_(aq) (25 mL) and extracted with CH₂Cl₂ (2 \times 25 mL). The combined organics were dried over MgSO₄, filtered, and the solvent was removed under reduced pressure. The crude residue was then taken up in acetone (1.0 mL) and SnCl₂•2H₂O (128 mg, 0.57 mmols) in 50% acetic acid (AcOH) in H₂O (1.0mL) was added dropwise. After stirring at room temperature for 3 hours, the precipitate was collected by filtration and washed with cold methanol to give 111 mg (65%) of compound 5 as a blue solid.

¹H NMR (500 MHz, CDCl₃): 8.74 (s, 2H), 7.77-7.71 (m, 10H), 7.56-7.39 (m, 14H), 7.19 (dd, *J*=5.5 Hz, 3.0 Hz, 4H), 7.10 (dd, *J*=5.0 Hz, 2.0 Hz, 4H), 4.28 (s, 4H), 1.20-1.19 (m, 84H)

¹³C NMR (125 MHz, CDCl₃): 182.0, 149.5, 147.7, 147.5, 145.9, 137.3, 136.0, 135.8, 134.16, 132.0, 129.2, 128.7, 128.6, 128.2, 128.1, 127.2, 127.1, 126.6, 126.5, 126.4, 111.5, 103.4, 88.7, 88.6, 55.5, 55.3, 18.9, 11.4

HRMS (ESI): C₁₁₀H₁₂₂O₂Si₄ [M+Na]⁺ 1609.8412, found 1609.7811

4.6 References

- (1) Forrest, S. R. *Nature*, **2004**, *428*, 911.
- (2) Singh, S.; Jones, W. J.; Siebrand, W.; Stoicheff, B. P.; Schneider, W. G. *J. Chem. Phys.* **1965**, *42*, 330.
- (3) (a) Siebbeles, L. D. A. *Nature Chem.* **2010**, *2*, 608. (b) Jadhav, P. J.; Mohanty, A.; Sussman, J.; Lee, J.; Baldo, M. A. *Nano Lett.* **2011**, *11*, 1495. (c) Ramanan, C.; Smeigh, A. L.; Anthony, J. E.; Marks, T. J.; Wasielewski, M. R. *J. Am. Chem. Soc.* **2011**, *134*, 386.
- (4) Smith, M. B.; Michl, J. *Chem. Rev.* **2010**, *110*, 6891, and references within.
- (5) Shockley, W.; Queisser, H. J. *J. Appl. Phys.* **1961**, *32*, 510.
- (6) Hanna, M. C.; Nozik, A. J. *J. Appl. Phys.* **2006**, *100*, 074510/1.
- (7) Lee, J.; Jadhav, P.; Baldo, M. A. *Appl. Phys. Lett.* **2009**, *95*, 033301.
- (8) Guo, J.; Ohkita, H.; Benten, H.; Ito, S. *J. Am. Chem. Soc.* **2009**, *131*, 16869.
- (9) (a) Lanzani, G.; Stagira, S.; Cerullo, G.; DeSilvestri, S.; Comoretto, D.; Moggio, I.; Cuniberti, C.; Musso, G. F.; Dellepiane, G. *Chem. Phys. Lett.* **1999**, *313*, 525. (b) Lanzani, G.; Cerullo, G.; Zavelani-Rossi, M.; De Silvestri, S.; Comoretto, D.; Musso, G.; Dellepiane, G. *Phys. Rev. Lett.* **2001**, *87*, 187402.
- (10) Gradinaru, C. C.; Kennis, J. T. M.; Papagiannakis, E.; van Stokkum, I. H. M.; Cogdell, R. J.; Fleming, G. R.; Niederman, R. A.; van Grondelle, R. *Proc. Natl Acad. Sci. U.S.A.* **2001**, *98*, 2364.
- (11) (a) Groff, R. P.; Avakian, P.; Merrifield, R. E. *Phys. Rev. B* **1970**, *1*, 815. (b) Tomkiewicz, Y.; Groff, R. P.; Avakian, P. *J. Chem. Phys.* **1971**, *54*, 4504. (c) Jundt, C.; Klein, G.; Sipp, B.;

Moigne, J. L.; Joucla, M.; Villaeys, A. A. *Chem. Phys. Lett.* **1995**, *241*, 84.

(12) (a) Wolf, H. C. *Solid State Phys.* **1959**, *9*, 1. (b) Avakian, P.; Abramson, E.; Kepler, R. G.; Caris, J. C. *J. Chem. Phys.* **1963**, *39*, 1127.

(13) Tomkiewicz, Y.; Groff, R. P.; Avakian, P. *J. Chem. Phys.* **1971**, *54*, 4504.

(14) (a) Sebastian, L.; Weiser, G.; Bässler, H. *Chem. Phys.* **1981**, *61*, 125. (b) Lee, K. O.; Gan, T. T. *Chem. Phys. Lett.* **1977**, *51*, 120. (c) Burgos, J.; Pope, M.; Swenberg, C. E.; Alfano, R. R. *Phys. Status Solidi B* **1977**, *83*, 249.

(15) (a) Merrifield, R. E. *J. Chem. Phys.* **1968**, *48*, 4318. (b) Merrifield, R. E.; Avakian, P.; Groff, R. P. *Chem. Phys. Lett.*, **1969**, *3*, 155. (c) Johnson, R. C.; Merrifield, R. E. *Phys. Rev. B*, **1970**, *1*, 896. (d) Suna, A. *Phys. Rev. B* **1970**, *1*, 1716.

(16) (a) Vets, N.; Smet, M.; Dehaen, W. *Synlett*, **2005**, *2*, 217. (b) Miao, Q.; Chi, X.; Xiao, S.; Zeis, R.; Lefenfeld, M.; Siegrist, T.; Steigerwals, M. L.; Nuckolls, C. *J. Am. Chem. Soc.* **2006**, *128*, 1340.

(17) Roberts, S. T.; McAnally, R. E.; Mastron, J. N.; Webber, D. H.; Whited, M. T.; Brutchey, R. L.; Thompson, M. E.; Bradforth, S. E. *J. Am. Chem. Soc.* **2012**, *134*, 6388.

(18) Gorodetsky, A. A.; Cox, M.; Tremblay, N. J.; Kymissis, I.; Nuckolls, C. *Chem. Mater.* **2009**, *21*, 4090.

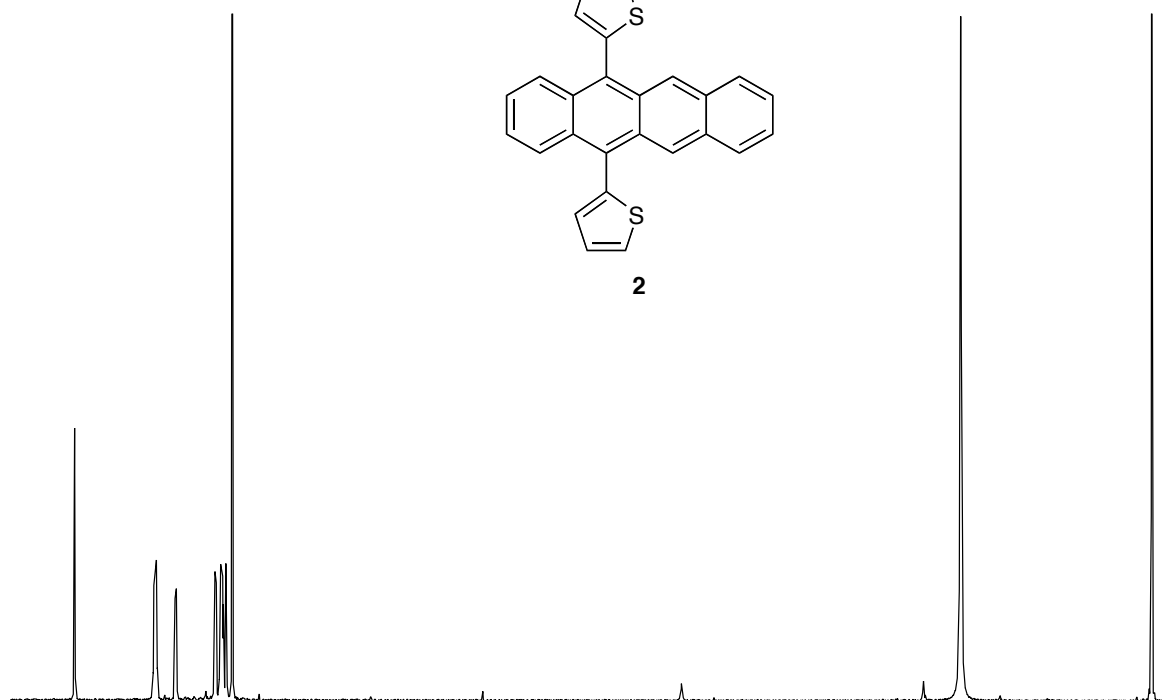
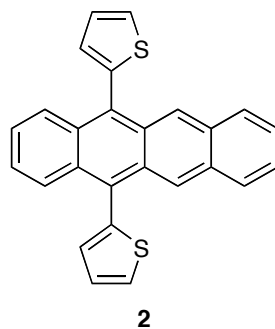
(19) (a) Yoo, S.; Domercq, B.; Kippelen, B. *Appl. Phys. Lett.* **2004**, *85*, 5427. (b) Mayer, A. C.; Lloyd, M. T.; Herman, D. J.; Kasen, T. G.; Malliaras, G. G. *Appl. Phys. Lett.* **2004**, *85*, 6272. (c) Pandey, A. K.; Nunzi, J.-M. *Appl. Phys. Lett.* **2006**, *89*, 213506. (d) Nanditha, D. M.; Dissanayake, M.; Hatton, R. A.; Curry, R. J.; Silva, S. R. P. *Appl. Phys. Lett.* **2007**, *90*, 113505. (e) Yang, J.; Nguyen, T.-Q. *Org. Electron.* **2007**, *8*, 566. (f) Postcavage, W. J.; Yoo, S.; Domercq, B.; Kippelen, B. *Appl. Phys. Lett.* **2007**, *90*, 253511. (g) Sullivan, P.; Jones, T. S. *Org. Electron.* **2008**, *9*, 656.

(20) Cory, R. M.; McPhail, C. L.; Dikmans, A. J. *Tetrahedron Lett.* **1993**, *34*, 7533.

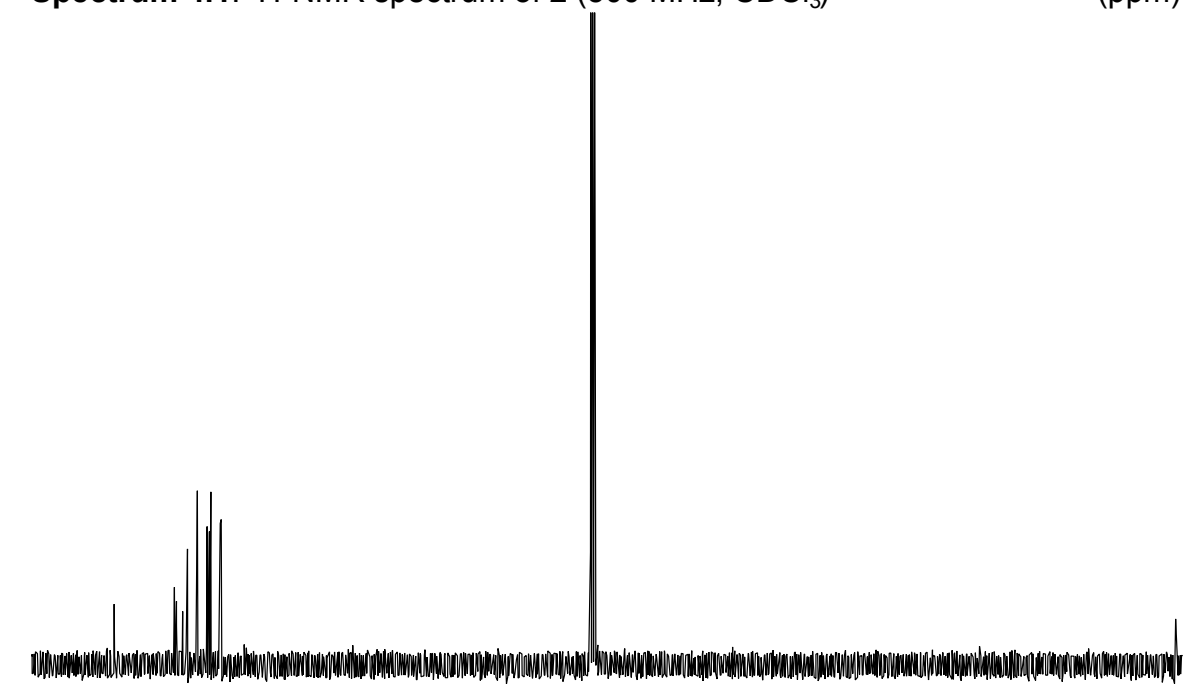
(21) Payne, M. M.; Delcamp, J. H.; Parkin, S. R. Anthony, J. E. *Org. Lett.* **2004**, *6*, 1609.

(22) Kaur, I.; Jia, W.; Kopreski, R.P.; Selvarasah, S.; Dokmeci, M. R.; Pramanik, C.; McGruer, N. E.; Miller, G. P. *J. Am. Chem. Soc.* **2008**, *130*, 16274.

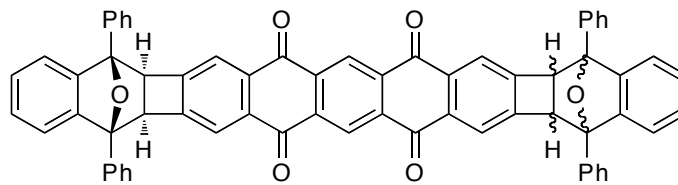
Chapter 4 Appendix
 $^1\text{H-NMR}$ and $^{13}\text{C-NMR}$ Spectra



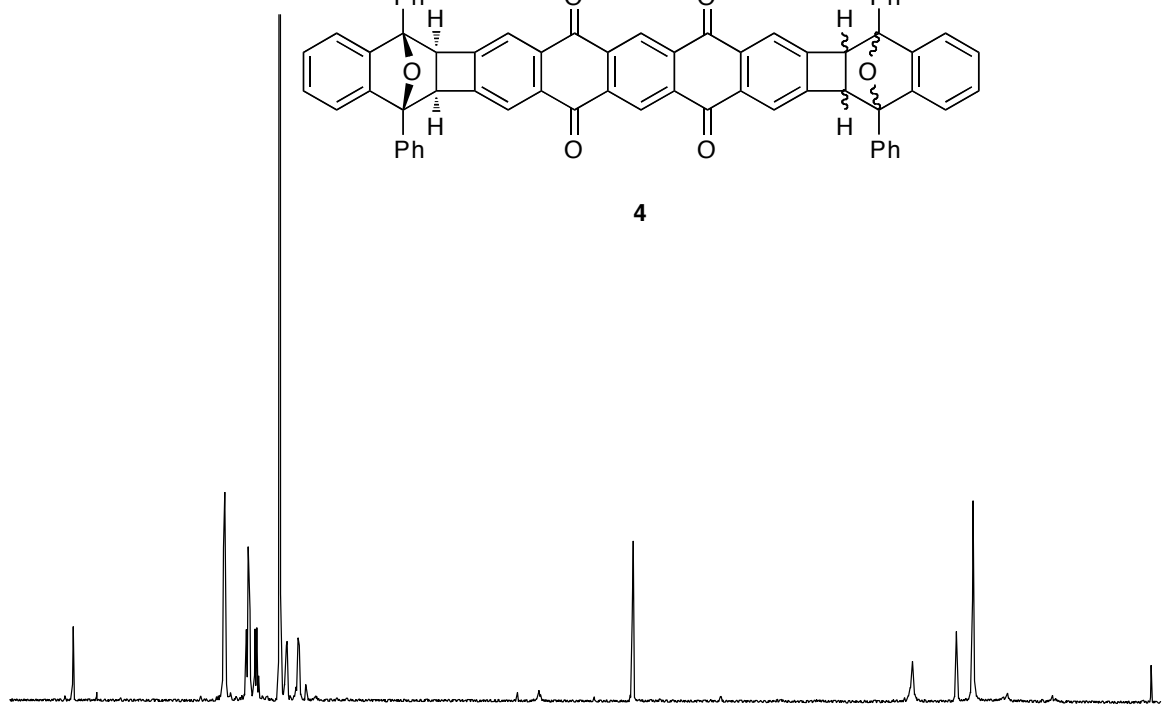
Spectrum 4.1. $^1\text{H-NMR}$ spectrum of **2** (500 MHz, CDCl_3) (ppm)



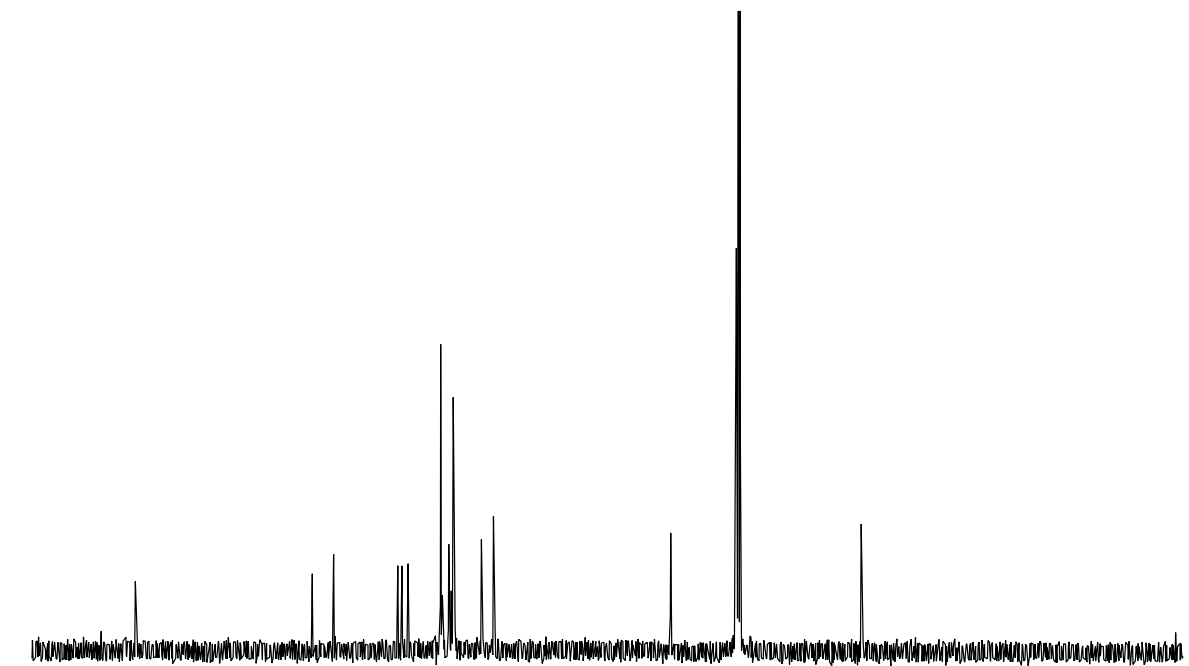
Spectrum 4.2. $^{13}\text{C-NMR}$ spectrum of **2** (125 MHz, CDCl_3) (ppm)



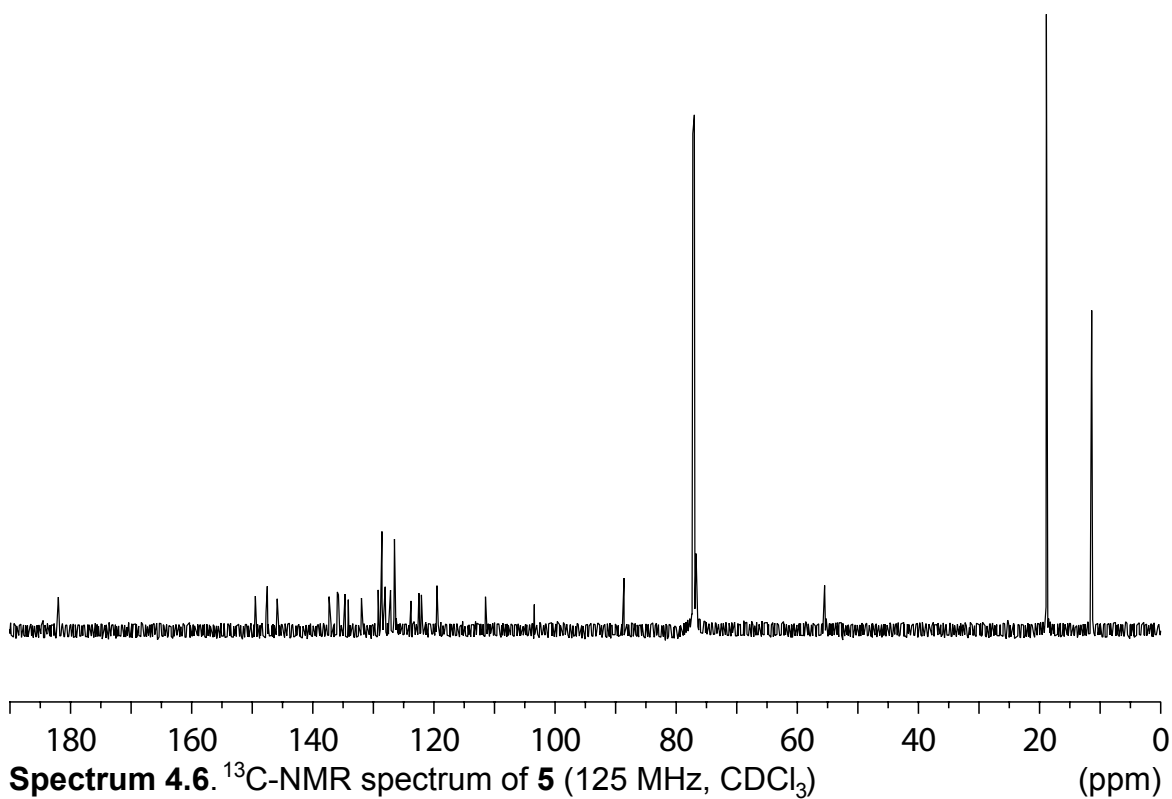
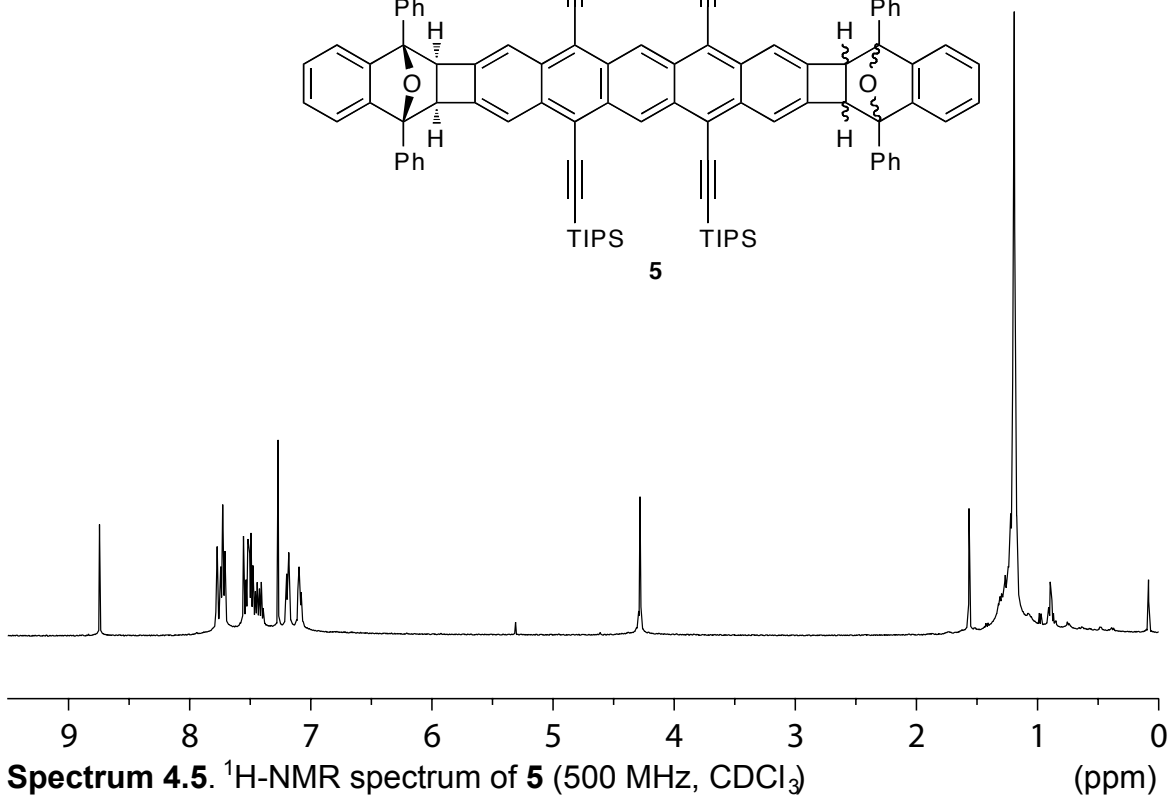
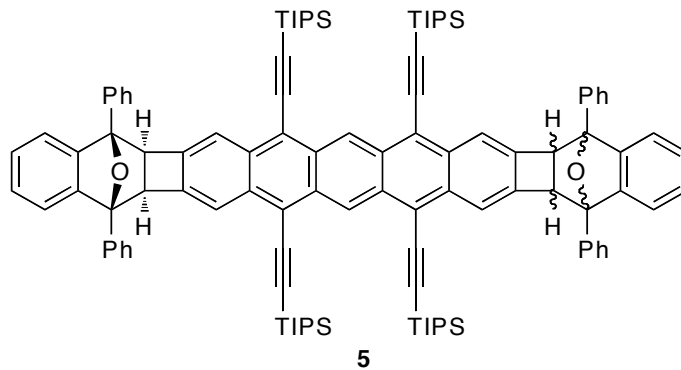
4



Spectrum 4.3. ¹H-NMR spectrum of 4 (500 MHz, CDCl₃) (ppm)



Spectrum 4.4. ¹³C-NMR spectrum of 4 (125 MHz, CDCl₃) (ppm)



Chapter 5

Towards Chain-Growth Diels-Alder Polymerization

5.1 Introduction

Design and synthesis play an important role in the creation of useful new materials. Polymer chemistry often borrows from the synthetic methodology developed for small molecules, however the different nature of macromolecules makes it a challenge to take full advantage of these transformations.¹ Polymerization reactions generally occur by either a step-growth or chain-growth mechanism (Figure 5.1). In step-growth polymerization, any two species can react regardless of the degree of polymerization. Therefore, oligomers form initially and high molecular weight material does not appear until monomer conversion reaches values greater than 98%.² During chain-growth polymerization, reaction between individual monomers is disfavored or slow until a propagating species is generated by reaction with an initiator. Chain-growth allows for narrower polydispersities (PDIs) and greater control over molecular weight than step-growth in the creation of tunable polymer architectures.

Although chain-growth polymerization is more efficient, it has historically been limited to relatively few reactions such as polymerization of vinyl monomers and ring-opening polymerizations, most of which are not useful in the synthesis of conjugated polymers. Recent advances have extended chain-growth polymerization to examples of condensation and cross-coupling polymerization.³ However, there remain many useful reactions for which this mechanism is unavailable. Specifically, the Diels-Alder reaction is very powerful in both polymer and small molecule synthesis due to its efficient and convergent nature.⁴ Two bonds are formed simultaneously with minimal side products and no reactive intermediates.

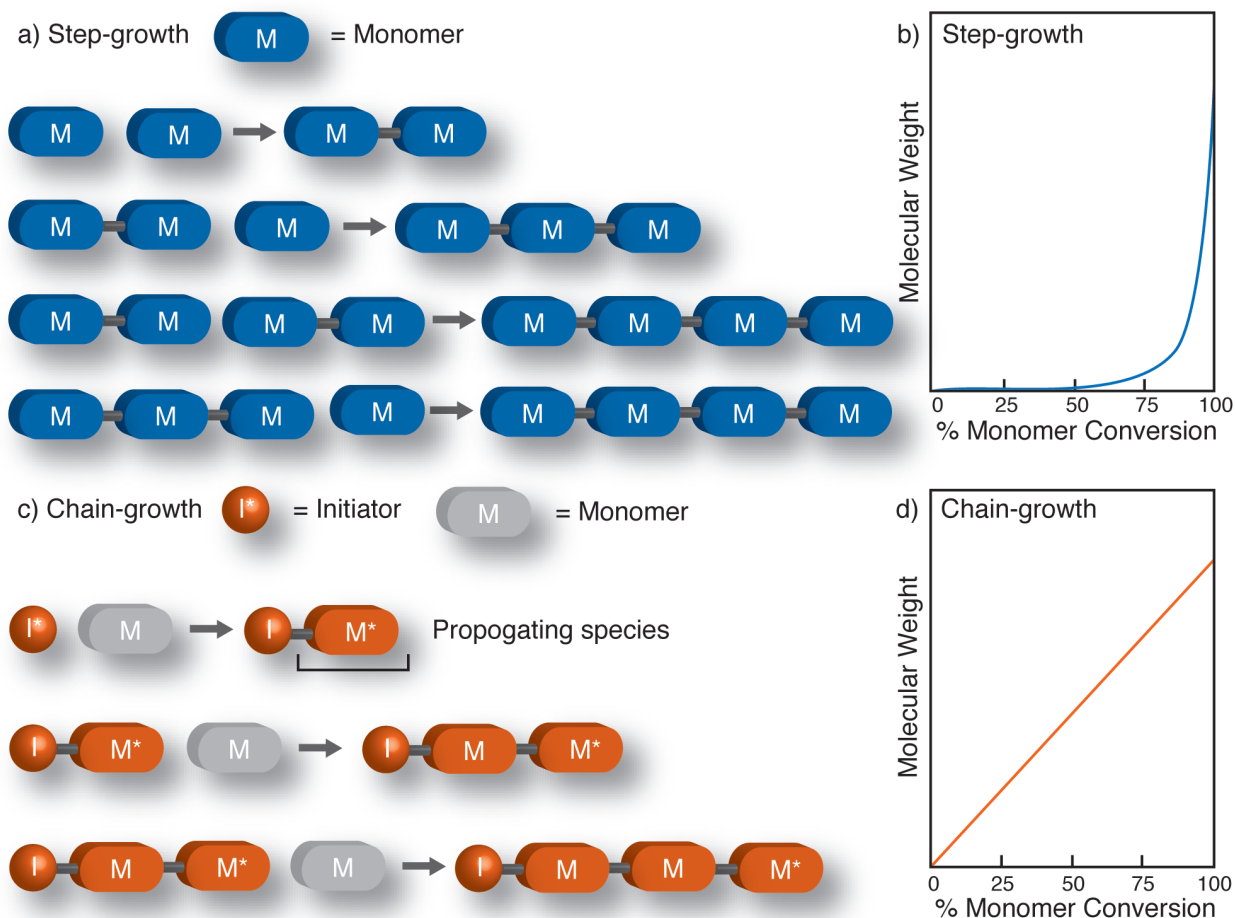


Figure 5.1. (a) Schematic representation, and (b) plot of molecular weight versus monomer conversion of step-growth polymerization. (c) Schematic representation, and (d) plot of molecular weight versus monomer conversion of chain-growth polymerization.

The Diels-Alder reaction offers a defect-free route to ladder polymers, but has thus far only been possible *via* a step-growth mechanism with monomers of the type A_2/B_2 or AB (Figure 5.2a,b). Converting Diels-Alder polymerization to a chain-growth process requires an AB monomer in which one functional group can be masked until activation by an initiator. We have conceived of such a monomer based on the Diels-Alder reactivity of 3,4-bis(methylene)cyclobutene (**1**) established in chapter 3 of this thesis (Figure 5.2c). Initial reaction of **1** with a diene initiator generates a reactive diene (represented in green) as a propagating species for further polymerization of **1**.

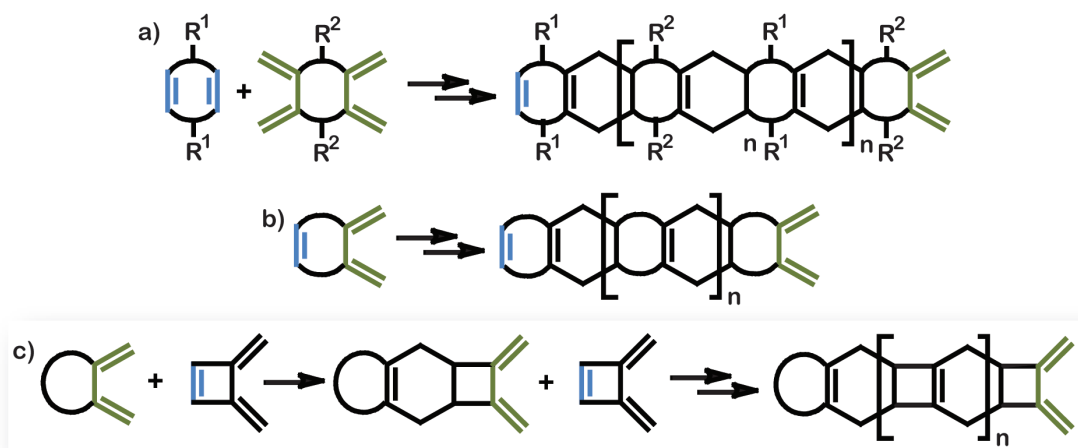
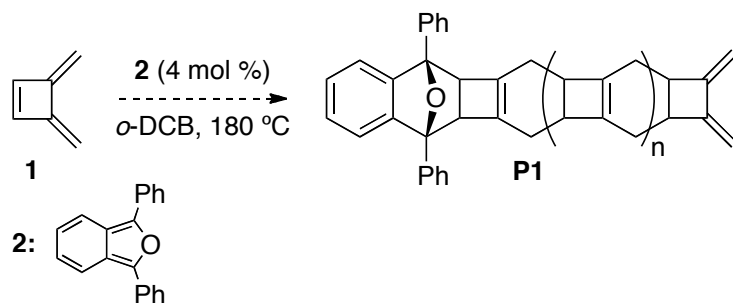


Figure 5.2. Two classical examples of Diels-Alder polymerization: (a) A_2/B_2 polymerization (b) AB polymerization. (c) Proposed chain-growth Diels-Alder polymerization of 3,4-bis(methylene)cyclobutene.

5.2 Initial Polymerization Studies

After establishing some Diels-Alder reactivity of **1** (cf. chapter 3), polymerization and oligomerization studies were undertaken. In the first polymerization attempt, **1** was combined with 4 mol % of initiator 1,3-diphenylisobenzofuran (**2**) in *o*-dichlorobenzene (*o*-DCB, Scheme 5.1). After 30 minutes at room temperature, the yellow, fluorescent color of **2** had disappeared, indicating that initiation had occurred. Heating the reaction mixture to 180 °C for four hours led to precipitation of an insoluble white solid. Low solubility prevented thorough characterization, however data from infrared spectroscopy was consistent with the desired polymer (Figure 5.3). The IR spectrum contained three major bands indicative of cyclohexyl C—H bonds ($\nu = 2816 \text{ cm}^{-1}$, $\nu = 1438 \text{ cm}^{-1}$), and cycloalkene C=C stretching ($\nu = 1665 \text{ cm}^{-1}$). There were no bands in the range of vinylic C—H stretching ($\nu \approx 3100\text{-}3000 \text{ cm}^{-1}$).



Scheme 5.1. Attempted polymerization of **1** to polymer **P1**

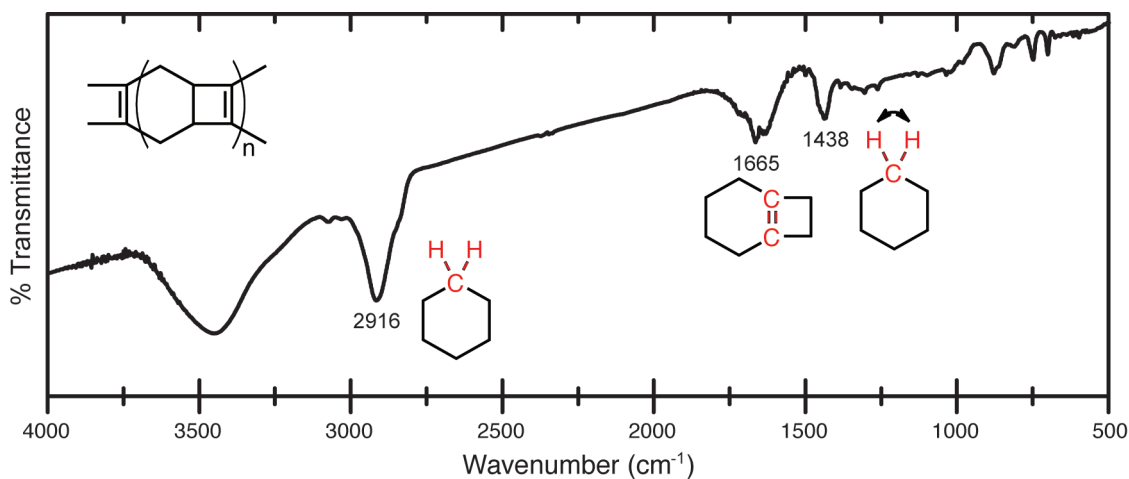


Figure 5.3. Infrared spectrum of **P1**.

To circumvent the problem of low solubility, dimer (**P1**, $n = 0$) formation was attempted using 50 mol % of **2**. The reaction formed a gel after heating to 150 °C for four hours in a sealed tube. The resulting solid upon solvent removal was likewise insoluble. The IR spectrum of the dimer resembles that of **P1** pretty close with the addition of vinylic C—H stretching bands ($\nu = 3062, 3069\text{ cm}^{-1}$) attributable to the unreacted end group (Figure 5.4b). When the dimerization conditions were repeated in the absence of **2**, a precipitate also formed, however at a much slower rate than the gel formation. Unfortunately, the IR of that solid also resembled that of **P1**, with an additional strong band at $\nu = 1719\text{ cm}^{-1}$ (Figure 5.4c). These preliminary results helped to identify two obstacles in utilizing parent hydrocarbon **1** as the monomer: very poor solubility

will be an issue with chains of any length including oligomers, and **1** is susceptible to side reactions under the necessary high temperature conditions.

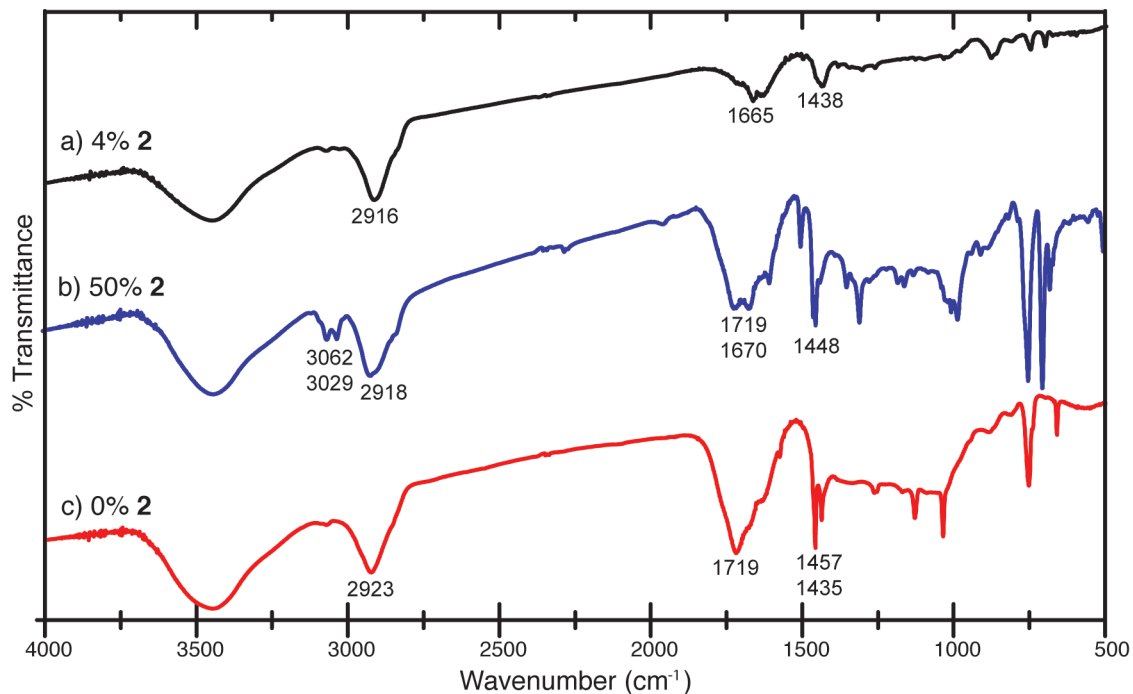


Figure 5.4. IR spectra of insoluble solids resulting from heating of **1** in the presence of (a) 4%, (b) 50 %, and (c) 0% of initiator **2**.

5.3 Improved Monomer Design

In addition to designing a monomer with increased functional group density for improved solubility, we also aimed to enhance Diels-Alder reactivity. It is well established in Diels-Alder chemistry that reactions of dienes locked in the *s-cis* conformation are favorable as the diene need not overcome the energetic barrier of twisting from the thermodynamically favored *s-trans* conformation.⁵ This advantage is classically exemplified by the facile Diels-Alder reactivity of cyclopentadiene. However the situation is more complicated for exocyclic dienes. As the 1,4-internuclear distance “r” in a diene increases, orbital overlap with dienophile becomes less

efficient and the rate of reaction decreases (Figure 5.5a).⁶ The calculated distance “r” for **1** is 3.41 Å (B3LYP/6-31g**), which is even larger than that of 3,4-dimethylenecyclobutane due to the increased ring strain (Figure 5.5b).

Tying the exocyclic methylene groups together in a furan ring would have the threefold advantage of decreasing “r” (Figure 5.5c), raising the HOMO level of the diene, and adding the opportunity for post-polymerization dehydration to a fully-conjugated ladder polymer. The synthesis of the parent furocyclobutadiene **3** was reported in 1972 *via* the flash vacuum pyrolysis (FVP) of a mixture of isomers of 1,2-diethynyloxirane.⁷ However as with **1**, this synthetic route does not allow the opportunity for appending additional functional groups to the monomer for enhancing either reactivity or polymer solubility. Therefore we set out to develop the synthesis of new architectures related to **3**.

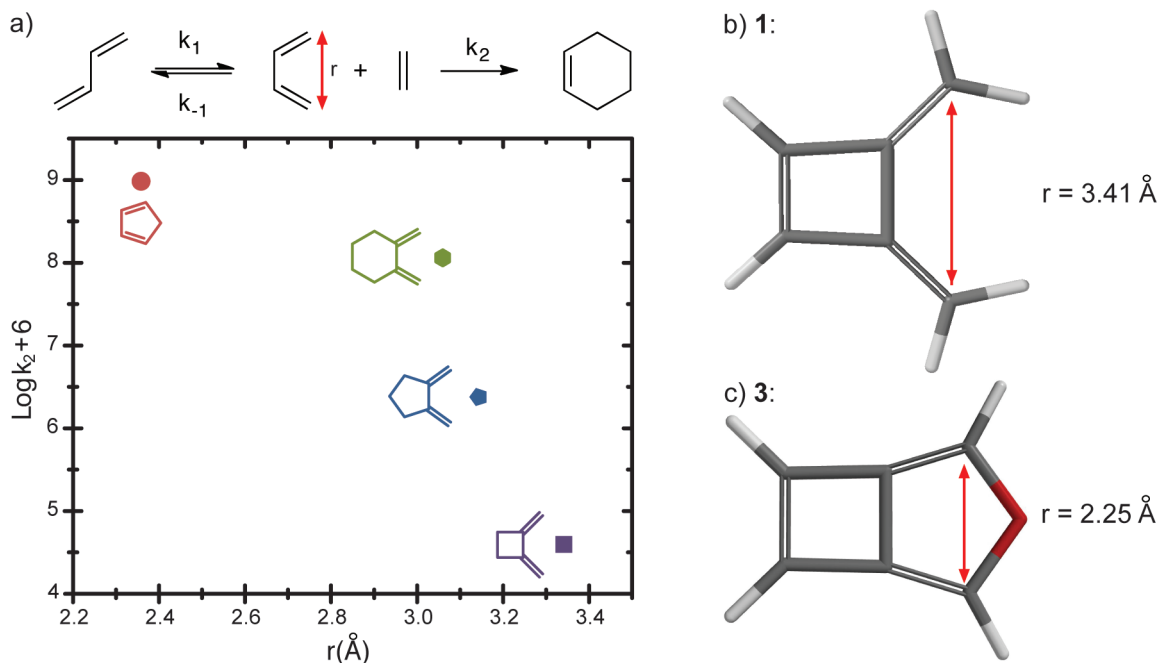
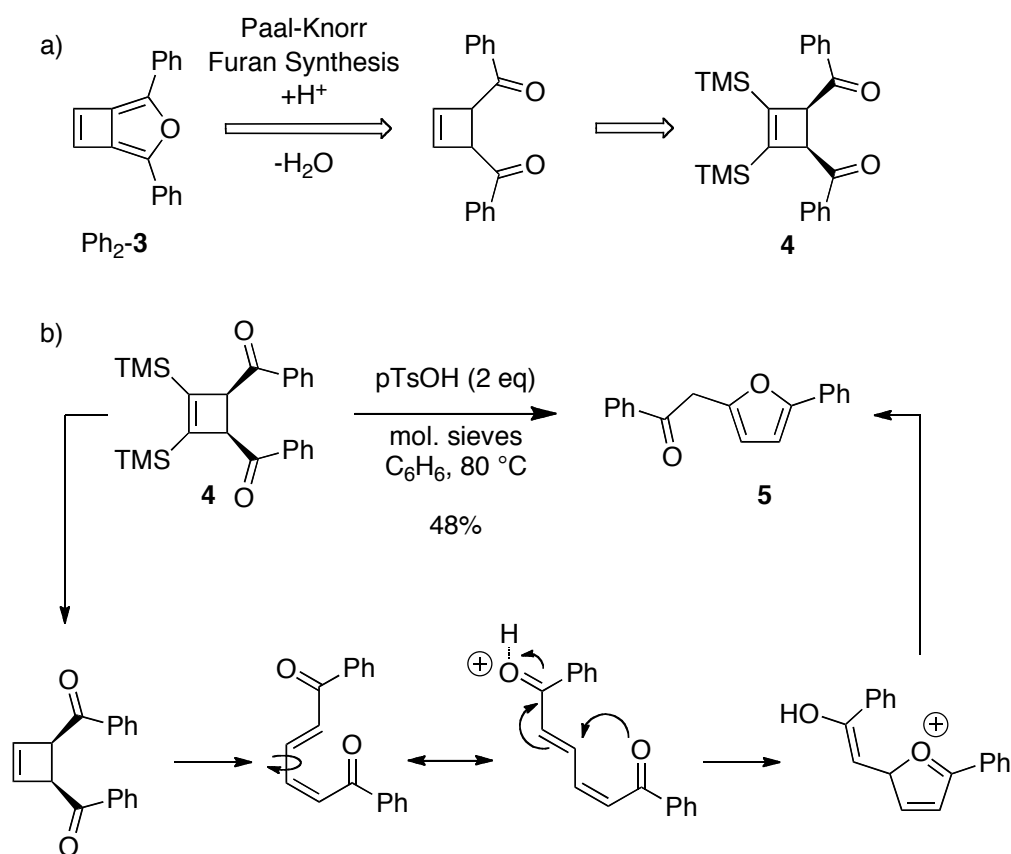


Figure 5.5. (a) Diels-Alder reactivity of *s-cis* dienes versus internuclear distance “r.” For the specific k values plotted, the dienophile is tetracyanoethylene (TCNE).⁶ Calculated geometries of (a) **1** and (b) **3** (Spartan, B3LYP/6-31g**).

The initial synthetic route was based on the Paal-Knorr furan synthesis, which is known to transform 1,4-diketones to furans (Scheme 5.2a).⁸ The synthesis of diketone **4** in one step from benzil and lithium trimethylsilylacetylide was reported in 2010.⁹ Unfortunately, upon heating **4** in the presence of acid, a cascade of reactions takes place beginning with the electrocyclic ring opening of the essential cyclobutene ring (Scheme 5.2b). Asymmetrical furan **5** was isolated as the major product. Ring closure of the proposed diene intermediate to **5** is known and the spectral data matched that previously reported.¹⁰ Several other dehydration conditions were screened. Conditions making use of Lewis acids (TMSCl/DMF, Sc(OTf)₃/PhCH₃) also resulted in the furan **5**, whereas basic conditions (POCl₃, pyr) tended to result in *cis-trans* isomerization.



Scheme 5.2. (a) Retrosynthetic analysis of **Ph₂-3** to **4**. (b) Attempted Paal-Knorr furan synthesis resulting in rearrangement of **4** to asymmetrical furan **5**.

5.4 Towards a Monomer for Chain-Growth Diels-Alder Polymerization

For a second revision of the monomer design, we chose to focus on the synthesis of an isobenzofuran[*b*]cyclobutadiene derivative (Figure 5.6), the synthetic route to which would provide more functional group versatility. For this synthetic route we returned to the intramolecular [2 + 2] cycloaddition of allenes¹¹ as well as some of the chemistry established in chapter 2 of this thesis.¹² In several cases in the literature, *o*-substituted phenyl bisallenes have been shown to ring-close to naphthocyclobutenes (Scheme 5.3a).¹³ Promisingly, in one report in 1978, similar chemistry was used in the synthesis of 1,3-diphenylisobenzofuran-containing compound **6** (Scheme 5.3b).¹⁴ The authors of that work report that compound **6** was relatively stable in the solid state, although they were unable to isolate the dibrominated precursor. The phenyl substituents on the cyclobutadiene ring likely play an important role in the stabilizing **6**, both sterically and electronically, however for our purposes it is best to leave those positions unsubstituted. Retrosynthetic analysis of the desired monomer **7** is shown in scheme 5.4.

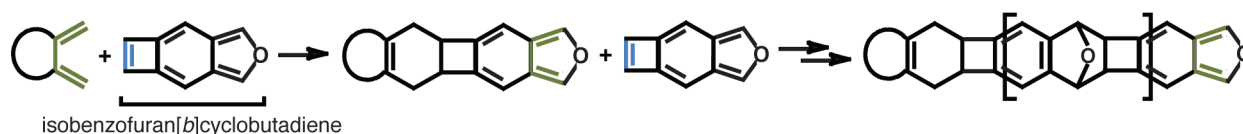
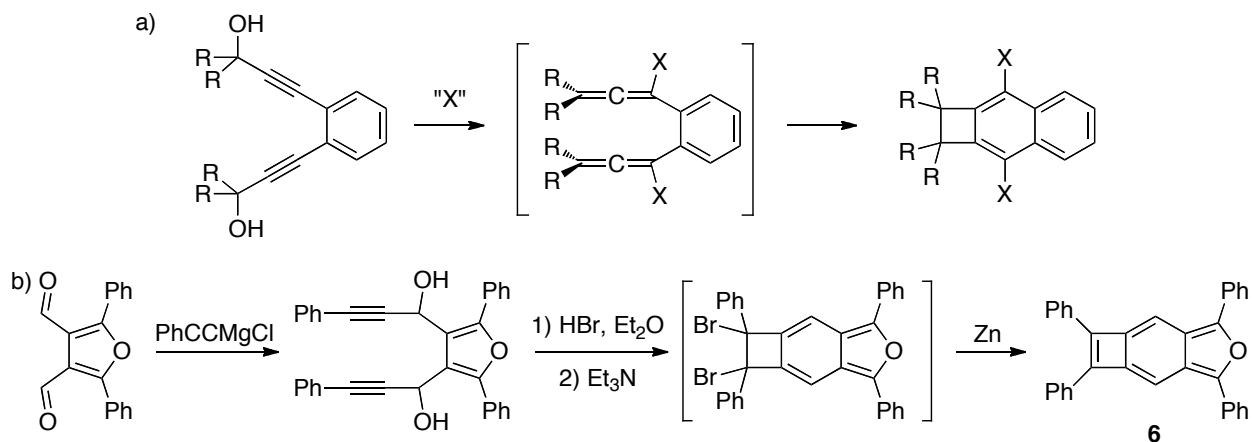
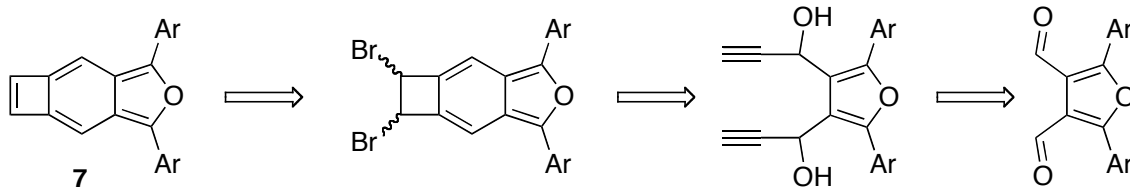


Figure 5.6. Proposed chain-growth Diels-Alder polymerization of isobenzofuran[*b*]cyclobutadiene monomer.



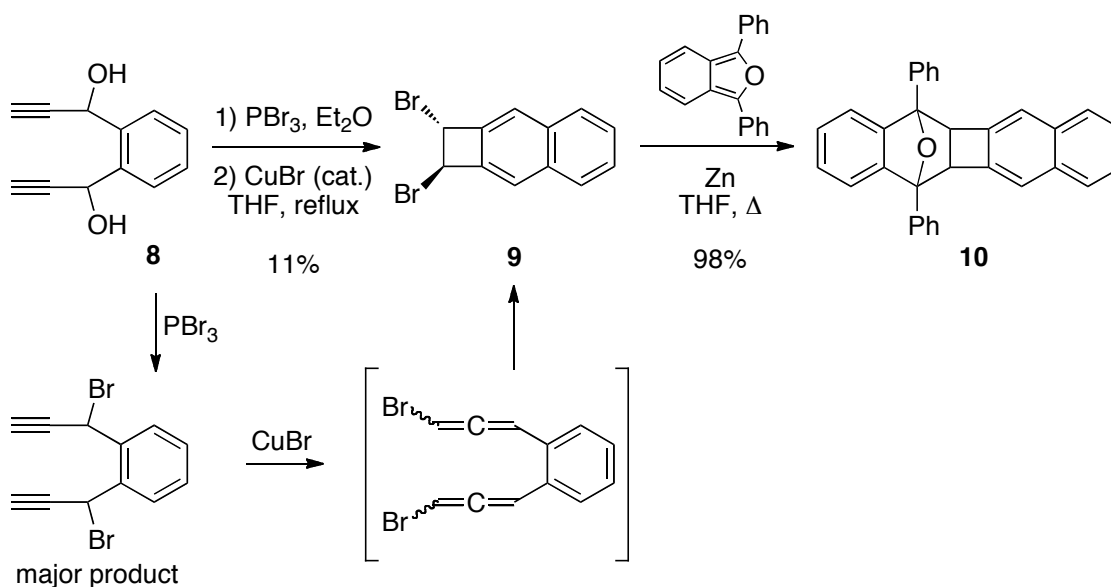
Scheme 5.3. (a) Generic example of [2 + 2] ring closure of *o*-substituted phenyl bisallenes to naphthocyclobutenes. (b) Reported synthesis of 1,3-diphenylisobenzofuran-containing **6**.



Scheme 5.4. Retrosynthetic analysis of monomer **7**.

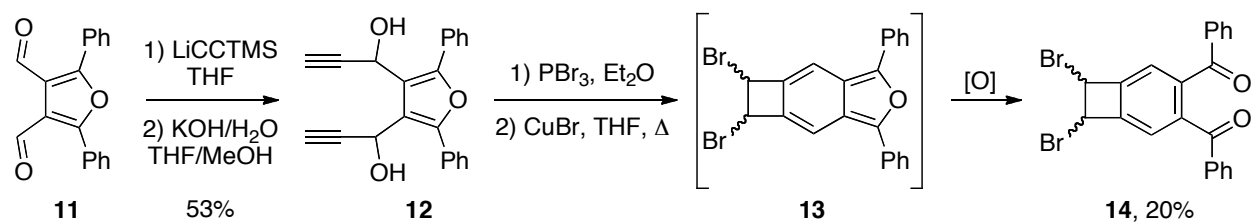
The synthesis of 1,2-dibromonaphtho[*b*]cyclobutene was undertaken first as a test case for the proposed monomer synthesis (Scheme 5.5). Diol **8** was prepared from *o*-phthalaldehyde according to the literature procedure.¹⁵ Treatment of **8** with phosphorous tribromide (PBr₃) resulted in a mixture of isomers, which is believed to be primarily stereoisomers of the propargyl bromide and smaller amounts of the allenyl bromide. The crude mixture was then heated to reflux in tetrahydrofuran (THF) in the presence of a catalytic amount of copper(I), first isomerizing to the bisallene and then ring closing to yield **9**. Compound **9** was isolated as a single isomer and the spectral data matches that previously reported for the *trans* isomer.¹⁶ Although the isolated yield is rather low (11%), compound **9** is the only detected small molecule product. Finally, compound **9** was reduced *in situ* to naphtho[*b*]cyclobutadiene by activated zinc and trapped with 1,3-diphenylisobenzofuran as Diels-Alder adduct **10** in very high yields. The

synthesis of compound **10** by different methods has been reported in the literature, however the characterization data in the previous reports was incomplete.¹⁷



Scheme 5.5. New synthetic route to 1,2-dibromonaphtho[*b*]cyclobutadiene **9** as a model system, and Diels-Alder trapping of naphtho[*b*]cyclobutadiene to give **10**.

Having confirmed the viability of this methodology with substrates such as **8**, the synthesis of the isobenzofuran[*b*]cyclobutadiene monomer **7** was undertaken. The starting material necessary to access the desired monomer *via* the proposed route is 2,5-diphenylfuran-3,4-dicarbaldehyde (**11**). Compound **11** was synthesized in four steps from ethyl benzoylacetate according to the procedure described in the literature.¹⁸ Nucleophilic addition of lithium trimethylsilylacetylide and subsequent deprotection provided diol **12** (Scheme 5.6). Compound **12** was then treated with PBr₃ and the resulting crude material was heated in the presence of catalytic copper(I). The isolated product was determined to be diketone **14** in a 20% yield.



Scheme 5.6. Attempted synthesis of monomer precursor **13**, resulting instead in diketone **14**.

The sensitivity of 1,3-diphenylisobenzofuran to singlet oxygen ($^1\text{O}_2$) in the solution state is well documented. A Diels-Alder reaction between the two results in the *endo*-peroxide,¹⁹ which then decomposes to the diketone *via* a mechanism that is not well understood.²⁰ Compound **13** appears to react with oxygen more rapidly than 1,3-diphenylisobenzofuran which is not surprising given the additional strain imparted to the heterocycle by fusion to a cyclobutene ring. Often isobenzofurans can be either recrystallized or precipitated directly from the reaction to allow their isolation in the solid state. Preliminary attempts to generate **13** under anaerobic conditions and isolate it by precipitation have thus far not been successful. Future work will focus on the direct preparation of **7** and its subsequent polymerization, thus circumventing the isolation of **13**.

5.5 Conclusion

The chain-growth mechanism of polymerization allows for greater control over the molecular weight and narrower polydispersities of polymers than does the step-growth mechanism. However, its application is limited to only certain reactions. The design of a monomer to extend chain-growth polymerization to the Diels-Alder reaction and preliminary results to that end are reported. The unique Diels-Alder reactivity of 3,4-bis(methylene)cyclo-

butene **1** served as inspiration for the proposed polymerization, however in practice low solubility and susceptibility to competing side reactions proved to be an obstacle.

A second generation monomer incorporating isobenzofuran was then designed to overcome some of the drawbacks presented by **1**. Model studies of the new methodology on 1,2-dibromonaphtho[*b*]cyclobutene **9**, as well as its subsequent reduction to naphtho[*b*]cyclobutadiene and Diels-Alder trapping were successful. The instability of dibrominated monomer precursor **13** has presented a challenge in the synthesis of isobenzofuran[*b*]cyclobutadiene monomer **7**. Investigation of a synthetic route to circumvent isolation of this intermediate are underway.

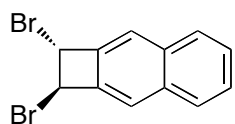
5.6 Experimental

Materials: All reactions were carried out under argon using standard Schlenk techniques unless otherwise noted. All solvents were of ACS reagent grade or better unless otherwise noted. Anhydrous tetrahydrofuran (THF), and diethyl ether (Et₂O) were obtained from J. T. Baker and dried on a solvent column purification system. Silica gel (40 μm) was purchased from SiliCycle Inc. All reagent grade materials were purchased from Alfa Aesar or Sigma-Aldrich and used without further purification. Zinc dust was activated by washing successively with 2% HCl, water, EtOH, and Et₂O. It was then dried under reduced pressure and used immediately.²¹ Diol **7** was prepared from *o*-phthaldialdehyde *via* nucleophilic addition of lithium trimethylsilylacetylide and deprotection according to the procedure reported by Liu, *et al.*¹⁵ Furan **11** (2,5-diphenylfuran-3,4-dialdehyde) was synthesized in four steps from ethyl benzoylacetate according to the literature procedure.¹⁸

NMR Spectroscopy: ^1H and ^{13}C NMR spectra for all compounds were acquired in CDCl_3 on a Varian Inova Spectrometer (500 MHz or 125 MHz, respectively). Chemical shifts (δ) are reported in parts per million (ppm) and referenced with residual CHCl_3 (7.27 ppm).

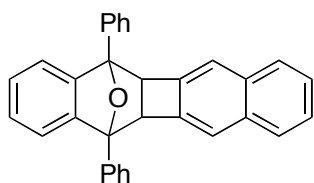
Mass Spectrometry: High-resolution mass spectra (HRMS) were obtained at the MIT Department of Chemistry Instrumentation Facility employing electrospray (ESI) as the ionization technique.

Synthetic Procedures:



Compound 9: Diol **8** (210 mg, 1.13 mmols) was dissolved in anhydrous Et_2O (6.0 mL) in a flame-dried round-bottom flask. The solution was cooled to $-10\text{ }^\circ\text{C}$ in a brine/ice bath and flushed with argon for 10 minutes. Phosphorous tribromide (PBr_3 , 0.07 mL, 0.74 mmols) was added dropwise and the reaction was stirred for 2 hours. After warming to room temperature, the reaction was quenched with H_2O (25 mL) and extracted with Et_2O ($2 \times 25\text{ mL}$). The combined extracts were neutralized with a saturated aqueous solution of sodium bicarbonate ($\text{NaHCO}_{3(\text{aq})}$, 25 mL), washed with brine (25 mL), then dried over anhydrous sodium sulfate (Na_2SO_4), decanted and concentrated under reduced pressure. The resulting crude residue was taken up in dry THF (6.0 mL) with catalytic copper(I) bromide (CuBr , 8 mg, 5 mol %). The reaction mixture was flushed with argon for 10 minutes then heated to $40\text{ }^\circ\text{C}$ for 4.5 hours. The reaction was allowed to cool to room temperature and then quenched with a saturated aqueous solution of

ammonium chloride ($\text{NH}_4\text{Cl}_{(\text{aq})}$, 50 mL) and extracted with Et_2O (2×50 mL). The combined extracts were dried over sodium sulfate (Na_2SO_4), decanted, and the solvent removed under reduced pressure. Flash column chromatography (SiO_2 , hexanes) yielded 38 mg (11%) of *trans*-**8** as a white solid. The spectral data of **8** was consistent with that reported in the literature for the *trans* isomer.¹⁶

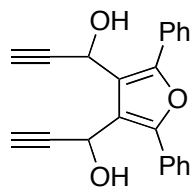


Compound 10: Compound **9** (9.3 mg, 0.030 mmols), 1,3-diphenylisobenzofuran (16.1 mg, 0.060 mmols), and activated zinc dust (100 mg, 1.49 mmols) were combined in anhydrous THF (1.5 mL). The reaction mixture was flushed with argon for 10 minutes then heated to reflux overnight. After cooling to room temperature, the reaction was diluted with dichloromethane (CH_2Cl_2 , 25 mL) and filtered through a pad of celite. Flash column chromatography (SiO_2 , 25-50% CH_2Cl_2 /Hexanes) yielded 12.3 mg (98%) of compound **10** as a white solid.

^1H NMR (500 MHz, CDCl_3): 7.78 (d, $J=2.0$ Hz, 4H), 7.66 (dd, $J=6.2$ Hz, 3.3 Hz, 2H), 7.52 (app t, $J=7.2$ Hz, 4H), 7.44 (app t, $J=6.1$ Hz, 2H), 7.29 (dd, $J=6.3$ Hz, 3.2 Hz, 2H), 7.20 (dd, $J=5.4$ Hz, 3.0 Hz, 2H), 7.16 (s, 2H), 7.12 (dd, $J=5.4$ Hz, 3.0 Hz, 2H), 4.34 (s, 2H)

^{13}C NMR (125 MHz, CDCl_3): 148.0, 140.8, 136.5, 134.3, 128.4, 128.2, 127.9, 126.99, 126.96, 124.8, 120.9, 119.4, 89.3, 54.8

HRMS (ESI): Calc for $\text{C}_{32}\text{H}_{22}\text{O}$ $[\text{M}+\text{H}]^+$ 423.1743, found 423.1733



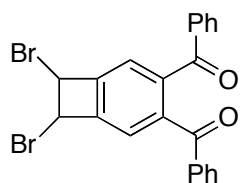
Compound 12, step 1: A flame-dried three-neck flask fitted with two addition funnels was charged with trimethylsilylacetylene (2.25 mL, 15.93 mmols) and dry THF (30 mL). The solution was cooled to $-78\text{ }^{\circ}\text{C}$ in a dry ice/acetone bath and flushed with argon for 10 minutes. *n*BuLi in hexanes (10.0 mL, 15.93 mmols) was then added dropwise *via* one of the addition funnels before stirring at $-78\text{ }^{\circ}\text{C}$ for 30 minutes. A solution of compound **11** (2.000 g, 7.24 mmols) in dry THF (15 mL) was then added dropwise *via* the second addition funnel. The reaction mixture was stirred at $-78\text{ }^{\circ}\text{C}$ for 15 minutes, and then warmed to $0\text{ }^{\circ}\text{C}$ in an ice/water bath and stirred for an additional 30 minutes. The reaction was quenched by pouring into $\text{NH}_4\text{Cl}_{(\text{aq})}$ (50 mL), then extracted with ethyl acetate (EtOAc, $2 \times 50\text{ mL}$). The combined extracts were washed with H_2O and brine (50 mL each), then dried over Na_2SO_4 , decanted, and the solvent removed under reduced pressure.

Step 2: The crude residue from step 1 was taken up in a 1:1 mixture of methanol (MeOH) and THF (30 mL) and cooled to $0\text{ }^{\circ}\text{C}$ in an ice/water bath. Potassium hydroxide (KOH, 120 mg, 2.1 mmols) in H_2O (5 mL) was added and the reaction was stirred for 1 hour. The volatiles were removed under reduced pressure and the residue was redissolved in CH_2Cl_2 (100 mL). The solution was washed with H_2O and brine (50 mL each), dried over Na_2SO_4 , decanted, and the solvent removed under reduced pressure. Flash column chromatography (SiO_2 , 25% EtOAc/hexanes) yielded 1.253 g (53%) of **12** as an off-white solid.

¹H NMR (500 MHz, CDCl₃): 7.69 (m, 4H), 7.50-7.48 (m, 4H), 7.44-7.41 (m, 2H), 5.80 (dd, *J*=8.4 Hz, 2.2 Hz, 2H), 3.70 (d, *J*=8.4 Hz, 2H), 2.77 (d, *J*=2.4 Hz, 1.4H), 2.70 (d, *J*=2.4 Hz, 0.6H)

¹³C NMR (125 MHz, CDCl₃): 151.3, 151.0, 130.0, 129.9, 129.1, 128.98, 128.96, 127.93, 127.87, 120.54, 120.51, 84.8, 83.6, 75.2, 75.1, 57.5, 57.3

HRMS (ESI): Calc for C₂₂H₁₆O₃ [M+Na]⁺ 351.0992, found 351.0988



Compound 14, step 1: Compound **12** (105 mg, 0.32 mmols) was suspended in dry Et₂O (3.0 mL), cooled to -10 °C in an ice/brine bath, and flushed with argon for 10 minutes. Phosphorus tribromide (20 μL, 0.21 mmols) was added and the reaction was stirred for 2 hours. The reaction was quenched with H₂O (25 mL) and then extracted with Et₂O (2 × 25 mL). The combined organics were neutralized with NaHCO_{3(aq)} (25 mL), then washed with H₂O and brine (25 mL each). The organic layer was dried over Na₂SO₄, decanted, and the solvent was removed under reduced pressure.

Step 2: The crude residue from step 1 was taken up in dry THF (6.0 mL) and CuBr (2 mg, 5 mol%) was added. The reaction mixture was bubbled with argon for 30 minutes before heating the reaction to 60 °C for one hour. After cooling to room temperature, the reaction was diluted with Et₂O (25 mL) and filtered through a pad of celite. The solvent was removed under reduced pressure. Flash column chromatography (SiO₂, 10% EtOAc/hexanes) yielded 30 mg (20%) of diketone **14**.

¹H NMR (500 MHz, CDCl₃): 7.73 (d, *J*=7.5 Hz, 4H), 7.56 (app t, *J*=7.5 Hz, 2H), 7.48 (s, 2H), 7.42 (app t, *J*=6.0 Hz, 4H), 5.51 (s, 2H)

¹³C NMR (125 MHz, CDCl₃): 195.6, 144.2, 143.7, 136.6, 133.4, 129.9, 128.5, 124.5, 48.3

HRMS (ESI): Calc for C₂₂H₁₄Br₂O₂ [M+H]⁺ 470.9423, found 470.9419

5.7 References

-
- (1) Hawker, C. J.; Wooley, K. L. *Science* **2005**, *309*, 1200.
 - (2) Odian, G. *Principles of Polymerization*; John Wiley & Sons, Inc.: Hoboken, 2004; pp 6-9.
 - (3) Yokoyama, A.; Yokozawa, T. *Macromolecules* **2007**, *40*, 4093.
 - (4) Carruthers, W. *Cycloaddition Reactions in Organic Synthesis*; Pergamon Press: Oxford, 1990.
 - (5) (a) Fringuelli, F.; Taticchi, A. *Dienes in the Diels-Alder Reaction*. John Wiley & Sons, Inc.: New York, 1990; p 125. (b) Fleming, I. *Frontier Orbitals and Organic Chemical Reactions*. **1978**, London: Wiley. pp. 29–109.
 - (6) Sauer, J.; Sustmann, R. *Angew. Chem. Int. Ed.* **1980**, *19*, 779.
 - (7) Vollhardt, K. P. C.; Bergman, R. G.; *J. Am. Chem. Soc.* **1972**, *94*, 8950.
 - (8) Kürti, L.; Czakó, B. *Strategic Applications of Named Reactions in Organic Synthesis*, Elsevier: Oxford, **2005**, pp. 326-327.
 - (9) Pal, R.; Clark, R. J.; Manoharan, M.; Alabugin, I. V. *J. Org. Chem.* **2010**, *75*, 8689.
 - (10) Bailey, P. S.; Hakki, W. W.; Bost, H. W. *J. Org. Chem.* **1955**, *20*, 1034.
 - (11) (a) Landor, S. R. *The Chemistry of Allenes*, Academic Press: London, **1982**. (b) Krause, N.; Hashmi, A. S. K. *Modern Allene Chemistry*, Wiley-VCH: Weinheim, **2004**. (c) Alcaide, B.; Almendros, P.; Aragoncillo, C. *Chem. Soc. Rev.* **2010**, *39*, 783.
 - (12) Parkhurst, R. R.; Swager, T. M. *Synlett*, **2011**, 1519.
 - (13) (a) Toda, F.; Tanaka, K.; Sano, I.; Isozaki, T. *Angew. Chem. Int. Ed.* **1994**, *33*, 1757. (b) Toda, F.; Tanaka, K.; Watanabe, M.; Tamura, K.; Miyahara, I.; Nakai, T.; Hirotsu, K. *J. Org. Chem.* **1999**, *64*, 3102. (c) Tanaka, K.; Takamoto, N.; Tezuka, Y.; Kato, M.; Toda, F.

Tetrahedron, **2001**, *57*, 3761. (d) Kitagaki, S.; Okumura, Y.; Mukai, C. *Tetrahedron Lett.* **2006**, *47*, 1849.

(14) Firouzabadi, H.; Maleki, N. *Tetrahedron Lett.* **1978**, *34*, 3153.

(15) Liu, Y. Zhou, S.; Li, G.; Yan, B.; Guo, S.; Zhou, Y.; Zhang, H.; Wang, P. G.; *Adv. Synth. Catal.* **2008**, *350*, 797.

(16) Shepherd, M. K. *J. Chem. Soc., Perkin Trans. 1*, **1985**, 2689.

(17) (a) Cava, M. P.; Hsu, A.-F. C. *J. Am. Chem. Soc.* **1972**, *94*, 6441. (b) Hsu, A.-F. C.; Cava, M. P. *J. Org. Chem.* **1979**, *44*, 3790.

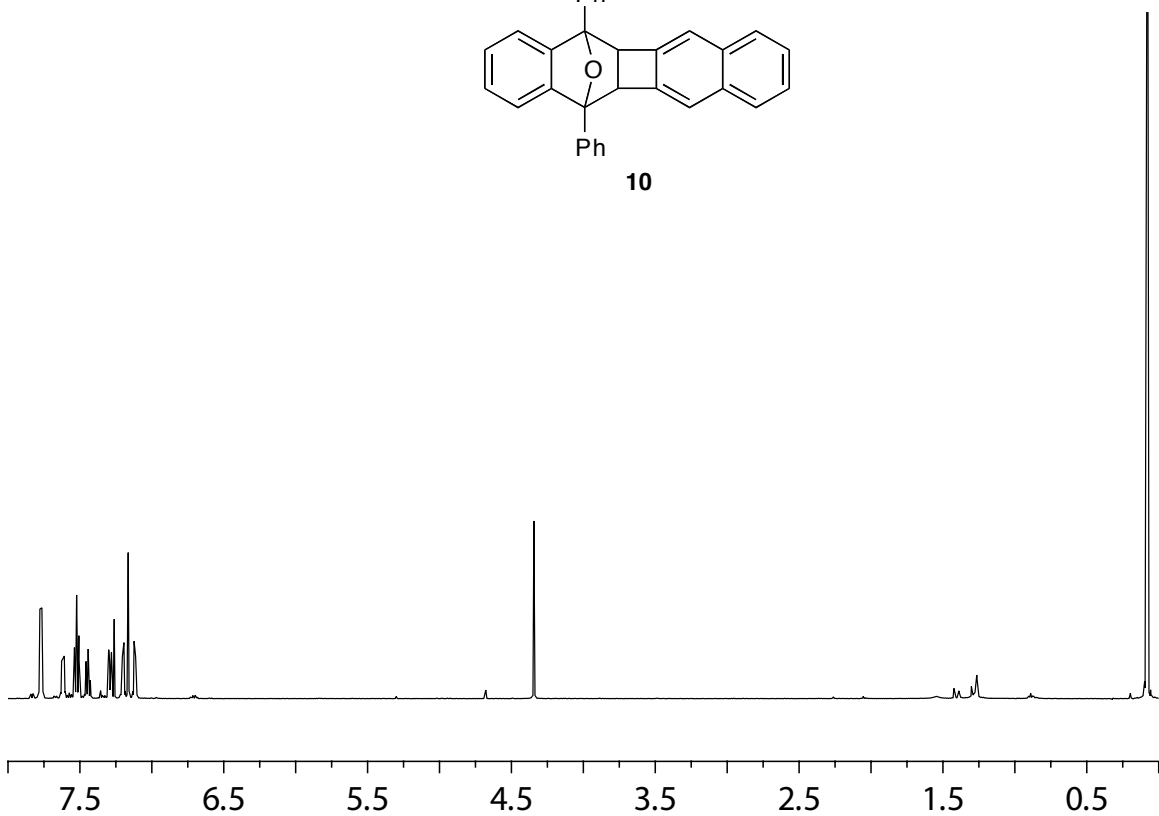
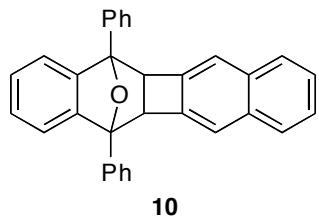
(18) (a) Wu, A.; Zhao, Y.; Chen, N.; Pan, A. *Synth. Commun.* **1997**, *27*, 331. (b) Hsu, D.-T.; Lin, C.-H. *J. Org. Chem.* **2009**, *74*, 9180.

(19) Rio, G.; Scholl, M.-J. *J. Chem. Soc., Chem. Commun.* **1975**, 474.

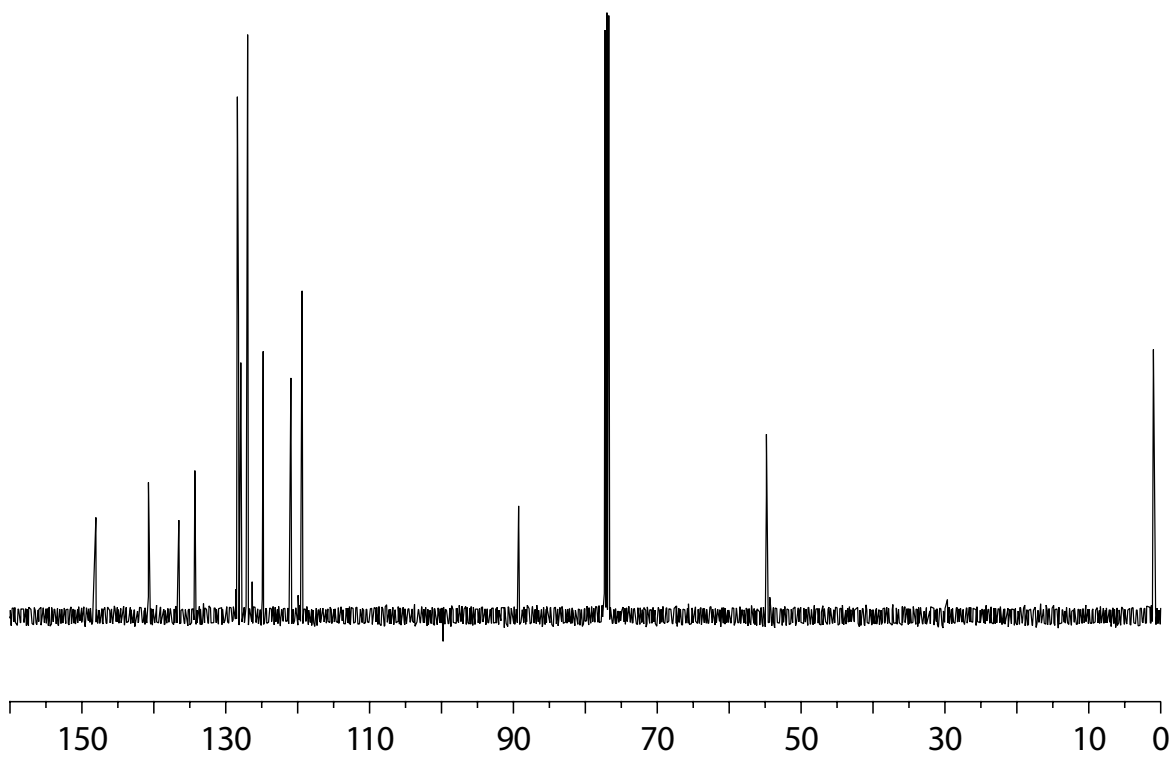
(20) Friedrichsen, W. *Adv. Heterocycl. Chem.* **1980**, *26*, 13.

(21) Gauvry, N.; Comoy, C.; Lescop, C.; Huet, F. *Synthesis*, **1999**, 574.

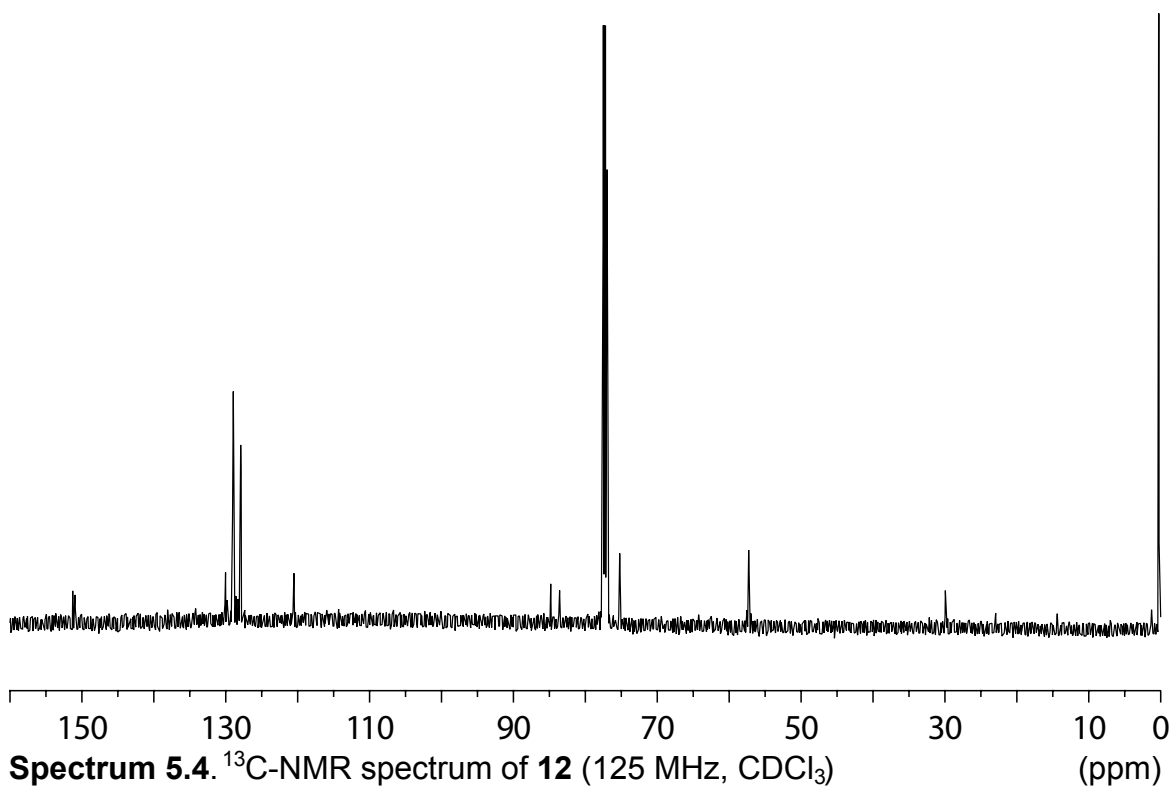
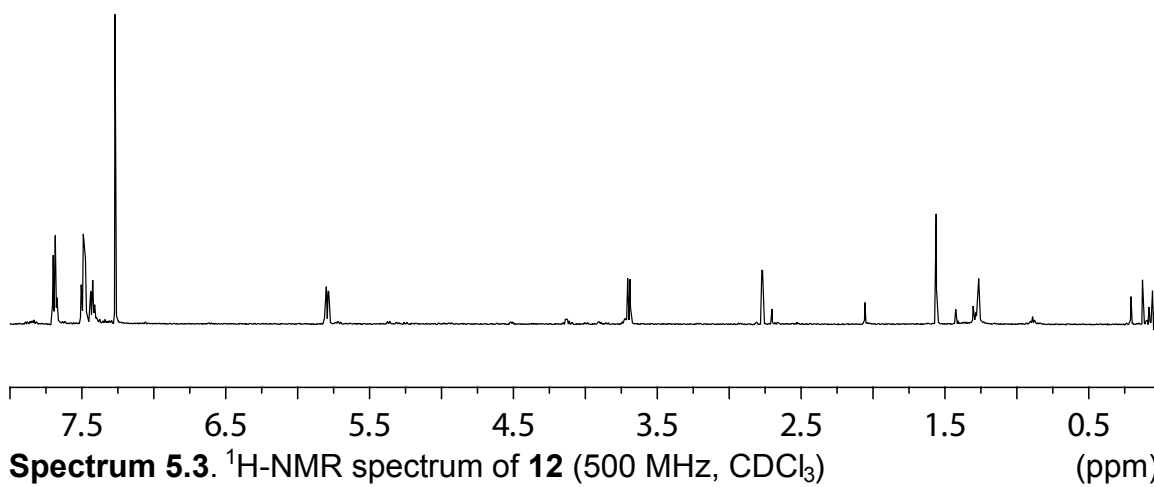
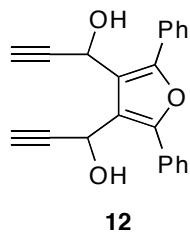
Chapter 5 Appendix
 ^1H -NMR and ^{13}C -NMR Spectra
And Additional Figures

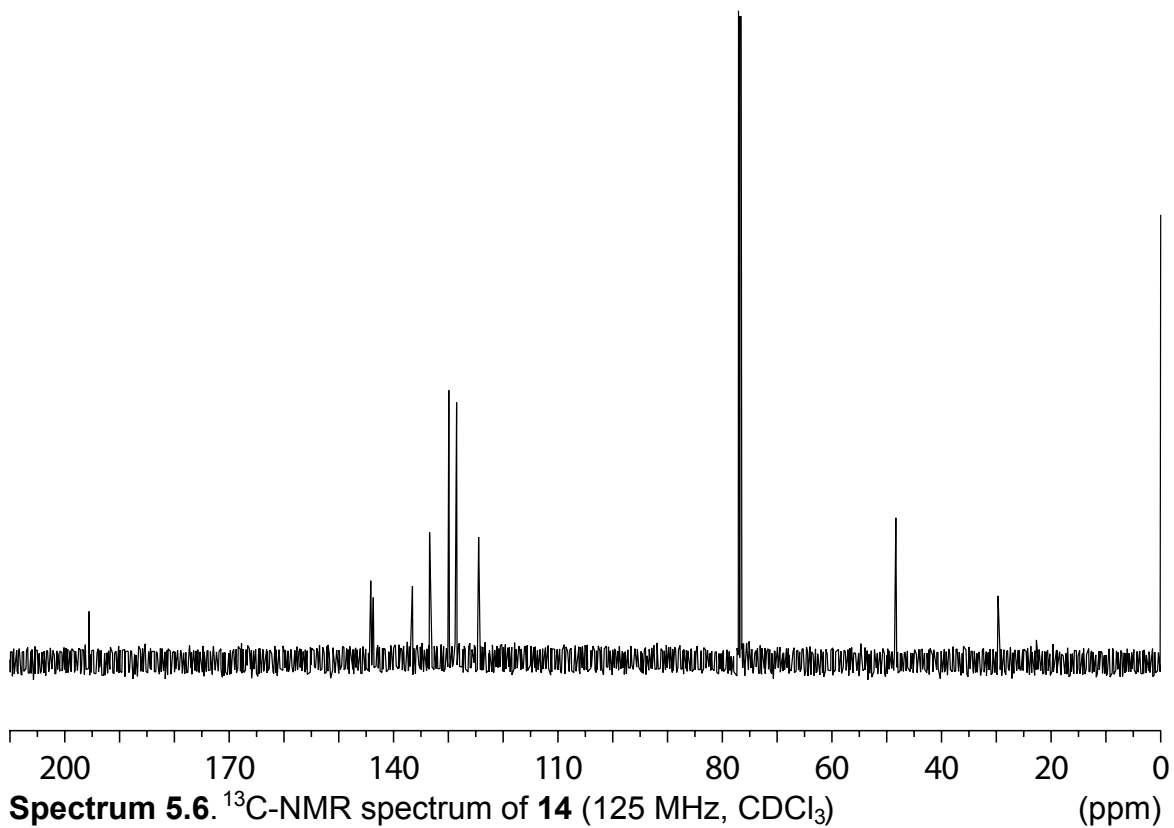
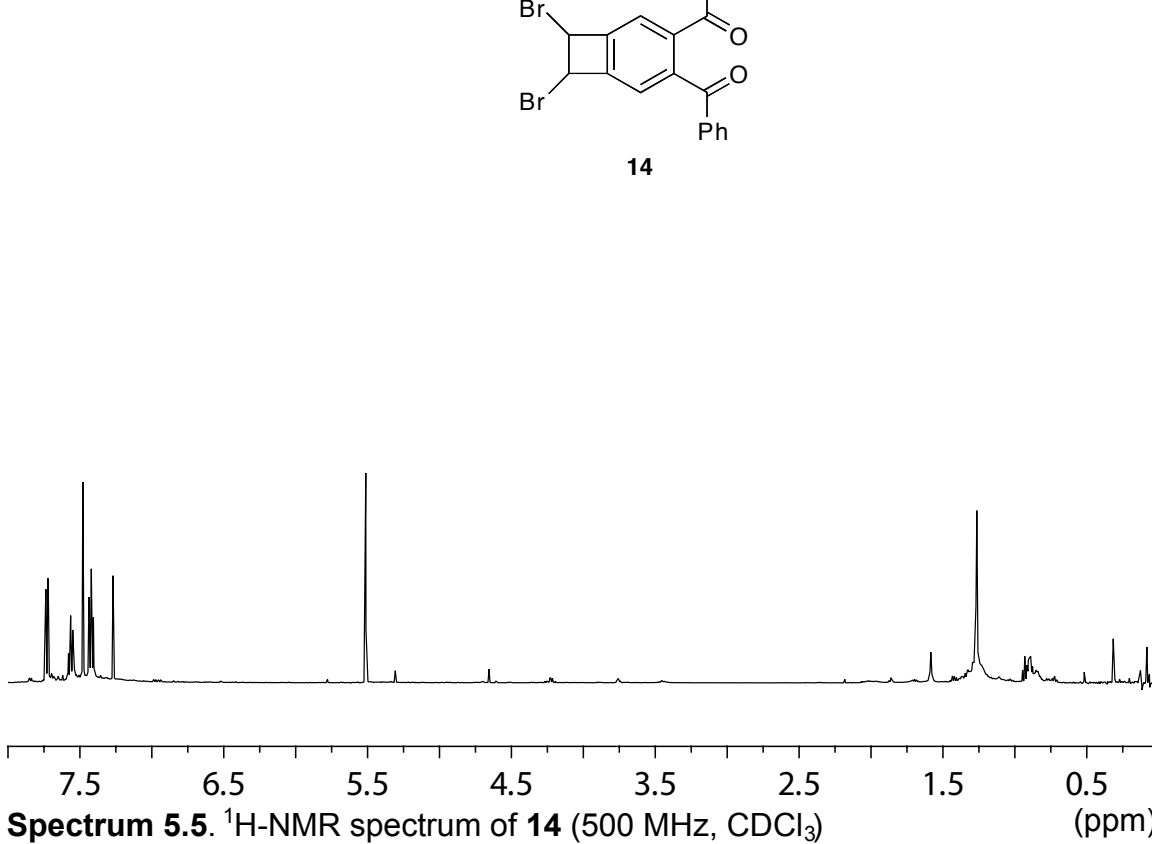
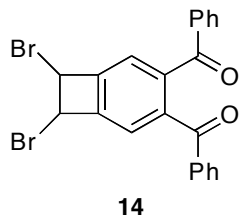


Spectrum 5.1. $^1\text{H-NMR}$ spectrum of **10** (500 MHz, CDCl_3) (ppm)



Spectrum 5.2. $^{13}\text{C-NMR}$ spectrum of **10** (125 MHz, CDCl_3) (ppm)





EDUCATION

Massachusetts Institute of Technology, Cambridge, MA June 2012

Doctor of Philosophy in Organic Chemistry - GPA: 4.9/5.0

- 2 first author publications, 1 review in press, 3 international conference presentations.

Hamilton College, Clinton, NY May 2007

Bachelor of Arts Summa Cum Laude in Chemistry and French - GPA: 94.5/98.0

- Academic Distinctions: Sigma Xi, Phi Beta Kappa, Dean's List eight semesters
- 2 international conference presentations.

University of Pierre and Marie Curie, Paris, France Sept. 2005-May 2006

Visiting student

- Completed coursework in quantum mechanics and thermodynamics in French.

RESEARCH EXPERIENCE

MIT Chemistry Department, Cambridge, MA Sept. 2007-present

Adviser: Timothy M. Swager

Research Assistant

- Synthesized and characterized a previously unknown family of highly strained and highly unsaturated organic molecules as precursors to interesting electronic materials.
- Designed and implemented new methodology for the synthesis of organic materials (both small molecules and polymers) with unique optoelectronic properties derived from the incorporation of high energy, strained functional groups. Currently collaborate with electrical engineers on investigation of above materials for use in solar cells.

Hamilton College Chemistry Department, Clinton, NY June 2004-May 2007

Adviser: Ian J. Rosenstein

Research Assistant

- Launched a research project to invent new methods for stereoselective synthesis of organic molecules using radical chemistry. Project culminated in a written thesis and an oral presentation.

Novartis Institutes for Biomedical Research, Cambridge, MA June 2005-Aug. 2005

Adviser: Markus Dobler

Summer Intern

- Explored the structure-activity relationship of anti-cancer drug candidates to better understand and improve mechanism of action. Investigated the effects of functionalization on a biologically active natural product. Project culminated in an oral and poster presentation.

TEACHING EXPERIENCE

MIT-China Educational Technology Initiative (MIT-CETI), Cambridge, MA March 2012-present

Fellow

- Currently developing curricula in organic electronics and American culture to be taught in English at universities in China and Taiwan June-July 2012.

MIT Chemistry Department, Cambridge, MA Sept. 2007-Dec. 2010

Teaching Assistant, Organic Chemistry I (Sept. 2010-Dec. 2010)

- Implemented new technology as an interactive teaching tool in the course to assess student understanding and encourage lecture attendance. Managed and analyzed student data from a class of 170 students.

Teaching Assistant, Introduction to Experimental Chemistry (Jan. 2008-May 2008)

- Instructed a laboratory course designed to introduce students to innovative research techniques such as the fabrication of light-emitting diodes (LEDs).

Howard Hughes Medical Institute (HHMI) Teaching Assistant, Principals of Chemical Science (Sept. 2007-Dec. 2007)

- Formulated and taught two one-hour lectures of 20 students per week. Incorporated interdisciplinary topics into the curriculum to increase student interest in the course.

PRESENTATIONS

- R. R. Parkhurst, T. M. Swager, "Design and Synthesis of Unique Electronic Materials from Derivatives of 3,4-Bis(methylene)cyclobutene" 14th International Symposium on Novel Aromatic Compounds (ISNA-14), **2011**, (awarded Best Poster Presentation Award).
- R. R. Parkhurst, T. M. Swager, "Synthesis of Phenylene-Containing Acenoid Structures," 240th ACS National Meeting, **2010** (oral presentation).
- R. R. Parkhurst, T. M. Swager, "Synthesis of Phenylene-Containing Acenoid Structures," 9th International Symposium on Functional Pi-Electron Systems (F-Pi-9), **2010** (poster presentation).
- R. R. Parkhurst, I. J. Rosenstein, "Investigation of Novel Methods for Stereoselective Synthesis Involving Radical Translocation," 234th ACS National Meeting, **2007** (poster presentation).
- R. R. Parkhurst, I. J. Rosenstein, "Investigation of Novel Methods for Stereoselective Synthesis Involving Radical Translocation," National Organic Symposium (NOS), **2007** (poster presentation).

PUBLICATIONS

- R. R. Parkhurst, T. M. Swager, "Synthesis of 3,4-Bis(benzylidene)cyclobutenes," *Synlett*, **2011**, *11*, 1519.
- R. R. Parkhurst, T. M. Swager, "Synthesis and Optoelectronic Properties of Phenylene-Containing Oligoacenes (POAs), submitted.
- R. R. Parkhurst, T. M. Swager, "Antiaromaticity in Non-Benzenoid Acenoid Structures and Ladder Polymers," *Top. Curr. Chem.*, in press.

LEADERSHIP AND ACTIVITIES

- MIT Women in Chemistry**, Cambridge, MA Sept. 2007-present
President (Mar. 2009-Aug. 2010), Member
- Organized professional and social events for 100 female graduate students and post-docs in the chemistry department as well as alumni. Chaired meetings of the organizing board and expanded annual program to include career panels with invited speakers.
- Swager Research Group** Cambridge, MA Jan. 2010-present
Subgroup Captain
- Coordinate bimonthly meetings in which 30-35 graduate and postdoctoral research assistants present progress reports. Commenced weekly literature and research discussions among a subgroup team of 8 researchers.
- MIT Chemistry Graduate Student Seminar Committee**, Cambridge, MA May 2009-Oct. 2010
Organizer
- Selected seminar speakers for the Chemistry Department. Served as a liaison to invited speaker, and oversaw scheduling and publicity of the event.
- ACS Graduate Student Symposium Planning Committee**, Cambridge, MA June 2008-Aug. 2010
Secretary
- Maintained comprehensive records of committee meetings and decisions during the organization of a Presidential Event on science policy at the Aug. 2010 meeting of the American Chemical Society (ACS). Coordinated logistics for invited speakers.
- SYNFACTS, Thieme Publishers**, Cambridge, MA July 2008-Dec. 2009
Co-Editor
- Selected recent scientific papers with implications for materials chemistry to be highlighted in the monthly publication SYNFACTS. Illustrated the impact of the above publications with a summary and figures.

HONORS AND FELLOWSHIPS

Best Poster Presentation Award (ISNA-14, 2011), Morse Travel Grant (MIT, 2011 and 2010); HHMI Teaching Assistantship (MIT, 2007); *The Merck Index* Women in Chemistry Scholarship Award of Special Recognition (2007); National Organic Symposium Undergraduate Travel Award (2007); Elihu Root Fellowship (Hamilton, 2007); Underwood Prize in Chemistry (Hamilton, 2007); Couper Phi Beta Kappa Book Prize (Hamilton, 2004); Merck/AAAS research stipend (2004); NSF-STEP (Science Talent Expansion Program) Fellowship (2003).

Acknowledgements

I can hardly believe that it's been five years already! First, I would like to thank *Tim Swager* for being such an amazing advisor. I believe you can see the advisor's personality reflected in the group he/she runs. Through his creative approach to science and unbeatable work ethic, Tim has set the standard for the Swager research group, and, in the process, cultivated a supportive and collaborative environment. Particularly in the past year, it has become clear to me how well Tim knows and understands each and every group member, a fact that makes his advice on life post-MIT invaluable. I'm so grateful to have had the opportunity to work for Tim as a graduate student.

I would also like to thank my thesis committee, *Rick Danheiser* and *Tim Jamison*, as well as the rest of the organic faculty. I have learned so much chemistry in the past five years from being in such a diverse department. Meetings with Rick each year have been very helpful and I very much appreciate his attention to detail. I think it is important to quickly mention other chemistry mentors along the way: *Profs. Rosenstein, Kinnel, and Brewer* at Hamilton for four amazing and inspiring years, as well as a lot of advice on graduate school, and to *Mr. Palmer and Dr. Haswell* for starting it all at B.H.S.

Kathy Sweeney and *Caitlin McDowell* have played a crucial role in keeping the group running the past few years. I cannot imagine the group without either of you, but I guess we will find out soon enough. Good luck in graduate school, Caitlin! I'm so glad that you got the job four years ago and that we've had the opportunity to become friends and colleagues because of it.

Jose Lobez, Jan Schnorr, and Oleysa Haze are amazing colleagues who have been there since the beginning. *Jose* – You're still the Harry Potter to my Hermione Granger (which I'm pretty sure makes me the smart one). It's hard to believe that I won't see you every day for the next five years, too. Thanks for listening to me cry over failed experiments (and only making fun of me 75% of the time). You're so talented and your ability to multi-task effectively is inspiring. I'm sure that you'll get everything that you want and more, just be patient. *Janster* – Very few people on this planet are as helpful and as giving of their time as you. There are a lot of good things coming your way karmically. Thanks for all your help around the lab, as well as everywhere else: picking locks, fixing computers, drawing muffins, etc. *OH* – I'm so glad that you joined the lab! You are such a great colleague and friend that I often forget there was ever a time you weren't there. Thanks for all the bubble tea breaks, good luck with all of your plans for the future. I expect daily puppy updates.

The Swager group is such an amazing group of people, unfortunately I can't thank everyone but I may come close. *Joel Batson* – We have become so close over the past couple of years, and I may not have survived the last year, in particular, without you. Being colleagues, friends, and roommates simultaneously is no small feat. Thanks for listening and bringing Phoebe and Wally into my life...just kidding...sort of. Thanks to all of me officemates over the years: *Shuang Liu* – Thanks for being such a good lab citizen and for all kinds of discussions over the past five years. *Grace Han* – I'm so glad you took the desk next to mine a year and have been such good company ever since. Good luck with the rest of your PhD! *Balta Bonillo* – Thanks for the company on the occasional late night and for always reminding me that I'd

survive the writing process. Thanks also to *Fei Wang* and *Julian Chan* for help getting started in the lab, and to *Mindy Levine* and *Kat Mirica* for advice on life and the future.

The Swager group thrives on an unofficial system of mentorship between upper level graduate students and post-docs and new members. I'm sure everyone in the lab has helped me at some point or another, but a few former group members stand out: *Trisha Andrew* – the overlord of fluorescence and general oracle of chemistry. You have the unmatched ability of being able to help everyone else around the lab while still getting your own work done. Thanks for introducing me to Buffy (ponytail). I can't wait to see all of the amazing research that comes out of your new lab. *Jeewoo Lim* – I've already promised you eternal friendship multiple times so I'm not sure what else I have to offer. Thanks for all the help and advice you've given me and for cleaning up everyone else's messes as safety officer.

Graduate school would not have been the same without the train wreck that is *Katie White*, *Arturo Pizano*, *Christina* and *Eric Zimanyi*, and *Dan Suess*. You all were an amazing support system, the perfect mix of empathy as fellow chemistry graduate students and the ability to discuss and enjoy a huge array of other things. I'm also so proud to have been a part of the administrative board of *Women in Chemistry*, so thanks to all of the women, past, present, and future, who've made that group possible. I think we have had a very creative and proactive five years and I hope some day to join the ranks of our many generous benefactors.

I was lucky enough to be able to be in graduate school at one of the best universities in the world *and* be close to friends and family. I couldn't have done it without the support of all of my loved ones outside of MIT in addition the people listed above. A few people who will likely never see this document but still deserve recognition: *Sarah Perkins*, *Betsey Holland*, *Cat Michaud*, *Sara Sabella*, *Heather Milkiewicz*, *Jess Lewis*, *Chris Minue*, *Allie Demas*.

Thanks of course to my parents, *Bob* and *Debra*, and to my sister, *Emalie*, for being a great support system over the past five years. I will definitely miss being able to see you whenever I want next year (even if I didn't take full enough advantage of it for the last five). My grandmother, to whom I dedicate this thesis, passed away last September at the age of 91. Her support opened up a lot of educational doors for me and gave me opportunities that I will never take for granted. We were linked not only by family ties, but also by I love of science and I'm honored to have made her proud.